

**OPTIMIZATION OF CIRCULATING miRNA LIBRARY PREPARATION FOR
NEXT-GENERATION SEQUENCING AND AN EXPLORATORY
PHARMACOGENOMICS INVESTIGATION OF PSORIATIC ARTHRITIS
PATIENTS TREATED WITH IL-12/23 or IL-17 INHIBITORS**

© Alison Margaret Semple Sutherland

This thesis was submitted to the School of Graduate Studies in partial fulfillment of the requirements for the degree of

Master of Science in Medicine (Human Genetics)
Discipline of Genetics, Faculty of Medicine
Memorial University of Newfoundland
St. John's Newfoundland and Labrador

May 2018

ABSTRACT

Optimization for circulating miRNA library preparations, multiplexing capacity, and sequencing with the Ion Torrent System was executed in order to process patient samples effectively. Multiple modifications were attempted in two published protocols before miRNA library preparations reached adequate quality for sequencing. A cohort of nine psoriatic arthritis patients, recruited for a pharmacogenomics investigation of treatment with IL-12/23 or IL-17 inhibitors, had blood samples drawn at baseline, as well as one- and three-month post treatment. The pharmacogenomics samples from baseline were sequenced and the resultant data underwent several analyses in order to identify predictive miRNA markers or profiles. Differential miRNA expression analyses were performed both between the American College of Rheumatology response criteria groupings and on clinical datasets, followed by a comprehensive literature review to examine potential implications of identified miRNAs. Pathway analyses, network analyses, and an *in silico* functional enrichment analysis were performed on the data to identify associations with signalling cascades, collectively targeted genes, and biological functions, respectively. The results of this exploratory study demonstrate the potential of the miRNA sequencing framework for identifying predictive miRNA markers and profiles associated with response to pharmaceuticals.

ACKNOWLEDGEMENTS

I would like to extend my upmost appreciation and gratitude to a number of people:

To my mother, father, brother, and grandparents who have given me love, strength, and support throughout my life.

To my supervisor, Dr. Darren O’Rielly, for his help throughout this project and the writing of this thesis. And to my co-supervisor, Dr. Proton Rahman, for his kindness, hospitality, and mentorship in the clinic.

To the members of my committee, Dr. Guanju Zhai for his knowledge and direction, and to Dr. Lourdes Peña-Castillo for her efficiency and overall brilliance.

To the staff of the Rahman-O’Rielly lab group – Amanda Dohey, for her kindness, consideration, and patience; Dianne Codner for her proficiency and assistance in the lab as well as for the sequencing of samples in this project; and Nadine Burry for her kind-heartedness and humour.

To Dr. Quan Li for his expertise in running the data analyses in this project.

To the research team at St. Clare’s Hospital – Donna Hackett for help with clinical data and consenting patients for this project, Sheena Leonard for administering the biologics, and Rose Arden her organization and helping me get in contact with Proton.

To Mathieu LaRivière for his consultations while establishing the RNA sequencing framework.

To Dr. Michael Woods and Dr. Ann Dorward, for their guidance, support, and overall efforts to enrich the student experience in the Discipline of Genetics.

To Amy Carroll for motivating me to apply for the Rothermere Fellowship, you changed my life and for that I am forever grateful.

To the staff at the Health Science Centre Library for all their help and kindness.

To the patients in the PsA cohort who donated samples for this project.

To the funding agencies who support the Rahman-O’Rielly Lab efforts.

To all of my friends from the genetics department with a special thanks to Yajun Yu and Tammy Benteau.

To the gentle hippies that are so dear to me, thank you for the hours of laughter and dancing with special thanks to Anna Callahan for her unfailing support, friendship, and compassion.

To Kevin Qiu, for being there from the first day to the last.

Finally, and perhaps most of all, I’d like to thank Chad Griffiths, for being so welcoming, for the inimitable friendship, for all of the laughter, for the dependability, for teaching me about Newfoundland, for teaching me about grammar and writing, for the editorial help, for the emotional support, for instilling confidence in me, and for enabling me to embark on a path I wouldn’t have gotten to (or been brave enough to go down), without your help.

TABLE OF CONTENTS

ABSTRACT	ii
ACKNOWLEDGEMENTS	iii
TABLE OF CONTENTS	v
LIST OF FIGURES	ix
LIST OF TABLES	xii
ABBREVIATIONS	xvi
1 INTRODUCTION	1
1.1 Psoriatic Arthritis and Clinical Features	1
1.1.1 Clinical Categorization of Psoriasis and Psoriatic Arthritis.....	2
1.1.2 Comorbidities.....	4
1.1.3 Classification Criteria.....	5
1.1.4 Monitoring Disease Progression and Response to Treatment.....	6
1.1.4.1 American College of Rheumatologist Criteria	6
1.1.4.2 Clinical Disease Activity Index	6
1.1.4.3 Health Assessment Questionnaire-Disability Index	7
1.1.4.4 Patient Reported Outcomes	8
1.1.4.5 Minimal Disease Activity.....	8
1.1.4.6 Erythrocyte Sedimentation Rate.....	8
1.2 Pathogenesis of PsA	9
1.2.1 Pathogenesis at the Level of the Tissue.....	9
1.2.2 Pathogenesis at the Molecular Level.....	12
1.2.2.1 TNF α	12
1.2.2.2 IL-12/23.....	13
1.2.2.3 IL-17	15
1.3 Genetics of PsA	16
1.3.1 Heritability of PS and PsA	16
1.3.2 Genetic Contributions to PsA within the MHC locus	17
1.3.3 Genetic Contributions to PsA outside the MHC locus.....	19
1.4 Treatment of PS and PsA	20
1.4.1 Topical Agents for the Treatment of PS.....	22
1.4.2 Oral Agents for the Treatment of PS and PsA	23
1.4.3 Small Molecule Inhibitors	25
1.4.4 Biologic agents.....	25
1.4.4.1 TNF α Inhibitors.....	26
1.4.4.2 IL-12/IL-23 Inhibitors	27
1.4.4.3 IL-17 Inhibitors	28
1.5 Prediction of Treatment Response	29
1.5.1 Pharmacokinetics	29
1.5.2 Pharmacodynamics.....	31

1.5.3	Pharmacogenetics and Pharmacogenomics	33
1.5.3.1	DNA Variations in Precision Medicine	33
1.5.3.2	DNA Variations Causing Differential Drug Response in Psoriatic Disease....	35
1.5.3.2.1	Differential Response to Topical Agents in PS Patients	35
1.5.3.2.2	Differential Response to Oral Agents in PS Patients	36
1.5.3.2.3	Differential Response to Traditional Systemic Agents in PS and PsA Patients.....	37
1.5.3.2.4	Differential Response to Biologic Agents in PS and PsA Patients	39
1.5.3.3	RNA Variations in Precision Medicine	41
1.5.3.3.1	messenger RNA	41
1.5.3.3.2	microRNA.....	42
1.5.3.4	mRNA Variations Causing Differential Drug Response in Psoriatic Disease.	46
1.5.3.4.1	Methotrexate	47
1.5.3.4.2	TNF α Inhibitors	47
1.5.3.4.3	IL-12/23 Inhibitors.....	48
1.5.3.4.4	IL-17 Inhibitors.....	49
1.5.3.5	miRNA Variations Causing Differential Drug Response in Psoriatic Disease	50
1.5.3.5.1	Methodologies of miRNA Extraction from Plasma	51
1.6	Rationale	54
2	MATERIALS AND METHODS.....	56
2.1	Ethics approval.....	56
2.2	Sample Ascertainment for Optimization of Library Preparation.....	57
2.3	Sample Ascertainment for PGx Study Cohort	57
2.4	Sample Processing	59
2.4.1	Small RNA Extraction from Plasma.....	59
2.4.2	DNase Treatment.....	61
2.4.3	Quality Assessment of Extracted RNA	62
2.4.4	Library Preparation.....	62
2.4.4.1	Ion Total RNA-Seq v2 Kit.....	64
2.4.4.1.1	Magnetic Bead Cleanup Module I	64
2.4.4.1.2	Hybridize and Ligate RNA	65
2.4.4.1.3	Reverse Transcription of RNA	66
2.4.4.1.4	Magnetic Bead Cleanup Module II - Purify and Size-Select cDNA.....	67
2.4.4.1.5	Amplify cDNA	68
2.4.4.1.6	Magnetic Bead Cleanup Module III - Purify the Amplified DNA.....	69
2.4.4.1.7	Assess the Yield and Size Distribution of the Amplified DNA	70
2.4.4.1.8	Pool and Dilute Small RNA Libraries for Template Preparation.....	72
2.4.4.2	Prepare Template for Sequencing.....	73
2.4.4.3	Hi-Q OneTouch2 200 Kit	73
2.4.4.3.1	Prepare Template-positive ISPs.....	73
2.4.4.3.2	Assess Quality of Unenriched, Template-positive ISPs.....	75
2.4.4.3.3	Enrich the Template-positive ISPs.....	76
2.4.4.4	Ion PI Hi-Q Sequencing 200 Kit.....	77
2.4.4.4.1	Prepare the Enriched Template-positive ISPs for Sequencing.....	77
2.4.4.4.2	Load the ION PI Chip v3	78
2.5	Grouping Patients by Clinical Response.....	79
2.6	PGx Patient Data Analyses.....	79

2.6.1	Comprehensive miRNA Analyses Pipeline	79
2.6.1.1	Read Pre-Processing	80
2.6.1.2	miRNA Variant Detection	82
2.6.1.3	Known and Novel miRNA Detection.....	82
2.6.1.4	Differential miRNA Expression Analyses of ACR50 Response Groupings and Clinical Data Sets.....	82
2.6.1.4.1	Gene Pathway Analyses Using Top-100 Differentially Expressed miRNAs	85
2.6.1.4.2	miRNA-mRNA Network Analyses and <i>in silico</i> Functional Analysis of Top 100 Differentially Expressed miRNAs.....	85
3	RESULTS	87
3.1	Optimization of Circulating miRNA Library Preparations	87
3.1.1	miRNA Library Preparation and Sequencing using the Thermo Fisher Protocol Modifications	90
3.1.1.1	Modified Thermo Fisher Protocol #1 (TF-Sample 1).....	90
3.1.1.2	Modified Thermo Fisher Protocol #2 (TF-Sample 2).....	92
3.1.1.3	Modified Thermo Fisher Protocol #3 (TF-Sample 3).....	95
3.1.1.4	Small RNA Control Sample	99
3.1.2	miRNA Library Preparation and Sequencing using the Cheng et al. Protocol Modifications	101
3.1.2.1	Modified Cheng et al. Protocol #1 (CH-Sample 1).....	101
3.2	Optimizing Chip Loading Capacity	104
3.2.1	CH-Sample 1B	104
3.2.2	CH-Sample 2A	105
3.2.3	CH-Sample 2B	106
3.2.4	CH-Sample 3A	107
3.2.5	CH-Sample 3B	108
3.2.6	CH-Sample 4.....	109
3.2.7	Chip Run Comparison.....	110
3.3	PGx PsA Cohort Library Preparation and Sequencing Results	111
3.4	Clinical Results and Response Groupings	113
3.5	Analyses of PGx Samples Using the Comprehensive miRNA Pipeline.....	114
3.5.1	Identified miRNA Variants and Identified Known and Novel miRNAs	117
3.5.2	Differential miRNA Expression between ACR50 Response Groupings	118
3.5.3	Differential miRNA Expression Incorporating Clinical Data	121
3.5.4	Pathway Analysis Using Top 100 Differentially Expressed miRNAs	123
3.5.5	Network Analysis/Predictive Binding of Top 100 Differentially Expressed miRNAs 127	
3.5.6	<i>In silico</i> Functional Analysis of Top Differentially Expressed miRNAs and Top Mutually Targeted Genes	135
4	DISCUSSION	137
4.1	Optimization of Circulating miRNA Library Preparations	138
4.1.1	Thermo Fisher Protocol Modifications	138
4.1.2	Cheng et al. Protocol Modifications.....	144

4.2	Preparing for Optimal Sequencing.....	145
4.2.1	Chip Loading Properties.....	145
4.2.2	Sequencing Quality of Samples under Different Loading Conditions	146
4.2.2.1	Samples that Sequenced Best at 7@8pM.....	147
4.2.2.2	Samples that Sequenced Best at 6@6pM.....	148
4.2.2.3	Trend Between Library Quality and Chip Loading Conditions.....	149
4.3	Clinical Information and Response Grouping.....	149
4.4	Data Analyses.....	151
4.4.1	miRNA Variant and Novel miRNAs Analyses	152
4.4.2	Differential miRNA Expression Analyses.....	153
4.4.2.1	Differential miRNA Expression Analyses of ACR50 Response Groupings .	154
4.4.2.2	Differential miRNA Expression Analyses Incorporating Clinical Data	160
4.4.2.3	Pathway Analysis Using Top 100 Differentially Expressed miRNAs.....	161
4.4.2.4	miRNA-mRNA Network Analyses and an <i>in silico</i> Functional Analysis of Top 100 Differentially Expressed miRNAs.....	162
4.5	Clinical Relevance	165
4.6	Limitations	167
4.7	Summary and Conclusions.....	171
4.8	Future Directions.....	173
APPENDICES	196

LIST OF FIGURES

Figure 1.1 – Schematic of IL-12/23 and IL-17 signalling pathways, which are implicated in the pathogenesis of PsA.....	14
Figure 1.2 - Schematic of miRNAs being excised from a cell, where they are referred to as ‘circulating miRNA’.....	45
Figure 2.1 – Flow chart of study participant recruitment process.....	58
Figure 2.2 – Procedures involved in sample processing beginning with whole blood and ending with analysis of sequencing data.	59
Figure 2.3 – An electropherogram of a barcoded small RNA library.	71
Figure 2.4 - Schematic of cDNA fragments that do not have a miRNA inserted, which make up the ~85 bps adaptor dimer peak on the library-quantification electropherogram.	72
Figure 2.5 - Schematic of cDNA fragments that have a miRNA inserted, which make up the ~100 bps sample peak on the library-quantification electropherogram.....	72
Figure 2.6 – Flow chart of comprehensive miRNA analyses pipeline. See Figure 3.16 for in-depth analyses of differentially expressed miRNAs.....	81
Figure 3.1 – Overview of the modification performed for the optimization of the library preparation protocol.	88
Figure 3.2 – Flow chart depicting protocol modifications and subsequent results in TF-Sample 1.....	90
Figure 3.3 - Electropherogram depicting the size distribution and concentration of small RNA in the TF-Sample 1 library.	91
Figure 3.4 - Flow chart depicting protocol modifications and subsequent results in TF-Sample 2A and TF-Sample 2B.	92
Figure 3.5 - Electropherogram depicting the size distribution and concentration of small RNA in the TF-Sample 2A library.....	94
Figure 3.6 - Electropherogram depicting the size distribution and concentration of small RNA in the TF-Sample 2B library.....	94

Figure 3.7 - Flow chart depicting protocol modifications and subsequent results in TF-Sample 3A, TF-Sample 3A*, and TF-Sample 3B.....	96
Figure 3.8 - Electropherogram depicting the size distribution and concentration of small RNA in the TF-Sample 3A library.....	97
Figure 3.9 - Electropherogram depicting the size distribution and concentration of small RNA in the TF-Sample 3A* library.	98
Figure 3.10 - Electropherogram depicting the size distribution and concentration of small RNA in the TF-Sample 3B library.....	98
Figure 3.11 - Flow chart depicting protocol modifications and subsequent results in Sample SmRNACon.	99
Figure 3.12 - Electropherogram depicting the size distribution and concentration of small RNA in the Small RNA Control library.	100
Figure 3.13 - Flow chart depicting protocol modifications and subsequent results in CH-Sample 1.....	101
Figure 3.14 - Electropherogram depicting the size distribution and concentration of small RNA in the CH-Sample 1A library.....	103
Figure 3.15 - Electropherogram depicting the size distribution and concentration of small RNA in the CH-Sample 1B library.....	103
Figure 3.16 – Flow chart depicting the analyses performed using the comprehensive miRNA analyses pipeline.....	116
Figure 3.17 – Boxplot visualization of the distribution of normalized reads sequenced from each sample.....	118
Figure 3.18 - MDS plot of Fold change of miRNA expression between responders and non-responders.	119
Figure 3.19 – Network analysis of top 100 differentially expressed miRNAs, between responders and non-responders.	128
Figure 3.20 - Network analysis of top 100 differentially expressed miRNAs, relative to CDAI values at 1 month, and the collectively targeted genes.....	129
Figure 3.21 - Network analysis of top 100 differentially expressed miRNAs, relative to CDAI values at 3 months, and the collectively targeted genes.....	130

Figure 3.22 - Network analysis of top 100 differentially expressed miRNAs, relative to HAQ-DI values at 1 month, and the collectively targeted genes.....	131
Figure 3.23 - Network analysis of top 100 differentially expressed miRNAs, relative to HAQ-DI values at 3 months, and the collectively targeted genes.....	132
Figure 3.24 – Network analysis of top 100 differentially expressed miRNAs, relative to ESR values at 1 month, and the collectively targeted genes	133
Figure 3.25 – Network analysis of top 100 differentially expressed miRNAs, relative to ESR values at 3 months, and the collectively targeted genes.....	134
Figure 3.26 – An example of an in silico functional enrichment analysis of genes collectively targeted by the top differentially expressed miRNAs in responders.....	136
Figure 4.1 – Summary of RNA sequencing framework for the broader project that enables mRNA and intercellular miRNA sequencing and collective data analysis. Highlighted is the focus of this project.....	173
Figure B1 - Electropherogram depicting the size distribution and concentration of small RNA in the library of Patient 2.	197
Figure B2 - Electropherogram depicting the size distribution and concentration of small RNA in the library of Patient 6.	198
Figure B3 - Electropherogram depicting the size distribution and concentration of small RNA in the library of Patient 7.....	199
Figure B4 - Electropherogram depicting the size distribution and concentration of small RNA in the library of Patient 8.	200
Figure B5 - Electropherogram depicting the size distribution and concentration of small RNA in the library of Patient 10.....	201
Figure B6 - Electropherogram depicting the size distribution and concentration of small RNA in the library of Patient 11.	202
Figure B7 - Electropherogram depicting the size distribution and concentration of small RNA in the library of Patient 12.....	203
Figure B8 - Electropherogram depicting the size distribution and concentration of small RNA in the library of Patient 13.....	204
Figure B9 – Electropherogram depicting the size distribution and concentration of small RNA in the library of Patient 14.....	205

LIST OF TABLES

Table 1.1 - CIASsification of Psoriatic ARthritis (CASPAR).....	5
Table 1.2 - Typical regime for treatment of PsA.....	22
Table 2.1 - Sample ascertainment including biologic prescribed, date of blood drawn and date of biologic administration.....	58
Table 2.2 - Summary of variations and modifications between small RNA extraction protocols used during optimization.....	61
Table 2.3 - Summary of variations and modifications between library preparation protocols used during optimization.....	63
Table 3.1 - Library preparation and sequencing metrics with descriptions and desired range.....	89
Table 3.2 - Results of the library quantification of TF-Sample 1.....	91
Table 3.3 - Results of circulating miRNA sequencing of TF-Sample 1.....	92
Table 3.4 - Results of the library quantification of TF-Sample 2A and TF-Sample 2B.....	94
Table 3.5 - Results of sequencing TF-Sample 2A and TF-Sample 2B.....	95
Table 3.6 - Results of the library quantification of TF-Sample 3A, TF-Sample 3A*, and TF-Sample 3B.....	97
Table 3.7 – Results of sequencing TF-Sample 3A* and 3B.....	99
Table 3.8 - Results of the library quantification of Sample SmRNACon.....	100
Table 3.9 – Results of the library quantification of CH-Sample 1A and CH-Sample 1B.....	102
Table 3.10 – Results of sequencing CH-Sample 1A and CH-Sample 1B.....	104
Table 3.11 - Results of multiple sequencing runs of CH-Sample 1B, loaded at different molarities and/or loaded with different number of samples on the sequencing chip.....	105
Table 3.12 - Results of multiple sequencing run of CH-Sample 2A, loaded at different molarities and/or loaded with different number of samples on the sequencing chip.....	106

Table 3.13 - Results of multiple sequencing run of CH-Sample 2B, loaded at different molarities and/or loaded with different number of samples on the sequencing chip.....	107
Table 3.14 - Results of multiple sequencing run of CH-Sample 3A, loaded at different molarities and/or loaded with different number of samples on the sequencing chip.....	108
Table 3.15 - Results of multiple sequencing run of CH-Sample 3B, loaded at different molarities and/or loaded with different number of samples on the sequencing chip.....	109
Table 3.16 - Results of multiple sequencing run of CH-Sample 4, loaded at different molarities and/or loaded with different number of samples on the sequencing chip.....	110
Table 3.17 - Results of multiple sequencing runs with chips loaded at different molarities and/or loaded with different number of samples on the sequencing chip.....	111
Table 3.18 – Summary of library preparation and sequencing results the PGx patient samples. Bolded values are important library metrics for assessing quality of the prepared libraries.	112
Table 3.19 – Patient information including patient ID, the biologic the patient was prescribed, the patient’s age, and the patient’s sex.	113
Table 3.20 - Clinical values of HAQ-DI, CDAI, and ESR that were used to monitoring disease progression and treatment response.....	114
Table 3.21 - Clinical groupings of responders and non-responders to biologics treatment.	114
Table 3.22 - Summary of sequencing results used for the comprehensive miRNA pipeline.	115
Table 3.23 – Novel miRNAs identified in responders or non-responders.....	117
Table 3.24 - Differential expression analyses metric and descriptions.....	119
Table 3.25 – Top seven differentially expressed miRNAs between ACR50 response grouping, where no significance was reached after correcting for multiple testing.....	120
Table 3.26 – mRNA targets common to all of the top 100 differentially expressed miRNAs between ACR50 response grouping.....	120
Table 3.27 – Suggestively significant differentially expressed miRNAs associated with CDAI values at one-month post treatment with the statistically significant differentially expressed miRNAs incidated in the bordered cells.....	121

Table 3.28 - Statistically significant differentially expressed miRNAs associated with CDAI values at three-months post treatment.....	122
Table 3.29 - Statistically significant differentially expressed miRNAs associated with HAQ-DI values at one-month post treatment.....	122
Table 3.30 - Suggestively significant differentially expressed miRNAs associated with HAQ-DI values at three-months post treatment with the statistically significant differentially expressed miRNA incicated in the bordered cell.....	122
Table 3.31 – Suggestively significant differentially expressed miRNAs associated with ESR values at three-months post treatment with the statistically significant differentially expressed miRNAs incicated in the bordered cells.....	123
Table 3.32 - Differentially expressed miRNAs found to be associated with more than one analysis.	123
Table 3.33 – Pathway analysis metrics and descriptions.....	124
Table 3.34 – Top five pathways associated with differentially expressed miRNAs between clinical response groupings.....	124
Table 3.35 - Top five pathways associated with differentially expressed miRNAs relative to the CDAI1 dataset.....	125
Table 3.36 - Top five pathways associated with differentially expressed miRNAs relative to the CDAI3 dataset.....	125
Table 3.37 - Top five pathways associated with differentially expressed miRNAs relative to the HAQ-DI1 dataset.....	125
Table 3.38 - Top five pathways associated with differentially expressed miRNAs relative to the HAQ-DI3 dataset.....	126
Table 3.39 - Top five pathways associated with differentially expressed miRNAs relative to the ESR1 dataset.	126
Table 3.40 - Top five pathways associated with differentially expressed miRNAs relative to the ESR3 dataset.....	126
Table 4.1 – Trend in library concentration and chip loading capacity.....	147
Table 4.2 – The published literature related to drug response in identified differentially expressed miRNAs between ACR50 response groupings and in clinical datasets.....	156

Table 4.3 - The published literature pertaining to related disease pathogenesis in identified differentially expressed miRNAs identified between ACR50 response groupings and in clinical datasets.....158

ABBREVIATIONS

ACR	American College of Rheumatologist
ABCB1	Adenosine Triphosphate Binding Cassette Subfamily B Member 1
ABCC1	Adenosine Triphosphate Binding Cassette Subfamily C Member 1
ABCG2	Adenosine Triphosphate Binding Cassette Subfamily G Member 2
ACT1	Activator 1
ADCY6	Adenylate Cyclase 6
ADME	Absorption, Distribution, Metabolism, and Excretion
ADORA2A	Adenosine A2a Receptor
AGO2	Protein Argonaute-2
ANKHD1	Ankyrin Repeat and KH Domain-Containing Protein 1
AP-1	Activator Protein 1
AQP5	Aquaporin 5
AS	Ankylosing Spondylitis
ATIC	5-Aminoimidazole-4-Carboxamide Ribonucleotide Formyltransferase IMP Cyclohydrolase
BAM	Binary Alignment Map
BAX	B-Cell chronic lymphocytic leukemia Lymphoma 2-Associated X Protein
BCL2	B-Cell chronic lymphocytic leukemia Lymphoma 2
Bmp7	Bone Morphogenetic Protein 7
bp	Base Pairs
BTG3	B-Cell Translocation Gene 3
BTRC	Beta-Transducin Repeat Containing E3 Ubiquitin Protein Ligase
C/EBP	CCAAT Enhancer-Binding Protein
CARD15	Caspase Recruitment Domain-Containing Protein 15
CASPAR	Classification of Psoriatic Arthritis
CCL20	Chemokine (C-C Motif) Ligand 20
CCND1	Cyclin D1
CCNE1	Cyclin E1
CD4+	Cluster of Differentiation 4
CD8+	Cluster of Differentiation 8
CDAI	Clinical Disease Activity Index
cDNA	Complementary DNA
CELSR2	Cadherin, Epidermal growth factor Lymphocyte activation gene Seven-Pass G-Type Receptor 2
CH	Cheng et al.
ChIP-Seq	Chromatin Immunoprecipitation-Sequencing
CNOT6L	CCR4-NOT Transcription Complex Subunit 6-Like
CNV	Copy Number Variation
CXCL1	C-X-C Motif Chemokine Ligand 1

CYP	Cytochrome P450
DE	Differentially Expressed
DEFB4	Defensin Beta 4
DGCR8	Digeorge Syndrome Chromosomal (Or Critical) Region 8
DHFR	Dihydrofolate Reductase
DMARD	Disease Modifying Anti-Rheumatic Drug
DNA	Deoxyribonucleic Acid
ECM	Extracellular Matrix
EGFR	Epidermal growth factor receptor
EGR2	Early Growth Response 2
ELISA	Enzyme-Linked Immunosorbent Assay
EPC2	Enhancer of Polycomb Homolog 2
ERAP	Endoplasmic Reticulum Aminopeptidase
ERGIC2	Endoplasmic Reticulum-Golgi Intermediate Compartment Protein 2
ERK	Extracellular-Signal-Regulated Kinase
ES	Enrichment System
ESR	Erythrocyte Sedimentation Rate
EZH2	Enhancer of Zeste Homolog 2
EZR	Ezrin
FAS	Field Application Scientist
FBXL19	F-Box and Leucine Rich Repeat Protein 19
FCGR	Fc Gamma Receptor
FDA	Food and Drug Administration
FDR	False Discovery Rate
Fok1	Flavobacterium okeanokoites
FOXO1	Forkhead Box O1
GATK	Genome Analysis Toolkit
GO	Gene Ontology
GWAS	Genome-Wide Association Study
GZMB	Granzyme B
H ₂ O	Nuclease-Free Water
HAQ-DI	Health Assessment Questionnaire-Disability Index
HBD-2	Human Beta-Defensin-2
hg19	Human Genome Reference 19
HGS	Hepatocyte Growth Factor-Regulated Tyrosine Kinase Substrate
HLA	Human Leukocyte Antigen
hsa	Homo Sapien
HSP90B1	Heat Shock Protein 90 Beta Member 1
HTR1B	5-Hydroxytryptamine (Serotonin) Receptor 1B, G Protein-Coupled

IBD	Inflammatory Bowel Disease
IFN- α	Interferon Alfa
IFN- γ	Interferon Gamma
IL	Interleukin
IL1B	Interleukin 1 Beta
IRS1	Insulin Receptor Substrate 1
IRX5	Iroquois Homeobox 5
ISP	Ion Sphere Particle
Jak	Janus kinase
KEGG	Kyoto Encyclopedia of Genes And Genomes
KIR	Killer Immunoglobulin-Like Receptor
KIR2DS	Killer-Cell Immunoglobulin-Like Receptors 2DS
KRT16	Keratin, Type I Cytoskeletal 16
KRTAP3-2	Keratin Associated Protein 3-2
LCN2	Lipocalin 2
LogCPM	Log Counts Per Million
LogFC	Log of Fold Change
LR	Logarithm Ratio
Mag-Bead	Magnetic Bead Cleanup Module
MAPK	Mitogen-Activated Protein Kinase
M-CSF	Macrophage Colony-Stimulating Factor
MDA	Minimal Disease Activity
MDR1	Multidrug-Resistance P-Glycoprotein
MDS	Multi-Dimensional Scaling
MHC	Major Histocompatibility Complex
MICA	Major Histocompatibility Complex Class 1-Related Gene A
miRNA	Micro Ribonucleic Acid
MITF	Microphthalmia-Associated Transcription Factor
mRNA	Messenger Ribonucleic Acid
MTHFR	Methylenetetrahydrofolate Reductase
MTX	Methotrexate
MYB	V-Myb Avian Myeloblastosis Viral Oncogene Homolog
MYRIP	Myosin VIIA and Rab Interacting Protein
NAT2	N-Acetyltransferase 2
NF- κ B	Nuclear Factor Kappa-Light-Chain-Enhancer of Activated B Cells
NGF	Nerve Growth Factor
NGS	Next-Generation Sequencing
NK	Natural Killer
NF	Newfoundland

NME7	Nucleoside Diphosphate Kinase 7
nmol	Nanomole
NOTCH1	Neurogenic Locus Notch Homolog Protein 1
NSAID	Non-Steroidal Anti-Inflammatory Agents
nts	Nucleotides
ODF2	Outer Dense Fiber of Sperm Tails 2
OSCAR	Osteoclast-Associated Receptors
OT2	OneTouch™ 2 System
P2RX7	Purinergic Receptor P2X, Ligand-Gated Ion Channel, 7
PBMC	Peripheral Blood Mononucleocytes
PCR	Polymerase Chain Reaction
PGM	Personal Genome Machine
PGx	Pharmacogenomics
pM	Picomolar
pri-miRNA	Primary Micro Ribonucleic Acid
PRO	Patient Reported Outcomes
PS	Psoriasis
PsA	Psoriatic Arthritis
PSORS1	Psoriasis Susceptibility Loci 1
PTH LH	Parathyroid Hormone like Hormone
PTPN22	Protein Tyrosine Phosphatase, Non-Receptor Type 22
qPCR	Quantitative Polymerase Chain Reaction
RA	Rheumatoid Arthritis
RANKL	Receptor Activator of Nuclear Factor Kappa-B Ligand
RB1	Retinoblastoma-Associated Protein
RISC	Ribonucleic Acid -Induced Silencing Complex
RNA	Ribonucleic Acid
RNAi	Ribonucleic Acid Inactivation
rpm	Revolutions Per Minute
rRNA	Ribosomal Ribonucleic Acid
RT	Reverse Transcription
RUNX1T1	Runt-Related Transcription Factor 1; Translocated To, 1 (Cyclin D-Related)
RYK	Receptor-Like Tyrosine Kinase
S100A7	S100 Calcium Binding Protein A7
SLC19A1	Solute Carrier Family 19 Member 1
SLCO1C1	Solute Carrier Organic Anion Transporter Family Member 1c1
SNPs	Single Nucleotide Polymorphisms
SNV	Single Nucleotide Variation
SODD	Silencer of Death Domains

SpA	Spondyloarthritis
SPRY1	Sprouty RTK Signaling Antagonist 1
SSSCA1	Sjogren Syndrome/Scleroderma Autoantigen 1
STAT	Signal Transducer and Activator of Transcription
TAF4B	TATA-Box Binding Protein Associated Factor 4 Beta
Taq1	Thermus Aquaticus 1
TBC1D9	Tubulin Specific Chaperone Cofactor 1 Domain Family, Member 9
TF	Thermo Fisher
TFS™	Thermo Fisher Scientific™
TGF-β	Transforming Growth Factor Beta
Th	T-Helper
TLR	Toll-Like Receptor
TNFRSF	Tumor Necrosis Factor Receptor Superfamily
TNFα	Tumor Necrosis Factor Alpha
TNIP1	Tumor Necrosis Factor Alpha-Induced Protein 3-Interacting Protein 1
TRADD	Tumor Necrosis Factor Receptor Type 1-Associated Death Domain
TRAF	Tumor Necrosis Factor Receptor-Associated Factor
TRAF3IP2	Tumor Necrosis Factor Receptor-Associated Factor 3 Interacting Protein 2
TRAPPC8	Trafficking Protein Particle Complex Subunit 8
TRBP2	Trans-Activation Response Element RNA-Binding Protein
tRNA	Transfer Ribonucleic Acid
Tyk2	Tyrosine kinase
TYMS	Thymidylate Synthetase
UTR	Untranslated Region
UV	Ultraviolet
V	Volume of Distribution
VDR	Vitamin D Receptor
λ1	First-Degree Relatives
× g	Times Gravity
μl	Microliter
6@6pM	6 Libraries Loaded at 6pM Each
6@8pM	6 Libraries Loaded at 8pM Each
7@8pM	7 Libraries Loaded at 8pM Each
9@6pM	9 Libraries Loaded at 6pM Each

CHAPTER 1

1 INTRODUCTION

1.1 Psoriatic Arthritis and Clinical Features

Psoriatic arthritis (PsA) is a disease that causes joint pain, inflammation, and stiffness in patients with psoriasis (PS) (Gladman & Ritchlin, 2016). PS is defined as red, scaly, hardened epithelial tissue that ranges from minimal patches to generalized involvement (National Clinical Guideline Centre UK, 2012). The notion that PS and arthritis were not comorbidities but rather one disease was supported by concurrent relapse and remission (Lane & Crawford, 1937). Dermatologists noted that the atrophic arthritis occurred more frequently in PS patients, while rheumatologists noted that PS occurred more frequently in patients with atrophic arthritis than those with osteoarthritis (Wright, 1956).

The prevalence of PS is approximately 1.3-2.2% globally and is on average higher in Caucasian populations (National Clinical Guideline Centre UK, 2012). Within PS populations, arthritis occurs in approximately 30% of cases, resulting in a Psoriatic Arthritis prevalence of 0.3-1.0% in the general population (Eder, Haddad, Rosen, Lee, Chandran, Cook, & Gladman, 2016; Sankowski, Lebkowska, Cwikla, Walecka, & Walecki, 2013). PsA occurs at equal frequency in men and women. The frequency of PsA varies depending on the incidence of PS and environmental factors such as the ultraviolet (UV) indexes per annum (Sankowski et al., 2013).

The incidence of PS on the island of Newfoundland (NF) is double that of any other Caucasian population worldwide (Gulliver et al., 2011). This is due in part to NF's small founding population of 20,000-25,000 Irish and English settlers in 1760 (Zhai et al., 2016). The genetic isolation as well as the low UV indexes per annum contribute to the increased prevalence of PS in NF (Gulliver et al., 2011). Given that arthritis is developed by one third of PS patients it can be reasonably assumed that there is also an increased incidence of PsA in NF, although it has not been officially documented (Rahman & Elder, 2005).

1.1.1 Clinical Categorization of Psoriasis and Psoriatic Arthritis

There are several subcategories of PS: plaque PS, guttate PS, erythrodermic PS, flexural PS, seborrheic PS, and pustular PS. The most common form is chronic plaque PS (or PS Vulgaris) which occurs in 85-90% of patients (National Clinical Guideline Centre UK, 2012). Unless otherwise indicated, the term PS refers to plaque PS. Plaque PS often occurs in 'difficult to treat sites' and can impact function and mobility. Guttate PS is defined by small drop-shaped red spots that are acute, persist for approximately one month, and precede a streptococcal infection in ~60% of cases. Erythrodermic PS is a rare and aggressive form of PS involving the whole body. Flexural PS, which is often less scaly, is located at a point of flexion. Seborrheic PS, affects the scalp, face, and torso with flaky and itchy skin. Pustular PS is distinctive by its "pus"-filled bumps and can be generalized or localized. Multiple categories of PS can occur simultaneously or subsequently within the same individual (National Clinical Guideline Centre UK, 2012; Weger, 2010).

The arthritis associated with PsA is an inflammatory arthritis, as opposed to a degenerative arthritis such as osteoarthritis. The inflammation leads to swelling and often pain in the affected joints. Due to its inflammatory nature, PsA is associated with morning stiffness that improves with movement. PsA patients predominantly develop peripheral arthritis, which affects the large joints, but can also develop peri-arthritis, which affects the structures surrounding the joint, and spondylitis, which affects the spine. PsA often presents as oligoarthritis (less than five joints involved) and, as the disease progresses with time, a polyarticular subtype is more common (five or more joints involved). Spondylitis involves the sacroiliac joint, as well as cervical, thoracic or lumbar spine causing chronic pain, reduced flexibility of the spine, decreased chest expansion, and difficulty with cervical rotation (Gladman, 2015).

Dactylitis, commonly known as sausage finger, refers to the inflammation of an entire digit. In dactylitis, the inflammation targets not only the joints of the finger but also the tendon sheaths and the soft tissues. Dactylitis is observed in approximately 30% of patients at disease presentation and approximately 48% of patients during the course of the disease (Gladman, 2015). Enthesitis is the inflammation of the enthesial site, the point of insertion of a tendon or a ligament on the bone. Enthesitis is a symptom common to all spondyloarthropathies but is most frequently seen in PsA. Upon diagnosis, approximately 35% of patients present with enthesitis and approximately half the patients with PsA will develop it over the course of their disease. Nail involvement is a risk factor for the manifestation of PsA and is a good indicator that PS patients may develop PsA. The nail lesions present as pits, hardening and thickening of the nail (hyperkeratosis), the separation

of the nail from the bed (onycholysis), and the crumbling of the nail bed. There is often a correlation between the nail involvement and inflammation the joint of the same finger (Gladman, 2015).

PsA falls within the disease category of seronegative spondyloarthropatheis (SpA). Other classical SpAs include Ankylosing Spondylitis (AS), arthritis that affects the spine; Inflammatory Bowel Disease (IBD), arthritis linked to IBD (i.e., enteropathic spondylitis); Reactive Arthritis, which is triggered by a bacterial infection; and Undifferentiated Spondyloarthropathies, arthritis that does not meet the classification criteria for the aforementioned conditions (Wright, 1978).

1.1.2 Comorbidities

There are numerous comorbidities associated with PsA, most of which relate to systemic inflammation and psycho-social factors. Conditions due to systemic inflammation cause increased insulin resistance, endothelial cell dysfunction, and the hardening of arteries, which affect multiple organ systems and lead to different clinical manifestations (Haddad & Zisman, 2017). Metabolic syndrome and diabetes mellitus are both independently correlated with PsA severity. PS is associated with an increased chance of developing cardiovascular disease, with similar trends documented for PsA (Haddad & Zisman, 2017). Other extra-articular immune-mediated comorbidities include IBD, Crohn's disease, and iritis. Psycho-social aspects involved with PsA such as depression, anxiety, and a lower quality of life. There is also a large financial burden on patients being

treated for their PS and PsA due to the high cost of pharmaceuticals, which can exacerbate psycho-social distresses (Haddad & Zisman, 2017).

1.1.3 Classification Criteria

The classification criteria for PsA was originally described by Wright and Moll in 1973 (Moll & Wright, 1973). Over the years many researchers have contributed to these criteria, as well as classifying subgroups (Gladman, 2015; Helliwell & Taylor, 2005; Torre Alonso, 2010). The criteria presently used for PsA was created by the CIASsification of Psoriatic Arthritis (CASPAR) study group. Upon examination by a rheumatologist, a PsA patient must receive ≥ 3 points in 5 classification criteria as described in **Table 1.1** (Carmona, 2012; Taylor et al., 2006).

Table 1.1 - CIASsification of Psoriatic ARthritis (CASPAR)

The CASPAR Classification Criteria for PsA		
Criterion	Description	Points
Current psoriasis and/or a personal or family history of psoriasis	Psoriasis currently present on skin or scalp as judged by a rheumatologist or dermatologist. A personal or family history of psoriasis (family history pertains to an affected first- or second-degree relative)	2 (current presentation) or 1 (personal or family history)
Observation of current psoriatic nail dystrophy	Onycholysis, nail pitting, or hyperkeratosis	1
Negative for rheumatoid factor	ELISA (enzyme-linked immunosorbent assay) or nephelometry	1
Current or history of dactylitis	Swelling of an entire digit, or a history of dactylitis recorded by a rheumatologist.	1
Radiographic indication of new bone formation	New bone formation near joint margins (but excluding osteophyte formation) on radiographic images of the hand or foot.	1

1.1.4 Monitoring Disease Progression and Response to Treatment

PsA disease activity, progression, and response to treatment can be monitored by a variety of criteria. Outline below are the American College of Rheumatologist Criteria (ACR), the Clinical Disease Activity Index (CDAI), Health Assessment Questionnaire-Disability Index (HAQ-DI), as well as a systemic marker of inflammation such as the Erythrocyte Sedimentation Rate (ESR) (Orbai & Ogdie, 2016).

1.1.4.1 American College of Rheumatologist Criteria

The ACR Criteria is the most well-recognized outcome measure for PsA treatment (Gladman et al., 2004). The ACR criteria dichotomously categorizes a patient as either a responder or a non-responder to treatment by the percentage of improvement between two time points. ACR20/50/70 is an equal to or greater than 20%/50%/70% improvement in disease activity, respectively. The ACR criteria, which is assessed recurrently during treatment, indicates improvement in swollen or tender joints. A joint count is taken based on at least three of the following measures: patient assessment, physician assessment, pain scale, disability/functional questionnaire (HAQ-DI), and/or acute phase reactant (erythrocyte sedimentation rate [ESR]) (PhUSE Wiki contributors, 2012).

1.1.4.2 Clinical Disease Activity Index

The Clinical Disease Activity Index (CDAI) is a validated score for Rheumatoid Arthritis (RA) that considers multiple factors including: a 28-point swollen joint count and a 28-point tender joint count (of the shoulders, elbows, wrists, metacarpophalangeal joints, proximal interphalangeal joints including thumb, and knees), a patient global disease

activity score (a self-assessment completed by the patient of overall disease activity on a scale of 1-10, 10 being the highest), and an evaluator's global disease activity score (a score assigned by the clinician of overall disease activity on a scale of 1- 10, 10 being the highest). The CDAI score is interpreted as "remission" if $CDAI \leq 2.8$, as "Low Disease Activity" if $CDAI > 2.8$ and ≤ 10 , as "Moderate Disease Activity" if $CDAI > 10$ and ≤ 22 , and as "High Disease Activity" if $CDAI > 22$ (Carmona, 2012). Given that the CDAI does not involve an acute phase reactant or any complex calculations, its can be measured relatively easily in clinic.

1.1.4.3 Health Assessment Questionnaire-Disability Index

The Health Assessment Questionnaire-Disability Index (HAQ-DI) is a measure of disease impact on quality of life, originally developed for monitoring disability of Rheumatoid Arthritis patients over time (Gunda, Syeda, & Jugl, 2015). The HAQ has been adapted for spondyloarthritis and for patients that have PS (Husted, Gladman, Long, & Farewell, 1995). The HAQ-DI assesses eight categories: dressing and grooming, arising, eating, walking, hygiene, reach, grip, and common daily activities. The patient self-reports the amount of difficulty they have performing the tasks in each category. Patients can rate their level of disease-caused disability for each category as "usual" (meaning the task is as easy as usual), "some" (meaning the task is performed with some difficulty), or "much" (meaning the task is performed with much difficulty) (Gunda et al., 2015).

1.1.4.4 Patient Reported Outcomes

Patient Reported Outcomes (PROs) are self-reports of health from the patient's own perspective. PROs are used to assess the patient's experience of symptoms, function, and their general quality of life. PROs include measures for pain, fatigue, sleep, and mobility (Orbai & Ogdie, 2016).

1.1.4.5 Minimal Disease Activity

Minimal Disease Activity (MDA) is a composite score commonly used for assessing low disease activity in patients with PsA. The MDA criteria evaluates articular disease, peri-articular disease, PS, and PROs. These aspects are measured by a tender and swollen joint count, enthesitis, PS activity (measured using body surface area affected and/or a severity index), a visual analogue scale for pain, a global disease activity, and a health assessment questionnaire. Five of seven aforementioned aspects must be considered in order to satisfy the criteria for MDA (Coates, Fransen, & Helliwell, 2010).

1.1.4.6 Erythrocyte Sedimentation Rate

Erythrocyte sediment rate (ESR) is a standard laboratory test that is used as a biomarker for inflammation and is the most traditional acute phase reactant. The ESR is a measure of red blood cell aggregation, determined by the distance travelled down a vibration-free, room-temperature vertical column over a one hour period and is expressed in mm/hr. A normal ESR for men is < 6.5 mm/hr and normal ESR for women is <16 mm/hr (Olshaker & Jerrard, 1997).

1.2 Pathogenesis of PsA

The pathogenesis of PsA has many contributing factors such as environmental influences and genetic components that prompt an immunological response. PsA can manifest due to environmental factors such as viral or bacterial infections and trauma. These triggers often precipitate PS, the effects of which can progress to include enthesial micro-damage leading to joint involvement (Roberts, J., O’Rielly, D.D., Rahman, P., 2017). Extensive evidence of PsA familial aggregation indicates a clear genetic component in the development of disease. Genetic associations of PsA are found primarily in human leukocyte antigen (HLA) alleles and others within the major histocompatibility complex (MHC) region. These genetic associations affect gene and subsequent protein expression, influencing pathways implicated in both innate and adaptive immune responses – specifically involving Cluster of Differentiation 8 positive (CD8+) T-lymphocytes and T-helper (Th)-17-lymphocyte signaling. Further insight has been gained in the Interleukin (IL)-23/Th-17 axis through gene and protein expression changes by treatment with IL-12/23 inhibitors, or more directly through IL-17A inhibitor. This has revealed the significance of the Th-17 signaling pathway in the pathogenesis of PsA (Roberts, J., O’Rielly, D.D., Rahman, P., 2017).

1.2.1 Pathogenesis at the Level of the Tissue

PsA manifests as inflammation at multiple sites and in multiple tissues, primarily the skin, synovium, entheses, and bone.

In the skin of PS patients, dendritic cells engulf foreign antigens and present them to T-cells, thereby activating them (Diani, Altomare, & Reali, 2015). It is widely hypothesized that infection or injury induces ‘danger signals’ triggering an autoimmune response, known as the Koebner phenomena (Barnas & Ritchlin, 2015). Models propose that dendritic cells (DC) sense stressed keratinocytes and invading microorganisms, and respond by excreting cytokines and chemokines (Diani et al., 2015). These signalling molecules bind to the antibacterial peptide LL37; that complex then binds to and activates the TLR-9 on plasmacytoid DC. TLR-9 activation leads the plasmacytoid DC to activate dermal DCs with IFN- α , which then migrates to lymph nodes. Within the lymph node, DCs produce IL-12 and IL-23, causing naive T-lymphocytes to differentiate into Th-1 and Th-17 cells that migrate back to the skin. In the dermis, Th-1 cells release IFN- α and Tumor Necrosis Factor Alpha (TNF α) and Th-17 cells release TNF α , IL-1, IL-17, and IL-22. The IL-22 release causes increased keratinocyte proliferation which leads to increased IL-1, IL-6 and TNF α release (Barnas & Ritchlin, 2015). TNF α promotes expression of adhesion molecules on endothelial cells and aids neutrophil migration (Diani et al., 2015). An abundance of neutrophils within the epidermis progress to form psoriatic plaques (Barnas & Ritchlin, 2015).

In the synovium of PsA patients, there is greater vascularity and lining-layer hyperplasia than other types of spondyloarthritis. Vascularization of the synovium is a known response to inflammation. Synovial hyperplasia can be explained by a higher proportion of CD8+ T-cells, which are cytotoxic, found in the tissue (Butt, 2009). In PsA synovial tissue, TNF α , IL-1B, IL-6, and IL-18 are found to have similar expression profiles

as seen in other spondyloarthropathies. Several studies have found that mast cells in the synovium of PsA patients express IL-17 (Barnas & Ritchlin, 2015).

PsA patients often have inflammation of the enthesis and the tissue structures surrounding it. A healthy enthesis organ dissipates mechanical stress and lacks vasculature. Mechanical stress or damage causes cells in the adjacent synovium to release inflammatory signals, which leads to the production of growth factors and cytokines. It is therefore thought that the inflammatory response in PsA originates in the enthesis. IL-23 receptor-expressing cells are present in the enthesial interface of tendons or ligaments. When IL-23 binds these cells there is increased production of IL-17A, IL-22, and Bmp7 – all of which are cytokines that perpetuate the inflammatory state (Barnas & Ritchlin, 2015).

In PsA patients, there is often a substantial amount of structural remodeling in the bone affecting skeletal joints. Disease-associated inflammation causes bone loss and new bone formation at the enthesial insertion. The altered bone remodeling can manifest: arthritis mutilans, eccentric bone erosions (particularly within the spine), and rapid new bone formation (Butt, 2009). The discovery of the IL-23/Th-17 axis provided new insight into the pathogenesis of bone remodeling in PsA. Inflammation causes an increase in circulating CD14⁺ cells, and a subset of these are triggered for differentiation into osteoclasts by M-CSF and RANKL. Osteoclastogenesis is also induced by TNF α , which induces upregulation of OSCAR on monocytes. Both RANKL and OSCAR activation send a secondary signal which leads to differentiation of monocyte to osteoclasts. Activated osteoclasts cause bone reabsorption and structural remodeling in the joint (Barnas & Ritchlin, 2015).

1.2.2 Pathogenesis at the Molecular Level

The molecular pathogenesis of PsA involves many inflammatory cytokines, primarily TNF α , IL-12/23, and IL-17.

1.2.2.1 TNF α

TNF α , which is also known as cachexin or cachectin, is a regulatory molecule of immune cells. TNF α can trigger apoptotic cell death, cachexia (wasting of the tissue), and inflammatory pathways. TNF α can be either membrane bound or soluble trimeric, either of which can bind the receptors TNFR1 and TNFR2. TNFR1 is expressed in most tissues, whereas TNFR2 is typically found in cells of the immune system. When the TNF α ligand binds either of these TNFRs, the receptor undergoes a conformational change. This change triggers the release of the inhibitory protein SODD which permits TRADD to bind the death domain. This binding activates three different pathways: NF- κ B, MAPK, and death signalling. In the nucleus, NF- κ B acts as a transcription factor for many proteins involved in cell survival, proliferation, inflammatory response, and anti-apoptotic factors. When the MAPK pathways are triggered it leads to cell differentiation, proliferation, and are generally pro-apoptotic. Death signalling pathways lead primarily to apoptosis (Gottlieb et al., 2005).

TNF α levels are increased in the synovial fluid and membranes in affected joints of PsA patients. Agents that target TNF α , such as etanercept, have been shown to improve the symptoms of PsA and TNF α levels (Mease, 2002). Both of these findings are evidence of the involvement of TNF α in the pathogenesis of PsA.

1.2.2.2 IL-12/23

The IL-12/23 pathway is highly complex and requires further investigation to clarify the exact mechanism of action in inflammation. What is currently known is that the IL-12 and IL-23 ligand bind together and activate a heterodimer receptor complex containing IL-12R that is paired with either IL-12RB or IL-23R. After the ligand binds the receptor, Jak2 and Tyk2 are activated. This activation, in turn, phosphorylates the STAT protein which dimerizes and undergoes nuclear translocation. Once in the nucleus, these STAT proteins cause transcriptional activation of target genes, which code for IL-17, IL-17F, and IL-23R as illustrated in **Figure 1.1** (Teng et al., 2015).

Both IL-12 and IL-23 are characterized as pro-inflammatory but they are also responsible for stimulating different immune responses. IL-12-induced signalling causes the differentiation of naive T-cells, proliferation and IFN- γ secretion by Natural Killer (NK) and T-cells, and increased cytotoxicity of NK cells and T-lymphocytes. IL-23-induced signalling stabilizes and maintains T-cells, increases memory T-cell activation and activates IL-17 mediated neutrophil recruitment at the site of trauma/infection (Teng et al., 2015). The IL-23/Th-17 axis has helped better elucidate the mechanism of PsA and all other spondyloarthropathies (Barnas & Ritchlin, 2015).

Genetic associations have been found between variations in genes coding for proteins involved in the IL-12/23 signalling pathway, suggesting a connection to PsA pathogenesis. There is overexpression of the IL-12 and IL-23 receptor subunits in psoriatic plaque and overexpression of IL-23 in the synovium of PsA patients. IL-12/23 inhibitors,

such as ustekinumab, have proven effective in relieving symptoms of PsA – providing further evidence of IL-12/23 signalling pathway involvement (Johnsson & McInnes, 2015).

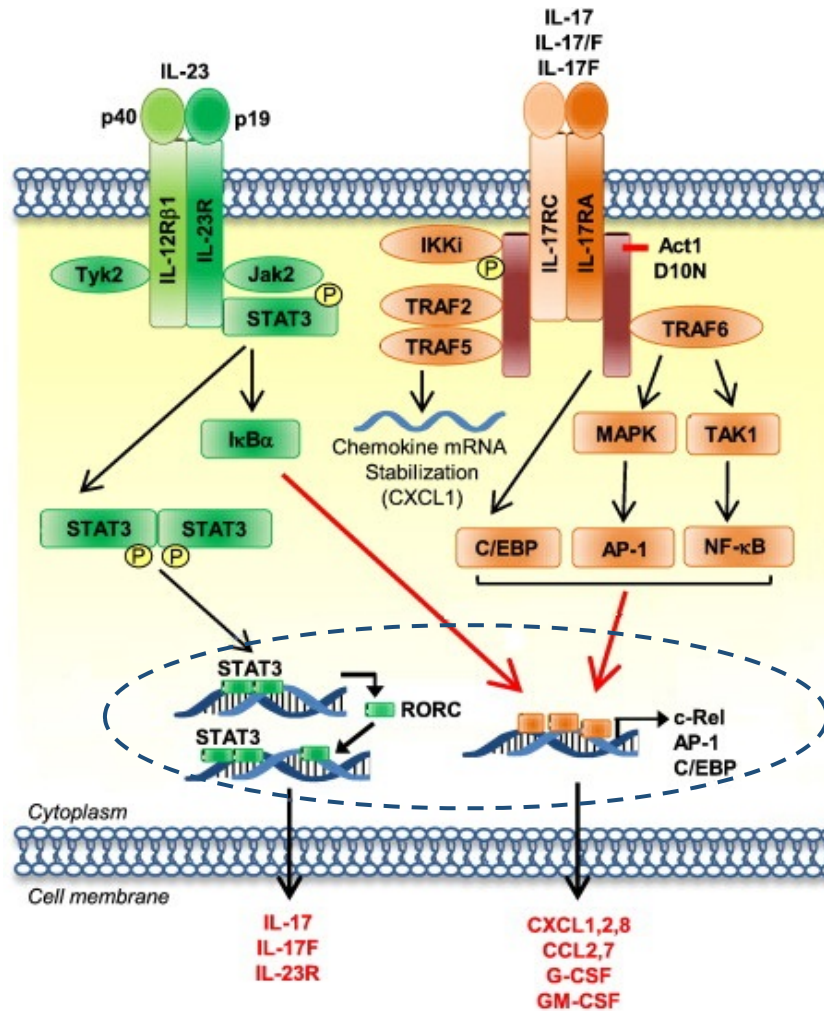


Figure 1.1 – Schematic of IL-12/23 and IL-17 signalling pathways, which are implicated in the pathogenesis of PsA. This figure was adapted with permission by Elsevier Publishing Company from (E. Suzuki, Mellins, Gershwin, Nestle, & Adamopoulos, 2014). **Appendix D** contains copyright permissions to use this figure.

1.2.2.3 IL-17

IL-17 is a pro-inflammatory cytokine produced by T-helper cells when induced by IL-23 (**Figure 1.1**). IL-17 acts synergistically with TNF α and IL-1 in promoting inflammation. When IL-17 signalling is redirected towards the host, autoimmune disorders develop. Signalling from IL-17 recruits monocytes and neutrophils to the site of inflammation (Miossec, 2017).

One of the six members of the IL-17 cytokine family binds an oligo-complex composed of various forms of the cell surface receptor IL-17R. Binding of these receptors leads to activation of the IL-17 cascade (Miossec, 2017). This cascade begins with the recruitment of ACT1 adaptor proteins. When ACT1 binds IL-17R, the recruitment of TRAF-6 and TRAF-3 occurs. ACT1 binding also activates intracellular kinases that interact and promote NF- κ B-dependent, AP-1-dependant, and C/EBP-dependent expression of cytokine and chemokines. Triggering the IL-17 cascade increases the production inflammatory proteins, such as TNF α , in cell types such as fibroblasts, endothelial cells, keratinocytes, and macrophages (Gaffen, Jain, Garg, & Cua, 2014).

Evidence that the IL-17 pathway contributes to the pathogenesis of PsA includes: IL-17 knockout animal models developing PsA, the increased expression of IL-17 positive T-cells in synovial fluid of PsA patients, the increased expression of IL-17R in synovial fibroblasts of PsA patients, and a decrease in disease activity in skin and joints seen with treatment IL-17 inhibitors (Raychaudhuri, Saxena, & Raychaudhuri, 2015).

When the TNF α , IL-12/23, and IL-17 signalling pathways are triggered concurrently with other pathways in the innate autoimmune response, an over production of inflammatory cytokines occurs. These cytokines promote an adaptive immune response, leading to the differentiation of T-lymphocytes. T-lymphocytes can differentiate into either CD4+ or CD8+ cells. When triggered by cytokines/chemokines, CD4+ cells differentiate into many types of Th-cells, but those that pertain to PsA are Th-1, Th-17, and Th-22 cells. Th-1 cells increase the cellular response of the immune system by aiding in the activation of CD8+ and NK cells. Th-17 cells play a large role in the pro-inflammatory arm of the immune system and are often associated with the pathogenesis of autoimmunity. These differentiated Th-cells release additional cytokines and chemokines triggering positive feedback in the signalling pathway of destructive autoimmunity in the skin, synovium, entheses, bones, digits, and nails (Barnas & Ritchlin, 2015).

1.3 Genetics of PsA

1.3.1 Heritability of PS and PsA

PsA is a complex disease that manifests due to genetic and environmental contributing factors. Heritability is often estimated through recurrence rate within family members of affected individuals and the rate of concordance in twins.

Both PsA and PS are highly heritable diseases and therefore there is an increased prevalence within families. The prevalence of PsA in first-degree relatives of PsA patients is 5.5%. First-degree relatives of PsA patients were found to have a 19-fold increase in

prevalence of PS (Rahman & Elder, 2005). Familial aggregations indicate heritability in both PsA and PS, classifying them as genetic disorders.

Strong heritability in PS and PsA is evident, with a recurrence risk ratio in first-degree relatives (λ_1) of ~ 8 (Pedersen, Svendsen, Ejstrup, Skytthe, & Junker, 2008). As well, there is a more than a 30-fold increase in the risk of developing PsA among the first-degree relatives of PS probands (Chandran, 2013). Familial aggregation of different types of SpAs present in individuals of the same kinship (Dougados & Baeten, 2011).

The rate of concordance amongst monozygotic and dizygotic twins can indicate the genetic and environmental contributions to disease. The rate of concordance of PsA in monozygotic twins is between 35-72% and between 12-23% for dizygotic twins. The incidence of PsA is approximately three-times higher in identical twins, indicating a strong genetic contribution in the development of the disease (Chandran et al., 2009). Because PsA is a multifactorial disease, there are also known environmental factors involving gut flora, infection, and smoking that impact the manifestation of PsA (Dougados & Baeten, 2011).

1.3.2 Genetic Contributions to PsA within the MHC locus

Linkage and associations studies on the genetics of PsA have been performed less frequently than with PS due to the decreased prevalence of PsA. In linkage studies, the most consistently observed genetic contribution to the development of PsA is located on chromosome 6p21.3, the MHC. Genetic variants in this region are, for the most part, class I HLA alleles and some are non-HLA MHC genes. (O'Rielly & Rahman, 2014) Nair et al.

determined that the *PSORS1* gene is actually the *HLA-Cw*0602* allele which has a strong association to PsA. (Nair et al., 2006)

Linkage studies have found that *HLA-B27* is associated with all spondyloarthropathies. With regard to PsA, *HLA-B27* is particularly associated with spondylitis and dactylitis (Gladman, Anhorn, Schachter, & Mervart, 1986; Gladman, Ziouzina, Thavaneswaran, & Chandran, 2013). HLA-antigens such as B38 and B39 are associated with peripheral polyarthritis (Gladman et al., 1986). Chandran et al. (2013) found that *HLA-C12/B38*, *HLA-B27*, and *HLA-C06/B57* haplotypes and alleles show the strongest association with PsA in a case-control and family-based study (Chandran et al., 2013). Disease progression has also been found to be associated with *HLA-B39*, with the presence of both *HLA-B27* and *HLA-DR7*, and with *HLA-DQw3* in the absence of *HLA-DR7* and *HLA Cw0602* (Ellinghaus et al., 2012).

There is mounting evidence for two associations between PsA and non-HLA genes within the MHC region (Al-Heresh et al., 2002; S. Gonzalez et al., 2002; Hohler et al., 2002). Polymorphisms in the promoter region of the *TNF α* gene, single nucleotide polymorphisms (SNPs) at position -238, and a SNP at position -308 each have associations to PsA in several Caucasian populations (Al-Heresh et al., 2002; S. Gonzalez et al., 2002; Hohler et al., 2002). The SNP at -308 has been found to be specifically associated with erosive changes in the PsA of affected individuals (Balding et al., 2003). Also within the *TNF α* gene, an association has been found between a SNP located at -857 and PsA; however, no association with PS has been found (Reich et al., 2007).

The second non-HLA association within the MHC is to *MICA*. An association has been found between a triple microsatellite repeat in exon 5 of the *MICA* gene and various immunological disorders such as RA, AS, and Bechet's Disease. The *MICA* gene is in extensive linkage disequilibrium with PsA-associated *HLA* alleles, establishing a weak association (Gao et al., 2006; Lucas et al., 2008; Ribas, Oliveira, Petzl-Erler, & Bicalho, 2008).

1.3.3 Genetic Contributions to PsA outside the MHC locus

Only a few studies have identified genetic contributions from outside the MHC to the development of PsA. *KIR* genes have been investigated given that MHC class 1 molecules interact with this receptor and perpetuate PsA-associated inflammatory pathways (K. C. Hsu, Chida, Geraghty, & Dupont, 2002). Associations have been observed between the development of PsA with polymorphisms in *KIR2DS1* and *KIR2DS2* so long as the corresponding HLA ligand for the inhibitory receptors were not present; there have been similar findings in PS (Nelson et al., 2004; Y. Suzuki et al., 2004; Williams et al., 2005). An association with PsA was found to the *IL-1 α* 889C polymorphism, however this finding has not been successfully replicated (Peddle, Butt, Snelgrove, & Rahman, 2005). There is also evidence for an association with a variant in *PTPN22* and PsA; however, this association was not seen in PS (Bowes et al., 2015).

One linkage study, conditioned on paternal inheritance of PsA, identified a locus proximal to PSORS8 (16q) (Karason et al., 2003). Within the same study, *CARD15* was identified as a contributor to the disease. This finding was then replicated in a NF cohort

but has not been replicated in other cohorts (Karason et al., 2003; Rahman et al., 2003). An association was identified between the *ERAP1/2* genes. The association between a SNP in the *ERAP 2* gene was strongest in individuals who were *HLA-B27* negative. Contrarily, an association was also found between PsA patients who are *HLA-B27* positive and possess a SNP in *ERAP1* (Popa et al., 2016). Two polymorphisms in the promoter regions of *IL-6* and *IL1B* were found to be associated with the peripheral pattern of PsA and higher disease activity in the peripheral joints, respectively (Cubino et al., 2016). Most recently, an association was found with a rare coding allele in the *IFIH1* gene (Budu-Aggrey et al., 2017).

An association between *IL-2* and *IL-21* and PsA has been shown in a Genome Wide Association Study (GWAS) (Liu et al., 2008). GWASs that investigated PsA found some associations with genes outside of the MHC region. The strongest of these associations is with *IL-12B*, *IL-23R*, *TNIP1*, *TRAF3IP2*, *FBXL19*, and *REL* (Huffmeier et al., 2010; Liu et al., 2008; Stuart et al., 2010). A GWAS identified a strong association between PS and a haplotype in the *IL-23R* gene (Nair et al., 2008). This finding was also replicated in two studies defining the same association with PsA (Filer et al., 2008; Rahman et al., 2009).

1.4 Treatment of PS and PsA

The treatment regime for the management of PS symptoms includes topical treatments, traditional systemic agents, small molecule inhibitors, and biologic agents. Therapeutics are prescribed based on the severity and location of disease as well as relevant comorbidities. For mild PS affecting a small region, topical steroids are most commonly

recommended (Sutherland, Power, Rahman, & O'Rielly, 2016). Other topical management options include vitamin D analogs, tar, and retinoids (American Academy of Dermatology Work Group, 2011). PS that is moderate to severe is often treated with topical therapies in conjunction with phototherapy or oral systemic agents. Patients with severe PS are typically prescribed traditional oral systemic therapies such as retinoids, methotrexate (MTX), and cyclosporine. Should the patient's PS persist after these treatments, biologic agents are then considered (Sutherland et al., 2016). Generally biologics have better treatment efficacy than oral systemic agents. The three most commonly prescribed types of biologics for PS include anti-TNF α agents (i.e., adalimumab, etanercept, and infliximab), anti-IL-17 agents (i.e., secukinumab), and anti-IL-12/23 agents (i.e., ustekinumab) (American Academy of Dermatology Work Group, 2011).

PsA is treated by a regime of Non-Steroidal Anti-Inflammatory Drugs (NSAIDs), traditional systemic agents, Disease Modifying Anti-Rheumatic Drugs (DMARDs), and biologic agents (**Table 1.2**). The aim of treatment is to reduce stiffness, limit pain, and increase mobility and function. First-line treatment for PsA is the use of NSAIDs. If symptoms persist, systemic agents such as MTX and leflunomide are then considered. Sulfasalazine, another systemic agent, is less frequently prescribed due to its inefficacy relative to other treatment options. An orally administered phosphodiesterase-4 inhibitor, Apremilast, has recently been approved in North America. As with PS, biologic agents are more effective than oral systemic agents in the management of PsA (Sutherland et al., 2016). Three types of biologic agents have been deemed appropriate for the management of PsA: anti-TNF α agents (i.e., adalimumab, certolizumab, etanercept, golimumab, and

infliximab), anti-interleukin-12/23 agents (i.e., ustekinumab), and anti-IL-17 agents (secukinumab) (McInnes et al., 2017).

Table 1.2 – Typical regime for treatment of PsA.

Treatment Regime for PsA Patients	
Topical Agents	Corticosteroids
	Vitamin D3 Analogues
	Topical Retinoids
	Anthralin and Tars
	Phototherapy
Traditional Oral Agents	Oral Retinoids
	Non-Steroidal Anti-inflammatory Agents
	Methotrexate
	Cyclosporine
	Leflunomide
	Sulphasalazine
Small Molecule Inhibitor Agents	Apremilast
Biologic Agents	TNF α inhibitors
	IL-12/IL-23 inhibitors
	IL-17 inhibitors

Despite a range of options, there is great variability in patient response to the treatment regime for PS and PsA, with a high percentage of patients experiencing non-response and adverse events while undergoing therapy (Sutherland et al., 2016).

1.4.1 Topical Agents for the Treatment of PS

Topical agents prescribed for PS are corticosteroids, vitamin D₃ analogues, topical retinoids, anthralin and tars, as well as phototherapy. The most commonly used topical

treatment of PS symptoms for the past 50 years has been corticosteroids. These high-potency topical steroid treatments, are considered to be most efficacious, followed by vitamin D₃ analogues. The most commonly prescribed vitamin D₃ analogues is calcipotriol. Calcipotriol simulates calcitriol, the active form of vitamin D₃ that is naturally produced by the body, which decreases redness, scaling, itchiness, and plaque elevation in psoriatic skin. Tazarotene is a commonly prescribed topical retinoid to treat PS. The proposed mechanism of tazarotene is through modulating the proliferation and differentiation of keratinocytes. Anthralin is another topical treatment for PS that has anti-proliferative and anti-inflammatory effects. Tar therapy is one of the original methods of PS treatment; however, currently it is less commonly prescribed (Canadian Psoriasis Guidelines Addendum Committee, 2016). Controlled exposure to UV light is a widely utilized and well-established PS therapy (Menter et al., 2008). UV light is administered based on the complexion of the patient as well as the location and intensity of symptoms (Canadian Psoriasis Guidelines Addendum Committee, 2016).

1.4.2 Oral Agents for the Treatment of PS and PsA

Oral agents prescribed to treat PS and/or PsA include oral retinoids, NSAIDs, and DMARDs – such as methotrexate, cyclosporine, leflunomide, and sulphasalazine.

Acitretin is the only oral retinoid that is currently prescribed in Canada to treat PS. There are severe restrictions on the use of this pharmaceutical because of its teratogenic potential, and is therefore contraindicated for women of childbearing age. The therapeutic capability of acitretin is realized in combination with topical calcipotriol (Canadian

Psoriasis Guidelines Addendum Committee, 2016). NSAIDs are a first-line treatment for a wide range of symptoms in PsA patients. NSAIDs are proven effective in treating peripheral arthritis, axial involvement, enthesitis, and dactylitis (Ritchlin et al., 2009).

Pharmaceutical agents that act systemically by modifying immune response are referred to as traditional systemic agents (Sutherland et al., 2016). These systemic agents, otherwise known as DMARDs, include MTX and cyclosporine for PS treatment and include MTX, leflunomide, and sulphasalazine for PsA treatment (Canadian Psoriasis Guidelines Addendum Committee, 2016).

MTX is a first-line systemic agent prescribed to treat moderate to severe PS and PsA (Sutherland et al., 2016). MTX promotes the release of adenosine which subsequently suppresses inflammation (Puig, 2014). MTX has proven to be effective in suppressing the cutaneous and articular manifestations of the disease. There are some adverse events associated with MTX, mainly hepatotoxicity, leading to one third of patients discontinuing the therapy (Sutherland et al., 2016).

Cyclosporine is a DMARD that suppresses the immune system by inhibiting calcineurin. Calcineurin inhibition impedes B-cell activation and T-cell proliferation by blocking the inflammatory signalling cascade. Cyclosporine has proven effective in treating PS and marginally effective in treating PsA, therefore it is rarely prescribed by rheumatologists. Patient response to cyclosporine varies significantly due to differential intestinal absorption rates (Sutherland et al., 2016). Leflunomide is an immunosuppressant that inhibits the activation and proliferation of T-cells by inhibiting pyrimidine synthesis (Kaltwasser, 2007). Leflunomide has proven to be effective in suppressing the cutaneous

and articular manifestations of the disease (Ritchlin et al., 2009). Leflunomide has a high response rate and a favourable safety profile (Kaltwasser, 2007). Sulphasalazine is moderately effective in improving the symptoms of peripheral synovitis in PsA, and to a greater extent improving cutaneous and peripheral articular features (Ritchlin et al., 2009; Sutherland et al., 2016).

1.4.3 Small Molecule Inhibitors

Cells that regulate immune response highly express small molecules, such as phosphodiesterase 4. Apremilast is an orally administered small molecule inhibitor that is approved for treatment of PS and PsA. Inhibiting phosphodiesterase 4 can suppress immune response and regulate autoimmunity. Apremilast has proven to be efficient in treating both PsA and moderate-to-severe PS (Deeks, 2015).

1.4.4 Biologic agents

Biologics are a relatively new class of pharmaceuticals which are manufactured from biological sources or processes. Because biologics are not synthesized, like in the manufacturing processes of other pharmaceuticals, they are much more costly to produce (Rader, 2008). The high cost associated with production and inflation on pharmaceuticals have resulted in biologics costing between \$380 and \$4500 per treatment resulting in an annual cost of between \$17,000 and \$31,200 (Ustekinumab Injection, 2016). Biologics target different inflammatory pathways involved in autoimmune reaction and have proven to be efficacious in the treatment of PS and PsA (Rader, 2008). Biologic agents such as TNF α , IL-12/23, and IL-17 inhibitors are increasingly being prescribed to treat moderate-

to-severe PS or PsA in patients who do not respond to traditional systemic therapies (Sutherland et al., 2016).

1.4.4.1 TNF α Inhibitors

There are five anti-TNF α agents prescribed for the treatment of PsA: etanercept, a recombinant human TNF α receptor protein; infliximab, a human-mouse chimeric anti-TNF α monoclonal antibody; adalimumab, a fully human anti-TNF α monoclonal antibody; certoluzimab, a (mouse-human) chimeric monoclonal antibody; and golimumab, a human monoclonal antibody (Canadian Psoriasis Guidelines Addendum Committee, 2016). It is common for PsA patients to be prescribed biologics as monotherapies, or in combination with traditional systemic agents (Sutherland et al., 2016).

TNF α inhibitors act by binding either free-floating TNF α cytokines or by binding the TNF α cell surface receptors thereby inhibiting the inflammatory signalling cascades that cause autoimmunity. With regards to cutaneous symptoms, TNF α binds to the surface of pro-inflammatory leukocytes, including neutrophils, monocytes, and activated T-cells, triggering the production of inflammatory chemokines which in turn perpetuates inflammation in that region (Koch, 2005). Arthritic symptoms are improved with TNF α inhibitors by decreasing bone loss and by improving osteoblast function and differentiation (Gilbert et al., 2000). In both serum and lesioned skin, TNF α levels return to normal in patients who respond to TNF α inhibitor treatment. The decrease in TNF α levels is proportional to the decrease in cutaneous and articular symptoms (Mizutani, Ohmoto, Mizutani, Murata, & Shimizu, 1997). Consistent with these clinical findings are patient-

reported outcomes indicating significant improvement in function and quality of life after treatment with TNF α inhibitors (Carron et al., 2017).

1.4.4.2 IL-12/IL-23 Inhibitors

The inflammatory cytokines IL-12 and IL-23 are known to play a role in the pathogenesis of PS and PsA (Lopez-Ferrer, Laiz, & Puig, 2017). Ustekinumab is a human monoclonal antibody that has demonstrated high efficacy in targeting IL-12/IL-23 inflammatory pathways by binding the IL-12/23 cell surface receptor (Krueger et al., 2007). Ustekinumab has proven efficacious in treating moderate-to-severe PS and is regarded as efficacious for treating PsA. Similar response profiles were observed in PS and PsA patients taking ustekinumab, with a patient response rate of approximately 50% (Lopez-Ferrer et al., 2017). There are minimal adverse events associated with ustekinumab treatment, though side effects include headache, abdominal pain, and infection (Chien, Elder, & Ellis, 2009).

Although proven effective in treating PsA, ustekinumab has shown to be effective in treating cutaneous symptoms more so than in articular disease (Johnsson & McInnes, 2015). Symptoms of PsA, such as enthesitis, dactylitis, spondylitis, and nail involvement have shown to improve with IL-12/23 treatment (Johnsson & McInnes, 2015; Pasch, 2016). Similarly, significant improvements have been documented through patient-reported outcomes by those undergoing treatment with ustekinumab (Rahman et al., 2016).

1.4.4.3 IL-17 Inhibitors

The inflammatory cytokine IL-17 has a known association with the pathogenesis of PS and PsA through the IL-23/Th-17 axis. Secukinumab and ixekizumab are both biologic agents that target the IL-17 signalling pathways by binding the IL-17 cell surface receptor (McInnes et al., 2015; Leonardi et al., 2012).

Secukinumab is an anti-IL-17A human monoclonal antibody that functions by inhibiting the IL-17 inflammatory pathway. Secukinumab is approved worldwide for treating PS and has recently been approved for the treating PsA. The IL-17A and the IL-17A receptors, which are expressed in the synovium and mediate enthesial inflammation, are inhibited by secukinumab; this results in a decrease in both joint damage and tissue remodeling (McInnes et al., 2015). An overall reduction of periarticular features, such as enthesitis and dactylitis, has been frequently seen with secukinumab treatment (Gladman & Ritchlin, 2016). Secukinumab has also proven efficacious in treating nail and skin features associated with PsA (Mease & McInnes, 2016). Consistent with these clinical findings are patient-reported outcomes indicating significant improvement in function and quality of life after secukinumab treatment (Mease et al., 2015). Adverse events associated with secukinumab treatment include upper-respiratory infections and nasopharyngitis. Response rates to secukinumab are similar to those of other biologics prescribed for PS and PsA treatment. Response rates were higher in patients who were naive to anti-TNF α and not being treated concomitantly with MTX (McInnes et al., 2015).

Ixekizumab is a humanized monoclonal antibody used to treat PS and PsA by inhibiting IL-17A (Leonardi et al., 2012). Ixekizumab is prescribed to patients with PsA

and moderate-to-severe PS. Cutaneous and articular features have shown improvement with Ixekizumab treatment (Gladman & Ritchlin, 2016). Consistent with these clinical findings are patient-reported outcomes indicating significant improvement in function and quality of life after ixekizumab treatment (Edson-Heredia et al., 2016). Up to 40% of patients treated with ixekizumab show partial or complete disease remission of their skin disease. As with other biologics, some patients treated with ixekizumab experienced increased rate of infection, reaction at the site of infection, upper-respiratory tract infection, as well as pain and inflammation of the oropharyngeal region (Nash et al., 2017).

1.5 Prediction of Treatment Response

There are many biological traits that are associated with predicting response to treatment. Prediction of treatment response is typically examined through four main approaches: pharmacokinetics, pharmacodynamics, pharmacogenetics, and pharmacogenomics. The known associations between these fields and PsA are outlined below.

1.5.1 Pharmacokinetics

Pharmacokinetics is the impact that the body has on an administered pharmaceutical. There are four main mechanisms involved in the study of pharmacokinetics: absorption, distribution, metabolism, and excretion (ADME). Relating to all of these variables is the concept of drug clearance, which is the elimination of a pharmaceutical from the body. Clearance estimates over time produce either a linear or nonlinear pharmacokinetic model.

A linear pharmacokinetic model is limited by the half-life of the pharmaceutical assuming it will remain consistent regardless of its concentration with one bolus administration distributed instantaneously. A nonlinear pharmacokinetic model is limited by the saturation of one pharmacokinetic aspect, such as a major metabolic pathway (Ratain & Plunkett, 2003).

Interpatient pharmacokinetic variability is dependent on differential ADME rates. Absorption of pharmaceuticals is dependent of factors such as gastrointestinal and renal tubular function. The drug absorption percentage can be discussed in the context of bioavailability. Bioavailability is determined in part by liver function and in part by drug metabolism rates in the gastrointestinal tract. Pharmaceutical distribution rates vary based on body size and fat percentage, while irregular drug distribution will decrease clearance rates. Excretion rates, which are highly variable between patients and difficult to predict, are impacted by liver function (metabolism) and renal function (clearance) (Ratain & Plunkett, 2003).

When determining dosage levels in clinic, multiple patient characteristics must be considered. Age, sex, body fat, blood flow, and organ function are key traits in pharmacokinetics. With advanced age there is a decrease in many regulatory and functional processes within the cell (Ratain & Plunkett, 2003). The decrease in general cellular activity results in a reduction in metabolic rate/gastrointestinal absorption as well as in hepatic and renal clearance potential (Mangoni & Jackson, 2004). Sex has a social and biological influence on pharmacokinetics. In general, there has been fewer investigations into pharmacokinetics in females. These discrepancies should be addressed as studies have

indicated that women have worse safety profiles, with increased incidence and severity of adverse events (Franconi & Campesi, 2014). Body fat percentage plays a large role in pharmacokinetics due to its contribution to total mass and influence on the metabolism of lipophilic drugs. Each of the aforementioned characteristics affect organ function and subsequent pharmacokinetics, especially within the gastrointestinal tract, the liver, and the kidneys (Ratain & Plunkett, 2003).

When treating PsA with biologics (TNF α , IL-12/23, or IL-17 inhibitors) the pharmacokinetic properties that contribute to inter-patient variability include: slow clearance, long half-lives, and limited tissue distribution. The intramuscular injections of biologics involve slow absorption, with maximal plasma concentrations recorded for approximately 1-8 days post treatment. The distribution of biologic agents is limited by fluid circulation from blood into interstitial spaces, diffusion of the drug across a tissue, pinocytosis (invagination of extra-cellular fluid into a cell), and receptor-mediated endocytosis. Excretion of biologics is challenging because they are too large to undergo glomerular filtration. Biologics are therefore metabolized and primarily eliminated by catabolism of the protein into its amino acid subunits, which are then reused for the synthesis of new proteins (Kamath, 2016).

1.5.2 Pharmacodynamics

Pharmacodynamics relates to the impact that an administered pharmaceutical has on the body. In clinical trials pharmacodynamic investigations examine the relationship between dose and response to determine the maximally tolerated dosage and dose-limiting

toxicities in patients. Interpatient variation in dosage-to-toxicity can be attributed to two factors: differential pharmacokinetic characteristics and/or heightened sensitivity to certain pharmaceuticals. Establishing which pharmacodynamic factor is contributing to excessive toxicity must be determined before dosage is adjusted (Ratain & Plunkett, 2003).

To quantify a drug's pharmacodynamics properties, the maximal effect and the median dose (dosage necessary for 50% of the maximal effect) must be established. When establishing these pharmacodynamic quantifications, it is important to consider that the impact of a pharmaceutical is dependent on its interaction with a cell-surface receptor. Based on this, pharmaceutical exposure can be saturable or nonsaturable, producing either a sigmoidal or linear pharmacodynamic plot, respectively (Ratain & Plunkett, 2003).

When treating PsA with biologics the pharmacodynamics properties of TNF α , IL-12/23, and IL-17 inhibitors that contribute to inter-patient variability include: the ligand-receptor interaction after binding of drug, the reduction of target cells by the down-regulation of target antigens, and the consequences on signalling pathways after blocking initiation receptors. Numerous factors can influence the pharmacodynamics of biologics, such as antigen expression levels, the affinity of the target antigen, the distribution of an antigen within a tissue and which tissues it is expressed. Other characteristics of biologics that contribute to inter-patient variability include their charge, hydrophobicity, and glycosylation (Kamath, 2016).

1.5.3 Pharmacogenetics and Pharmacogenomics

Pharmacogenetics is the study of how genetic variation affects differential response to pharmaceuticals. Pharmacogenetic investigations are undertaken with a hypothesis and use a targeted approach that examines regions of the genome associated with the pathogenesis of a disease or pharmaceutical metabolism. Pharmacogenomics, takes a broader approach, evaluating genome-wide variations that contribute to differential treatment response. Pharmacogenomic investigations are comprehensive evaluations that are “hypothesis-free” or “hypothesis generating”, which identify regions of the genome associated with pharmaceutical response. Those associations are then scrutinized by various “-omic” approaches to establish the impact of biological functions on response to treatment and determine possible causation (Sutherland et al., 2016).

Together, pharmacokinetic, pharmacodynamic, pharmacogenetic, and pharmacogenomic factors should be taken into consideration before a patient begins treatment with biologics. Studies investigating these factors in PsA treatments differ in number, scale, and statistical power. Often, associations found have not reached significance levels appropriate for clinical utility. Genetic variations involved in differential drug response can occur in the deoxyribonucleic acid (DNA), ribonucleic acid (RNA), and can be affected by epigenetic modifications that impact the regulation of gene expression.

1.5.3.1 DNA Variations in Precision Medicine

There are many types of DNA variations that affect gene expression and gene function, including single nucleotide variations (SNVs) and copy number variations

(CNVs). The most common DNA variations are SNVs, in which one nucleotide differs from the reference genome on one or both strands of DNA. SNVs differ from SNPs in that they have a minor allele frequency of >1%. CNVs are variations in the number of copies of a certain sequence that possess 95% homology in the repeated units and are less than 1000kb in length (Feuk, Carson, & Scherer, 2006).

The aforementioned DNA variations can be investigated for associations to interpatient variability to drug response within the disciplines of pharmacogenetics and pharmacogenomics. There are a number of methods used to investigate pharmacogenetic DNA variants. Genotyping assays and next-generation sequencing (NGS) technologies are the two main approaches to targeted pharmacogenetic studies. Genotyping assays such as polymerase chain reaction (PCR), Sanger Sequencing, and restriction fragment length polymorphism are simple and cost-efficient procedures. NGS technologies such as Illumina or Ion Torrent platforms are more complex and costly procedures for sequencing panels of targeted variants. Similarly, NGS technologies, which sequence whole-exome, transcriptome, and methylome, are used to comprehensively investigate pharmacogenomics to identify genetic variants. These approaches involve sequencing a patient's whole genome or whole exome (the coding regions of the genome) to identify associations with treatment response. Those associations are then investigated for causation.

1.5.3.2 DNA Variations Causing Differential Drug Response in Psoriatic Disease

Pharmacogenetic profiles of efficacy and toxicity have been compiled for patients undergoing treatment for PS and PsA. Genetic variations are primarily associated with pharmacokinetic and pharmacodynamic pathways. The DNA variations associated with response to topical treatments are found primarily within genes coding for vitamin D absorption. Variations that impact response to oral agent treatment are generally found in genes that code for drug-metabolizing enzymes, drug-transportation proteins, and cell-surface receptors. Variant associations to response to biologics have predominantly been found in the signalling pathways that these pharmaceuticals act on, such as TNF α , IL-12/23, and IL-17 (Sutherland et al., 2016).

1.5.3.2.1 Differential Response to Topical Agents in PS Patients

1.5.3.2.1.1 Vitamin D₃ Analogues

Pharmacogenetic variants associated with topical agents for the treatment of PS have been found primarily in genes involved in Vitamin D absorption. The *TaqI* polymorphic site in the vitamin D receptor (*VDR*) correlates with a decreased calcipotriol response in PS patients (Dayangac-Erden, Karaduman, & Erdem-Yurter, 2007). Contravening this finding, Hasall et al. demonstrated that the *VDR* polymorphism *TaqI*, A-1012G, and *FokI* are associated with an efficacious calcipotriol response (Halsall, Osborne, Pringle, & Hutchinson, 2005).

1.5.3.2.1.2 Phototherapy

The pharmacogenetics of phototherapy has yet to be systematically evaluated, although some studies have been completed. One study of PS patients found that the presence of an indel in the *GSTMI* was associated with an increased probability of achieving clearance of PS symptoms (Smith, Weidlich, Dawe, & Ibbotson, 2011). Ryan et al. determined that patients treated with narrow-band UVB therapy who possessed a certain genotype in *TaqI VDR* had a significantly reduced time to remission (Ryan, Renfro, Collins, Kirby, & Rogers, 2010).

1.5.3.2.2 Differential Response to Oral Agents in PS Patients

1.5.3.2.2.1 Non-Steroidal Anti-Inflammatory Drugs

It is known that NSAIDs are metabolized by cytochrome P450 enzymes, yet establishing pharmacogenetic profiles of response remains challenging (Jani, Barton, & Ho, 2015). When compared with PS patients possessing the *CYP2C9*1* allele (wildtype), those who have the *CYP2C9*2* and *CYP2C9*3* alleles were found to have reduced metabolic clearance of NSAIDs. Reduced clearance of these pharmaceuticals can lead to toxicity and must be considered when determining dosage (Martinez et al., 2004).

1.5.3.2.3 Differential Response to Traditional Systemic Agents in PS and PsA Patients

1.5.3.2.3.1 Methotrexate

Ample research has been done into polymorphisms associated with response to MTX treatment in PS patients. Polymorphisms associated with differential response can be categorized as effectors of MTX transport across the cell membrane (*ABCC1*, *ABCG2* and *SLC19A1*) and as effectors of enzymes involved signalling pathways and metabolism of MTX (*MTHFR*, *DHFR*, *TYMS*, *ATIC* and *ADORA2A*) (Ranganathan & McLeod, 2006).

Three variants in the *ABCC1* gene and two variants in the *ABCG2* gene are associated with PS patients who responded to MTX treatment (Warren et al., 2008). The presence of a, 28 base-pair, triplet tandem repeat in the 5' untranslated region (UTR) of *TYMS* was correlated with patients who failed to respond to MTX (Campalani et al., 2007).

Six variants in the *ABCC1* gene were found to be associated with PS patients who experienced at least one adverse event during MTX treatment. Additionally, a minor increase in the occurrence of MTX toxicity was observed in patients with a SNP in either *ADORA2A* or in *SLC19A1* (Warren et al., 2008). A deletion in the *TYMS* gene was also found to be associated with the occurrence of hepatotoxicity. Similarly, a variant in *ATIC* was found to be associated with a greater risk of side effects including nausea, elevated alanine, and aminotransferase (Campalani et al., 2007).

Research into the pharmacogenetics of MTX in PsA patients is not as extensive as those done for PS patients. Chandran et al. examined polymorphisms in genes in the folate pathway in relation to efficacy and toxicity of MTX in PsA patients (Chandran et al., 2010). They found variant in *DHFR* was associated with a significant increase in response to

MTX. Some evidence was found for a genotype in *MTHFR* that correlates to an increased incidence of hepatotoxicity (Chandran et al., 2010).

1.5.3.2.3.2 Cyclosporine

There is high inter-individual variability in PS patient response when treated with cyclosporine. This variable response is attributed hepatic levels of metabolizing cytochrome P450 (CYP)-3A isozymes (i.e., CYP3A4) and MDR1-ABCB1 (Naesens, Kuypers, & Sarwal, 2009). The CYP3 enzyme is known to influence oral bioavailability and systemic clearance of cyclosporine (O'Rielly & Rahman, 2011). One study showed a genotype in *ABCB1* was more common in non-responders when compared to responders (Vasilopoulos et al., 2014).

1.5.3.2.3.3 Sulphasalazine

There has been some studies done on the pharmacogenetics of sulphasalazine, the efficacy and toxicity of which is monitored by sulphapyridine serum levels. To be secreted via the kidneys, an acetate group is bound to sulphasalazine by NAT2 to form N-acetyl sulphasalazine (Das & Dubin, 1976). Inter-individual variability in the acetylation of sulphasalazine is correlated with differential plasma concentrations: patients who are rapid acetylators (i.e., efficient secretors) are less prone to adverse events and may require increased dosage to maintain efficacy (Wiese et al., 2014). *NAT2* has seven variants which have been positively correlated to sulphasalazine acetylation rates (Hein & Doll, 2012). Patients who are heterozygous for these variants are known to be either slow or

intermediate acetylators, while those who are homozygous for these variants are known to be either rapid or intermediate acetylators) (Davila & Ranganathan, 2015; Hein & Doll, 2012).

1.5.3.2.4 Differential Response to Biologic Agents in PS and PsA Patients

Research has been done in the pharmacogenetics of biologics therapy in PsA patients because this pharmaceutical class has a low response rate (~50%) and very high financial costs associated with treatment (between \$380 and \$4500 per treatment) (Ustekinumab Injection, 2016).

1.5.3.2.4.1 TNF α inhibitors

Two types of TNF α inhibitors are currently used to treat PsA: fusion-chimeric proteins (etanercept) and monoclonal antibodies (infliximab and adalimumab). There is high variability in PsA patient response to these biologics, with up to 40% of patients showing minimal-to-no disease remission. Due its low overall incidence, few pharmacogenetics studies have been done on PsA patients; however, many studies have been done on patients with PS. Often pharmacogenetic studies on biologics are often under-powered so it is common for research to group patients being treated with different TNF α inhibitors so that statistical significance can be achieved (Sutherland et al., 2016).

Studies on TNF α inhibitor-treated PS patients found variants in *TNF α* , *TNFRSF1A*, *TNFRSF1*, and *TNFRSF10A* lead to positive response to treatment (Vasilopoulos et al., 2012;Tejasvi et al., 2012;Gallo et al., 2013;Tong et al., 2013;Murdaca et al., 2014;Morales-Lara et al., 2012). Together these studies indicate the crucial role of genetic variation in

TNF α signalling-associated genes and response to TNF α inhibitors. In addition to these TNF α signalling-associated genetic variants, response to TNF α inhibitors is also affected by variants in genes associated with Th-17 signalling, such as *IL-23* and *IL-17*. Studies have found associations between positive response to treatment and variants in *IL-23R* and *IL-17F* (Gallo et al., 2013; Prieto-Perez et al., 2015).

Fc gamma receptors (FCGRs) are expressed on most immune cells and regulate functions such as cytokine release, apoptosis, and cytotoxicity. Associations have been found between the genes that code for these receptors and positive response to anti-TNF α therapy. Variants in genes such as *FCGR2A*, *FCGR3A*, *SLCO1C1* were found to be associated with a greater clearance of PS symptoms when treated with TNF α inhibitors (M. Julia et al., 2013; A. Julia et al., 2015; Ramirez et al., 2012).

1.5.3.2.4.2 IL-12/IL-23 inhibitors

Studies examining the pharmacogenetics of IL-12/23 inhibitors have primarily shown associations to HLA genes or genes in the IL-12/23 pathway. Numerous studies that have investigated the response to ustekinumab found the efficacy to be more frequent and more rapid in *HLA-Cw6*-positive patients (Chiu et al., 2014; Talamonti et al., 2013). A multi-parameter logistical regression analysis identified *HLA-Cw6* to be a more accurate indicator of positive response to ustekinumab if a variant in *IL-12B* was also present. Furthermore, *HLA-Cw6* proved to be a more accurate indicator of positive response to ustekinumab in the absence of variants in *IL12B* and/or the *IL-6* (Galluzzo et al., 2015). Prieto Perez et al. identified an association between a variant in *IL-17F* and patients who

did not respond to ustekinumab treatment (Prieto-Perez et al., 2015). This is in keeping with the established relationship between the IL-12/IL-23 signalling cascade and IL-17 genes.

1.5.3.2.4.3 IL-17 inhibitors

Thus far no published studies have investigated the pharmacogenetics of IL-17 inhibitors.

1.5.3.3 RNA Variations in Precision Medicine

1.5.3.3.1 messenger RNA

messenger RNAs (mRNAs) are genetic transcripts that code for proteins and are the mechanism by which genes are expressed. mRNA is transcribed from DNA by RNA polymerase II within the nucleus. After transcription is complete a 5' methyl-guanine cap and a 3' polyadenyline tail are added. Once processed the mRNA transcript is packaged with mRNA-binding proteins and exported into the cytoplasm. Once in the cytoplasm the mRNA transcripts are bound by either a ribosomal complex for translation or a microRNA (miRNA) complex for translational inhibition (Cole, 2001).

Pharmacogenetic and pharmacogenomic investigations of RNA variants are primarily done by microarray or sequencing. Targeted pharmacogenetics approaches involve panels of selected genes with known or suspected associations with treatment response, which are examined with DNA microarrays composed of probes that are complementary to mRNA transcripts (Katagiri & Glazebrook, 2009).

Transcriptomics is the comprehensive analysis of the all RNA transcripts in a sample. This type of investigations uses microarray or sequencing methods to identify associations with treatment response. These investigations examine all known mRNA transcripts to identify differential expression and attempt to determine causation.

1.5.3.3.2 microRNA

microRNAs (miRNAs) are 17-22nt sequences which act as a regulators of gene expression by binding mRNA transcripts and either suppressing or inhibiting their translation (Mi, Zhang, Zhang, & Huang, 2013). miRNA biogenesis begins when RNA polymerase II transcribes the miRNA-containing loci. This transcript forms one or more hairpin structures which are referred to as primary miRNA (pri-miRNA). The stem of the primary miRNA is then bound by DGCR8, which is then bound by DROSHA, thus making the microprocessor complex. This complex trims the transcript into a ~60-70nt precursor miRNA (pre-miRNA). EXPORTIN5 then exports the precursor miRNA into the cytoplasm and releases it. The precursor miRNA is then recognized by DICER. DICER binds TRBP2 and cleaves the stem loops of the hairpin, making a short double-stranded miRNA. The Argonaute 2 (AGO2) interacts with DICER causing it to release the bound miRNA. AGO2 then binds the double-stranded miRNA and releases one strand of the miRNA. The strand of miRNA that remains bound to AGO2 is referred to as the guide strand. When one miRNA strand is selected to be the guide strand more frequently than the other it is considered the “major product” of that precursor miRNA and is often (but not always) denoted by the absence of a star or the suffix -5p. The “minor product” is often denoted by a star or the suffix -3p (Bartel, 2004).

The guide miRNA strand interacts with AGO2 and other proteins to form RISC (RNA-Induced Silencing Complex), which is responsible for miRNA-induced gene silencing through RNAi (RNA Inactivation). RISC guides the miRNA to a target mRNA based on complete (or nearly complete) complementarity to the mRNA transcript (Bartel, 2004). miRNA binding of mRNA is dependent on the seed region of the miRNA, which binds the 3' untranslated region. The seed region is a conserved seven base pair sequence, commonly positioned from nucleotide 2 – 7 from the 5' end of the miRNA transcript, where initial binding of an mRNA occurs (Grimson et al., 2007).

When RISC binds to an mRNA transcript it leads to translational repression/silencing or mRNA cleavage (Grimson et al., 2007). If there is imperfect binding of the miRNA to the mRNA transcript, translational repression/silencing is more likely to occur. Imperfect binding causes RISC to remain bound to the mRNA transcript making it impossible for translational machinery to bind and for translation to begin. Immediate post-binding mRNA cleavage is most likely to occur with increased pairing between the miRNA and mRNA transcripts (Bartel, 2004). This occurs more frequently with mRNA binding of siRNAs (often an exogenous small RNA transcript, which has a similar function to miRNAs) (Grimson et al., 2007). After mRNA cleavage, the miRNA remains intact and can continue binding and cleaving additional mRNA transcripts (Bartel, 2004).

1.5.3.3.2.1 Circulating miRNAs

miRNAs primarily function in the cytoplasm but are known to be excised by a cell and invaginated by a neighboring cell, leading to intercellular communication via

regulation of gene expression. The exact mechanism of release from the cell is currently unknown but is hypothesized to occur during a loss of integrity in the plasma membrane and/or during cell death. These extracellular pre-miRNAs and mature miRNAs are bound to either high-density lipoproteins or the AGO2 protein, or they are encapsulated in microvesicles or exosomes which in turn inhibits RNase digestion in the plasma (Mi et al., 2013). Once released from a cell into the plasma, these microparticles can be absorbed by the blood stream; they are then referred to as ‘circulating miRNAs’ (**Figure 1.2**). Circulating miRNAs are a major form of intercellular communication (Creemers, Tijssen, & Pinto, 2012).

miRNAs are frequently investigated as potential biomarkers in many conditions because of their potential to non-invasively aid in diagnostics, prognostics, or therapeutic response prediction. Circulating miRNA biomarkers were initially investigated in cancer research. For example, when compared to levels in healthy controls, miR-141 was significantly increased in individuals who had metastatic prostate cancer. Similarly, a miRNA profile of increased miR-486 and miR-30 and decreased miR-1 and miR-499 levels was found in patients with non-small-cell lung cancer. These and many other studies have shown the predictive potential of circulating miRNAs that could one day have clinical utility (Mi et al., 2013).

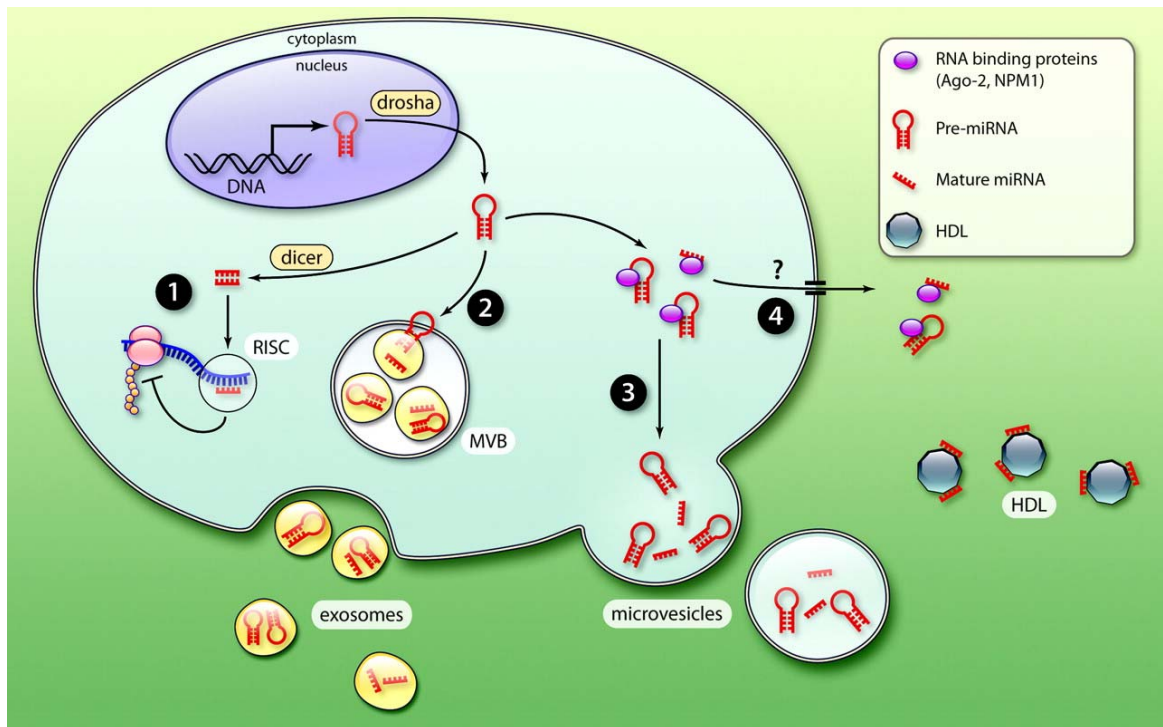


Figure 1.2 - Schematic of miRNAs being excised from a cell, where they are referred to as ‘circulating miRNA’. This figure was used with permissions from Wolters Kluwer Publishing Company; (Creemers, Tijssen, & Pinto, 2012). **Appendix E** contains copyright permissions to use this figure.

The use of circulating miRNAs as biomarkers is currently being examined in inflammatory disease. miRNAs are known to regulate immune response and the development of immune-related cells, both of which are factors that contribute to inflammatory disease pathogenesis (Mi et al., 2013). For instance, miR-150 expression is known to be critical to the development of mature T- and B-cells, but its over-expression severely decreases the formation of mature T-cells (Zhou, Wang, Mayr, Bartel, & Lodish, 2007). Up-regulation of miR-151-5p and miR-28-5p was observed in two independent circulating miRNA studies on ulcerative colitis patients (Paraskevi et al., 2012).

Pharmacogenetic and pharmacogenomic investigations of miRNA variants are primarily done by microarray or sequencing. Targeted pharmacogenetics approaches involve panels of selected miRNAs with known or suspected associations with treatment response, which are examined with DNA microarrays composed of probes that are complementary to miRNA transcripts (Katagiri & Glazebrook, 2009). Similar investigations can be done targeting differential miRNA expression potentially associated with treatment response, which are examined with microarrays composed of probes specially designed to bind miRNAs (Shingara et al., 2005).

The comprehensive analyses of the miRNA transcripts has been given the name “miRomics”. This type of investigation uses microarray and sequencing methods to identify associations between differentially expressed miRNAs with treatment response. These investigations examine all known miRNA transcripts to identify differential expression and attempt to determine causation.

1.5.3.4 mRNA Variations Causing Differential Drug Response in Psoriatic Disease

Transcriptomic investigations of drug response in patients undergoing treatment for PS and PsA have identified associations with differential mRNA profiles. These studies identified differential mRNA expression of genes that are primarily responsible for T-cell regulation and cytokine production. A few transcriptomic investigations into drug response in PsA and PS patients have been done that are primarily associated with pharmacokinetic and pharmacodynamic pathways. These genetic variations that impact response to PS/PsA

treatment are generally found in genes that code for drug-metabolizing enzymes, drug transportation proteins, and cell-surface receptors. These associations have predominantly been found in signalling pathways that these pharmaceuticals act on, such as TNF α , IL-12/23, and IL-17 inhibitors (Sutherland et al., 2016).

1.5.3.4.1 Methotrexate

Pharmacogenomics investigations have been performed on PS and PsA patient cohorts treated with MTX. In a microarray analysis of gene expression in PS patients, a significant down-regulation of the mRNAs involved with helper T-cells (i.e., Th-1, Th-17 and Th-22) was observed (Goldminz et al., 2015). There has been only one comparative transcriptomic analysis done on PsA patients, comparing those being treated with MTX and those who were not undergoing treatment. Through microarray, responders to MTX were found to have an increased expression of 12 genes and a decreased expression of 33 genes (Cuchacovich, Perez-Alamino, Zea, & Espinoza, 2014). Further comprehensive investigations are required to identify additional genetic variations associated with MTX response.

1.5.3.4.2 TNF α Inhibitors

Studies have used a targeted approach to examine the influence of etanercept on gene expression in PS patients. These studies have displayed a significant reduction in mRNA expression levels in *TLR-2* and *-9* and key notch signalling pathway genes

(*NOTCH1*, *NOTCH2* and *JAGGED1*) when matched to untreated PS controls (Skarmoutsou et al., 2015; Vageli et al., 2015). Another study demonstrated an increase in mRNA levels of survivin and capase3 transcripts in lesional and non-lesional skin after etanercept treatment. These results suggest etanercept's mechanism of action is correlated to a decrease of keratinocyte regulation and the subsequent increase in keratinocyte apoptosis (Lembo et al., 2016). A decreased in expression levels of 161 genes and increased expression levels of 27 genes was observed in patients being treated with TNF α inhibitors when compared to an untreated control group (Cuchacovich et al., 2014).

A study examining response to adalimumab found an overall suppression of genes involved in the Th-17 signalling pathway in the skin and PBMCs of PS patients. Specifically, this study found a down-regulation of Th-17 polarizing cytokines (*IL-23A*, *TGF- β 1*, *IL-1 β*), Th-17 cytokines (*IL-17*, *IL-22*), Th-1 polarizing cytokines (*IFN- α* , *TNF α*), chemokines (*IL-8*, *CCL20*), and antimicrobial peptides (*HBD-2*, *S100A7*) (Balato et al., 2014). Another study identified a decrease in *NOTCH1* mRNA levels in the skin of responders to adalimumab (Skarmoutsou et al., 2015).

1.5.3.4.3 IL-12/23 Inhibitors

Multiple studies have examined gene expression profiles of PS patients undergoing treatment with IL-12/23 inhibitors; however, no studies have been published that examine the effects of ustekinumab on PsA patients. Several genes known to be involved in the pathogenesis of PS have displayed a significant down-regulation in responders to ustekinumab treatment (Gudjonsson & Krueger, 2012). Another investigation identified a

significant reduction in *NGF* expression and an increase in *GATA3* and *IL-22RA1* expression (Baerveldt et al., 2013). Responders to ustekinumab had an increase in *IL-20*, *IL-21* and *p40* expression in lesional skin in their pre-treatment transcriptomes (Gedebjerg, Johansen, Kragballe, & Iversen, 2013). Another study demonstrated the down-regulation of expression of genes crucial to the Notch signalling pathway, *NOTCH1* and *NOTCH2*, in the skin biopsies of PS patients undergoing ustekinumab therapy (Skarmoutsou et al., 2015).

1.5.3.4.4 IL-17 Inhibitors

PS patients treated with secukinumab exhibited down-regulation of genes coding for chemokines and cytokines. This change in transcriptomic profile showed a significant decrease in Th-17-associated genes (*IL-17A*, *IL-17F*, *IL-21*, *IL-22*, *IL-8*, *DEFB4*, *CCL20*), Th-1-associated genes (*IFN- γ* , *IL-12B*), proliferation marker (*KRT16*), and innate immunity-associated genes (*TNF α* , *IL-6*) (Hueber et al., 2010).

Pharmacogenomic investigations have been done on PS patients taking ixekizumab, which is currently in clinical trials (Boyd & Kavanaugh, 2015). mRNA expression levels in lesional skin from PS patients treated with ixekizumab showed a down-regulation of *IL-19*, *IL-8*, *CXCL1*, *CCL20*, *GZMB* and *LCN2* when compared to mRNA levels at baseline and after 6 weeks of therapy (Krueger et al., 2012). The suppression of these genes was more significant than in the transcriptomes of patients treated with etanercept. This indicates that ixekizumab has a larger impact on the PS transcriptome at baseline. Comparisons between psoriatic skin pre- and post treatment with ixekizumab also

revealed that of the 1200 genes that were differentially expressed, 643 genes became normalized after two weeks (Krueger et al., 2012). Wang and colleagues found similar results, noting the majority of genes that were up-regulated in PS patients were significantly suppressed in response to ixekizumab therapy (Wang et al., 2014). Intriguingly, there was a significant down-regulation of genes associated with cardiovascular disease and atherosclerosis – comorbidities commonly associated with PS (Ryan et al., 2011; Wang et al., 2014).

1.5.3.5 miRNA Variations Causing Differential Drug Response in Psoriatic Disease

Very few studies have investigated differential miRNA expression in response to treatment of PS, while none investigated differential miRNA expression in response to treatment of PsA. A study on PS patients undergoing treatment with MTX found that decreased levels of miR-223 and miR-143 in the PBMCs of these patients were directly correlated to disease severity (Lovendorf, Zibert, Gyldenlove, Ropke, & Skov, 2014). Investigations into miRNA expression demonstrated that miR106b, miR142-3p, miR-223, and miR-126 were significantly down-regulated in PS patients who responded to etanercept when compared with non-responders (Pivarsci, Meisgen, Xu, Stahle, & Sonkoly, 2013). Thus far only a few studies have investigated the field of pharmacogenomics of PsA, and therefore further studies are required on the differential miRNA expression as a marker of response to treatment.

1.5.3.5.1 Methodologies of miRNA Extraction from Plasma

Since circulating miRNAs were identified as a potential source of stable and non-invasive biomarkers, researchers have been optimizing miRNA extraction procedures from plasma to achieve high miRNA yields with minimal contamination. Proper plasma isolation, RNA extraction, RNA size separation, and miRNA quantification are all required to produce optimum results (McAlexander, Phillips, & Witwer, 2013; Moret et al., 2013).

To ensure highest possible yields, all miRNA extraction procedures must be performed in an RNase-free environment to minimize RNase degradation until the RNA has been reverse transcribed into cDNA. Plasma isolation should be performed as soon as possible after venipuncture to reduce contamination from hemolysis. Centrifugation of whole blood causes separates it into layers from which the plasma is transferred to a fresh tube. Often, a second centrifugation is performed to remove cellular contents from the plasma, which can bias results with an intracellular miRNA profile from platelets and white blood cells. If possible ultracentrifugation should be considered to ensure no contamination. miRNAs are well preserved in frozen plasma (-80°C) allowing for miRNA extractions to be performed at a later time (McAlexander et al., 2013; Moret et al., 2013).

RNA extraction from plasma is normally performed by mixing the plasma with a phenol-chloroform solution that separates the RNA into an aqueous phase after centrifugation. The RNA is then precipitated out of the aqueous phase using ethanol; however, this process is less efficient with small RNAs than with larger species and can be optimized using differential concentrations of ethanol. Techniques for miRNA isolation from total RNA include size separation by filtered column or by magnetic beads. Column

separation is a more traditional approach that is low cost and effective in size separation but results in lower yield because some miRNAs remain in the filter after elution. Magnetic-bead separation is a newer technique that is more costly but highly effective in size separation with minimal loss of miRNAs throughout the procedure (McAlexander et al., 2013; Moret et al., 2013).

After miRNA is properly extracted, samples can then be quantified and standardized either for differential expression analyses using microarray or for library preparation using NGS. Currently, quantification methods are far from optimal. Standard spectrophotometer quantification methods are not suitable for plasma-extracted RNA due to the paucity of miRNAs and carryover contaminants. The small size of miRNA limits the efficiency of most conventional biological amplification processes and adds bias to expression quantifications. It has also been reported that RNA extracted from plasma can be contaminated with inhibitors of quantitative polymerase chain reaction (qPCR). qPCR is inefficient at miRNA quantification on a genomic scale and is more suitable for validation purposes. Unlike qPCR, microarray technology labels each miRNA molecule and does not include any amplification step, thereby removing that source of potential bias. The optimization and standardization of methods for miRNA extraction from plasma will improve the clinical utility of circulating miRNA biomarkers with regards to diagnosis, prognosis, and predicting response to treatment (McAlexander et al., 2013; Moret et al., 2013).

There are well established protocols for sequencing intracellular miRNA, which is much more abundant than circulating miRNA. Using extracted miRNA from plasma for

genomic analysis using NGS technologies is difficult in nature due to small size of miRNA, low yields when extracted from plasma, and suboptimal quantification techniques. The small size of the miRNAs necessitates adaptors that increase fragment length and the low yield necessitates increasing amplification cycles. Library preparation procedures often require a known concentration of miRNA in a sample to reduce variability between the resultant concentrations of prepared libraries; however, the lack of appropriate quantification techniques limits this potential point of standardization. Limiting factors such as these were points of optimization during the development of library preparation methods for sequencing on Ion Torrent or Illumina platforms (Head et al., 2014). At the time of this investigation, a literature review failed to find publications on sequencing circulating miRNAs from human plasma using NGS technologies. Two papers had been published that sequenced the contents of exosomes excised by human cell lines and serum; however, these investigations involved procedural modifications and did not include other species of non-exosomal microRNAs (Schageman et al., 2013; Lunavat et al., 2015). The co-author of Lunavat et al. (2015), published the protocol used to successfully prepare libraries in this investigation.

Overall, miRNA extraction and library preparation methods have improved; however further optimization is required to maximize this potential for biomarkers. Method selection varies depending on the laboratories capacity and should be employed and compatibility between reagent chemistry and sequencing platforms should always be considered. Once established, additional in-house modification may be required to optimize the sequencing of circulating miRNAs.

1.6 Rationale

PS prevalence in NF is double that of any other Caucasian population worldwide (Gulliver et al., 2011). This is due in part to genetic isolation of a small founding population and in part due to the low UV indexes per annum (Gulliver et al., 2011). Given that arthritis is developed by one third of PS patients it can be reasonably assumed that there is also an increased incidence of PsA in NF, although it has not been officially documented (Rahman & Elder, 2005).

Biologics are the current gold standard for the treatment of moderate to severe PsA. Predicting response to biologics is important because between 35-50% of patients do not respond and continue to experience disease progression (Gladman & Ritchlin, 2016). This class of pharmaceuticals poses a large financial burden both on the individual and the health care system making response prediction of particular importance (Gladman & Ritchlin, 2016). Despite research advances in the pharmacogenomics of PsA, few predictors of response have been discovered (Sutherland et al., 2016).

Examining miRNA gives insight to the intracellular communication occurring at the level of the tissue (Kosaka et al., 2010). At the clinical level this is particularly important in PsA as an alternative to biopsies of deteriorating psoriatic joints, which may cause decreased mobility and increase complications. As seen in studies (Paraskevi et al., 2012; Wu et al., 2010), circulating miRNAs are highly stable, conveniently collectable, and non-invasive sources of biomarkers (Mi et al., 2013). The scope of previous miRNA studies (in PS) were limited to microarray and qPCR of targeted miRNAs (Sutherland et al., 2016). Using the NGS platform for miRNA research is preferred over microarray and qPCR due

to its superior detection sensitivity, greater dynamic range of detection, higher accuracy of measuring differential expression levels, and does not require target selection (Tam, de Borja, Tsao, & McPherson, 2014).

Given the high prevalence of psoriatic disease, the high interpatient variability and cost associated with biological therapy, the lack of access to tissue of primary pathology, and the advent of NGS to sequence circulating miRNA, the research objectives of this project are:

- 1) To develop and optimize a procedure for preparing circulating miRNA libraries for sequencing with Ion Torrent Technology; and
- 2) To examine circulating miRNA library preparation, circulating miRNA sequencing, and circulating miRNA differential expression data analyses in a PGx-PsA patient cohort as an exploratory investigation of these methodologies.

CHAPTER 2

2 MATERIALS AND METHODS

Ethics approvals were obtained and patient recruitment began for the PsA pharmacogenomics project. A cohort of PsA patients was treated with biologic agents and had blood samples taken pre-treatment, one-month post treatment, and three-months post treatment. For this project, an optimized protocol for miRNA library preparation was needed. After an optimal library preparation protocol was established, multiplexing capacity of chip loading for the Ion Torrent System was established. The pharmacogenomics (PGx) patient samples were then sequenced and the data underwent numerous analyses. Differential miRNA expression analyses, pathway analyses, network analyses, and an *in silico* functional analysis were performed to investigate miRNAs that could be contributing to differential response to PsA treatment.

2.1 Ethics approval

The "Pharmacogenomic Markers for Psoriatic Arthritis Treatment" study was approved by the Newfoundland and Labrador Health Research and Ethics Board; Researcher Portal File Number: 20170466, Reference Number: 2016.195. This study was also approved by the Eastern Health Research Proposals Approval Committee. The ethics approval granted states that the patients may be approached by rheumatologists for interest in study and their consent was obtained by a research nurse prior to taking part in the study.

2.2 Sample Ascertainment for Optimization of Library Preparation

Three plasma samples, referred to as TF-Sample 1, TF-Sample 2, and TF-Sample 3, were used to assess the quality and performance of the Thermo Fisher protocol; these samples were aliquots of the same pooled plasma that was extracted and de-identified from multiple individuals. Samples, referred to as CH-Sample 1, CH-Sample 2, and CH-Sample 3, and CH-Sample 4 were used to test and optimize the Cheng et al. protocol and to test the chip loading capacity; these samples were aliquots of plasma that were extracted and de-identified from a single individual. CH-Sample 5 and CH-Sample 6 were processed using the Cheng et al. protocol and were used to test chip loading capacity; these samples were aliquots of plasma that were extracted and de-identified from a single individual. (Cheng, Sharples, Scicluna, & Hill, 2014)

2.3 Sample Ascertainment for PGx Study Cohort

Nine participants were ascertained for this study during their routine appointments at Dr. Proton Rahman's Rheumatology Clinic at St. Clare's Mercy Hospital. To be eligible for the cohort patients must 1) satisfy CASPAR criteria for PsA, 2) be greater than 18 years of age, 3) be of non-aboriginal descent, 4) were about to begin treatment with a biologic (either secukinumab or ustekinumab), and 5) be naive to treatment with biologics or have been washed out from biologics treatment for more than three months. If the patient was eligible for the study they were then seen by the research nurse. The nurse would explain the study in detail, and if the patient was willing their consent would be obtained (see

Appendix C for consent form). Patients who agreed to participate in the research study had their blood drawn (up to 30mL), the biologic administered via sub-cutaneous injection, and were asked to return to the clinic to attain response status after one- and three-months post treatment (Figure 2.1). Patients' blood was drawn between two weeks prior and one week after biologic was injected (Table 2.1).

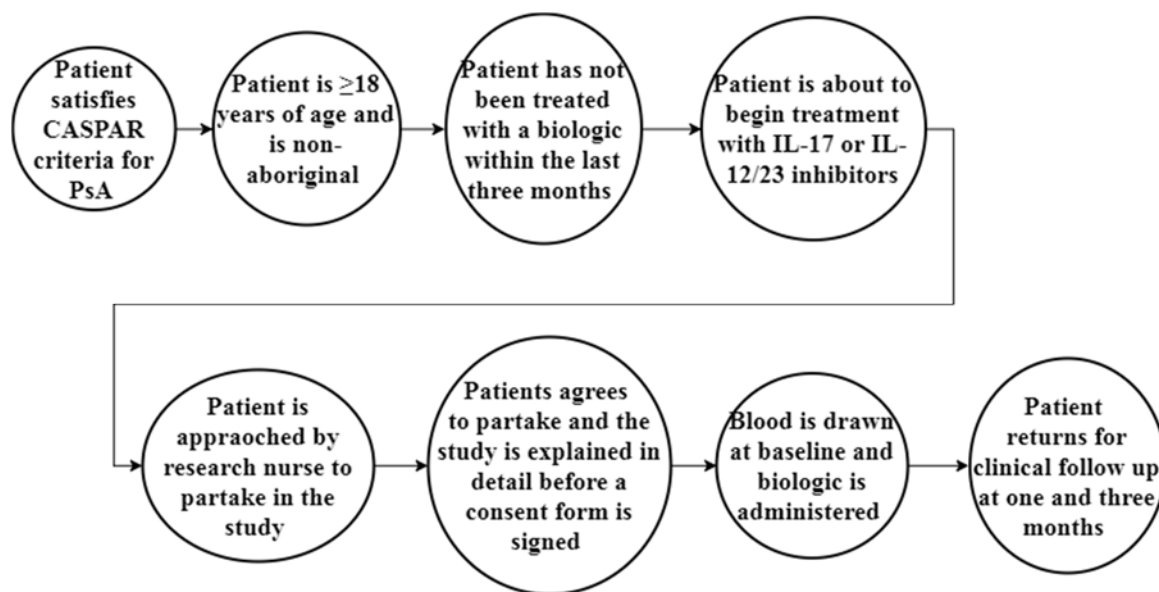


Figure 2.1 – Flow chart of study participant recruitment process.

Table 2.1 - Sample ascertainment including biologic prescribed, date of blood drawn and date of biologic administration.

Patient #	Biologic	Pre-Date Blood Drawn	Date Biologic Started
02	Stelara	1-Nov-16	3-Nov-16
06	Cosentyx	7-Dec-16	14-Dec-16
07	Cosentyx	14-Dec-16	21-Dec-16
08	Cosentyx	9-Jan-16	25-Jan-17
10	Cosentyx	9-Feb-17	15-Feb-17
11	Cosentyx	6-Mar-17	6-Mar-17
12	Cosentyx	7-Mar-17	12-Mar-17
13	Stelara	27-Mar-17	21-Mar-17
14	Cosentyx	5-Apr-17	16-Apr-17

2.4 Sample Processing

Whole blood samples were collected from PSA patients in Ethylenediaminetetraacetic acid tubes. The plasma was separated by the centrifugation at $800 \times g$ for 10 minutes at room temperature and then stored in aliquots of 1mL at -80°C . miRNAs were isolated from the plasma and treated with DNase. These samples then underwent library preparation and were quantified to ensure quality results. High quality prepared libraries were then loaded onto a chip and sequenced using the Ion Torrent System. The sequencing data generated from the Ion Torrent Server underwent numerous analyses (**Figure 2.2**).

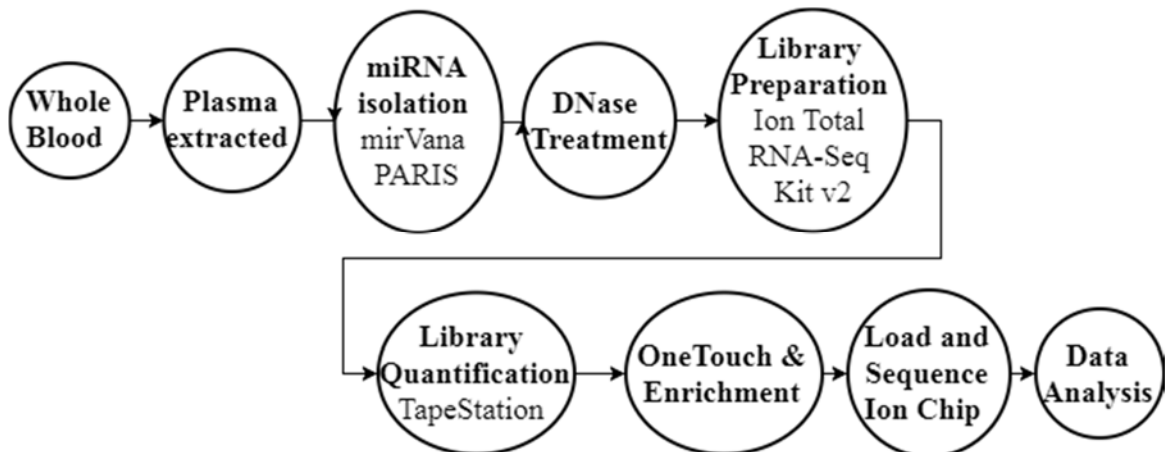


Figure 2.2 – Procedures involved in sample processing beginning with whole blood and ending with analysis of sequencing data.

2.4.1 Small RNA Extraction from Plasma

A *mirVana*TM *PARIS*TM Kit (Thermo Fisher ScientificTM [herein referred to as TFSTM], Catalogue#: AM1556. Waltham, MA., USA), following a modified *mirVana*TM *PARIS*TM RNA and Native Protein Purification Kit protocol (see **Table 2.2**; where inter-

protocol discrepancies exist Table 2.2 can be referenced for exact numerical values), was used to extract small RNA species from plasma. (Invitrogen by Life Technologies, 2012) A total of 1mL of plasma was added to 1025 μ l of 2X Denaturing Solution (TFSTM), mixed, and incubated on ice for 5 minutes. Following incubation, 2025 μ l of Acid-Phenol Chloroform (TFSTM) was added, vortexed for 45 seconds, and centrifuged for 5 minutes at 10,000 \times g. The interphase was visually inspected to ensure that it was sufficiently compact. The upper aqueous phase was transferred to a fresh tube and the volume recorded, ensuring that the lower phase was not disturbed.

To capture small species of RNA (<200 nt), a volume of 100% ethanol (Greenfield Speciality Alcohol Inc. TM, Catalogue#: P016EAAN. Toronto, ON., CA) equal to 1.25 \times the volume of the aqueous phase was added to the solution and vortexed for 30 seconds. An RNA capture filter was placed in a fresh collection tube and 700 μ l of aqueous phase-ethanol solution was transferred onto the filter. Contents of the collection tube were then centrifuged for 15 seconds at 10,000 \times g and the flow-through was discarded. This process was repeated until the entire aqueous phase-ethanol solution was filtered. 700 μ l of Wash 1 Solution (TFSTM) was added to the filter, centrifuged for 5-10 seconds at 10,000 \times g, and the flow-through discarded. This was followed by 500 μ l of Wash 2/3 Solution (TFSTM) and centrifuged through the filter for 5-10 seconds at 10,000 \times g. The Wash 2/3 Solution process was then repeated. Contents of the collection tube were then centrifuged for 1 minute to remove any residual fluid from the filter. The filter was then transferred to a fresh collection tube. 40 μ l of 95 $^{\circ}$ C nuclease-free water (H₂O [TFSTM]) was added to the middle of the filter to elute the small RNA species. The elution solution was incubated for 1 minute, and then

spun for 30 seconds at $10,000 \times g$. This step was then repeated with an additional 40 μ l of elution solution. The $\sim 75\mu$ l of pooled eluate was stored at -80°C .

Table 2.2 - Summary of variations and modifications between small RNA extraction protocols used during optimization

Step in Procedure	<i>mirVana</i>TM PARISTM Kit Protocol	<i>mirVana</i>TM PARISTM RNA and Native Protein Purification Kit Protocol	Additional Modifications to <i>mirVana</i>TM PARISTM RNA and Native Protein Purification Kit Protocol
Sample Input	625 μ l	200 μ l	1000 μ l
2X Denaturing Solution	625 μ l	205 μ l	1025 μ l
Acid-Phenol Chloroform	1250 μ l	410 μ l	2025 μ l
Volume and Technique Used for Eluting Sample	100 μ l (Dispensed on to filter at one time)	100 μ l (50 μ l dispensed twice and combined through centrifugation)	80 μ l (40 μ l dispensed twice and combined through centrifugation)

2.4.2 DNase Treatment

A TURBO DNA-*free*TM Kit (TFSTM, Catalogue#: AM1907, Waltham, MA., USA) was used to guarantee all DNA contamination was removed from the extracted small RNA samples. The samples, which contained less than 200 μ g of nucleic acid per mL, underwent a routine DNase treatment. A total of 0.1 \times the sample volume of 10X TURBO DNase buffer (TFSTM) and 1 μ l TURBO DNase (TFSTM) was added to $\sim 75\mu$ l of the small RNA sample. The mixture was incubated at 37°C for 30 minutes. The total sample volume was then calculated and 0.1X sample volume of DNase Inactivation Reagent (TFSTM) was added. The solution was then mixed well and incubated at room temperature for 5 minutes.

The tube was flicked 2-3 times during the incubation to ensure that the DNase Inactivation Reagent (TFS™) was re-dispersed. The mixture was then centrifuged at $10,000 \times g$ for 1.5 minutes to pellet the DNase Inactivation Reagent (TFS™). The DNA-free small RNA containing supernatant was then transferred into a fresh tube and stored at -80°C .

2.4.3 Quality Assessment of Extracted RNA

Before going into library preparation, the presence of the small RNA samples was assessed. The small RNA samples were measured using a NanoDrop™ (TFS™, Waltham, MA., USA) to confirm the presence of miRNA in the sample, rather than measure the sample concentration. The NanoDrop™ 1000 instrument was tared using water, the RNA program was selected, and $1\mu\text{l}$ of the sample was added. All samples were tested in duplicate.

2.4.4 Library Preparation

Two different protocols were investigated in an attempt to optimize circulating miRNA library preparation (**Table 2.3**). First, a modified version of Thermo Fisher's protocol for intracellular miRNA extraction and library preparation (Invitrogen by Life Technologies, 2012) was used to isolate and prepare libraries for extracellular or circulating miRNA. A second protocol entitled "*Small RNA Library Construction for Exosomal RNA from Biological Samples for the Ion Torrent PGM™ and Ion S5™ System*", herein referred to as the "Cheng et al. protocol", was subsequently modified and used. (Cheng, Sharples, Scicluna, & Hill, 2014)

Table 2.3 – Summary of variations and modifications between library preparation protocols used during optimization

Step in Procedure	Thermo Fisher Ion Total RNA-Seq v2 Total Exosome RNA Protocol	Cheng et al. Protocol	Additional Modifications to Cheng et al. Protocol
Magnetic Bead Clean up Module I	On magnet incubation (x2): 5 mins Elution volume: 30µl	On magnet incubation (x2): 5 mins Elution volume: 30µl	On magnet incubation (x2): 7-9 mins Elution volume: 15µl
Speed Vac	N/A	30µl → 3µl	15µl → 3µl
Hybridize and Ligate RNA	R&D Systems Optimized adaptors	Ion Adaptor Mix v2	
Reverse Transcription Reaction	H ₂ O: 2µl 10X RT Buffer: 4µl 2.5 nM dNTP mix: 2µl Ion RT Primer v2: 8µl	H ₂ O: 5µl 10X RT Buffer: 4µl 2.5 nM dNTP mix: 2µl Ion RT Primer v2: 5µl	
Magnetic Bead Cleanup Module II	Beads: 5µl Binding Sol: 250µl H ₂ O: 60µl Ethanol: 275µl On magnet incubation: 2-5 mins No supernatant transfer Air dry time: 2-3 mins	Beads: 7µl Binding Sol: 140µl No H ₂ O added Ethanol: 120µl On magnet incubation: 5 mins Supernatant transferred for second size selection H ₂ O: 72µl Ethanol: 78µl Beads: 7µl On magnet incubation: 5 mins Air dry time: 1-2 mins	On magnet incubation: 7-9 mins On magnet incubation: 7-9 mins
Amplification of cDNA	16 cycles of 94°C for 30 seconds, 62°C for 30 seconds, 68°C for 30 seconds	14 cycles of 94°C for 30 seconds, 62°C for 30 seconds, 68°C for 30 seconds	
Magnetic Bead Cleanup Module III	Beads: 5µl Binding Sol: 280µl H ₂ O: 27µl	Beads: 7µl Binding Sol: 140µl No H ₂ O added	

Step in Procedure	Thermo Fisher Ion Total RNA-Seq v2 Total Exosome RNA Protocol	Cheng et al. Protocol	Additional Modifications to Cheng et al. Protocol
Magnetic Bead Cleanup Module III	Ethanol: 230µl On magnet incubation: 2-5 mins Air dry time: 2-3 mins	Ethanol: 110µl On magnet incubation: 5 mins Supernatant transferred for second size selection H ₂ O: 35µl Ethanol: 35µl Beads: 7µl Air dry time: 1-2 mins	On magnet incubation: 7-9 mins

2.4.4.1 Ion Total RNA-Seq v2 Kit

2.4.4.1.1 Magnetic Bead Cleanup Module I

The process of enrichment was done twice to size select the desired small RNA species. Magnetic beads were used to capture and remove large RNA species (mRNA and rRNA) then, with increased ethanol concentrations, small-RNA species were selected for as follows:

Nucleic Acid Binding Beads (TFSTTM) were re-suspended and 7µl was added to a well of a 96-well plate (see **Table 2.3**) where inter-protocol discrepancies exist **Table 2.3** can be referenced for exact numerical values). Binding Solution Concentrate (TFSTTM) was added and mixed thoroughly. The small RNA sample (~75µl) was combined with beads and binding solution (**Table 2.3**). To bind any remaining large RNA species to the beads, 105µl of 100% ethanol (Greenfield Speciality Alcohol Inc.TM) was added and mixed thoroughly by pipetting the solution up and down 10 times. The plate was incubated for 5

minutes at room temperature, followed by incubation on the 96-well magnetic stand (Agencourt™) (see **Table 2.3**). Once the solution was clear, the supernatant was transferred to a fresh well.

To bind small RNA species, the plate was removed from the magnetic stand and 30µl of H₂O, 570µl of 100% ethanol, and 7µl of beads were added to the sample and mixed thoroughly. The mixture was incubated for 5 minutes at room temperature off the magnetic stand. The sample was incubated (see **Table 2.3**) on a magnetic stand. After the solution had cleared, the supernatant was discarded. Then, 150µl of Wash Solution Concentrate (TFS™) was added to the sample and incubated for 30 seconds. While the plate was on the magnetic stand, the supernatant was discarded. The beads were left to air dry for 1-2 minutes to remove all traces of ethanol solution.

The plate was then removed from the magnetic stand and the small RNAs were eluted from the beads using (see **Table 2.3**) 15µl of 80°C H₂O (TFS™). The plate was incubated for 1 minute off the magnetic rack and then placed back on the magnetic rack for 1 minute. Once the solution was clear, the eluate was transferred into a fresh tube (see **Table 2.3**).

The eluted sample was concentrated by a speed vacuum centrifuge to a final volume of 3µl, allowing the entire sample to be used in the hybridization reaction (see **Table 2.3**).

2.4.4.1.2 Hybridize and Ligate RNA

In order to reverse transcribe small RNA, adaptors must be hybridized and ligated to the small RNA species. A hybridization mastermix was prepared on ice with 3µl of

Hybridization Solution (TFS™) and 2µl of adaptors (see **Table 2.3**) in a 0.2ml PCR tube (TFS™, Catalogue#: AB0620, Waltham, MA., USA). The mastermix was then added to the 3µl of enriched small RNA sample. The solution was mixed well and centrifuged briefly before being loaded into the SimpliAmp Thermal Cycler (TFS™, Catalogue#: A24811, Waltham, MA., USA) for 10 minutes at 65°C, followed by 16°C for 5 minutes. The sample was immediately placed on ice.

The 2X Ligation Buffer was heated to 37°C, to ensure no white precipitate was present. A ligation master mix was prepared by combining 10µl of the 2X Ligation Buffer (TFS™) and 2µl of Ligation Enzyme Mix (TFS™). The 12µl ligation mastermix was vortexed, centrifuged briefly, and added to the 8µl of hybridization mastermix. The solution was mixed thoroughly and spun down before being loaded into the SimpliAmp Thermal Cycler for 16 hours at 16°C with the lid of the thermal cycler open.

2.4.4.1.3 Reverse Transcription of RNA

In order to amplify the adaptor-bound small RNA species, the fragments were reverse transcribed into cDNA. A reverse transcription mastermix (see **Table 2.3**) was prepared on ice with the following components: H₂O, 10X Reverse Transcription Buffer (TFS™), 2.5nM dNTP Mix (TFS™), and Ion Reverse Transcription Primer v2 (TFS™). The 16µl reverse transcription mastermix was then combined with the 20µl ligation reaction, centrifuged, incubated at 70°C for 10 minutes, and snap-cooled on ice. Then 4µl of 10X SuperScript III Enzyme Mix (TFS™) was added to the sample. The sample was vortexed gently, spun down, and incubated at 42°C for 30 minutes. This was a possible

stopping point where the sample was either stored at -20°C overnight or was purified and size-selected immediately.

2.4.4.1.4 Magnetic Bead Cleanup Module II - Purify and Size-Select cDNA

As was done in Magnetic Bead Cleanup Module I, the process of enrichment through magnetism is done twice on the same sample to size select the desired small cDNA product. The magnetic beads were used to capture and remove larger cDNA transcripts (>200bp) and with increased ethanol concentrations select for small cDNA transcripts (<200bp).

Nucleic Acid Binding Beads were completely re-suspended and added to a well on a 96-well plate (see **Table 2.3**). Binding Solution Concentrate (TFS™) was added (see **Table 2.3**) to the magnetic beads and mixed thoroughly. The 40µl reverse-transcription reaction was added to the well. To bind larger cDNA, 100% ethanol was added (see **Table 2.3**) to each sample, mixed thoroughly, and incubated for 5 minutes at room temperature. The plate was then incubated (see **Table 2.3**) on the magnetic stand. Once the solution was clear, the supernatant was transferred to a fresh well (see **Table 2.3**).

To bind the smaller cDNA transcripts, the plate was removed from the magnetic stand and 72µl of H₂O, 78µl of 100% ethanol, and 7µl of re-suspended beads were added and mixed thoroughly (see **Table 2.3**). The mixture was incubated for 5 minutes at room temperature off the magnetic stand. The sample was then placed on a magnetic stand to incubate (see **Table 2.3**). After the solution had cleared, the supernatant was discarded (see **Table 2.3**).

While the processing plate remained on the magnetic stand, 150µl of Wash Buffer Concentrate (TFS™) was added and incubated for 30 seconds. The supernatant was then discarded and the beads were air dried (see **Table 2.3**). The sample was then removed from the magnetic plate and 12µl of 37°C H₂O was added and mixed thoroughly. The sample was incubated at room temperature for 1 minute off of the magnetic stand. The processing plate was placed back on the magnetic stand and incubated for 1 minute. The 12µl eluate was then collected and transferred to a fresh tube and stored at -80°C.

2.4.4.1.5 Amplify cDNA

To enable multiplexing, the adaptor-bound small cDNA transcripts were labelled by a distinct barcode for down-stream identification. The barcoded, adaptor bound small cDNA transcripts were then amplified to increase the number of transcripts in the sample. A PCR and barcode mastermix was prepared by combining 45µl of Platinum PCR SuperMix High Fidelity (TFS™), 1µl of Ion Xpress RNA 3' Barcode Primer (TFS™), and 1µl of selected Ion Xpress RNA Barcode (TFS™). One half of the cDNA sample (6µl) was then added to the PCR mastermix, mixed, centrifuged, and loaded into the SimpliAmp Thermal Cycler under the following conditions: 94°C for 2 minutes, 2 cycles of 94°C for 30 seconds, 50°C for 30 seconds, 68°C for 30 seconds; followed by 14 or 16 cycles (see **Table 2.3**) of 94°C for 30 seconds, 62°C for 30 seconds, 68°C for 30 seconds, and 68°C for 5 minutes.

2.4.4.1.6 Magnetic Bead Cleanup Module III - Purify the Amplified DNA

Nucleic Acid Binding Beads were completely re-suspended, and added to a well on a 96-well plate (see **Table 2.3**). Binding Solution Concentrate (TFS™) was added (see **Table 2.3**) to the magnetic beads and mixed thoroughly. 53µl of amplified cDNA sample was added to the well. To bind larger cDNA, 100% ethanol was added (see **Table 2.3**) to each sample and was mixed thoroughly. The sample was incubated for 5 minutes at room temperature and then incubated (see **Table 2.3**) on a magnetic stand. Once the solution was clear, the supernatant was transferred to a fresh well (see **Table 2.3**).

To bind smaller cDNA transcripts the sample was removed from the magnetic stand and 35µl of H₂O, 35µl of 100% ethanol, and 7µl of beads were added and mixed thoroughly (see **Table 2.3**). The mixture was incubated for 5 minutes at room temperature, and then placed on a magnetic stand to incubate (see **Table 2.3**). Once the solution was clear, the supernatant was discarded (see **Table 2.3**).

While the processing plate remained on the magnetic rack, 150µl of Wash Buffer Concentrate was added and incubated for 30 seconds. The supernatant was then discarded and the beads were air-dried (see **Table 2.3**). The sample was then removed from the magnetic stand and 37°C H₂O was added (see **Table 2.3**) and mixed thoroughly. The sample was incubated at room temperature for 1 minute, and then placed on the magnetic stand to incubate for 1 minute. The eluate containing the prepared small RNA library was then collected (see **Table 2.3**), transferred to a fresh tube, and stored at -80°C.

2.4.4.1.7 Assess the Yield and Size Distribution of the Amplified DNA

The yield and size distribution of the small cDNA transcripts was assessed using the Agilent 2200 TapeStation and D1000 Screen Tape System (Agilent™, Catalogue#: 5067-5582, Santa Clara, CA., USA). All reagents were brought to room temperature, and 3µl of buffer (Agilent™) was added to each well of the TapeStation strip (Agilent™). In the first well of the strip 1µl of ladder (Agilent™) was added. In subsequent wells 1µl of sample was loaded. The strip was then loaded into an IKA vortexer (IKA® Works, Inc., Catalogue#: 0004049600, Wilmington, NC., USA), vortexed for 1 minute at 2000rpm, and centrifuged briefly. After being spun down, the tube strip was then loaded into the 2200 TapeStation (Agilent™, Catalogue#: G2965AA, Santa Clara, CA., USA) and the concentration of the sample was measured.

The targeted size of the barcoded cDNA fragment falls between 94 base pair (bps) and 114 bps. Applying size regions of interest to the plot allows measurement of molarity of the barcoded cDNA (94-114 bps, referred to as “regional molarity”) to the total library (50-300 bps, referred to as “total molarity”) and the resulting ratio to be determined. To ensure quality sequencing results a Field Application Scientist (FAS) from TFS™ recommended that the regional molarity percentage of the samples be greater than 50%.

The electropherograms produced during library quantification represent the size distributions of the reads in a given library. The y-axis is the measure of fluorescence units, representing the sample concentration, and the x-axis is a measure of read length in base pairs, beginning at the 25 bps marker and ending at the 1500 bps marker (**Figure 2.3**). The red lines on the electropherogram indicate the read lengths spanning from 50-300 bps.

Because of the numerous size selection processes the protocol the reads in a prepared library should all fall within these lines. The green lines on the electropherogram indicate the read lengths spanning the desired fragment size lengths of 94-114 bps. There are four distinctive “peaks” that can be observed in prepared libraries. The peak composed of fragments approximately 85 bps in length represents an adaptor dimer, which occurs when two adaptors bind ($2 \times \sim 30$ bps) without a miRNA inserted between them and are barcoded (20 bps) (**Figure 2.4**). The peak composed of fragments approximately 104 bps long represents cDNA fragments that have miRNA inserted between the adaptors, and are barcoded (**Figure 2.5**).

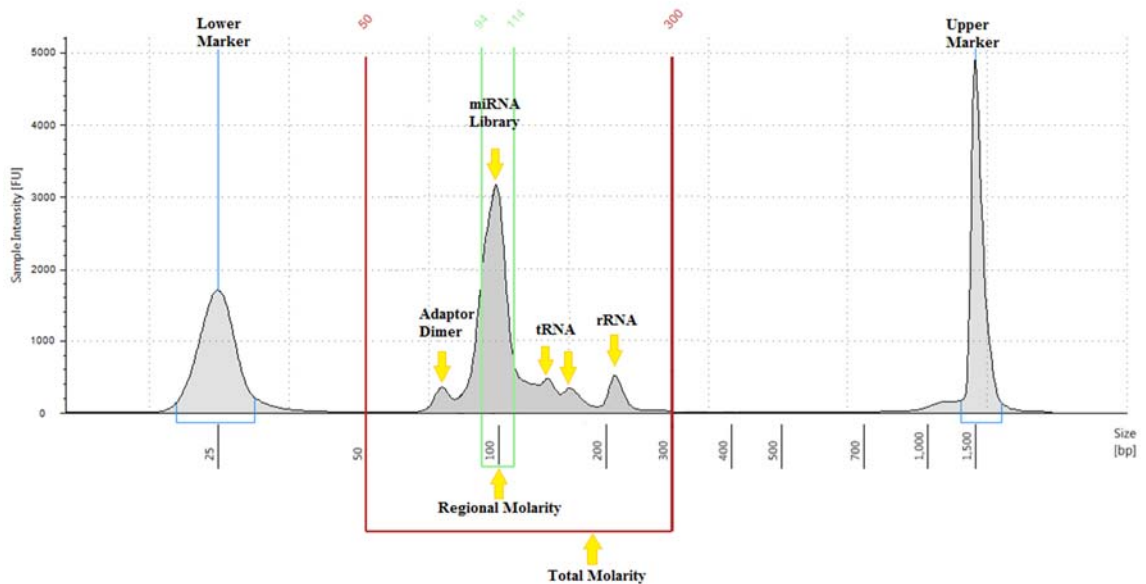


Figure 2.3 – An electropherogram of a barcoded small RNA library (~104 bps) that has an adaptor dimer (~85 bps) and some large RNA species present (~150-240 bps). The red lines indicate the Total Molarity (50-300 bps) and the green lines indicate the Regional Molarity (94-114 bps).

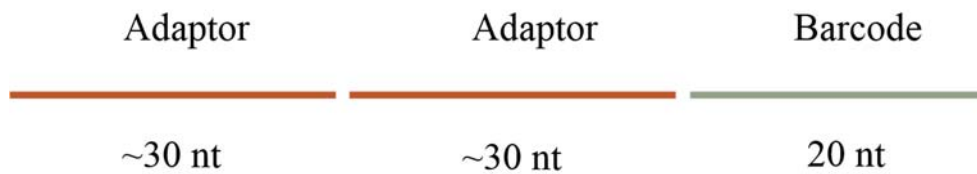


Figure 2.4 - Schematic of cDNA fragments that do not have a miRNA inserted, which make up the ~85 bps adaptor dimer peak on the library-quantification electropherogram.



Figure 2.5 - Schematic of cDNA fragments that have a miRNA inserted, which make up the ~100 bps sample peak on the library-quantification electropherogram.

When samples do not undergo proper size selection, the library would often contain large RNA species including transfer RNAs (tRNAs) and ribosomal RNAs (rRNAs). tRNAs are typically 76-90 nts in length, whereas rRNA species most likely to be present in the prepared libraries were the 5S subunit (~121 nts) and the 5.8S subunit (156 nts) (**Figure 2.3**).

2.4.4.1.8 Pool and Dilute Small RNA Libraries for Template Preparation

Once the molarity of each barcoded cDNA library (50-300 bps size range used) was determined, all libraries were diluted to 100pM. An equal amount of each library was

pooled for templating onto Ion Sphere particles™ (ISPs). All sequencing for this project was performed by a laboratory assistant in the Rahman-O’Rielly lab.

2.4.4.2 Prepare Template for Sequencing

The Ion Torrent sequencing system has limited sensitivity and therefore cDNA libraries must undergo amplification prior to sequencing. This amplification is done by emulsifying PCR using ISPs (TFS™). During this procedure one cDNA fragment is bound to an ISP, which then undergoes oil emulsification to ensure no other fragments are bound. These ISPs bound with cDNA templates (T+ISPs) then undergo amplification in the OneTouch System where the cDNA is used as a template and the fragment is replicated exponentially.

To quantify the T+ISP, the T+ISPs are fluorescently labelled, with one fluorophore bound to the Ion Sphere particles and one fluorophore bound the cDNA template that is bound to the ISP. The quantity of these fluorophores is measured and a ratio is generated that represents the proportion of template-positive ISPs in a sample. Inter-run variability in the proportion of T+ISPs in a sample is expected and is removed during normalization. The higher the proportion of T+ISPs in a sample the higher the quality of sequencing results can be anticipated.

2.4.4.3 Hi-Q OneTouch2 200 Kit

2.4.4.3.1 Prepare Template-positive ISPs

Samples were templated onto ISP’s and amplified on the Ion OneTouch™ 2 System (OT2) (TFS™, Catalogue#:4474779. Waltham, MA., USA) by emulsion PCR. The

ION PI Master Mix (TFS™) and ISP's were brought to room temperature. The enzyme mix and pooled library were kept on ice. The input concentration of the pooled libraries was between 6-8pM in a volume of 100µl. ISPs and Master Mix were vortexed at maximum speed for one minute to re-suspend particles then briefly spun down. The following components were added to 2mL of ION PI Master Mix: 80µl of H₂O, 120µl of Ion PI Enzyme Mix (TFS™), 100µl of ISPs, and 100µl of diluted libraries. The amplification solution was vortexed, spun briefly, and added through the sample port of the Reaction Filter 800µl at a time. 200µl of Ion OT Reaction Oil (TFS™) was added through the sample port. The reaction filter was then inverted ensuring the sample port was rotated clockwise over the other two ports and loaded onto the OneTouch2 instrument (TFS™) within 15 minutes of preparation.

Breaking solution was added to the Recovery Tubes (TFS™) in the OT2 instrument and the run was started. A final spin was done at the end of the run to pellet the template-positive ISPs. The recovery tubes were removed and all but approximately 100µl of recovery solution was removed from each tube and discarded. The remaining 100µl was used to re-suspend the template-positive ISPs by pipetting. The suspensions were then combined in a fresh LoBind tube (Eppendorf™, Catalogue#: 022431005, Hamburg, DE.). To recover any remaining sample from the tubes, 100µl of H₂O was used to rinse the recovery tubes and then added to the LoBind tube (Eppendorf™). The combined suspensions were brought up to 1mL with H₂O and vortexed for 30 seconds. The template-positive ISP suspensions were then centrifuged at $15,500 \times g$ for 8 minutes. All but approximately 20µl of the supernatant was discarded. The remaining 20µl was diluted up

to 100µl with ISP Resuspension Solution. The solution was then vortexed for 30 seconds and spun briefly.

2.4.4.3.2 Assess Quality of Unenriched, Template-positive ISPs

A Qubit® 2.0 Fluorometer (TFS™, Catalogue#: Q32866. Waltham, MA., USA) and the ION Sphere Quality Control Kit (TFS™, Catalogue#: 4468656. Waltham, MA., USA) were used to assess the quality of the unenriched, template-positive ISPs. Two fluorescent labels were used to determine what percentage of the ISP were bound with templates. One label (Alexa Fluor 488 [TFS™]) was bound to the ISP itself and another (Alexa Fluor 647 [TFS™]) was bound to the template-bound ISP. The ratio of bound ISPs over total ISPs is depicted by the 647:488 fluorescence ratio.

Each emulsified sample was run separately on the Qubit® by loading 2µl of the unenriched ISPs into a 0.2 mL PCR tube, 19µl of Annealing Buffer (TFS™), and 1µl of probes. The solution was mixed well, and the samples were loaded into the SimpliAmp Thermal Cycler and run at 95°C for 2 minutes followed by 37°C for 2 minutes. Then 200µl of Quality Control Wash Buffer (TFS™) was used to wash off the unbound probes. Once added, the solution was vortexed properly and centrifuged at maximum speed for 3 minutes. Ensuring not to disrupt the ISP pellets, all but 10µl of supernatant was discarded. The wash step was repeated twice more for a total of three washes. After the final wash, 190µl of Quality Control Wash Buffer was added and mixed well for a total volume of 200 µl. The sample was then loaded into a Qubit™ Assay Tube (TFS™, Catalogue#: Q32856. Waltham, MA., USA), the Qubit Instrument (TFS™) and the percentage of bound ISPs was calculated.

2.4.4.3.3 Enrich the Template-positive ISPs

The sample was then enriched for template-positive ISPs using the Ion PI™ Hi-Q Template OT2 200 Kit (TFS™, Catalogue#: A26434, Waltham, MA., USA). Melt-off Solution (TFS™) was prepared fresh using 280µl of Tween Solution (TFS™) and 40µl of NaOH (TFS™). MyOne C1 Beads (TFS™) were vortexed and 100µl was transferred into a fresh 1.5mL LoBind tube. The tube was then placed on a magnetic rack for 2 minutes. The supernatant was removed and discarded without disturbing the pelleted beads. Then, 1mL of One Touch Wash Solution (TFS™) was added and the tube was removed from the magnetic rack. After being vortexed for 30 seconds and briefly centrifuged the tube was placed back on the rack for 2 minutes. The supernatant was once again removed and discarded. A total of 130µl of MyOne Bead Capture Solution (TFS™) was added to the tube which was removed from the rack, vortexed, and spun briefly.

An 8-well strip was prepared for loading into the OneTouch Enrichment System (ION One Touch ES; TFS™). Ensuring that all reagents and solutions were mixed well before transferring the following was added to the strip: well 1, template-positive ISPs (TFS™) (100 µl); well 2, MyOne C1 resuspended beads (TFS™) (130 µl); wells 3-5, One Touch ES Wash Solution (TFS™) (300µl each); well 6 & 8, empty; well 7, Melt-Off Solution (TFS™) (300 µl). Once loaded with the other components the OT ES was run. After the run was complete, the 0.2mL tube containing the enriched ISPs was centrifuged for 5 minutes at $15,500 \times g$. All but 10µl of the supernatant was then removed, and 200µl of H₂O was added and mixed well. The solution was then re-centrifuged at $15,500 \times g$ for 5 minutes. The tube was visually inspected for a brown pellet.

If the pellet is present, then the solution was pipetted up and down to re-suspend the pellet. The tube was then placed on a magnetic rack for 4 minutes. The supernatant was transferred into a new 0.2mL tube without disturbing the pellet, then centrifuged at 15,500 × g for 5 minutes. All but 10µl of the supernatant was removed and H₂O was then mixed well into the solution for a final volume of 100 µl. If the pellet was not present, all but 10µl of the supernatant was removed and discarded. The solution was brought to 100µl with H₂O and the pellet was re-suspended. The re-suspended solution continued on to sequencing.

2.4.4.4 Ion PI Hi-Q Sequencing 200 Kit

Once the Ion Proton System for Next-Generation Sequencing System (TFS™, Catalogue#: 4476610. Waltham, MA., USA) was properly initialized and the planned run created, the enriched template-positive ISPs were prepared and the chip was loaded for sequencing using the Ion PI Hi-Q Sequencing 200 Kit (TFS™, Catalogue#: A26433. Waltham, MA., USA).

2.4.4.4.1 Prepare the Enriched Template-positive ISPs for Sequencing

The Control ISPs (TFS™) were re-suspended and 5µl was mixed well with the enriched, template-positive ISPs. The solution was then centrifuged for 5 minutes at 15,500 × g. Without disturbing the pellet, all but 10µl of supernatant was discarded. 15µl of Annealing Buffer (TFS™) and 20µl Sequencing Primer (TFS™) were added to the solution which was briefly vortexed and spun. The reaction was then loaded into the SimpliAmp Thermal Cycler (95° for 2 minutes, 37° for 2 minutes). Then 10µl of Loading Buffer (TFS™) was added and the solution was vortexed and spun.

2.4.4.4.2 Load the ION PI Chip v3

The entire prepared sample (55µl) was dispensed into the Ion P1 Chip v3 (TFS™) loading well. The chip was then spun in the minifuge for 10 minutes. Foaming solution was created by adding 49µl of 50% Annealing Buffer (TFS™) with 1µl of ION PI Foaming Solution (TFS™) and injecting 100µl of air with a p200 pipette and tip into the mixture and mixing well. An additional 100µl of air was injected into the mixture and mixed again. Excess reagents were washed from the chip by adding 100µl of foam into the chip loading port. The liquid expelled from the exit well was removed. 55µl of 50% Annealing buffer was dispensed into the chip loading well, and the chip was spun in the minifuge for 30 seconds. Liquid was removed from the exit well. 100µl of foam was injected into chip loading port. 55µl of 50% Annealing Buffer was dispensed into chip loading well, and the chip was spun in the minifuge for 30 seconds. Excess liquid was removed from the exit well. 100µl of Flushing Solution (TFS™) was injected into the chip loading port three times, while avoiding transferring bubbles from the pipette tip. The expelled liquid was removed from the exit well after each injection. Then 6µl of Hi-Q Sequencing Polymerase (TFS™) was then combined with 60µl of 50% Annealing Buffer and mixed. 65µl of the Polymerase Solution (TFS™) was then injected into the chip loading port, and the expelled liquid was remove from the exit well. The chip was left to incubate for 5 minutes at room temperature before being loaded into the Ion Proton System for Next-Generation Sequencing System (TFS™) and initiating the sequencing run.

The patient samples loaded onto PI chips were barcoded such that the three time points for each patient could be loaded onto the same chip. Because of the barcoding system

that was established to accommodate the larger project, the pre-treatment samples could not all be loaded onto the same chip and were therefore loaded on two separate chips (see Future Directions – **Section 4.8**).

2.5 Grouping Patients by Clinical Response

The primary endpoint indicated by the rheumatologist was ACR50 responders, as this was deemed a more meaningful outcome than ACR20. A patient is deemed an ACR50 responder when a 50% improvement in tender or swollen joint counts is achieved and there is a 50% improvement in at least three of the other five criteria outlined in the introduction (PhUSE Wiki contributors, 2012). Clinical parameters used in this categorization included CDAI, PRO's, HASQ-DI, and an acute phase reactant (ESR).

2.6 PGx Patient Data Analyses

The comprehensive miRNA analyses were performed with patients categorized as ACR50 responders (patient 2, 10, 13, and 14) and ACR50 non-responders (patient 6, 7, 8, 11, and 12), as indicated by the rheumatologist. Data collected from the sequencing of these samples was processed with the comprehensive miRNA analyses pipeline and used for subsequent analyses.

2.6.1 Comprehensive miRNA Analyses Pipeline

The sequencing results from the Ion Proton System for Next-Generation Sequencing were exported out as a FASTQ file, which contains the raw sequencing reads

of each sample and provides a numeric quality score for each nucleotide in the raw sequencing reads (Cock, Fields, Goto, Heuer, & Rice, 2010). In order to analyze the sequencing results, the FASTQ files were loaded into a miRNA-Seq pipeline (**Figure 2.6**) designed by the Rahman-O’Rielly Data Analyst.

2.6.1.1 Read Pre-Processing

The Ion Torrent FASTQ raw read files were submitted for pre-trim quality assessment by the FastQC software. This software reports on the quality of the reads and enables the user to customize the trimming of adapters and nucleotides from the 3’ and 5’ ends that have low-quality read depth. The adapters were then trimmed off of the raw reads using the Cutadapt (Marcel Martin, MIT-licensed) software and the file was then submitted for post-trim quality assessment by the FastQC software (Babraham Bioinformatics) (Martin, 2011).

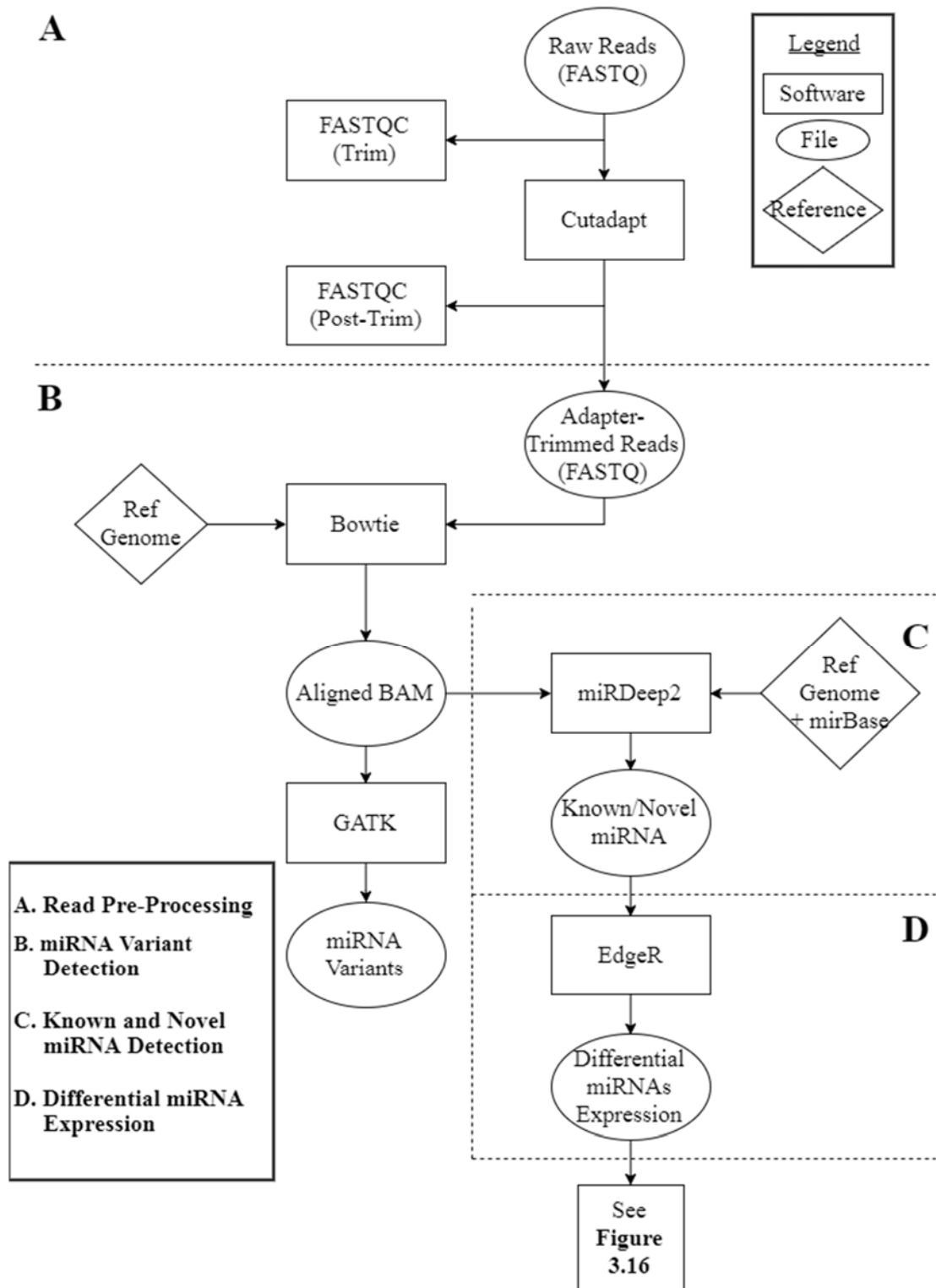


Figure 2.6 – Flow chart of comprehensive miRNA analyses pipeline. See **Figure 3.16** for in-depth analyses of differentially expressed miRNAs.

2.6.1.2 miRNA Variant Detection

For each sample the Bowtie alignment software (John Hopkins University) is used to align the adaptor-trimmed reads in a FASTQ file and generates the Binary Alignment Map (BAM) file to the human reference genome (hg19), which contains the genomic positions of the short reads in a binary and compressed format (H. Li et al., 2009). The aligned BAM file was then submitted to Genome Analysis ToolKit (GATK) software (Broad Institute) which called the detected miRNA variants.

2.6.1.3 Known and Novel miRNA Detection

The aligned reads in BAM file format were then submitted for mapping using miRDeep2 mapper software (Max Delbrück Center) (Friedlander, Mackowiak, Li, Chen, & Rajewsky, 2012). The miRDeep2 module was used to detect the reads that mapped to miRNA loci and compared them to the miRBase database, which is curated with known, annotated miRNAs. A summary report file and a file that quantifies known and novel miRNAs from that sample were then generated for differential miRNA expression analysis.

2.6.1.4 Differential miRNA Expression Analyses of ACR50 Response Groupings and Clinical Data Sets

The known and novel miRNAs' expression was then analyzed using the edgeR software (Bioconductor) to detect differentially expressed miRNAs between response groupings and on clinical datasets. The read counts were normalized before comparison to decrease the potential for read biases. The edgeR software normalizes the read data by dividing the read count by the total number of reads; this value is then rescaled to counts

per million (I. Gonzalez, 2014). Boxplots and multi-dimensional scaling (MDS) plots were generated to visualize the read distribution and clustering of the samples. The data was separated by the dichotomous response groupings, ACR50 responders vs. non-responders, and the expression level of a miRNA in responders was compared to the average expression level of that miRNA in the non-responders.

Increased and decreased expression is indicated by the fold change value (logFC), when this value is greater than zero there is increased miRNA expression and when this value is less than zero there is decreased miRNA expression. In the analysis, the logFC of miRNA 'x' was calculated as $\log(\text{expression of miRNA } x \text{ in responders})$ minus the $\log(\text{expression of miRNA } x \text{ in non-responders})$. Thus, a logFC value greater than zero indicates higher expression of the corresponding miRNA in responder, while a logFC value less than zero indicates higher expression of the corresponding miRNA in non-responders.

Linear regression was performed to determine if there was an association between differentially expressed miRNAs and ACR50 response groups or clinical datasets (HAQ-DI, CDAI, and ESR). These findings were deemed statistically significant at a False Discovery Rate (FDR) <0.05 , corrected using the Benjamini–Hochberg procedure. Given that this is an exploratory study, findings with $0.05 > \text{FDR} < 0.2$ (selected by the Rahman-O’Rielly bioinformatician based on previous experience and literature assessment) were deemed suggestively significant (Motta et al., 2013; Weilner et al., 2015). Increasing the cut off will detect more lenient associations, because these analyses were exploratory in nature this was done to test the methodology.

When no suggestive significance was reached, the top 100 differentially expressed miRNAs were prioritized for investigations of collectively targeted genes to attempt to identify significant associations. This analysis was performed to determine the probability of miRNA-mRNA binding. This was done by examining the structure and accessibility of the site of potential binding, otherwise known as miRNA-recognition elements (Reyes-Herrera, Ficarra, Acquaviva, & Macii, 2011). The target gene prediction was based on the dataset from microrna.org, which is a well-curated database with conserved miRNAs and accurate mirSVR scores (Betel, Koppal, Agius, Sander, & Leslie, 2010). mirSVR scores are generated based on contextual features of binding and target site information using a single integrated model trained with support vector regression (a supervised, machine learning algorithm) (Betel et al., 2010). The mirSVR scores are interpreted as a likelihood of target downregulation, as the mirSVR approaches zero the meaningfulness of the potential downregulation drops as the number of target prediction quickly rises. The predicted binding score for these analyses was set at a cut off of mirSVR >0.3, resulting in a lower number of predictions that have a higher probability of occurring.

Review of the literature published on the identified differentially expressed miRNAs (from both response groupings and clinical datasets) was performed using miRBase and PubMed. miRBase was used to establish if the identified miRNA was the major or minor product was done in order to determine potential variation in nomenclature for searching on PubMed. Each miRNA was searched using the hsa- prefix, the simple miR nomenclature, as well as the * or -3p/-5p suffixes. The search results were reported on if the study pertained treatment response or pathogenesis of related disorders.

2.6.1.4.1 Gene Pathway Analyses Using Top-100 Differentially Expressed miRNAs

A gene pathway analysis was done using the Fisher's-exact-T test the findings were adjusted by FDR. The database used for this pathway analysis was the Kyoto Encyclopedia of Genes and Genomes (KEGG) (Kanehisa Laboratories). The miRNA pathway analysis was performed using the top 100 differentially expressed miRNAs (~5% of total known miRNA) to determine which pathways are common to these miRNAs and response groupings or clinical datasets (data not shown).

2.6.1.4.2 miRNA-mRNA Network Analyses and *in silico* Functional Analysis of Top 100 Differentially Expressed miRNAs

The top 100 differentially expressed miRNAs and the collectively targeted genes for response groupings or clinical dataset underwent a network analysis where the miRNA-mRNA interactions were visualized by Cytoscape software (Cytoscape Consortium); similarly, the data underwent an *in silico* functional enrichment analysis and functional module interactions were also visualized by Cytoscape software. The GO (Gene Ontology) Consortium project is a database of standardized nomenclature for genes and gene products relevant to molecular functions, biological processes, or cellular locations. Using this controlled vocabulary, genes and gene products are grouped into bins (otherwise known as gene sets of functional groupings) based on their relatedness. In the context of this project, genes collectively targeted by differentially expressed miRNAs were entered into the GO software and associations were identified to significantly enriched gene sets based on biological processes.

These associations are indicated with lines of varying thicknesses, which are representative of Kappa scores. A Kappa score is a measure of correlation between two terms. In the context of this data a thicker line indicates a stronger interaction, between miRNA and mRNA or between miRNA-mRNA predicted binding and a biological process, and a higher probability that the correlation has been experimentally validated (either *in vitro* or *in silico*). Therefore, there is a positive correlation between the line thickness and predicted miRNA-mRNA binding. The network analysis visualized the miRNA that collectively target the same mRNA, and the *in silico* functional analysis visualized the biological processes that are collectively associated with the miRNA-mRNA interactions.

CHAPTER 3

3 RESULTS

3.1 Optimization of Circulating miRNA Library Preparations

The first objective of this project was to develop and optimize a procedure for preparing successful circulating miRNA libraries for sequencing with Ion Torrent Technology. Two different protocols were investigated in an attempt to optimize circulating miRNA library preparation. Briefly, the modified Thermo Fisher protocol yielded low-quality results and therefore additional modifications were made in an attempt to improve library quantification and sequencing quality. After many unsuccessful library preparations using various modifications to the original Thermo Fisher protocol, a second protocol entitled “*Small RNA Library Construction for Exosomal RNA from Biological Samples for the Ion Torrent PGM™ and Ion S5™ System*” called the Cheng et al. protocol, modifications of which successfully sequenced samples.

This section provides the results of the investigations that contributed to the optimization of library preparation for circulating miRNA. This procedure is technically challenging, labour intensive, and with minimal quality analysis steps; therefore, it was common to have uninformative results. The results that did not contribute to the optimization of the procedure were not included (n=8, see **Appendix A** for examples).

The procedures utilized to optimize miRNA libraries and the samples used to achieve this (**Figure 3.1**) as well as the library preparation and sequencing metrics (**Table**

3.1) are provided. The successful libraries were then used to test the chip loading capacity using a varying number of samples at varying molarities (**Figure 3.1**).

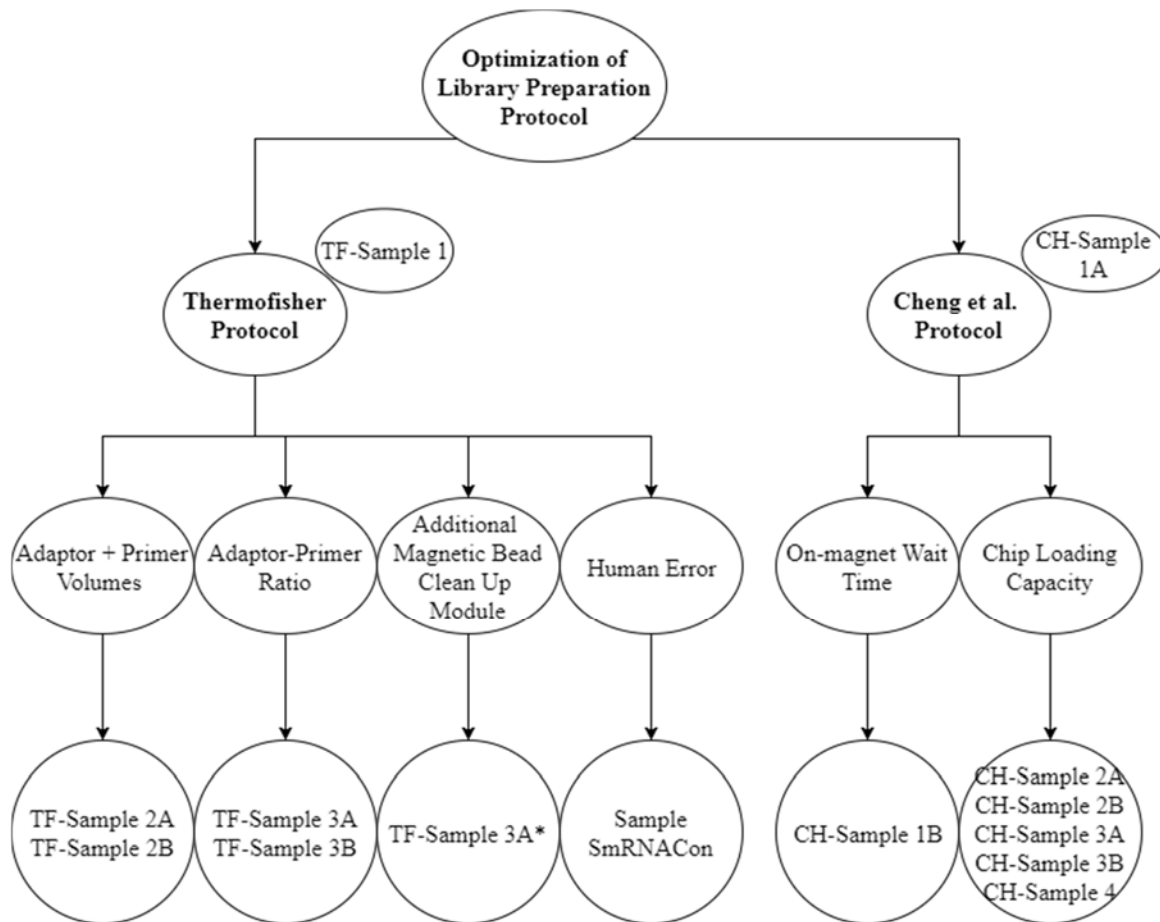


Figure 3.1 – Overview of the modification performed for the optimization of the library preparation protocol. The Thermo Fisher (TF) and Cheng et al. (CH) protocols underwent various modifications to determine the optimal procedure for miRNA library preparation.

Table 3.1 - Library preparation and sequencing metrics with descriptions and desired range.

Library & Sequencing Metrics	Description
Total Molarity	This value indicates total concentration of the prepared library that falls within the anticipated read lengths of a miRNA sample library (50-300 bps– indicated by the red lines on the electropherogram). The highest possible regional molarity is optimal when considering the electropherogram profile, which should have a sample peak within the desired read length (94-114 bps). The total molarity of libraries quantified over the course of this project range between 47.1- 362nmol/l.
Regional Molarity	This value indicates the concentration of the prepared library that falls within the desired read length (94-114 bps– indicated by the green lines on the electropherogram), and therefore is likely to contain miRNA. The highest possible regional molarity is optimal while considering the electropherogram profile, which should have a sample peak within the desired read length. The regional molarity of libraries quantified over the course of this project range between 5.32-165nmol/l.
Percent Regional Molarity	The percent region molarity is calculated by the regional molarity divided by the total molarity. This value indicates the percentage of the prepared library that falls within the desired read length. A percent regional molarity of ~50% is likely to produce quality sequencing results; however, the electropherogram profile should be taken into consideration when determining if the library is of adequate quality to sequence.
Mean Read Length	The average size of cDNA fragments, with an optimal length of 15-35 bps.
Total Reads	The number of cDNA fragments in the library, with the highest possible quantity being optimal.
Reads Passing Filter	The number of cDNA fragments that are of sufficient quality, with the highest possible quantity of total reads being optimal
Aligned Reads	The number of cDNA fragments that mapped to the hg19 reference genome, with the highest possible quantity of aligned reads being optimal.
Percent Mapped Reads	The proportion of reads passing filter that aligned to the hg19 reference genome, with the highest percentage possible.
miRNA Reads	The number of reads that map to an annotated/known miRNA regions of the genome, optimally exceeding 1 million.
Percent miRNA Reads	The percentage of reads passing filter that mapped to a known miRNA region of the genome, optimally exceeding 10%.
Number Of miRNA Detected	The number of different miRNA detected in each library, with an optimal total number of 400-800.

3.1.1 miRNA Library Preparation and Sequencing using the Thermo Fisher Protocol Modifications

3.1.1.1 Modified Thermo Fisher Protocol #1 (TF-Sample 1)

TF-Sample 1 was the first sample processed through the circulating miRNA sequencing pipeline using the modified Thermo Fisher protocol for intracellular miRNA extraction and library preparation (**Figure 3.2**).

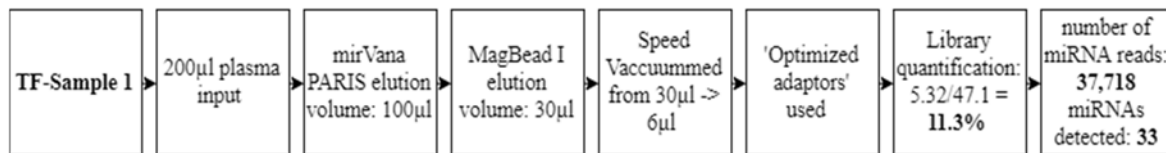


Figure 3.2 – Flow chart depicting protocol modifications and subsequent results in TF-Sample 1.

The library of TF-Sample 1 was quantified as having a total molarity of 47.1 nmol/l and a regional molarity of 5.32 nmol/l, resulting in an inadequate regional molarity percentage of 11.3% (**Table 3.2**). Quality assessment revealed a large adaptor dimer peak at 85 bps with an insufficient sample peak corresponding to miRNA at 102 bps (**Figure 3.3**). The library of TF-Sample 1 sequenced 59,075 miRNA reads that passed quality filters, 63.85% of which mapped to known miRNAs, detecting a total of 33 different miRNAs. However, most metrics failed to meet the minimum requirements of a successfully prepared library (**Table 3.3**).

Table 3.2 – Results of the library quantification of TF-Sample 1.

Library Quantification Metrics	Desired Thresholds	TF-Sample 1
Total Molarity	High	47.1 nmol /l
Regional Molarity	High	5.32 nmol /l
Percent Regional Molarity	~50%	11.3%.

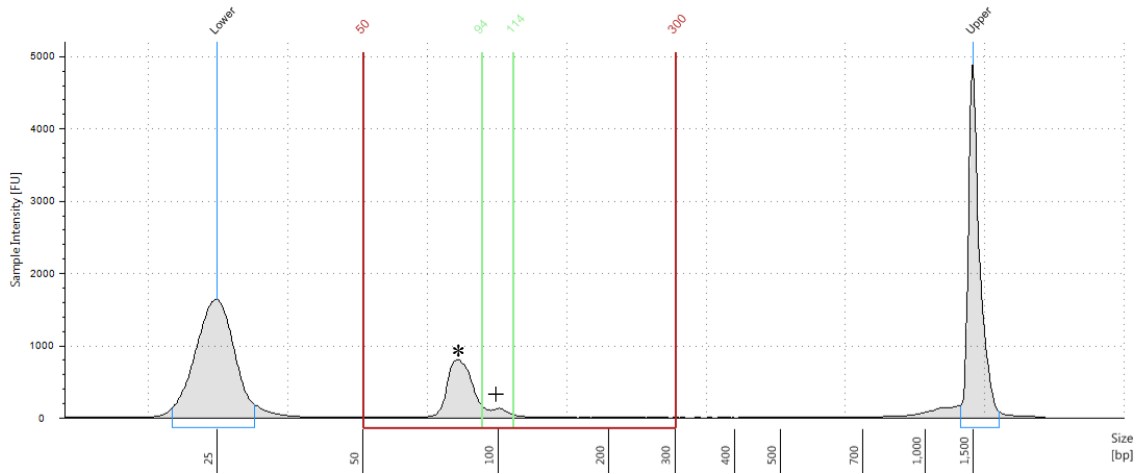


Figure 3.3 - Electropherogram depicting the size distribution and concentration of small RNA in the TF-Sample 1 library. The y-axis is the measure of fluorescence units, representing the sample concentration, and the x-axis is a measure of base pairs, representing the length of the cDNA fragment. The first and third peak indicate the lower and upper marker, known to be 25 and 1500 base pairs long. The peak in the middle is representative of TF-Sample 1 library, where the * indicates the adaptor dimer and the + indicates the sample. The red lines on the electropherogram indicate the read lengths spanning from 50-300 bps, indicating the total molarity. The green lines on the electropherogram indicate the read lengths spanning 94-114 bps, indicating the regional molarity.

Table 3.3 – Results of circulating miRNA sequencing of TF-Sample 1.

Sequencing Metrics	Desired Thresholds	TF-Sample 1
Mean Read Length	15-35 bps	17 bps
Total Reads	10M	133,744
Reads Passing Filters	Highest % of total	59,075
Aligned Reads	Highest % of total	46,247
Percent Mapped Reads	High	78.29%
miRNA Reads	>1M	37,718
Percent miRNA Reads	>10%	63.85%
miRNA Detected	400-800	33

3.1.1.2 Modified Thermo Fisher Protocol #2 (TF-Sample 2)

In an attempt to reduce the adaptor dimer, half of the indicated adaptor and primer input was added during library preparation and the plasma input was increased to 625µl on the recommendation of the FAS (**Figure 3.4**).

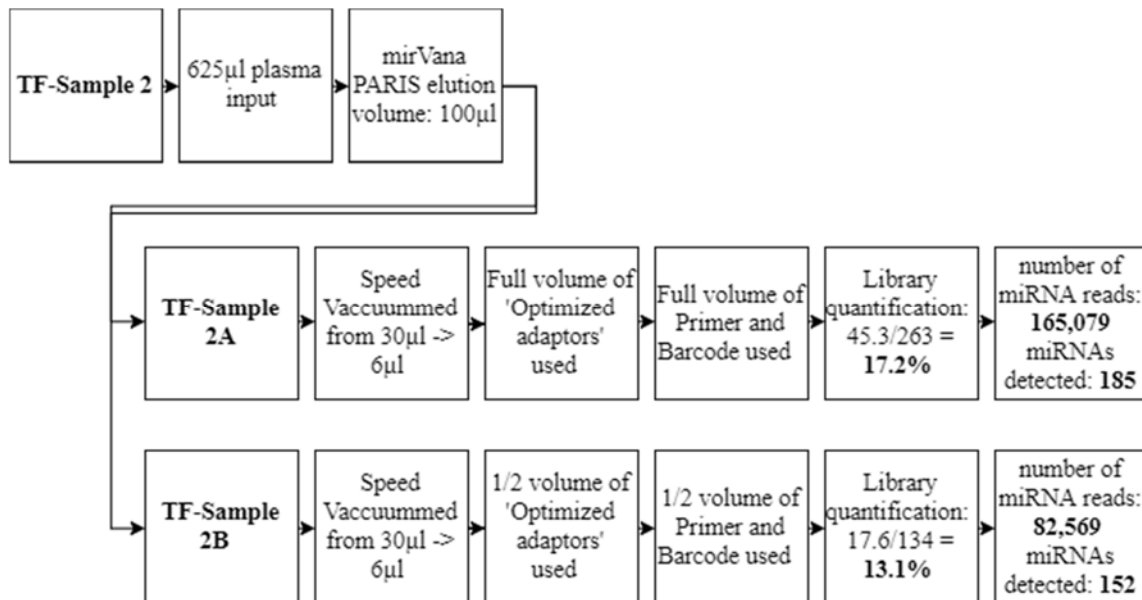


Figure 3.4 - Flow chart depicting protocol modifications and subsequent results in TF-Sample 2A and TF-Sample 2B.

When the input volume of plasma was increased (TF-Sample 2A), all metrics relating to molarity were increased compared with TF-Sample 1 (**Table 3.4**). Similarly, all sequencing metrics were also increased relative to TF-Sample 1 except percent miRNA reads. TF-Sample 2A was quantified as having a total molarity of 263 nmol/l and a regional molarity of 45.3 nmol/l, resulting in a regional molarity percentage of 17.2% (**Table 3.4**). The electropherogram showed a very large adaptor dimer peak at 89 bps, a small peak in the shoulder at approximately 102 bps, and another small peak at 148 bps (**Figure 3.5**). All sequencing metrics for TF-Sample 2A failed to meet criteria except mean read length and percent miRNA reads. Library sequencing generated 165,079 miRNA reads that passed quality filters, 43.74% of which mapped to known miRNAs, detecting a total of 185 different miRNAs.

When the adapter and primer inputs were decreased by half, there was a corresponding decrease in total and regional molarity, while the percent regional molarity remained virtually unchanged. Likewise, the majority of sequencing metrics also increased compared with TF-Sample 2A. TF-Sample 2B was quantified as having a total molarity of 134 nmol/l and a regional molarity of 17.6 nmol/l, resulting in a regional molarity percentage of 17.6% (**Table 3.4**). The electropherogram showed a very large adaptor dimer peak at 89 bps, a small peak in the shoulder representing the sample at ~101 bps, and another small peak at ~146 bps (**Figure 3.6**). All sequencing metrics for TF-Sample 2B failed to meet criteria except mean read length and percent miRNA reads. Library sequencing generated 82,569 miRNA reads that passed quality filters, 30.64% of which mapped to known miRNAs, detecting a total of 152 different miRNAs (**Table 3.5**).

Table 3.4 - Results of the library quantification of TF-Sample 2A and TF-Sample 2B.

Library Quantification Metrics	Desired Thresholds	TF-Sample 2A	TF-Sample 2B
Total Molarity	High	263 nmol/l	134 nmol/l
Regional Molarity	High	45.3 nmol/l	17.6 nmol/l
Percent Regional Molarity	~50%	17.2%.	17.6%.

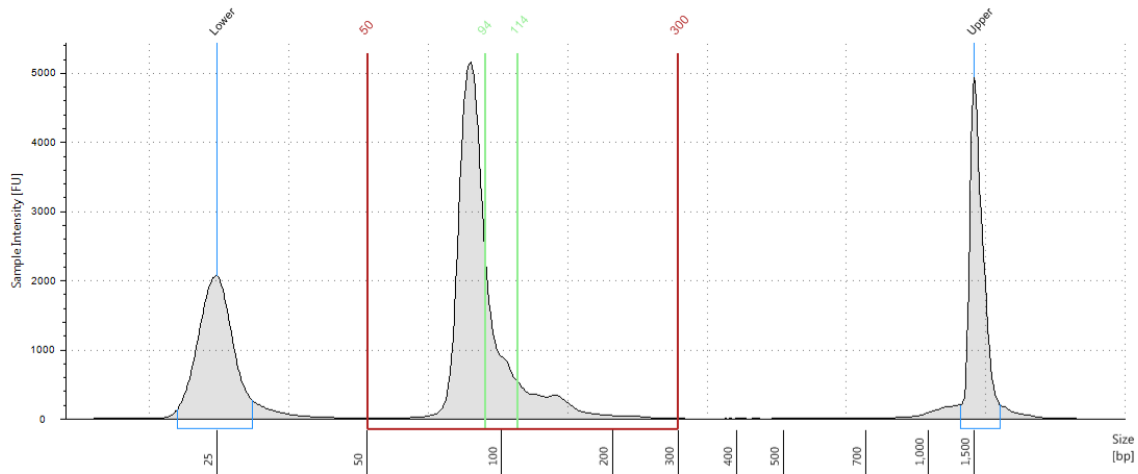


Figure 3.5 - Electropherogram depicting the size distribution and concentration of small RNA in the TF-Sample 2A library.

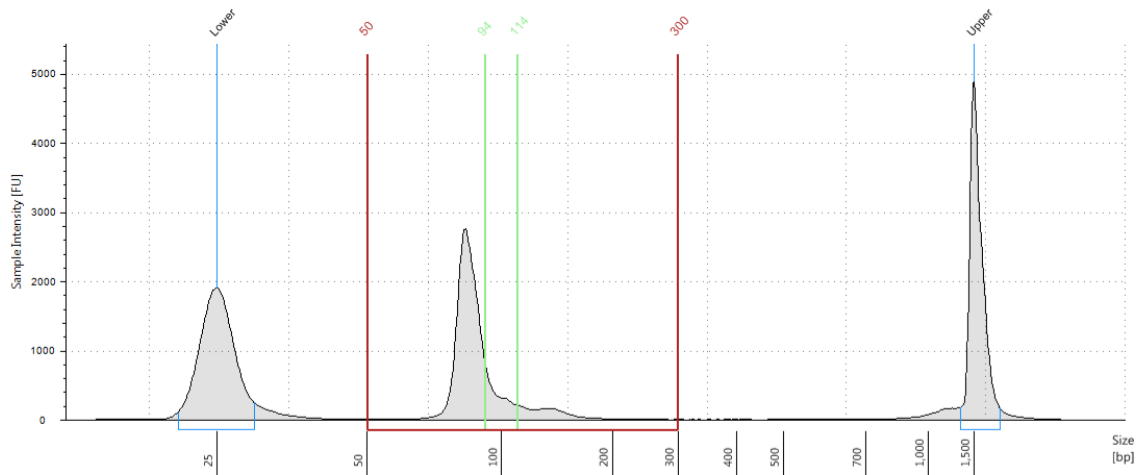


Figure 3.6 - Electropherogram depicting the size distribution and concentration of small RNA in the TF-Sample 2B library.

Table 3.5 – Results of sequencing TF-Sample 2A and TF-Sample 2B.

Sequencing Metrics	Desired Thresholds	TF-Sample 2A	TF-Sample 2B
Mean Read Length	15-35 bp	22 bp	28 bp
Total Reads	10M	793,158	473,909
Reads Passing Filters	Highest % of total	377,393	269,470
Aligned Reads	Highest % of total	334,319	238,980
Percent Mapped Reads	High	88.59%	88.69%
miRNA Reads	>1M	165,079	82,569
Percent miRNA Reads	>10%	43.74%	30.64%
miRNA Detected	400-800	185	152

3.1.1.3 Modified Thermo Fisher Protocol #3 (TF-Sample 3)

In an attempt to decrease the adaptor dimer, the adaptor input was reduced by half and a comparison was done between half the primer/barcode input and the full primer/barcode input using TF-Sample 3 (**Figure 3.7**).

TF-Sample 3A (half volume of primer and barcode) was quantified as having a total molarity of 133 nmol/l and a regional molarity of 21.7 nmol/l, resulting in a regional molarity percentage of 16.3% (**Table 3.6**). The electropherogram showed a very large adaptor dimer peak at 86 bps, a small sample peak at approximately 102 bps, and a small tRNA peak at 117 bps (**Figure 3.8**). TF-Sample 3A* (i.e., TF-Sample 3 that went through an additional cleanup process) was quantified as having a total molarity of 63.7 nmol/l and a regional molarity of 10.6 nmol/l, resulting in a regional molarity percentage of 16.6% (**Table 3.6**). The electropherogram showed a large adaptor dimer peak at 85 bps, a small sample peak at 104 bps, and a small tRNA peak at 116 bps (**Figure 3.9**). Library sequencing

generated 1,191,795 miRNA reads that passed quality filters, 31.47% of which mapped to known miRNAs, detecting a total of 307 different miRNAs (**Table 3.7**).

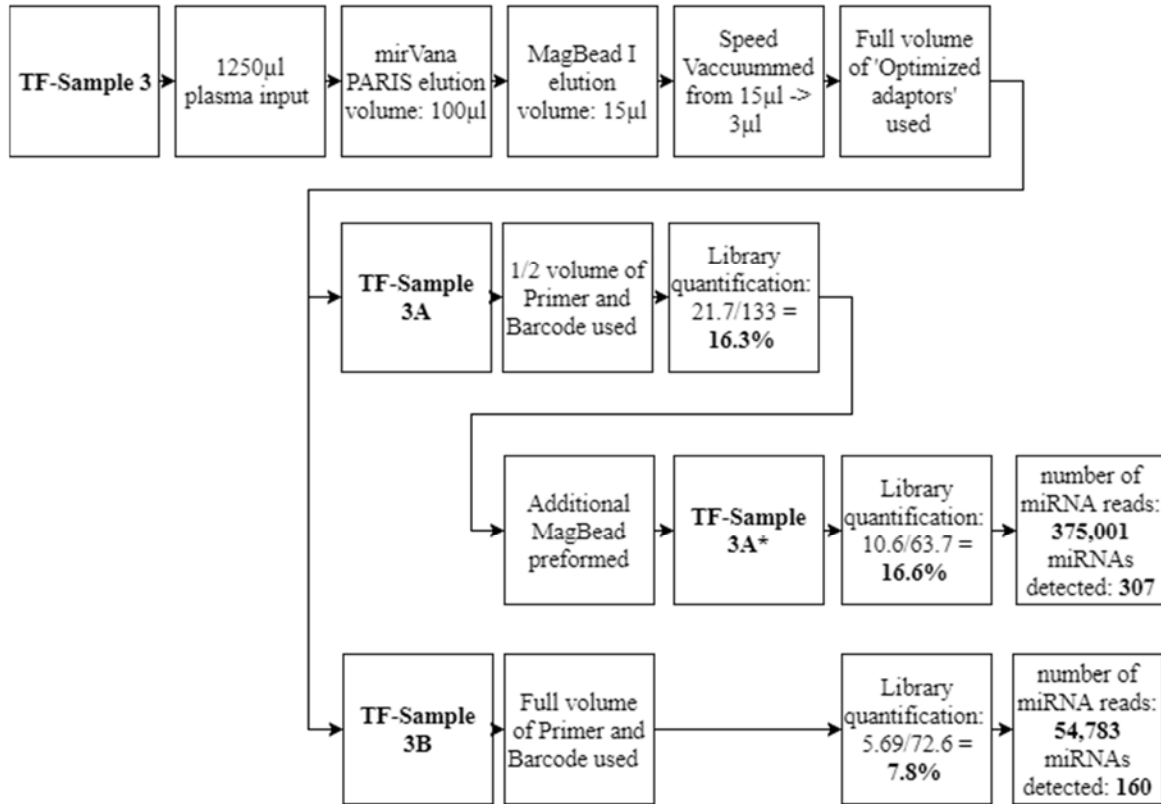


Figure 3.7 - Flow chart depicting protocol modifications and subsequent results in TF-Sample 3A, TF-Sample 3A*, and TF-Sample 3B.

TF-Sample 3B (full volume of primer and barcode) was quantified as having a total molarity of 72.6 nmol/l and a regional molarity of 5.69 nmol/l, resulting in a regional molarity percentage of 7.8% (**Table 3.6**). The electropherogram showed a large adaptor dimer peak at 84 bps as well as an extended shoulder of the slope which spanned the sample peak region (**Figure 3.10**). Library sequencing generated 128,149 miRNA reads that passed

quality filters, 42.75% of which mapped to known miRNAs, detecting a total of 160 different miRNAs (**Table 3.7**).

Table 3.6 - Results of the library quantification of TF-Sample 3A, TF-Sample 3A*, and TF-Sample 3B.

Library Quantification Metrics	Desired Thresholds	TF-Sample 3A	TF-Sample 3A*	TF-Sample 3B
Total Molarity	High	133 nmol/l	63.7 nmol/l	72.6 nmol/l
Regional Molarity	High	21.7 nmol/l	10.6 nmol/l	5.69 nmol/l
Percent Regional Molarity	~50%	16.3%	16.6%	7.8%

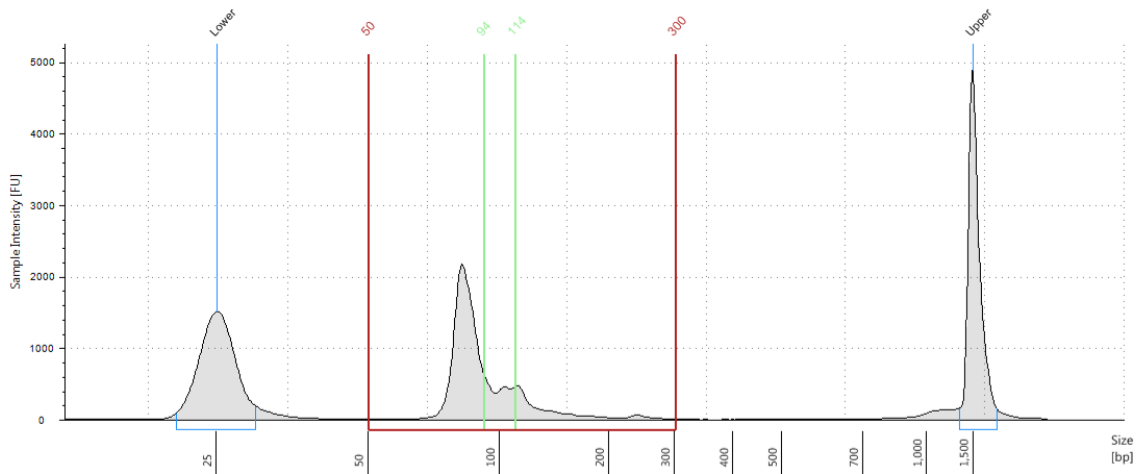


Figure 3.8 - Electropherogram depicting the size distribution and concentration of small RNA in the TF-Sample 3A library.

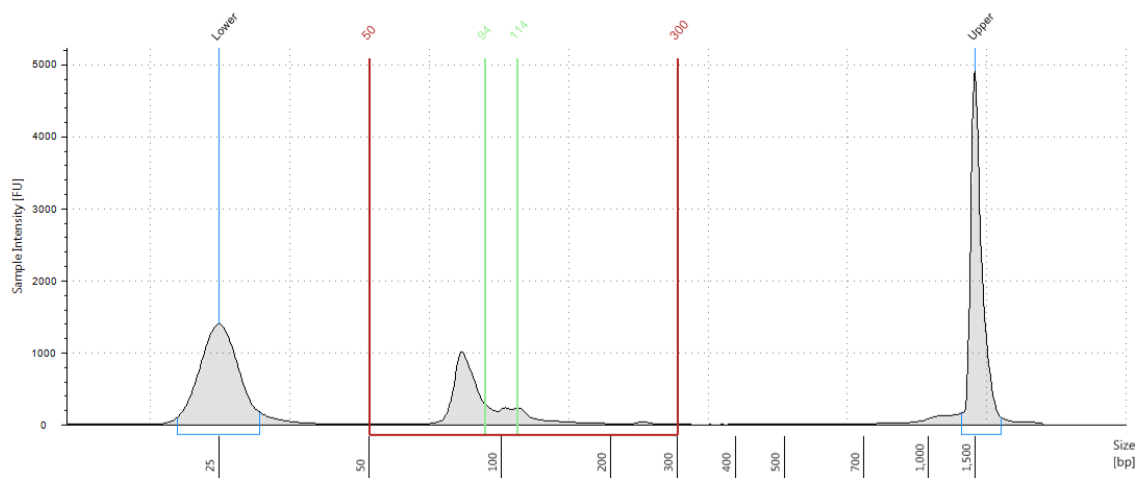


Figure 3.9 - Electropherogram depicting the size distribution and concentration of small RNA in the TF-Sample 3A* library.

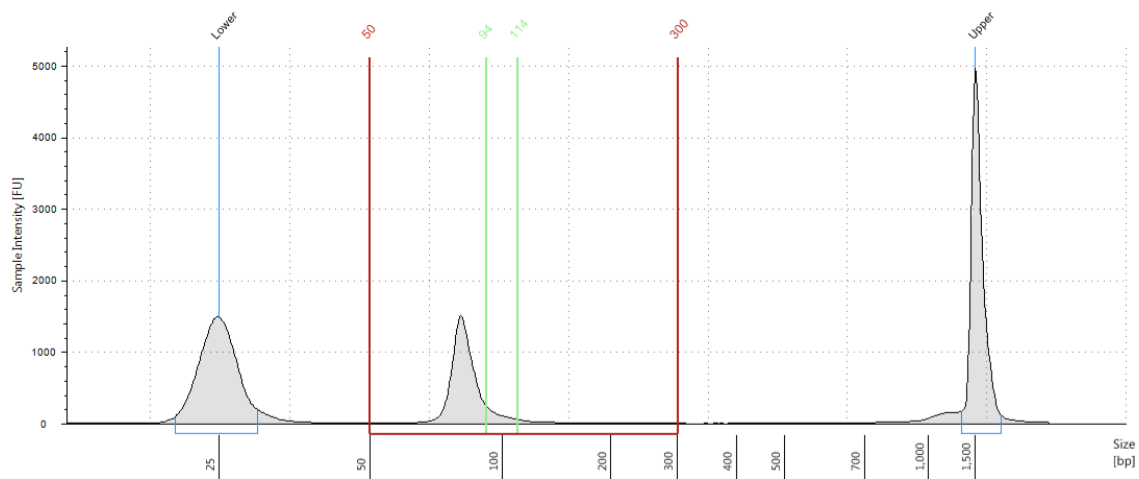


Figure 3.10 - Electropherogram depicting the size distribution and concentration of small RNA in the TF-Sample 3B library.

Table 3.7 – Results of sequencing TF-Sample 3A* and 3B.

Sequencing Metrics	Desired Thresholds	TF-Sample 3A*	TF-Sample 3B
Mean Read Length	15-35bp	32 bp	21 bp
Total Reads	10M	1,566,703	254,889
Reads Passing Filters	Highest % of total	1,191,795	128,149
Aligned Reads	Highest % of total	1,121,911	119,705
Percent Mapped Reads	High	94.14%	93.41%
miRNA Reads	>1M	375,001	54,783
Percent miRNA Reads	>10%	31.47%	42.75%
miRNA Detected	400-800	307	160

3.1.1.4 Small RNA Control Sample

At this point in the investigation, given the suboptimal results, assurance was needed that the procedure was being adhered to and proper laboratory techniques were being used. In order to control for human error, a Small RNA Control reagent included in the Ion RNA-Seq kit served as a standardized sample concentration used for library preparation (**Figure 3.11**).

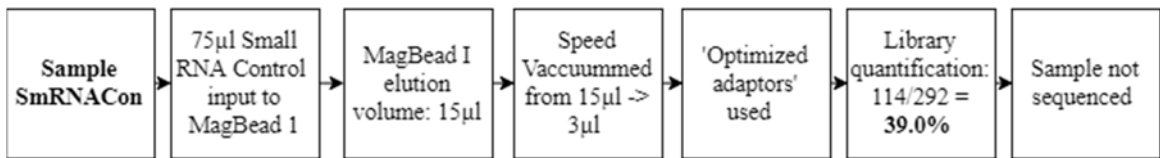


Figure 3.11 - Flow chart depicting protocol modifications and subsequent results in Sample SmRNACon.

“Sample SmRNACon” was quantified as having a total molarity of 292 nmol/l and a regional molarity of 114 nmol/l, resulting in a regional molarity percentage of 39%

(Table 3.8). The electropherogram showed a very large sample peak at 108 bps, a smaller peak at 164 bps and another large peak at 248 bps (Figure 3.12).

Table 3.8 - Results of the library quantification of Sample SmRNACon.

Library Quantification Metrics	Desired Thresholds	Sample SmRNACon
Total Molarity	High	292 nmol /l
Regional Molarity	High	114 nmol /l
Percent Regional Molarity	~50%	39%.

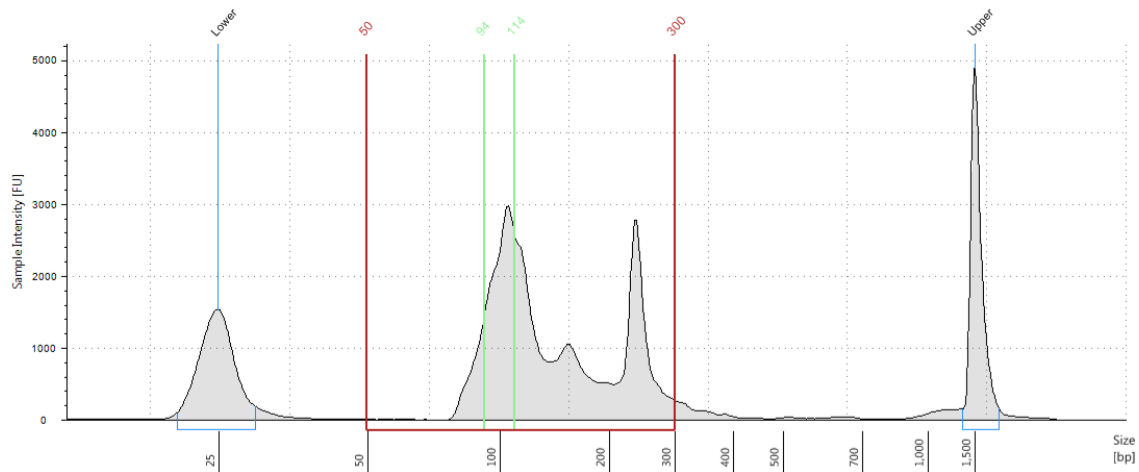


Figure 3.12 - Electropherogram depicting the size distribution and concentration of small RNA in the Small RNA Control library.

3.1.2 miRNA Library Preparation and Sequencing using the Cheng et al. Protocol Modifications

3.1.2.1 Modified Cheng et al. Protocol #1 (CH-Sample 1)

After establishing that the FAS-recommended protocol was inadequate for producing the desired library quality, a new protocol for library preparation published by Cheng et al. was attempted using CH-Sample 1. (Cheng et al., 2014)

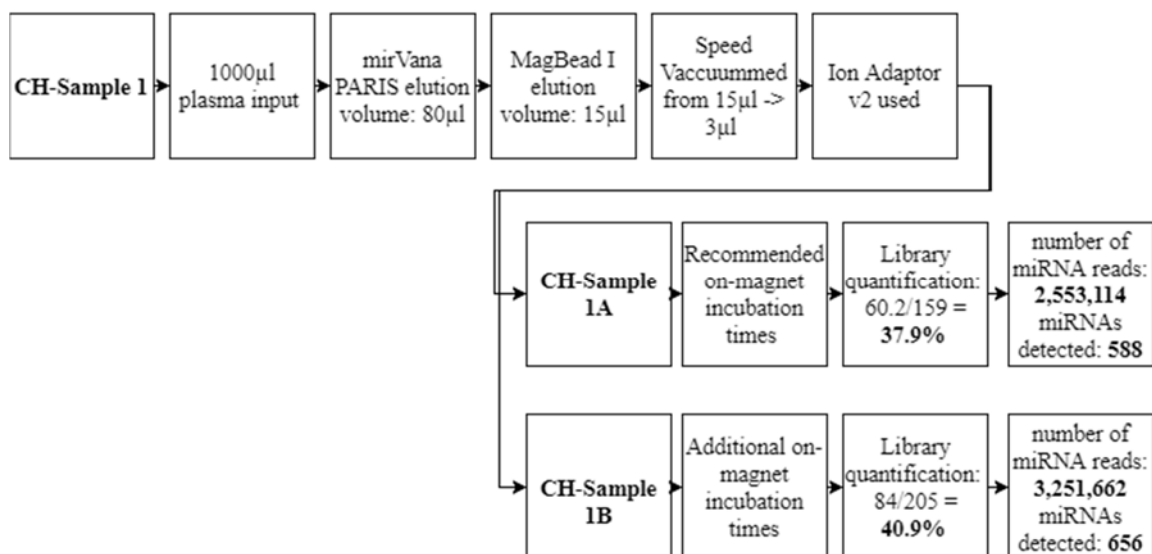


Figure 3.13 - Flow chart depicting protocol modifications and subsequent results in CH-Sample 1.

CH-Sample 1A was quantified as having a total molarity of 159 nmol/l and a regional molarity of 60.2 nmol/l, resulting in a regional molarity percentage of 37.9% (Table 3.9). The electropherogram showed a very small adaptor dimer peak at 87 bps, a very large miRNA sample peak at 117 bps, a small tRNA peak at 165 bps, and two small rRNA peaks at 186 bps and 246 bps (Figure 3.14). The library sequenced 10,395,297 reads

that passed quality filters, 24.56% of which mapped to known miRNAs, detecting a total of 588 different miRNAs.

The library generated using CH-Sample 1 was of acceptable quality; however, it contained undesired larger species of RNA. To reduce the quantity of larger RNA species, CH-Sample 1B was processed with additional on-magnet wait times (2 extra minutes) to increase the precision of the size selection process. CH-Sample 1B was quantified as having a total molarity of 205 nmol/l and a regional molarity of 84 nmol/l, resulting in a regional molarity percentage of 40.9% (**Table 3.9**). The electropherogram of showed a small adaptor dimer peak at 86 bps, a very large sample miRNA peak at 117 bps, a very small tRNA at approximately 166 bps, and a very small rRNA peak at 242 bps (**Figure 3.15**). The library generated 10,765,595 reads that passed quality filters, 30.20% of which mapped to known miRNAs, detecting a total of 656 different miRNAs (**Table 3.10**).

Table 3.9 – Results of the library quantification of CH-Sample 1A and CH-Sample 1B.

Library Quantification Metrics	Desired Thresholds	CH-Sample 1A	CH-Sample 1B
Total Molarity	High	159 nmol/l	205 nmol/l
Regional Molarity	High	60.2 nmol/l	84 nmol/l
Percent Regional Molarity	~50%	37.9%	40.9%

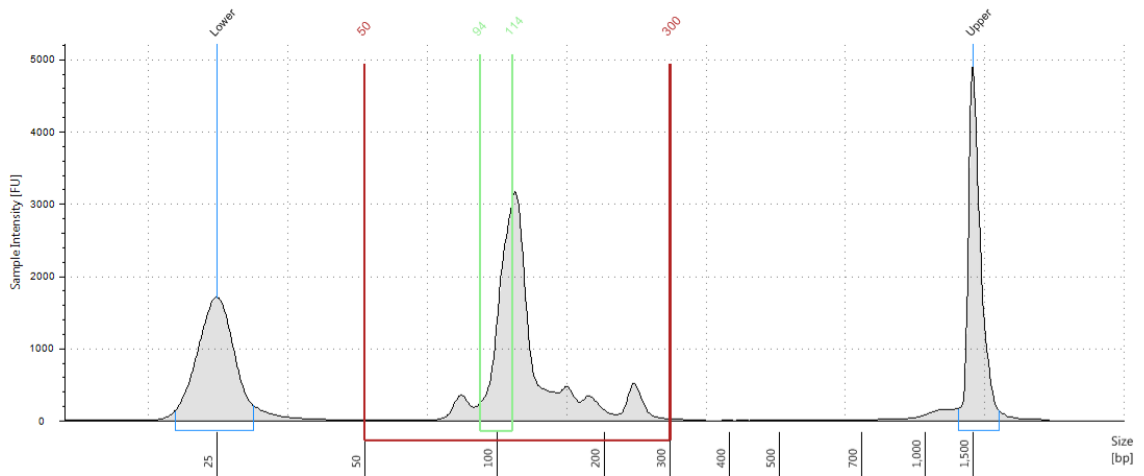


Figure 3.14 - Electropherogram depicting the size distribution and concentration of small RNA in the CH-Sample 1A library.

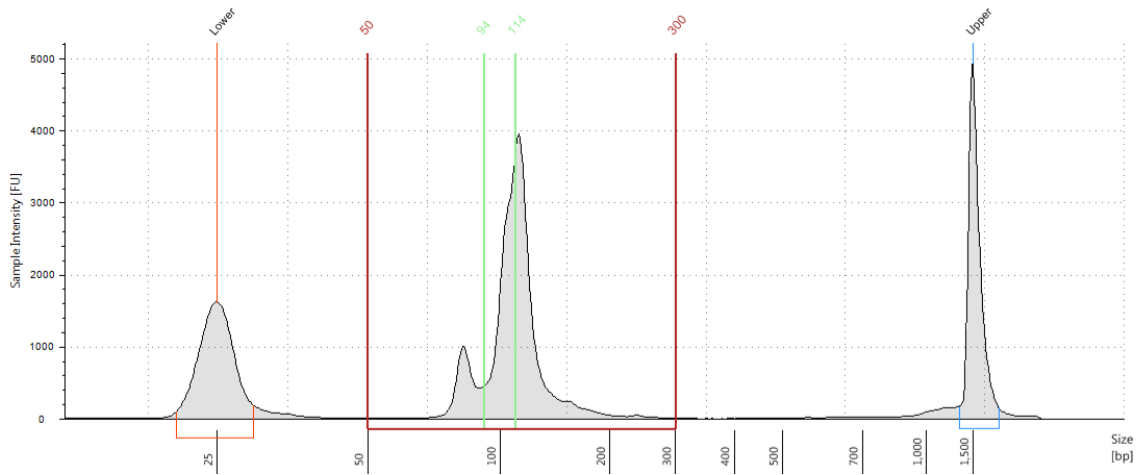


Figure 3.15 - Electropherogram depicting the size distribution and concentration of small RNA in the CH-Sample 1B library.

Table 3.10 – Results of sequencing CH-Sample 1A and CH-Sample 1B.

Sequencing Metrics	Desired Thresholds	CH-Sample 1A	CH-Sample 1B
Mean Read Length	15-35bp	37 bp	28 bp
Total Reads	10M	10,724,283	11,295,958
Reads Passing Filters	Highest % of total	10,395,297	10,765,595
Aligned Reads	Highest % of total	9,970,735	10,262,687
Percent Mapped Reads	High	95.92%	95.33%
miRNA Reads	>1M	2,553,114	3,251,662
Percent miRNA Reads	>10%	24.56%	30.20%
miRNA Detected	400-800	588	656

3.2 Optimizing Chip Loading Capacity

Once an optimized library preparation protocol was established, the optimization of chip loading began. In order to maximize the number of libraries that could be sequenced on one chip without decreasing the quality of sequencing metrics, 4 separate chip runs were performed. The first run, 6@8pM, had 6 libraries (regional morality percentage of >35%) loaded on the chip at 8 pM each. The second run, 7@6pM, had 7 successful libraries loaded on the chip at 6 pM each. The third run, 6@6pM, had 6 successful libraries loaded on the chip at 6 pM each. The fourth run, 9@6pM, had 9 successful libraries loaded on the chip at 6 pM each. Each sample that was loaded onto the chips during these runs is outlined below with its associated quality metrics.

3.2.1 CH-Sample 1B

The library of CH-Sample 1B sequenced at 6@8pM had 2,681,996 miRNA reads and detected 606 miRNAs. The library sequenced at 7@8pM had 3,251,662 miRNA reads

and detected 656 miRNAs. The library of sequenced at 6@6pM had 2,655,820 miRNA reads and detected 612 miRNAs. The library of sequenced at 9@6pM had 1,207,334 miRNA reads and detected 492 miRNAs (**Table 3.11**).

Table 3.11 - Results of multiple sequencing runs of CH-Sample 1B, loaded at different molarities and/or loaded with different number of samples on the sequencing chip.

CH-Sample 1B					
Total Molarity	205 nmol/l				
Regional Molarity	84 nmol/l				
Percent Regional Molarity	40.9%				
Chip Loading Conditions	Desired Thresholds	6@8pM	7@8pM	6@6pM	9@6pM
Mean Read Length	15-35bp	27 bp	28 bp	27 bp	27 bp
Total Reads	10M	9,120,699	11,295,958	8,904,659	4,168,540
Reads Passing Filters	Highest % of total	8,605,744	10,765,595	8,417,074	3,915,399
Aligned Reads	Highest % of total	8,170,418	10,262,687	8,005,450	3,714,112
Percent Mapped Reads	High	94.94%	95.33%	95.11%	94.86%
miRNA Reads	>1M	2,681,996	3,251,662	2,655,820	1,207,334
Percent miRNA Reads	>10%	31.17%	30.20%	31.55%	30.84%
miRNA Detected	400-800	606	656	612	492

3.2.2 CH-Sample 2A

The library of CH-Sample 2A sequenced at 6@8pM had 3,849,111 miRNA reads and detected 719 miRNAs. The library sequenced at 7@8pM had 3,506,927 miRNA reads and detected 719 miRNAs. The library sequenced at 6@6pM had 4,492,068 miRNA reads

and detected 775 miRNAs. The library sequenced at 9@6pM had 2,982,039 miRNA reads and detected 686 miRNAs (**Table 3.12**).

Table 3.12 - Results of multiple sequencing run of CH-Sample 2A, loaded at different molarities and/or loaded with different number of samples on the sequencing chip.

CH-Sample 2A					
Total Molarity	69.5 nmol/l				
Regional Molarity	37.1 nmol/l				
Percent Regional Molarity	53.4%				
Chip Loading Conditions	Desired Thresholds	6@8pM	7@8pM	6@6pM	9@6pM
Mean Read Length	15-35bp	23 bp	23 bp	23 bp	23 bp
Total Reads	10M	11,898,004	10,892,710	13,844,706	9,325,402
Reads Passing Filters	Highest % of total	9,336,216	8,636,110	10,819,580	7,247,430
Aligned Reads	Highest % of total	8,697,941	8,076,508	10,102,958	6,761,555
Percent Mapped Reads	High	93.16%	93.52%	93.38%	93.30%
miRNA Reads	>1M	3,849,111	3,506,927	4,492,068	2,982,039
Percent miRNA Reads	>10%	41.23%	40.61%	41.52%	41.15%
miRNA Detected	400-800	719	719	775	686

3.2.3 CH-Sample 2B

The library of CH-Sample 2B sequenced at 6@8pM had 3,548,187 miRNA reads and detected 713 miRNAs. The library sequenced at 7@8pM had 3,326,817 miRNA reads and detected 697 miRNAs. The library sequenced at 6@6pM had 4,186,769 miRNA reads

and detected 753 miRNAs. The library sequenced at 9@6pM had 2,277,177 miRNA reads and detected 632 miRNAs (**Table 3.13**).

Table 3.13 - Results of multiple sequencing run of CH-Sample 2B, loaded at different molarities and/or loaded with different number of samples on the sequencing chip.

CH-Sample 2B					
Total Molarity	93.9 nmol/l				
Regional Molarity	44.4 nmol/l				
Percent Regional Molarity	47.3%				
Chip Loading Conditions	Desired Thresholds	6@8pM	7@8pM	6@6pM	9@6pM
Mean Read Length	15-35bp	22 bp	22 bp	22 bp	22 bp
Total Reads	10M	10,870,402	10,210,875	13,080,873	7,283,505
Reads Passing Filters	Highest % of total	8,011,803	7,660,753	9,656,956	5,332,995
Aligned Reads	Highest % of total	7,488,973	7,185,659	9,054,920	4,982,695
Percent Mapped Reads	High	93.47%	93.80%	93.77%	93.43%
miRNA Reads	>1M	3,548,187	3,326,817	4,186,769	2,277,177
Percent miRNA Reads	>10%	44.29%	43.43%	43.35%	42.70%
miRNA Detected	400-800	713	697	753	632

3.2.4 CH-Sample 3A

The library of CH-Sample 3A sequenced at 6@8pM had 6,765,690 miRNA reads and detected 766 miRNAs. The library sequenced at 7@8pM had 7,381,776 miRNA reads and detected 802 miRNAs. The library sequenced at 6@6pM had 7,715,774 miRNA reads and detected 791 miRNAs. The library sequenced at 9@6pM had 3,749,194 miRNA reads and detected 657 miRNAs (**Table 3.14**).

Table 3.14 - Results of multiple sequencing run of CH-Sample 3A, loaded at different molarities and/or loaded with different number of samples on the sequencing chip.

CH-Sample 3A					
Total Molarity	250 nmol/l				
Regional Molarity	153 nmol/l				
Percent Regional Molarity	61.2%				
Chip Loading Conditions	Desired Thresholds	6@8pM	7@8pM	6@6pM	9@6pM
Mean Read Length	15-35bp	24 bp	24 bp	24 bp	24 bp
Total Reads	10M	15,077,181	16,660,648	17,307,747	8,517,446
Reads Passing Filters	Highest % of total	13,474,507	15,026,824	15,472,821	7,578,241
Aligned Reads	Highest % of total	12,736,343	14,242,989	14,640,686	7,150,327
Percent Mapped Reads	High	94.52%	94.78%	94.62%	94.35%
miRNA Reads	>1M	6,765,690	7,381,776	7,715,774	3,749,194
Percent miRNA Reads	>10%	50.21%	49.12%	49.87%	49.47%
miRNA Detected	400-800	766	802	791	657

3.2.5 CH-Sample 3B

The library of CH-Sample 3B sequenced at 6@8pM had 4,629,033 miRNA reads and detected 694 miRNAs. The library sequenced at 7@8pM had 6,722,682 miRNA reads and detected 767 miRNAs. The library sequenced at 6@6pM had 4,442,858 miRNA reads and detected 678 miRNAs. The library sequenced at 9@6pM had 2,241,975 miRNA reads and detected 573 miRNAs (**Table 3.15**).

Table 3.15 - Results of multiple sequencing run of CH-Sample 3B, loaded at different molarities and/or loaded with different number of samples on the sequencing chip.

CH-Sample 3B					
Total Molarity	331 nmol/l				
Regional Molarity	208 nmol/l				
Percent Regional Molarity	62.8%				
Chip Loading Conditions	Desired Thresholds	6@8pM	7@8pM	6@6pM	9@6pM
Mean Read Length	15-35bp	23 bp	24 bp	23 bp	23 bp
Total Reads	10M	10,406,120	15,181,195	9,943,531	5,101,471
Reads Passing Filters	Highest % of total	9,047,819	13,417,347	8,666,200	4,404,131
Aligned Reads	Highest % of total	8,480,245	12,656,294	8,147,169	4,116,465
Percent Mapped Reads	High	93.73%	94.33%	94.01%	93.47%
miRNA Reads	>1M	4,629,033	6,722,682	4,442,858	2,241,975
Percent miRNA Reads	>10%	51.16%	50.10%	51.27%	50.91%
miRNA Detected	400-800	694	767	678	573

3.2.6 CH-Sample 4

The library of CH-Sample 4 sequenced at 6@8pM had 3,865,195 miRNA reads and detected 634 miRNAs. The library sequenced at 7@8pM had 3,659,867 miRNA reads and detected 631 miRNAs. The library sequenced at 6@6pM had 4,556,733 miRNA reads and detected 658 miRNAs. The library sequenced at 9@6pM had 2,501,037 miRNA reads and detected 568 miRNAs (**Table 3.16**).

Table 3.16 - Results of multiple sequencing run of CH-Sample 4, loaded at different molarities and/or loaded with different number of samples on the sequencing chip.

CH-Sample 4					
Total Molarity	79.9 nmol/l				
Regional Molarity	30.6 nmol/l				
Percent Regional Molarity	38.3%				
Chip Loading Conditions	Desired Thresholds	6@8pM	7@8pM	6@6pM	9@6pM
Mean Read Length	15-35bp	21 bp	22 bp	21 bp	21 bp
Total Reads	10M	7,425,193	7,031,336	8,741,415	4,873,923
Reads Passing Filters	Highest % of total	6,061,797	5,808,195	7,141,614	3,940,071
Aligned Reads	Highest % of total	5,733,980	5,508,149	6,775,428	3,721,042
Percent Mapped Reads	High	94.59%	94.83%	94.87%	94.44%
miRNA Reads	>1M	3,865,195	3,659,867	4,556,733	2,501,037
Percent miRNA Reads	>10%	63.76%	63.01%	63.81%	63.48%
miRNA Detected	400-800	634	631	658	568

3.2.7 Chip Run Comparison

Run 1 had 6 samples loaded at 8 pM and sequenced a total of 64,797,599 reads; 25,339,212 of those were miRNA reads and a total of 4132 miRNAs were detected. Run 2 had 7 samples loaded at 8 pM and sequenced a total of 81,997,005 reads; 30,402,845 of those were miRNA reads and a total of 4860 miRNAs were detected. Run 3 had 6 samples loaded at 6 pM and sequenced 71,822,931 reads; 28,050,022 of those were miRNA reads and detected a total of 4267 miRNAs. Run 4 had 9 samples loaded at 6 pM and sequenced 65,402,227; 19,771,108 of those were miRNA reads and detected a total of 5147 miRNAs (Table 3.17).

Table 3.17 - Results of multiple sequencing runs with chips loaded at different molarities and/or loaded with different number of samples on the sequencing chip.

Chip Run Comparison	<u>Run 1</u>	<u>Run 2</u>	<u>Run 3</u>	<u>Run 4</u>
	6@8pM	7@8pM	6@6pM	9@6pM
% T-ISP's	7%	9%	6.4%	6.5%
Total reads	64,797,599	81,997,005	71,822,931	65,402,227
Total aligned reads	51,307,900	67,903,021	56,726,611	49,450,376
Total miRNA reads	25,339,212	30,402,845	28,050,022	19,771,108
Total miRNA detected	4132	4860	4267	5147

3.3 PGx PsA Cohort Library Preparation and Sequencing Results

A summary of library preparation results for the nine PsA patients is indicated in **Table 3.18**. PsA patient libraries were quantified as having total morlarities ranging from 111-275 nmol/l, regional molarities ranging from 49.4-165 nmol/l, and percent regional molarities rangning from 44.5-66.1%. For the electropherograms of the PsA patient libraries see **Appendix B**. A summary of sequencing results for the nine PsA patient samples, generated by the Ion Torrent System, are indicated in **Table 3.18**. Raw data collected from sequencing these samples was used for subsequent analyses performed through the comprehensive miRNA analyses pipeline.

Table 3.18 – Summary of library preparation and sequencing results of the PGx patient samples. Bolded values are important library metrics for assessing quality of the prepared libraries.

Library Metrics	Desired Thresholds	Patient 2	Patient 6	Patient 7	Patient 8	Patient 10	Patient 12	Patient 13	Patient 14
Total Molarity	High	142 nmol /l	111 nmol/l	130 nmol/l	190 nmol/l	162 nmol/l	234 nmol/l	180 nmol/l	275 nmol/l
Regional Molarity	High	83.5 nmol /l	49.4 nmol/l	69.2 nmol/l	115 nmol/l	98.7 nmol/l	135 nmol/l	119 nmol/l	165 nmol/l
Percent Regional Molarity	~50%	58.8%	44.5%	53.2%	60.5%	60.9%	57.7%	66.1%	60.0%
Mean Read Length	15-35bp	24 bp	27 bp	23 bp	25 bp	24 bp	27 bp	25 bp	26 bp
Total Reads	10M	12,285,203	15,257,693	13,805,888	11,407,235	13,777,447	19,618,782	18,011,848	19,430,276
Reads Passing Filters	Highest % of total	10,553,278	14,363,192	11,643,534	10,521,082	12,617,228	18,556,802	16,387,945	18,408,616
Aligned Reads	Highest % of total	9,901,417	13,659,253	11,004,407	9,958,734	11,903,955	17,683,645	15,528,710	17,509,053
Percent Mapped Reads	High	93.82%	95.10%	94.51%	94.66%	94.35%	95.29%	94.76%	95.11%
miRNA Reads	>1M	4,671,889	4,355,535	4,715,021	4,165,755	5,538,278	6,619,036	6,695,083	9,061,954
Percent miRNA Reads	>10%	44.27%	30.32%	40.49%	39.59%	43.89%	35.67%	40.85%	49.23%
miRNA Detected	400-800	741	686	731	683	725	776	794	810

3.4 Clinical Results and Response Groupings

Patients ranged from 37 to 64 years of age, with a mean age of 53.8 and a standard deviation of 7.0. There were 4 males (44.4%) and 5 females (55.6%) recruited for this study (**Table 3.19**). Two patients (22.2%) were prescribed the IL-12/23 inhibitor, ustekinumab (Stelera®), and seven patients (77.8%) were prescribed the IL-17 inhibitor, secukinumab (Cosentyx®) (**Table 3.19**).

Monitoring disease progression and determining treatment response was done using the recorded values for each criterion (**Table 3.20**), resulting in the categorization of patients into clinical response grouping (**Table 3.21**).

Table 3.19 – Patient information including patient ID, the biologic the patient was prescribed, the patient’s age, and the patient’s sex.

Patient ID	Drug	Age	Sex
2	Stelara	49	Male
6	Cosentyx	56	Female
7	Cosentyx	56	Female
8	Cosentyx	58	Male
10	Cosentyx	64	Female
11	Cosentyx	55	Female
12	Cosentyx	55	Male
13	Stelara	55	Female
14	Cosentyx	37	Male

Table 3.20 - Clinical values of HAQ-DI, CDAI, and ESR that were used to monitoring disease progression and treatment response.

Patient ID	HAQ-DI			CDAI			ESR (mm/hr)		
	Pre	1m	3m	Pre	1m	3 m	Pre	1 m	3m
2	0.22	0.11	0	29	2	0	13	4	2
6	1.25	0.8	1.2	28	23	41	5	0	6
7	1.05	1.2	0.7	22	20	31	40	50	38
8	0.85	0.85	0.75	53	22	18	29	14	19
10	1.35	1.55	1.85	47	47	16	24	15	24
11	1.25	1.25	1.1	39	26	22	34	26	26
12	2	1.85	1.7	51	48	49	27	40	25
13	0.95	1	0.7	30	18	3	10	10	8
14	0.7	0.5	0.5	21	4	1	2	2	2

Table 3.21 - Clinical groupings of responders and non-responders to biologics treatment.

Response groupings	Patient
ACR50 Non- Responders	6
	7
	8
	11
	12
ACR50 Responders	2
	10
	13
	14

3.5 Analyses of PGx Samples Using the Comprehensive miRNA Pipeline

Data generated by the comprehensive miRNA pipeline used for analyses (**Figure 3.16**) is outlined in **Table 3.22**. Three major datasets were generated from the comprehensive miRNA analyses pipeline: identified novel miRNAs, identified miRNA variants, and differential miRNA expression.

Table 3.22 - Summary of sequencing results used for the comprehensive miRNA pipeline.

Response groupings	Patient	Total Reads	Trimmed Reads	Aligned Reads	Precursor miRNA Reads	Mature miRNA Reads	Known miRNA with 5x coverage
Non-Responders	6	15,193,152	407,758	10,073,266	3,480	4,228,455	747
	7	13,748,316	276,721	7,579,642	3,294	4,556,267	792
	8	11,357,574	263,873	7,253,612	3,290	4,001,759	743
	11	15,093,112	236,845	10,810,641	4,208	5,801,842	795
	12	19,277,033	310,222	12,452,582	5,016	6,456,913	855
Responders	2	12,239,356	430,052	7,587,572	4,145	4,515,962	805
	10	13,710,176	341,803	8,440,832	3,622	5,338,171	796
	13	17,713,699	336,244	11,830,895	3,628	6,524,251	862
	14	19,100,094	210,621	13,966,733	10,939	8,743,105	874

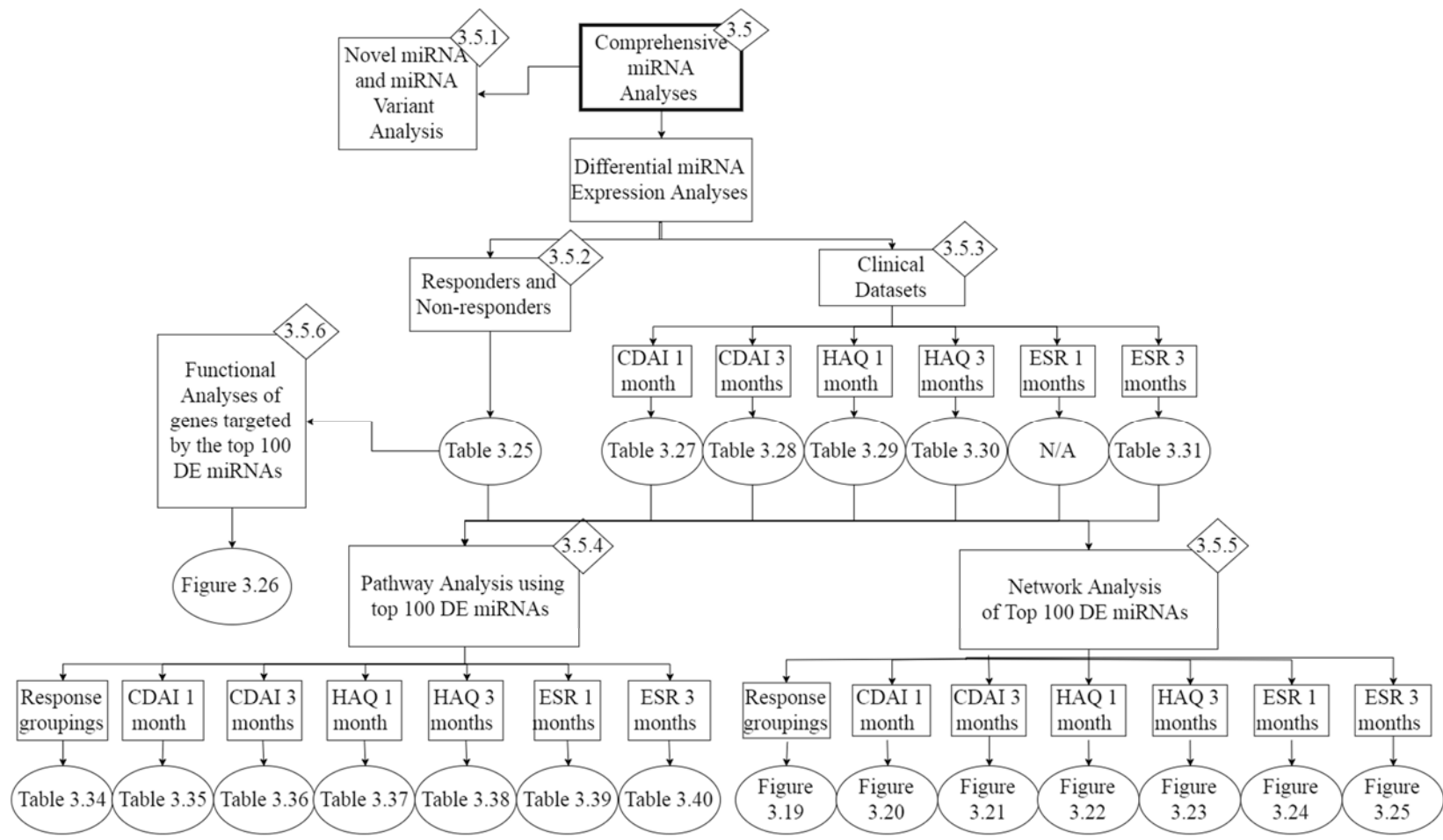


Figure 3.16 – Flow chart depicting the analyses performed using the comprehensive miRNA analyses pipeline (Section 3.5), including miRNA variant and novel miRNA analyses (Section 3.5.1), differential expression (DE) analysis between ACR50 responders and non-responders (Section 3.5.2), differential expression analyses relative to clinical datasets (Section 3.5.3), pathway analyses (Section 3.5.4), network analyses (Section 3.5.5), and a function enrichment analysis (Section 3.6.6). The tables corresponding to analyses only display the suggestively significant results.

3.5.1 Identified miRNA Variants and Identified Known and Novel miRNAs

In the 2822 detected miRNAs, there were 1936 variants identified (data not shown). In the nine PGx samples, a total of 2822 miRNAs were detected (data not shown). Of the 2822 miRNAs detected, 1902 have previously been identified. Therefore, the analysis detected 920 novel miRNAs that had not yet been annotated by miRDeep2/ miRBase (data not shown). Of the 920 novel miRNAs, nine miRNAs were found exclusively in the responder group and eight novel miRNAs were found exclusively in the non-responder group (Table 3.23).

Table 3.23 – Novel miRNAs identified in responders or non-responders. Where (+) indicates that patients possess that novel miRNA and (–) indicates that patient does not possess that novel miRNA.

chr	Responders				Non-Responders				
	02	10	13	14	06	07	08	11	12
chr2:88355218-88355276	+	+	+	-	-	-	-	-	-
chr3:185279931-185279996	+	-	+	+	-	-	-	-	-
chr5:32431097-32431160	+	+	+	-	-	-	-	-	-
chr5:171831837-171831897	+	+	+	-	-	-	-	-	-
chr6:28726146-28726212	+	+	+	-	-	-	-	-	-
chr7:77005493-77005573	+	+	+	-	-	-	-	-	-
chr9:95500873-95500934	+	-	+	+	-	-	-	-	-
chr13:43323439-43323498	+	+	-	+	-	-	-	-	-
chr2:27304884-27304952	-	-	-	-	-	+	-	+	+
chr2:96656064-96656124	-	-	-	-	-	+	-	+	+
chr3:41563653-41563715	-	-	-	-	-	-	+	+	+
chr4:81946113-81946170	-	-	-	-	-	-	+	+	+
chr6:8086643-8086702	-	-	-	-	+	-	+	-	+
chr6:137113031-137113087	-	-	-	-	-	+	+	-	+
chr17:7210149-7210207	-	-	-	-	-	+	-	+	+
chr19:1253356-1253424	-	-	-	-	-	+	-	+	+
chrX:153593853-153593910	-	-	-	-	+	+	-	-	+

3.5.2 Differential miRNA Expression between ACR50 Response Groupings

The read counts underwent normalization, and the distribution of the counts was visualized (**Figure 3.17**). A differential miRNA expression analysis was then performed under the hypothesis that differential miRNA expression levels exist between responders and non-responders.

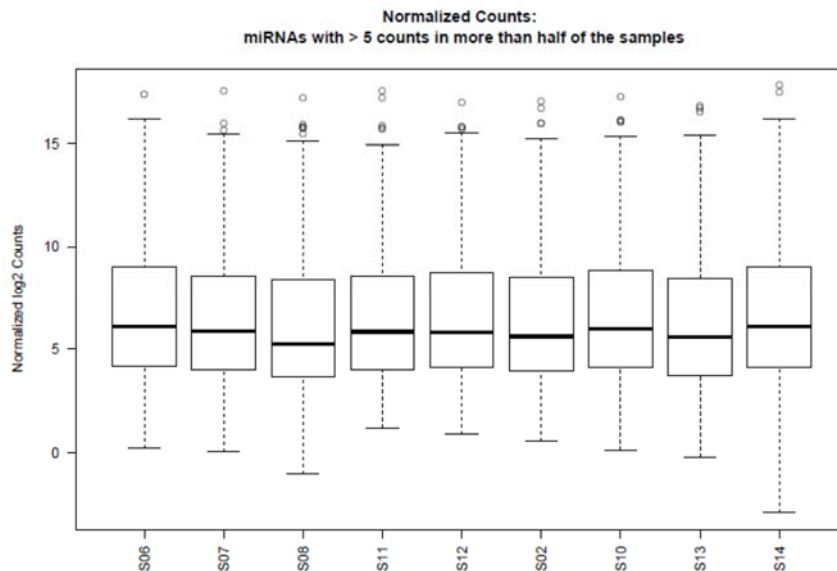


Figure 3.17 – Boxplot visualization of the distribution of normalized reads sequenced from each sample.

As shown on the MDS plot of fold change (**Figure 3.18**), the responder and non-responder groups did not cluster well in the differential expression analysis. The differential expression analyses metrics are outline and described in **Table 3.24**. The p-values for the differential miRNA expression associations between responders and non-responders were not significant after correcting for multiple testing (**Table 3.25**). Because no significant

associations were found, the top 100 differentially expressed miRNAs were prioritized for examination to identify mutually targeted genes (**Table 3.26**).

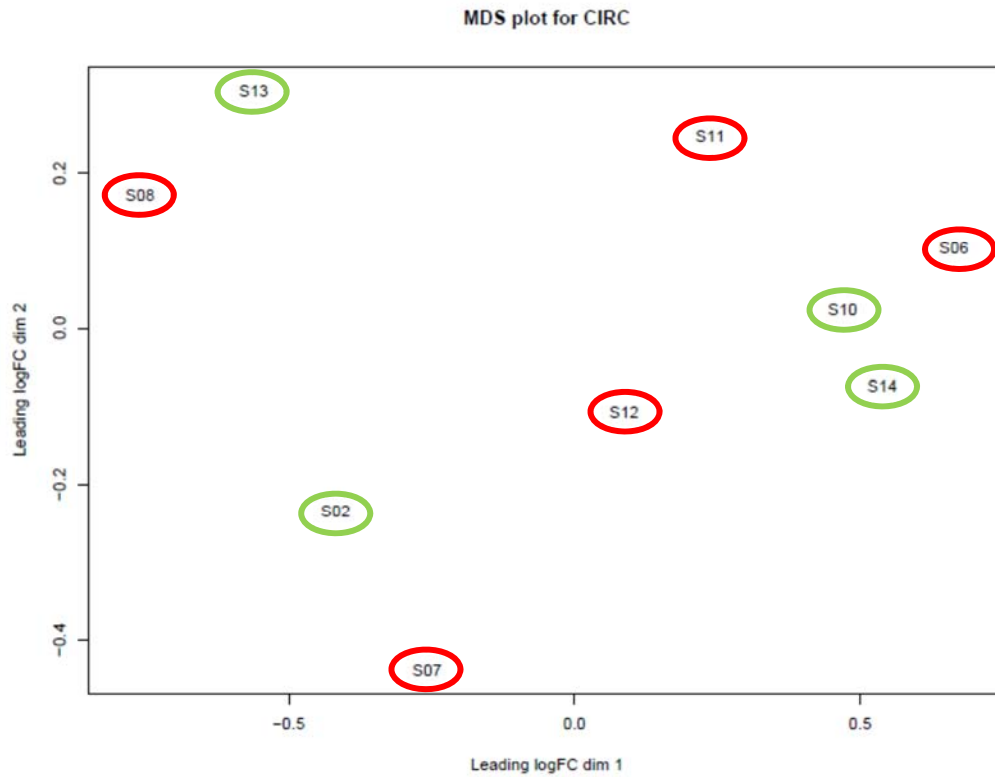


Figure 3.18 - MDS plot of Fold change of miRNA expression between responders (indicated in green) and non-responders (indicated in red).

Table 3.24 - Differential expression analyses metric and descriptions.

Differential Expression Analyses Metric	Description
LogFC (Log Fold Change)	Log of the fold change, of the differential expression, between groups
LogCPM (Log Counts Per Million)	Measure of expression level similar to fragments per kilobase of transcript per million mapped reads
LR (Logarithm Ratio)	Ratio between a change in two values
p-value	Measure of significance of the identified association

Table 3.25 – Top seven differentially expressed miRNAs between ACR50 response grouping, where no significance was reached after correcting for multiple testing.

Mature ID	Non-responders Read Counts					Responders Read Counts				Analysis Metrics				
	6	7	8	11	12	2	10	13	14	logFC	logCPM	LR	p-value	FDR
miR-106a-3p	4	3	5	5	5	7	8	15	7	-1.12	2.78	6.57	0.01	0.998
miR-96-5p	11	19	21	41	17	39	25	55	76	-1.15	5.10	6.17	0.01	0.998
miR-296-5p	15	13	24	24	9	55	32	31	21	-1.04	4.65	5.57	0.02	0.998
miR-3194-5p	14	2	6	3	9	6	25	7	32	-1.39	3.58	5.44	0.02	0.998
miR-150-5p	608	1565	489	436	743	2439	444	565	3842	-1.25	10.27	4.51	0.03	0.998
miR-183-5p	4	9	11	16	7	20	11	15	25	-0.91	3.77	4.17	0.04	0.998
miR-193a-5p	6	30	12	10	24	41	13	38	42	-1.02	4.62	4.16	0.04	0.998

Table 3.26 – mRNA targets common to all of the top 100 differentially expressed miRNAs between ACR50 response grouping.

Target Gene	Gene Description
HTR1B	5-hydroxytryptamine (serotonin) receptor 1B, G protein-coupled
SSSCA1	Sjogren syndrome/scleroderma autoantigen 1
AQP5	aquaporin 5
KRTAP3-2	keratin associated protein 3-2
HGS	hepatocyte growth factor-regulated tyrosine kinase substrate
BAX	BCL2-associated X protein
CCNE1	cyclin E1
RYK	receptor-like tyrosine kinase
IRS1	insulin receptor substrate 1
FOXO1	forkhead box O1
EZR	ezrin
TBC1D9	TBC1 domain family, member 9 (with GRAM domain)
EGR2	early growth response 2
P2RX7	purinergic receptor P2X, ligand-gated ion channel, 7
RUNX1T1	runt-related transcription factor 1; translocated to, 1 (cyclin D-related)
ODF2	outer dense fiber of sperm tails 2
CELSR2	cadherin, EGF LAG seven-pass G-type receptor 2
MYRIP	myosin VIIA and Rab interacting protein
CCND1	cyclin D1
ADCY6	adenylate cyclase 6
MYB	v-myb avian myeloblastosis viral oncogene homolog
MITF	microphthalmia-associated transcription factor
BTRC	beta-transducin repeat containing E3 ubiquitin protein ligase
BCL2	B-cell CLL/lymphoma 2

3.5.3 Differential miRNA Expression Incorporating Clinical Data

The differentially expressed miRNAs that reached suggestive significance for each set of clinical data (CDAI, HAQ-DI, and ESR) are outlined below; only miRNAs reaching a significance cut-off FDR of <0.05 (stastically significant) and <0.2 (suggestively significant) are displayed.

Differentially expressed miRNAs, reaching suggestive and statistical significance, associated with CDAI values at one-month and three-months post treatment are displayed in **Table 3.27** and **Table 3.28**, respectively. Differentially expressed miRNAs, reaching suggestive and statistical significance, associated with HAQ-DI values at one-month and three-months post treatment are displayed in **Table 3.29** and **Table 3.30**, respectively. No differentially expressed miRNAs reached suggestive significance for the ESR values at one-month post treatment. Statistically significant differentially expressed miRNAs associated with ESR values at three-months post treatment are displayed in **Table 3.31**. A summary of differentially expressed miRNAs that are associated with multiple datasets is displayed in **Table 3.32**.

Table 3.27 – Suggestively significant differentially expressed miRNAs associated with CDAI values at one-month post treatment with the statistically significant differentially expressed miRNAs incicated in the bordered cells.

CDAI 1 month														
Mature ID	Patient Read Counts									Analysis Metrics				
	6	7	8	11	12	2	10	13	14	logFC	logCPM	LR	p-value	FDR
miR-124-3p	4	1	1	0	1	4	0	4	43	-0.13	2.86	22.32	2.31E-06	1.3E-03
miR-1275	0	4	2	1	0	6	1	1	6	-0.09	1.49	18.12	2.08E-05	6.0E-03
miR-582-5p	2	7	7	5	4	19	5	5	49	-0.07	3.60	15.27	9.34E-05	1.8E-02
miR-150-5p	611	1535	460	453	768	2403	450	540	4042	-0.05	10.29	10.82	1.00E-03	0.15
miR-31-5p	3	8	3	2	5	24	3	1	19	-0.05	3.03	10.09	1.49E-03	0.17

Table 3.28 - Statistically significant differentially expressed miRNAs associated with CDAI values at three-months post treatment.

CDAI 3 months														
Mature ID	Patient Read Counts									Analysis Metrics				
	6	7	8	11	12	2	10	13	14	logFC	logCPM	LR	p-value	FDR
miR-582-5p	2	7	7	5	4	19	5	5	49	-0.06	3.60	13.72	2.13E-04	0.12

Table 3.29 - Statistically significant differentially expressed miRNAs associated with HAQ-DI values at one-month post treatment.

HAQ-DI 1 month														
Mature.ID	Patient Read Counts									Analysis Metrics				
	6	7	8	11	12	2	10	13	14	logFC	logCPM	LR	p-value	FDR
miR-124-3p	4	1	1	0	1	4	0	4	43	-3.88	2.86	14.61	1.32E-04	0.08
miR-582-5p	2	7	7	5	4	19	5	5	49	-1.99	3.60	12.14	4.93E-04	0.14

Table 3.30 - Suggestively significant differentially expressed miRNAs associated with HAQ-DI values at three-months post treatment with the statistically significant differentially expressed miRNA incicated in the bordered cell.

HAQ-DI 3 months														
Mature ID	Patient Read Counts									Analysis Metrics				
	6	7	8	11	12	2	10	13	14	logFC	logCPM	LR	p-value	FDR
miR-1275	0	4	2	1	0	6	1	1	6	-2.60	1.49	21.61	3.34E-06	1.94E-03
miR-27a-5p	2	7	2	1	3	13	1	3	6	-1.57	2.17	12.26	4.64E-04	0.13
miR-582-5p	2	7	7	5	4	19	5	5	49	-1.78	3.60	10.87	9.80E-04	0.13
miR-124-3p	4	1	1	0	1	4	0	4	43	-3.72	2.86	10.74	1.05E-03	0.13
miR-31-5p	3	8	3	2	5	24	3	1	19	-1.57	3.03	10.66	1.10E-03	0.13
miR-4433b-3p	24	69	16	88	28	184	24	64	40	-1.31	5.91	9.23	2.38E-03	0.20
miR-150-5p	611	1535	460	453	768	2403	450	540	4042	-1.43	10.29	9.20	2.42E-03	0.20

Table 3.31 – Suggestively significant differentially expressed miRNAs associated with ESR values at three-months post treatment with the statistically significant differentially expressed miRNAs incicated in the bordered cells.

ESR 3 months														
Mature.ID	Patient Read Counts									Analysis Metrics				
	6	7	8	11	12	2	10	13	14	logFC	logCPM	LR	p-value	FDR
miR-124-3p	4	1	1	0	1	4	0	4	43	-0.14	2.86	15.93	6.59E-05	3.83E-02
miR-146a-3p	122	31	86	47	31	129	35	166	103	-0.07	6.39	14.47	1.42E-04	4.14E-02

Table 3.32 - Differentially expressed miRNAs found to be associated with more than one analysis.

Differentially Expressed miRNAs	Analyses
miR-150-5p	Responders vs. Non-responders CDAI 1 month HAQ-DI 3 months
miR-124-3p	CDAI 1 month HAQ-DI 1 month HAQ-DI 3 months ESR 3 months
miR-1275	CDAI 1 month HAQ-DI 3 months
miR-582-5p	CDAI 1 month CDAI 3 months HAQ-DI 1 month HAQ-DI 3 months
miR-31-5p	CDAI 1 month HAQ-DI 3 months

3.5.4 Pathway Analysis Using Top 100 Differentially Expressed miRNAs

The pathway analysis metrics and their descriptions are outline in **Table 3.33**. The top five pathways significantly associated with the differentially expressed miRNAs between responders and non-responders are outlined in **Table 3.34**. The top five pathways significantly associated with the differentially expressed miRNAs and HAQ-DI values at

one-month and three-months post treatment are outlined in **Table 3.35** and **Table 3.36**, respectively. The top five pathways significantly associated with the differentially expressed miRNAs and CDAI values at one-month and three-months post treatment are outlined in **Table 3.37** and **Table 3.38**, respectively. The top five pathways significantly associated with the differentially expressed miRNAs and ESR values at one-month and three-months post treatment are outlined in **Table 3.39** and **Table 3.40**, respectively.

Table 3.33 – Pathway analysis metrics and descriptions.

Pathway Analysis Metric	Description
KEGG pathway	Pathway found to be associated with differentially express miRNA and the collectively targeted genes
KEGG pathway ID	KEGG ID associated with pathway identified
p-value	Measure of significance of the identified association
#genes	Number of genes associated with that pathway
#miRNA	Number of miRNAs associated with that pathway

Table 3.34 – Top five pathways associated with differentially expressed miRNAs between clinical response groupings.

Pathways Associated Clinical Response Groupings					
#	KEGG pathway	KEGG pathway ID	p-value	#genes	#miRNAs
1	Proteoglycans in cancer	hsa05205	4.33E-19	138	72
2	Axon guidance	hsa04360	7.41E-12	92	68
3	TGF-beta signalling pathway	hsa04350	1.61E-10	59	57
4	Signalling pathways regulating pluripotency of stem cells	hsa04550	6.99E-08	93	60
5	Hippo signalling pathway	hsa04390	6.99E-08	97	69

Table 3.35 - Top five pathways associated with differentially expressed miRNAs relative to the CDAI1 dataset.

Pathways Associated with CDAI1					
#	KEGG pathway	KEGG pathway ID	p-value	#genes	#miRNAs
1	Proteoglycans in cancer	hsa05205	2.54E-08	126	68
2	TGF-beta signalling pathway	hsa04350	7.37E-08	58	59
3	ECM-receptor interaction	hsa04512	2.22E-07	52	55
4	Morphine addiction	hsa05032	4.15E-07	59	57
5	Lysine degradation	hsa00310	6.87E-07	35	48

Table 3.36 - Top five pathways associated with differentially expressed miRNAs relative to the CDAI3 dataset.

Pathways Associated with CDAI3					
#	KEGG pathway	KEGG pathway ID	p-value	#genes	#miRNAs
1	Proteoglycans in cancer	hsa05205	1.30E-09	120	66
2	Hippo signalling pathway	hsa04390	1.92E-09	94	64
3	Fatty acid biosynthesis	hsa00061	1.16E-08	7	11
4	TGF-beta signalling pathway	hsa04350	1.81E-07	52	49
5	Axon guidance	hsa04360	9.43E-07	77	61

Table 3.37 - Top five pathways associated with differentially expressed miRNAs relative to the HAQ-DI1 dataset.

Pathways Associated with HAQ-DI1					
#	KEGG pathway	KEGG pathway ID	p-value	#genes	#miRNAs
1	Morphine addiction	hsa05032	5.98E-08	58	55
2	Axon guidance	hsa04360	5.98E-08	91	59
3	Proteoglycans in cancer	hsa05205	2.31E-07	120	68
4	Circadian entrainment	hsa04713	2.58E-05	64	59
5	Hippo signalling pathway	hsa04390	2.58E-05	91	67

Table 3.38 - Top five pathways associated with differentially expressed miRNAs relative to the HAQ-DI3 dataset.

Pathways Associated with HAQ-DI3					
#	KEGG pathway	KEGG pathway ID	p-value	#genes	#miRNAs
1	TGF-beta signalling pathway	hsa04350	1.53E-07	56	55
2	Proteoglycans in cancer	hsa05205	2.15E-06	122	68
3	Hippo signalling pathway	hsa04390	6.59E-06	92	67
4	Lysine degradation	hsa00310	1.45E-05	33	48
5	ECM-receptor interaction	hsa04512	1.45E-05	45	53

Table 3.39 - Top five pathways associated with differentially expressed miRNAs relative to the ESR1 dataset.

Pathways Associated with ESR1					
#	KEGG pathway	KEGG pathway ID	p-value	#genes	#miRNAs
1	TGF-beta signalling pathway	hsa04350	2.09E-09	59	63
2	Proteoglycans in cancer	hsa05205	3.14E-09	130	70
3	Pathways in cancer	hsa05200	3.38E-07	236	76
4	ECM-receptor interaction	hsa04512	2.60E-06	51	57
5	Axon guidance	hsa04360	2.63E-06	83	67

Table 3.40 - Top five pathways associated with differentially expressed miRNAs relative to the ESR3 dataset.

Pathways Associated with ESR3					
#	KEGG pathway	KEGG pathway ID	p-value	#genes	#miRNAs
1	Axon guidance	hsa04360	1.11E-07	88	67
2	Proteoglycans in cancer	hsa05205	1.11E-07	120	67
3	TGF-beta signalling pathway	hsa04350	1.13E-06	57	55
4	N-Glycan biosynthesis	hsa00510	2.58E-05	31	35
5	Pathways in cancer	hsa05200	1.49E-04	225	77

3.5.5 Network Analysis/Predictive Binding of Top 100 Differentially Expressed miRNAs

A network analysis performed on the top 100 differentially expressed miRNAs between responders and non-responders is visualized in **Figure 3.19**. A network analysis performed on the top 100 differentially expressed miRNAs and CDAI values at one-month and three-months post treatment are visualized in **Figure 3.20** and **Figure 3.21**, respectively. A network analysis performed on the top 100 differentially expressed miRNAs and HAQ-DI values at one-month and three-months post treatment are visualized in **Figure 3.22** and **Figure 3.23**, respectively. A network analysis performed on the top 100 differentially expressed miRNAs and ESR values at one-month and three-months post treatment are visualized in **Figure 3.24** and **Figure 3.25**, respectively.

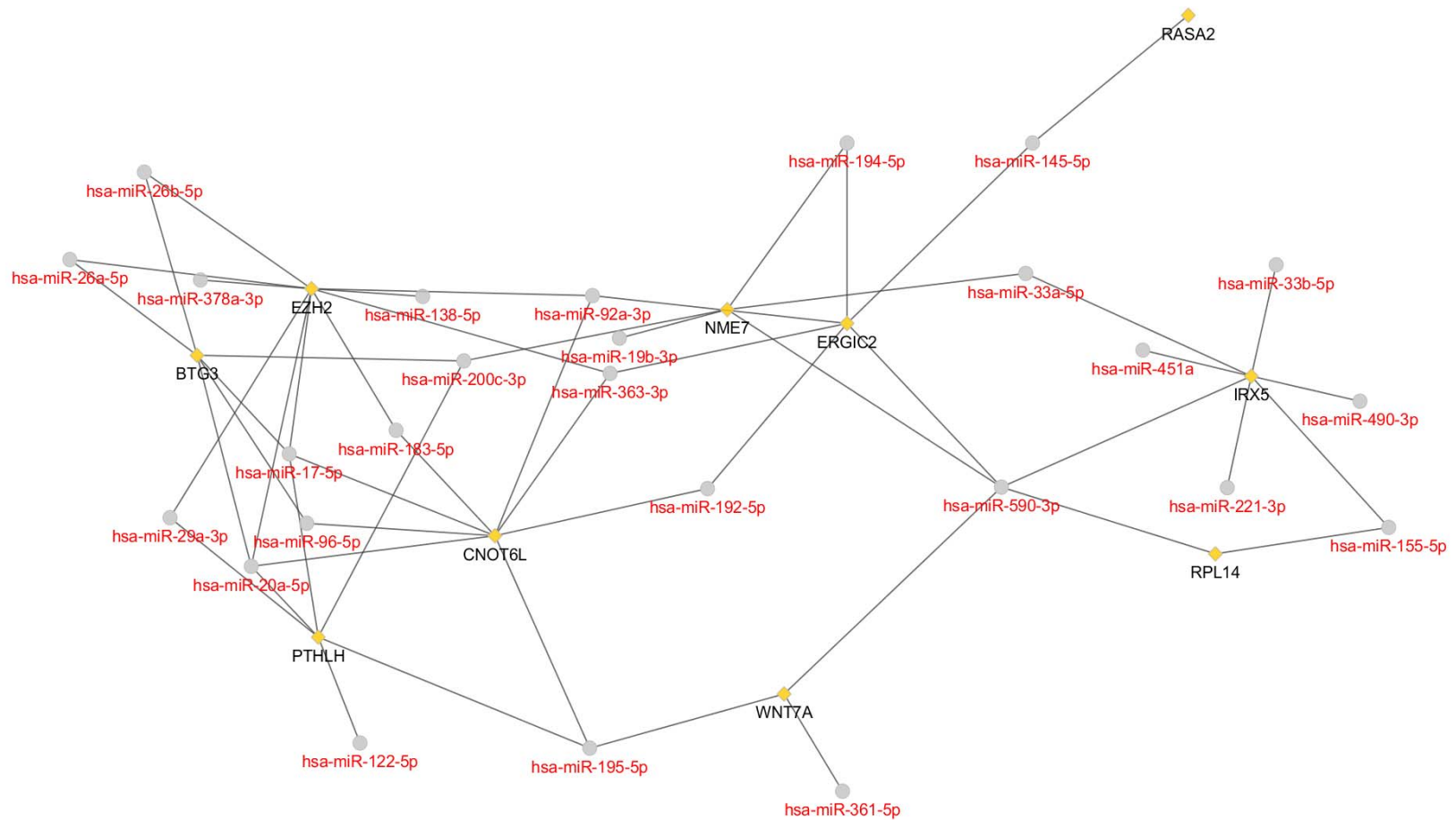


Figure 3.19 – Network analysis of top 100 differentially expressed miRNAs (red text), between responders and non-responders (black text), and the collectively targeted genes. All miRNA-mRNA interactions in this network, as depicted by all lines being of equal thickness, have an equal likelihood of occurrence.

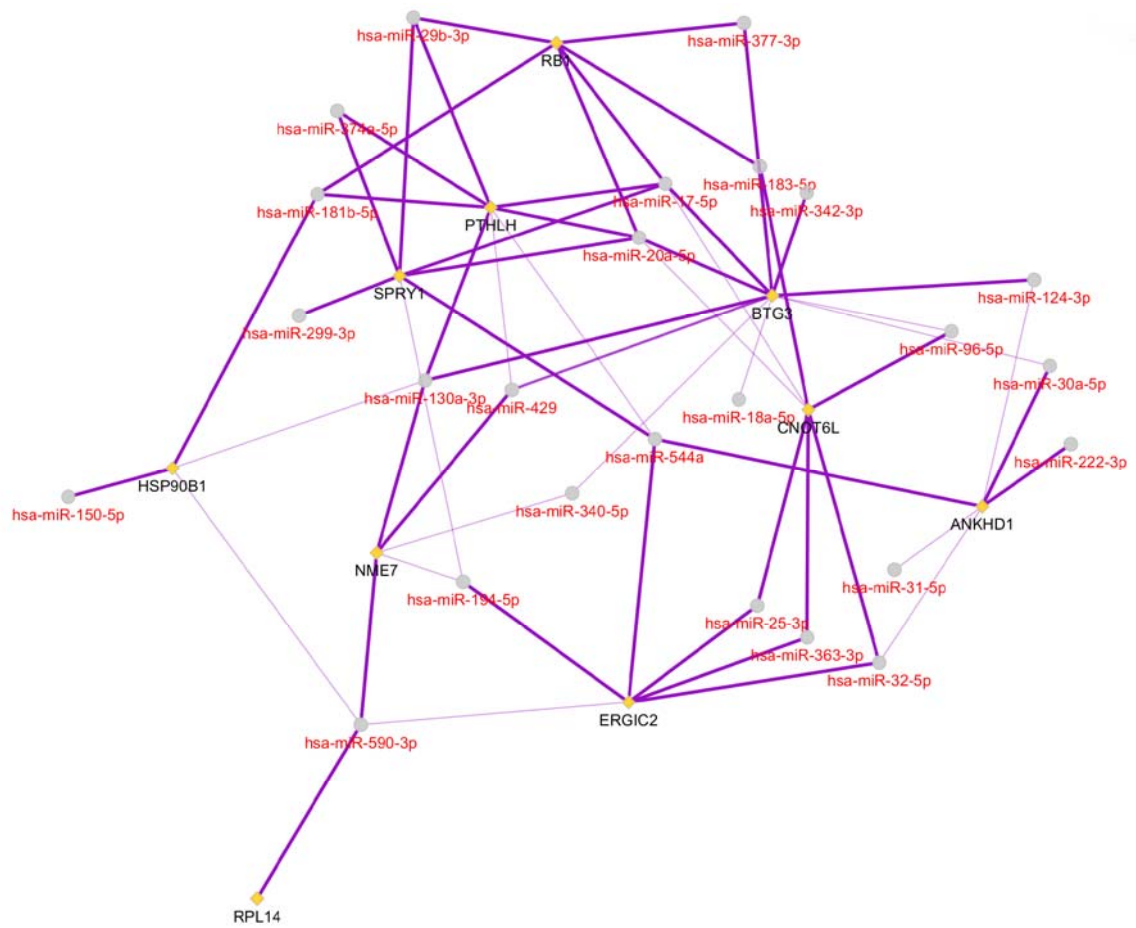


Figure 3.20 - Network analysis of top 100 differentially expressed miRNAs (red text), relative to CDAI values at 1 month, and the collectively targeted genes (black text). A miRNA-mRNA interaction has a higher likelihood of occurrence when indicated by thicker lines in the network.

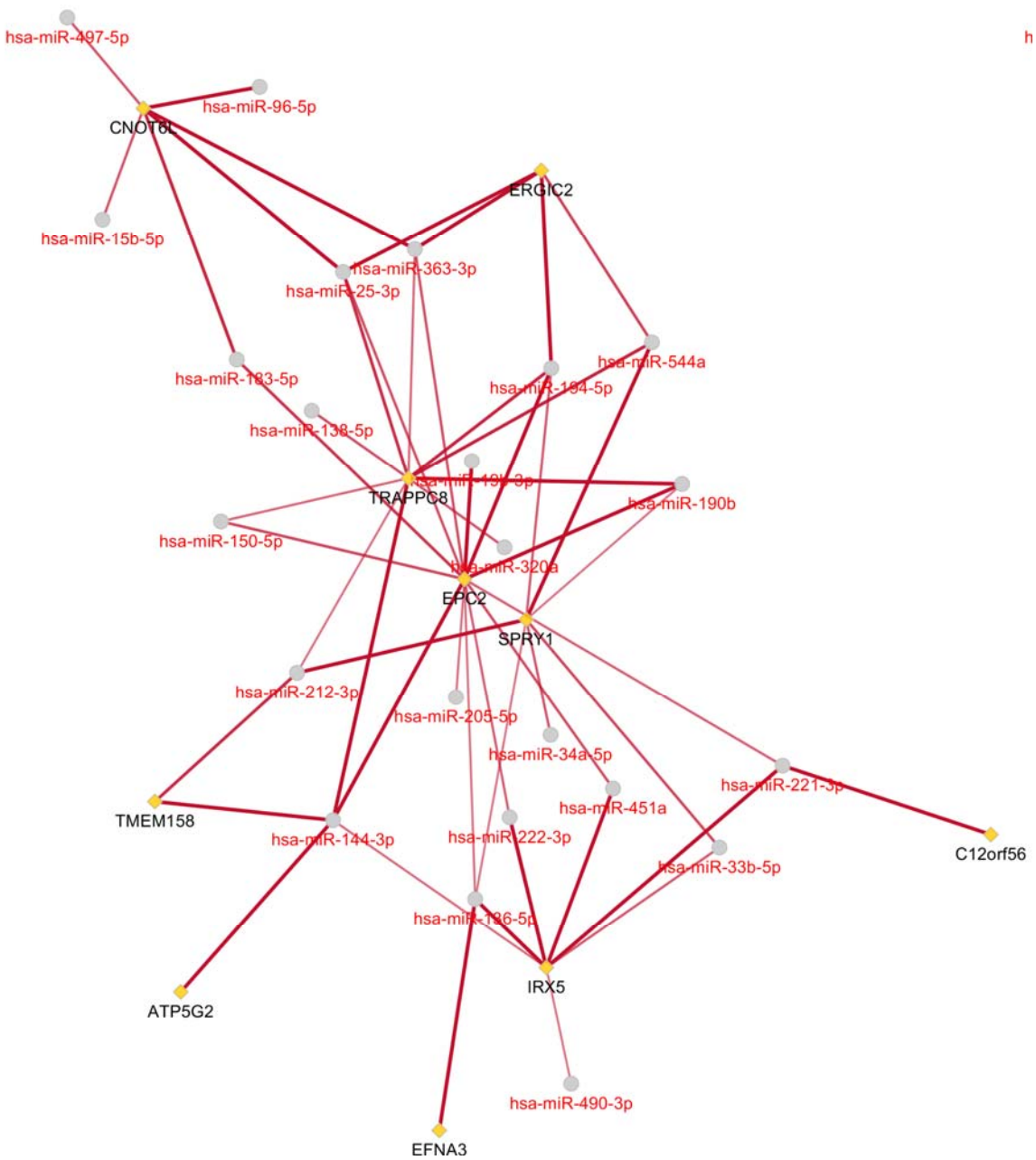


Figure 3.21 - Network analysis of top 100 differentially expressed miRNAs (red text), relative to CDAI values at 3 months, and the collectively targeted genes (black text). A miRNA-mRNA interaction has a higher likelihood of occurrence when indicated by thicker lines in the network.

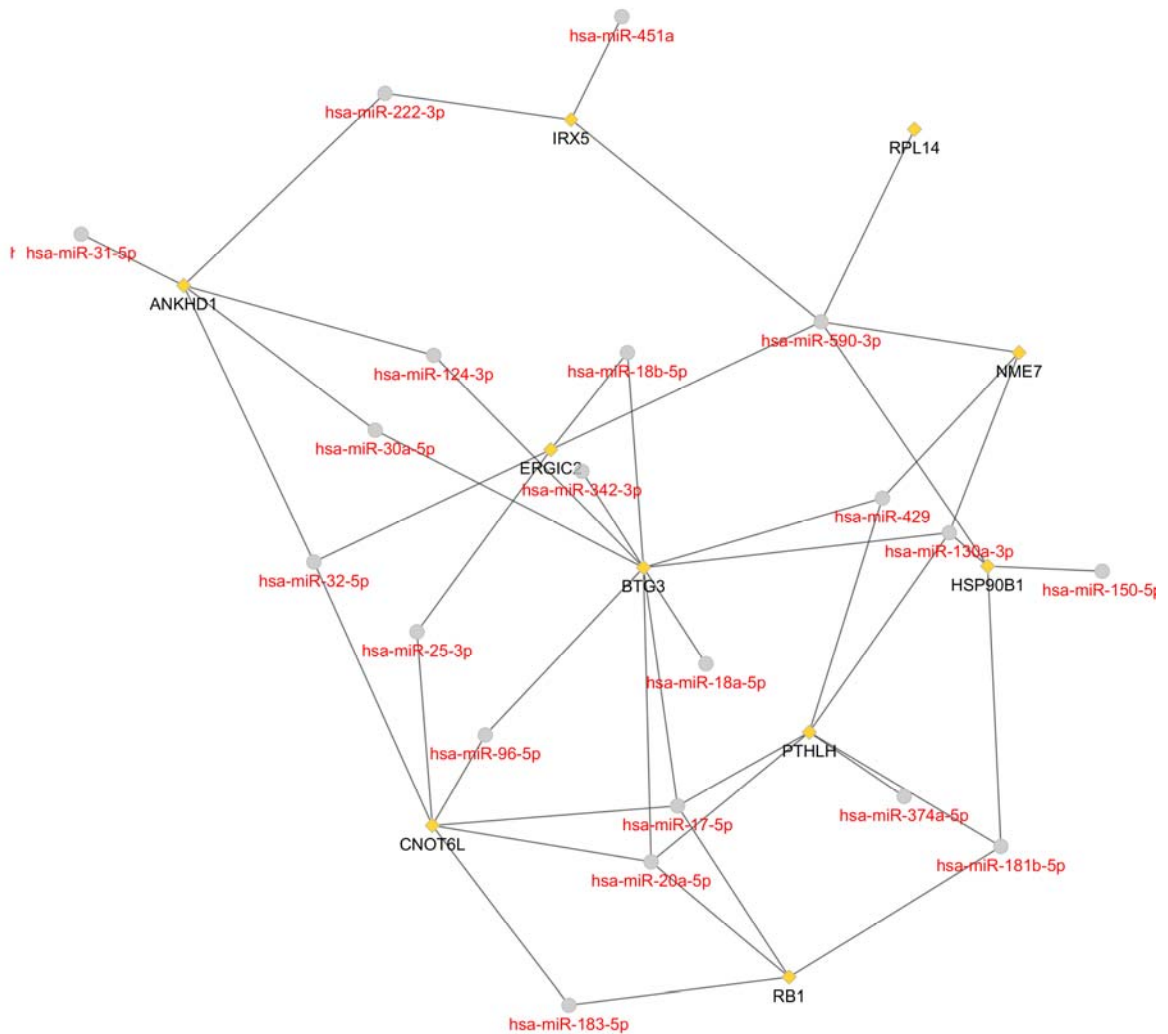


Figure 3.22 - Network analysis of top 100 differentially expressed miRNAs (red text), relative to HAQ-DI values at 1 month, and the collectively targeted genes (black text). All miRNA-mRNA interactions in this network, as depicted by all lines being of equal thickness, have an equal likelihood of occurrence. A miRNA-mRNA interaction has a higher likelihood of occurrence when indicated by thicker lines in the network.

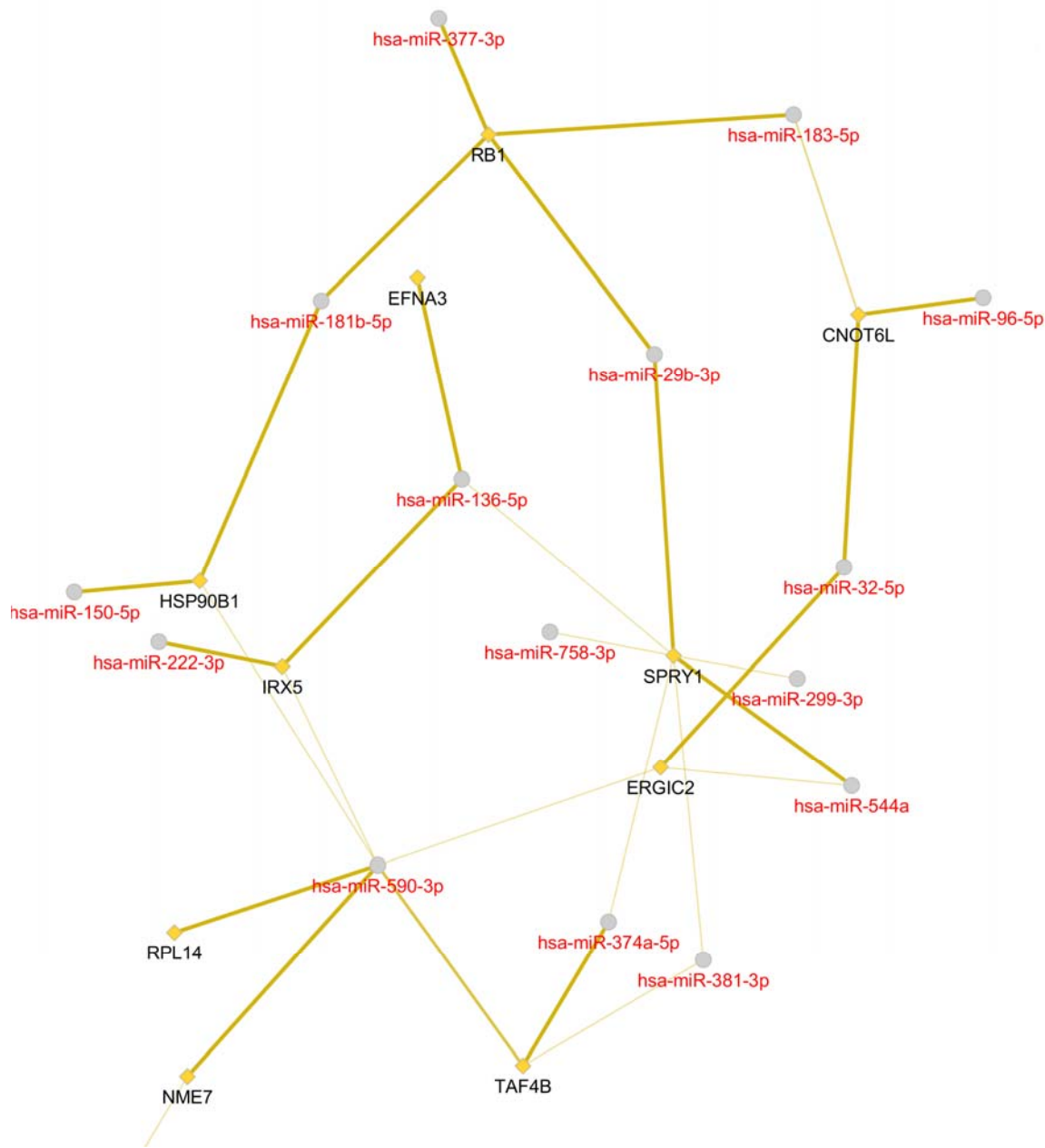


Figure 3.23 - Network analysis of top 100 differentially expressed miRNAs (red text), relative to HAQ-DI values at 3 months, and the collectively targeted genes (black text). A miRNA-mRNA interaction has a higher likelihood of occurrence when indicated by thicker lines in the network.

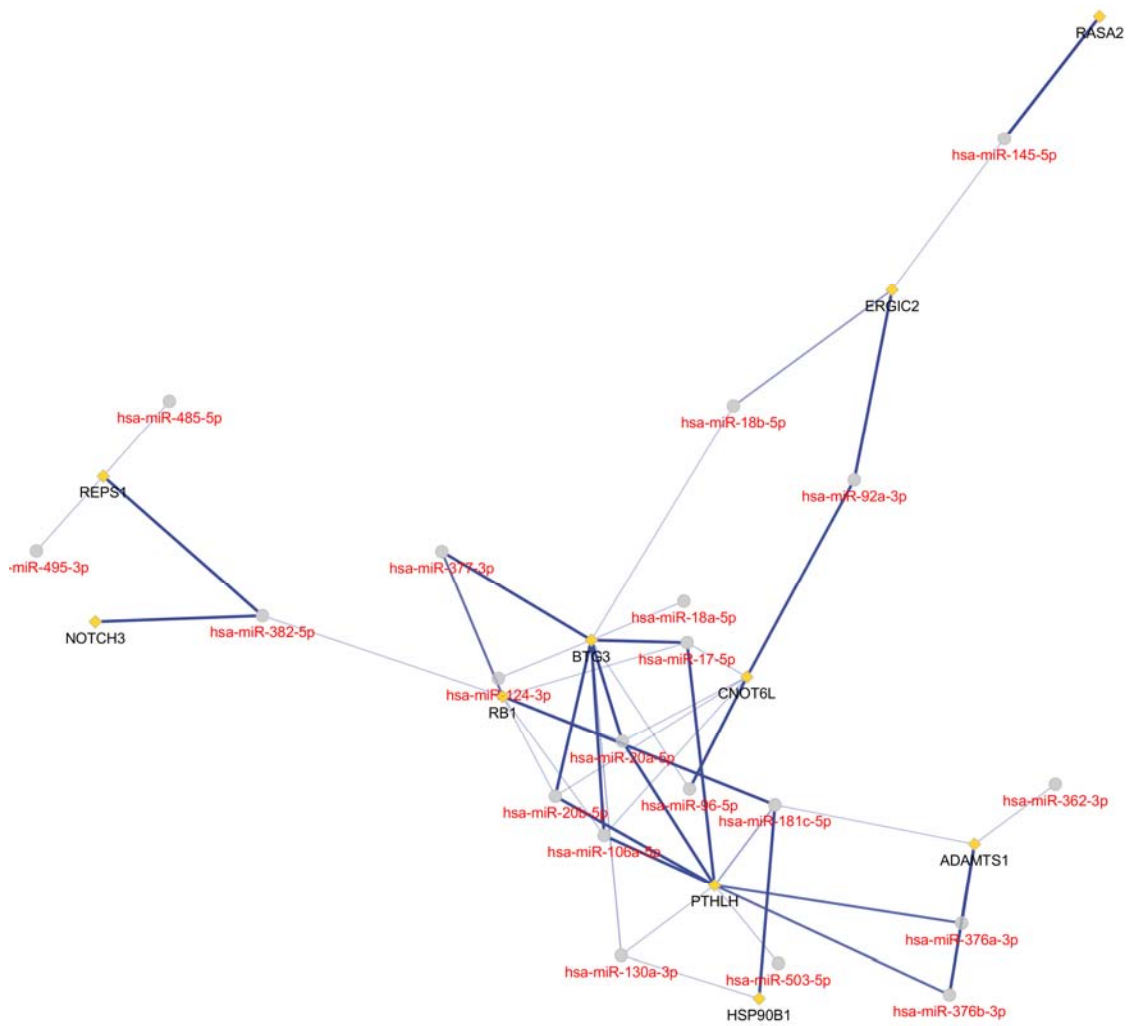


Figure 3.24 - Network analysis of top 100 differentially expressed miRNAs (red text), relative to ESR values at 1 month, and the collectively targeted genes (black text). A miRNA-mRNA interaction has a higher likelihood of occurrence when indicated by thicker lines in the network.

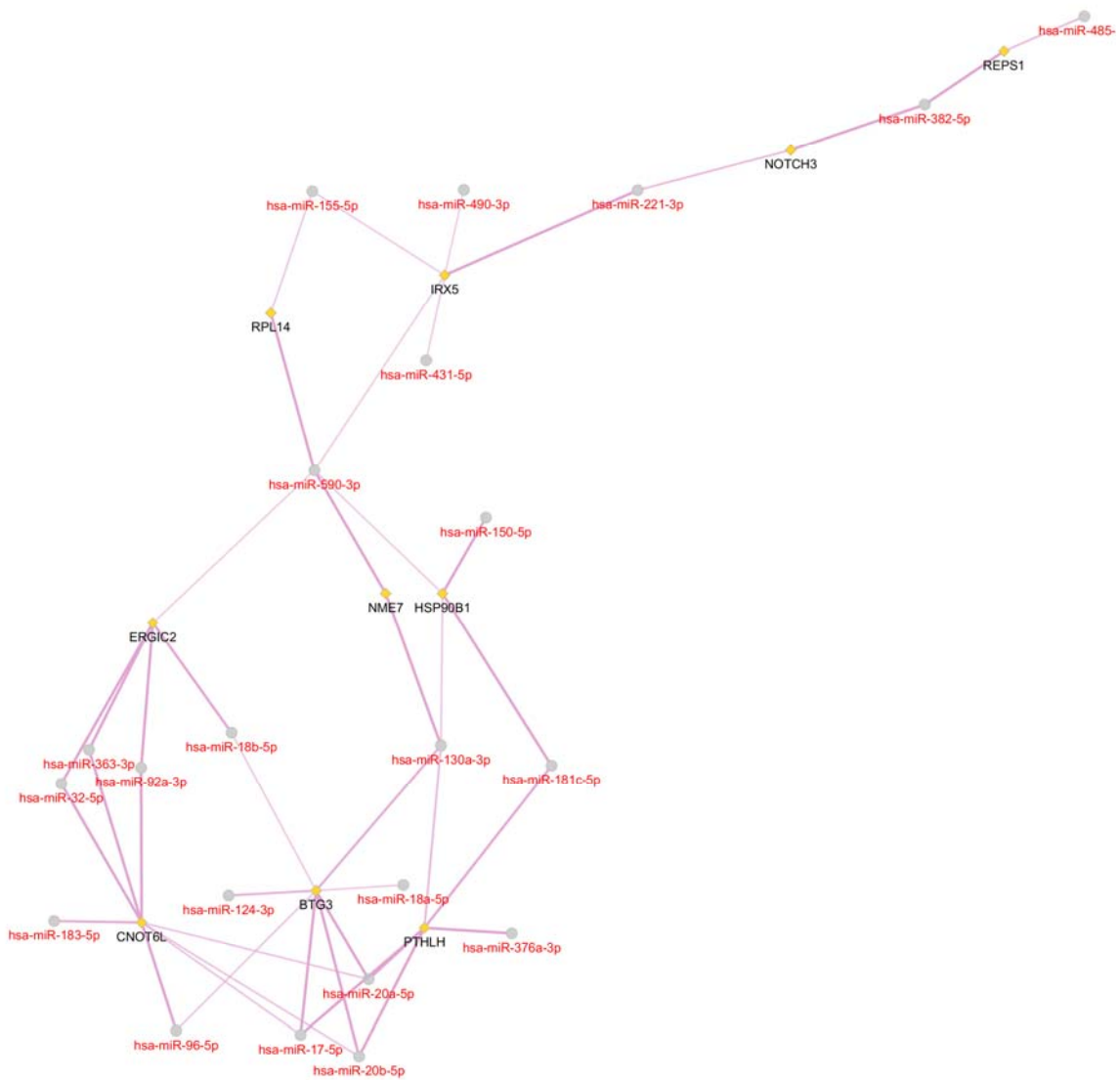


Figure 3.25 - Network analysis of top 100 differentially expressed miRNAs (red text), relative to ESR values at 3 months, and the collectively targeted genes (black text). A miRNA-mRNA interaction has a higher likelihood of occurrence when indicated by thicker lines in the network.

3.5.6 *In silico* Functional Analysis of Top Differentially Expressed miRNAs and Top Mutually Targeted Genes

The *in silico* functional analysis was performed with the top 100 differentially expressed miRNAs between responders and non-responders and the results are visualized in **Figure 3.26**. Within this *in silico* functional analysis three main functional modules were identified: a) skeletal muscle satellite cell maintenance involved in skeletal muscle regeneration, b) purine nucleoside biosynthetic process, and c) cytoplasmic mRNA processing body assembly.

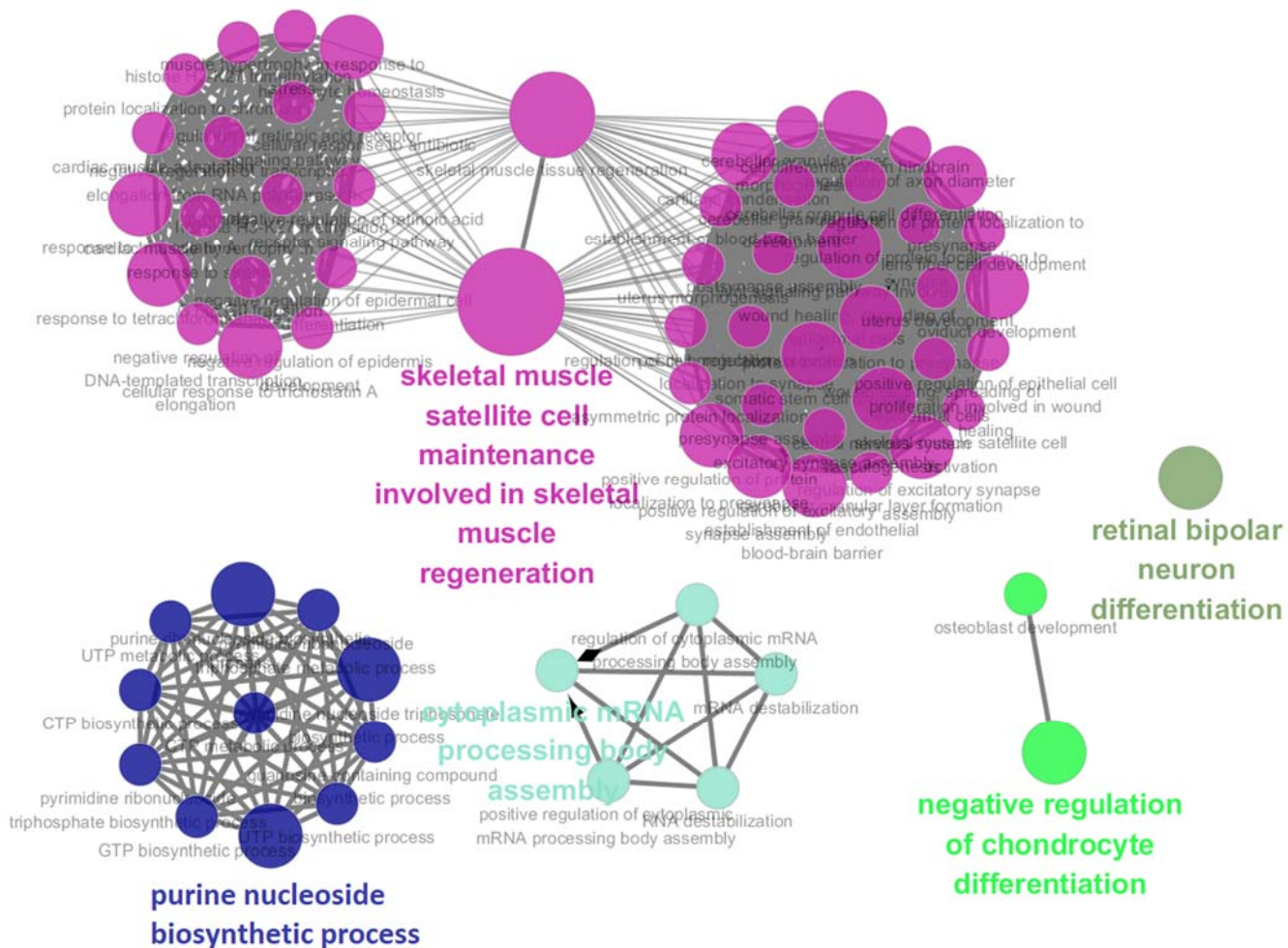


Figure 3.26 – An example of an *in silico* functional enrichment analysis of genes collectively targeted by the top differentially expressed miRNAs in responders.

CHAPTER 4

4 DISCUSSION

The optimization for circulating miRNA library preparations was first performed during this project in order to process patient samples effectively. After an optimal library preparation protocol was established, chip loading capacity was tested to create a reference for multiplexing patient samples efficiently. A cohort of PsA patients was treated with biologic agents and their blood samples were drawn pre-treatment, one-month post treatment, and three-month post treatment. The PGx patient samples were run on the Ion Torrent System and the resultant sequencing data underwent numerous analyses. Differential miRNA expression analyses were performed both between ACR50 response groupings and on clinical datasets. A comprehensive literature review was conducted on the identified differentially expressed miRNAs for potential implications in treatment response or disease pathogenesis. Subsequently, pathway and network analyses were performed on these results, which examined the miRNA profiles for associated signalling cascades and collectively targeted genes. Finally, an *in silico* functional analysis was performed using differentially expressed miRNA datasets generated between ACR50 response groupings to determine biological functions associated with the identified miRNA-mRNA network.

4.1 Optimization of Circulating miRNA Library Preparations

As stated in the introduction, the first objective of this project was to develop and optimize a procedure for preparing successful circulating miRNA libraries for sequencing using Ion Torrent Technology. With respect to miRNA sequencing using NGS technology, there are a number of quality measures that need to be met during library preparation and sequencing to ensure high-quality, accurate results (**Table 3.1**).

4.1.1 Thermo Fisher Protocol Modifications

It was quite evident that the TF protocol failed to meet the minimum criteria with respect to quality of the miRNA library preparation and downstream miRNA sequencing. In the electropherogram of TF-Sample 1, there was an excessive adaptor dimer peak at 85 bps, indicating heightened background noise, and there was an insufficient sample peak corresponding to miRNA at 102 bps, indicating that minimal fragments fell within the targeted size range. The mean read length was on the lower end of the desired metric due to the large adaptor dimer lowering the average length of reads in the sample. The total read count was predictably low given the low total sample concentration. The large adaptor dimer was composed of reads that were ~85 bps and as such were removed during filtering, resulting in a low percentage of total reads that passed filtering. A moderate amount of reads that passed filtering did align to the reference genome (alignment involves determining the position of a read relative to a reference genome). Similarly, a moderate percentage of those aligned reads mapped to miRNAs (mapping refers to the allocating aligned reads to miRNA loci). This suboptimal miRNA sequencing result was expected

due to the insufficiently small but appropriately sized (i.e., 94-144 bps) sample peak corresponding to miRNA. The suboptimal results for TF-Sample 1 library quantification were likely due to either the excessive adaptor dimers present and/or to the insufficient size of the sample peak corresponding to miRNA. The large adaptor dimer seen in the electropherogram could have been due to adaptor input excess or an inadequately proportioned adaptor-primer ratio, whereas the small sample peak observed in the electropherogram could have been due to human error or to the modified protocol being flawed.

Although the classic scientific method suggests that only one variable should be addressed at a time to determine why a procedure fails, the extremely low-quality results of the TF-prepared libraries necessitated multiple modifications to be implemented simultaneously. The excessive adaptor dimer present in each TF-prepared library, occupied unnecessary space on the chip and caused increased background noise thus reducing the quality of sequencing results. This was addressed by modifying both the adaptor volumes and adaptor-primer ratios. The insufficient sample peak corresponding to miRNA, which indicated that the input volume of the sample was too low or that the sample was being lost at during the procedure, was addressed by increasing the sample input consistently until the results improved.

After the suboptimal results of the TF-Sample 1 library, the first step was to optimize the input of these adaptors as well as increase the input volume of plasma. The majority of the metrics for molarity and sequencing quality were improved by increasing the input volume of plasma. Larger species of RNA in TF-Sample 2A (and 2B) also

contributed to the increased the total sample molarity. However, the lower-percent miRNA reads actually decreased as the content of the regional molarity was not miRNA species, but rather the shoulder of the adaptor dimer that fell in the regional molarity range of 94-104 bps on the electropherogram. The corresponding decrease in total and regional molarity when the adaptor and primer input was halved failed to affect percent regional molarity because the adaptor dimer shoulder area was decreased proportionally.

The majority of sequencing metrics were also decreased in TF-Sample 2B when compared with TF-Sample 2A, which is consistent with a decreased input of adaptors. Although the mean read length in TF-Sample 2A and 2B fell within the desired metric, it was towards the upper range for TF-Sample 2B likely due to larger species of RNA in the sample which can increase the mean read length. The total read counts for both TF-Sample 2A and TF-Sample 2B were both much lower than the desired metric. This was likely due to the reads that made up the large adaptor dimer that were removed during filtering, resulting in a low percentage of total reads passing filtering in both samples. Consequently, the majority of reads had been filtered out of both samples due to size such that only a moderate percentage of total reads mapped to the reference genome. A moderate amount of the reads that passed filtering aligned to the reference genome; this was expected due to the small but appropriate length sample peak. The number of miRNA reads fell well below the desired metric, although there was double the amount of miRNA reads in TF-Sample 2A than in TF-Sample 2B. This low number of miRNA reads resulted in a very low number of miRNAs detected, which was very similar in both TF-Sample 2A and TF-Sample 2B. These results show that decreasing the adaptor/primer input by half does not affect the

number of miRNAs detected but does affect the depth of coverage of those miRNA species (number of miRNA reads).

After addressing the adaptor input volume, the large adaptor dimers observed in the electropherogram of TF-Sample 2A and 2B could have been due to an inadequately proportioned adaptor-primer ratio. The small sample peak seen in the electropherogram of TF-Sample 2A and 2B could still have been due to human error or the modified protocol being flawed. After the suboptimal results of the TF-Sample 2A and 2B libraries, the second point of investigation was to optimize the adaptor-primer ratio.

The large adaptor dimer in the library of TF-Sample 3A, in addition to the presence of some larger species of RNA in the sample, resulted in increased total molarity. Given the persistent large adapter dimer still present in the library, an additional Magnetic Bead Cleanup Module was recommended to be performed by the FAS from TF in order to remove the adaptor dimer through the process of size selection. After the additional cleanup, the total molarity of TF-Sample 3A* had decreased by more than half, resulting in a substantial loss in library quality. Although the adaptor dimer peak, sample peak, and most of the larger species of RNA in the sample were low or removed during the additional clean up, all indices of molarity were also low, well below the desired thresholds. The mean read length fell within the upper range of the desired metric. The total read count for TF-Sample 3A* was higher than any other sample previously processed but was still well below the desired metric. Consequently, this additional procedure did not have the desired results and was not used going forward.

The total molarity of TF-Sample 3B was moderately high, the regional molarity was very low, and the percent regional molarity was very low. There was no visible sample peak within the desired range, suggesting that the sample might have been lost during processing. Because of this possibility, it was difficult to draw conclusions about the importance of barcode and primer volumes from this run. Assuming TF-Sample 3B was not lost in processing, the library quantification results indicate that decreasing the adaptor input by half (but not the primer inputs) resulted in a decrease of regional molarity by more than half. While the mean read length in TF-Sample 3B was in the acceptable range, the total read count for TF-Sample 3B was much lower than TF-Sample 3A* and was well below the desired metric. Because the majority of reads had been filtered out of both samples due to size, only a moderate percentage of total reads mapped to the reference genome. The number of miRNA reads fell well below the desired metric in both samples, with almost seven times the number of miRNA reads present in TF-Sample 3A* than in TF-Sample 3B. The low number of miRNA reads resulted in a low number of miRNAs detected. However, despite the greater number of miRNA reads in TF-Sample 3A*, the number of detected miRNAs was only double that of TF-Sample 3B. This demonstrated that, not only does TF-Sample 3A* have a larger number of detected miRNAs, but that there was greater coverage of these miRNAs. These results showed that decreasing the adaptor but not the primer or barcode inputs resulted in better sequencing quality from the samples; however, further improvements were required.

When compared with previous samples, the electropherogram profiles of TF-Samples 3A, 3A*, and 3B did not suggest that modifying the adaptor-primer ratio increases

the quality of the library produced. After addressing the adaptor input volume and the adaptor-primer ratio, the excessive adaptor dimers and insufficiently small but appropriately sized (i.e., 94-144 bp) sample peak corresponding to miRNA observed in the electropherogram of TF-Samples 3A, 3A*, and 3B could have been due to human error or to the modified protocol being flawed. Consequently, the third point of investigation was the possibility that human error was causing these suboptimal results.

To investigate if the source of suboptimal library preparations and sequencing results was attributable to human error, a standardized sample (with known concentration) was used for library preparation. With respect to small RNA, an optimal library result was produced using the Sample SmRNACon. The electropherogram profile of this sample differed greatly from the previous experiments because the Sample SmRNACon did not undergo size-selection processes (e.g., mirVana PARIS Kit or Magnetic Bead Cleanup Modules) to remove larger RNA species. As a result, there was a very large sample peak, a smaller peak that indicated the presence of tRNA species, and another large peak that indicated the presence of rRNA species. Consequently, the library result was slightly below the desired threshold for percent regional molarity with respect to miRNA. Noteworthy, the Ion Adaptor v2 reagent (part of the Ion Total RNA-Seq Kit v2) was used instead of the ‘R&D Systems Optimized’ adaptor reagent, suggesting that the previous suboptimal result could have been due to the adaptor reagent. This result proved that the protocol was being adhered to properly and that human error was not primarily responsible for the previous suboptimal results, and therefore this sample was not sequenced. After addressing the adaptor input volume, the adaptor-primer ratio, and the possible human error, the

previously observed suboptimal results could have been due to the modified protocol being flawed. After the successful results of the Sample SmRNACon library, the fourth point of investigation was to attempt a library preparation using a different published protocol.

4.1.2 Cheng et al. Protocol Modifications

The superiority of the CH protocol became evident with the library quantification of CH-Sample 1A. The total molarity and regional molarity were high and the percent regional molarity was slightly below the desired threshold. When compared with libraries prepared using the TF protocol, the electropherogram profile of this sample indicated that the CH protocol was superior and was therefore used for all library preparations from this point forward. The mean read length in CH-Sample 1A was longer than the desired metric, likely due to the presence of large RNA species. The total read counts exceed the desired threshold, which was expected based on the electropherogram profile. Likewise, very large proportion of the total read count that passed filtering and aligned to the reference genome, a large percentage of which mapped to known miRNAs, resulted in a miRNA read count that well exceeded the desired threshold. This was responsible for the detection of a large number of miRNAs. This sample generated optimal results in both library quantification and sequencing quality.

Despite the library preparation of CH-Sample 1A being successful, a small adaptor dimer was present as well as larger species of RNAs. To further refine the quality of libraries prepared, additional on-magnet incubation times were used in an attempt to remove the larger species of RNA. The total and regional molarity of CH-Sample 1B were very high and the percent regional molarity increased slightly compared with CH-Sample

1A and was marginally below the desired threshold. Although the peak for the adaptor dimer was increased compared with CH-Sample 1A, this was expected due to the overall higher library concentration. In contrast to CH-Sample 1A, the result with CH-Sample 1B indicated that the additional on-magnet wait times reduced the amount of large RNA species present and increased the sample concentration by ensuring that all fragments were bound and released from the magnetic beads at the right times. Therefore, additional on-magnet incubation times were used going forward. The mean read length in CH-Sample 1B was on the upper range of the desired metric but did not exceed its upper limit because the larger RNA species had been size selected out through increased on-magnet incubation times. The total read counts exceed the desired threshold which was expected based on the electropherogram profile. Likewise, a very large proportion of the total read count passed filtering and aligned to the reference genome – a large percentage of which mapped to known miRNAs and had a miRNA read count that well exceeded the desired threshold. This was responsible for the detection of a large number of miRNAs. This sample generated optimal results in both library quantification and sequencing quality.

4.2 Preparing for Optimal Sequencing

4.2.1 Chip Loading Properties

With regards to RNA-Seq, the P1 chip can be loaded with 60-80 million cDNA transcripts. When the number of samples loaded on the P1 chip is increased, the number of possible reads loaded from each sample is decreased. This is to say that the more samples

loaded the less information will be available from each of those samples. Each sample was loaded onto the chip at a molarity anticipated by the total number of samples loaded on that same chip. One variable that is affected by multiplexing/differential chip loading is average read depth, with the average read depth of each sample loaded onto a chip decreasing with a higher number of samples per chip or with an increase in the molarity of each sample. (Campbell et al., 2015) In general, the higher the proportion of T+ISPs in a sample, the higher the quality of sequencing results produced. Inter-run variability in the proportion of T+ISPs in a sample is expected and is removed during normalization.

Because of the variability between the chip loading capacity and the quality of sequencing results generated, the chip loading capacity for the RNA-Seq samples was evaluated before the PGx samples were loaded for sequencing. The purpose of this evaluation was to ensure that three time points (i.e., pre-treatment, post-treatment one month, and post-treatment three months) from the same individual could be loaded on to the same chip to eliminate inter-run variability (see Future Directions – **Section 4.8**). In the context of this project, the pre-treatment samples were loaded and sequenced at similar molarities to the chips that will be loaded with three time points in the broader project.

4.2.2 Sequencing Quality of Samples under Different Loading Conditions

Samples loaded under different conditions (different molarities and multiplexing with different number of samples) produced sequencing results that varied in quality. Two metrics, miRNA reads and miRNAs detected, were used to assess sequencing quality and a noticeable trend appeared whereby all of the samples assessed generated the highest

sequencing quality under two sequencing conditions (i.e., 7@8pM and 6@6pM) (Table 4.1).

Table 4.1 – Trend in library concentration and chip loading capacity.

Sample number	Best Chip Run
CH-Sample 1B	7@8pM
CH-Sample 2A	6@6pM
CH-Sample 2B	6@6pM
CH-Sample 3A	7@8pM
CH-Sample 3B	7@8pM
CH-Sample 4	6@6pM

4.2.2.1 Samples that Sequenced Best at 7@8pM

Three of the tested samples, CH-Sample 1B, CH-Sample 3A, and CH-Sample 3B, produced the best sequencing quality under the 7@8pM run condition. When the samples were sequenced with either 6@8pM or 6@6pM there was a midrange number of miRNA reads and a midrange number of miRNAs detected. This indicates that the differential molarities of these samples did not affect the number of miRNA reads or number of miRNAs detected. When sequenced with 9@6pM, the samples had the lowest number of miRNA reads and lowest number of miRNAs detected. This was the least informative sequencing run for these samples, demonstrating that increasing the number of samples to 9 per chip at 6pM considerably decreased the quality of sequencing results. Increasing the number of samples to 7 per chip at 8pM increased the quality of sequencing results. On the periphery, this finding is somewhat in contrast with next generation sequencing (exome or targeted panels) trends. However, the relatively low number of reads that comprise a

miRNA library (compared with exome sequencing) combined with the 6@8pM run not saturating the capacity of the P1 chip, allowed for the higher multiplexing capacity achieved with the 7@8pM run. In contrast, when the samples were sequenced with 7@8pM, they had the highest number of miRNA reads and miRNAs detected of all the sequencing runs performed. The 7@8pM sequencing run was the most informative for these samples, enabling quality differential expression analyses, miRNA variant detection, and novel miRNA discovery.

4.2.2.2 Samples that Sequenced Best at 6@6pM

Three of the tested samples, CH-Sample 2A, CH-Sample 2B, and CH-Sample 4, produced the best sequencing quality under the 6@6pM run condition. When the samples were sequenced with either 6@8pM or 7@8pM there was a midrange number of miRNA reads and a midrange number of miRNAs detected. This indicates that for these samples the number of samples loaded onto the chip at 8pM did not affect the number of miRNA reads or number of miRNAs detected. When sequenced with 9@6pM, the samples had the lowest number of miRNA reads and lowest number of miRNAs detected. This was the least informative sequencing run for these samples, demonstrating that increasing the number of samples to 9 per chip at 6pM considerably decreased the quality of sequencing results. Decreasing the number of samples to 6 per chip at 6pM increased the quality of sequencing results, suggests that decreasing the number of samples increases the number of sequenced reads and miRNA detected. The 6@6pM sequencing run was the most informative for these

samples, enabling quality differential expression analyses, miRNA variant detection, and novel miRNA discovery.

4.2.2.3 Trend Between Library Quality and Chip Loading Conditions

The dichotomous trend in sequencing results under differential loading conditions could be explained by the composition of the sample libraries. CH-Sample 1B, CH-Sample 3A, and CH-Sample 3B all had the best sequencing quality results when a moderate number of samples per chip were loaded at an increased molarity (7@8pM). The electropherograms of the sample libraries that sequenced best at 7@8pM all displayed a very large peak between 105-117 bps and had minimal adapter dimers and minimal large RNA species present, indicating quality library preparation. These results indicate that if the prepared library is of good quality then chip loading conditions should be 7@8pM. In contrast, CH-Sample 2A, CH-Sample 2B, and CH-Sample 4 all had the best sequencing quality results when there was a lower number of samples per chip at a decreased molarity (6@6pM). The electropherograms of the sample libraries that sequence best at 6@6pM all displayed adaptor dimers that were proportional in concentrations to the sample libraries. These results indicate that if adapter dimers are present, especially those that are of proportional concentration to the sample, then chip loading conditions should be 6@6pM.

4.3 Clinical Information and Response Grouping

While optimization for library preparation and chip loading capacities was underway, clinical assessment and blood sampling of PSA patients was underway. Blood

was drawn from PsA patients before they began treatment with biologic agents, one month after treatment began, and three-months after treatment began. The pre-treatment sample was used to establish a baseline miRNA profile. This baseline profile would then be compared to miRNA profile after one- and three-months of treatment. This approach would allow for an intra-individual differential miRNA expression analysis which is much more informative than inter-individual comparisons. The method of drawing blood pre-treatment was performed consistently across patients other than Patient 13. Patient 13 blood was drawn one week after the biologic had been administered. This was due to unforeseen clinical circumstances, as patient self-injected prior to having their blood drawn. Due to the exploratory nature of this project, Patient 13 was included as a baseline sample to increase the cohort size and subsequent data set. However, this is not a true baseline sample, as miRNA expression profiles would likely change one week after treatment began, and therefore Patient 13 will not be included in the analyses of the broader project.

PsA patients were either prescribed secukinumab (an IL-17 inhibitor) or ustekinumab (an IL-12/23 inhibitor). These treatment groups were collectively examined because of similar molecular and clinical results. Molecularly, the pharmaceuticals both target the same effector molecule, where secukinumab acts directly by inhibiting the IL-17 pathway and ustekinumab acts indirectly by inhibiting the IL-17 pathway. Clinically, there are very subtle differences in ACR50 response rates between these pharmaceuticals, with ustekinumab having a slightly higher incidence of mucocutaneous infections that are seen less commonly with secukinumab. These pharmaceuticals are often collectively examined and compared to treatment response to TNF α inhibitors, which targets a separate signalling

pathway and has a very different response profile to IL-12/23 or IL-17 inhibitors. An eventual goal of the broader PGx project is to better understand when to prescribe TNF α pathway inhibitors versus IL-17 pathway inhibitors (see Future Directions – **Section 4.8**). This project was focused on examining the IL-17 axis, which is inhibited by IL-17A and IL-12/23; TNF α inhibitors could be compared at a later date. It was with this rationale that patients treated with ustekinumab and secukinumab were grouped together for analyses.

The assessments performed to determine response status included the ACR50 (primary endpoint) and CDAI as global measurements of disease activity, disability as measured by HAQ-DI, and acute phase reactants as measured by ESR. The results of these assessments were collectively examined to determine each patient's response status. ACR50 and CDAI are very similar indicators of disease progression or clinical response. These two criteria normally result in the same response groupings. CDAI differs from ACR50 in that it does not require an acute phase reactant and is therefore more easily used in clinic. Because acute phase reactant results were available, the ACR50 was used to assess treatment response in the PGx cohort. Under these parameters, just under one half of the PsA patients who were included in this study met the ACR50 response criteria.

4.4 Data Analyses

The FASTQC software was originally developed for Illumina sequencing results and therefore is not optimized to analyze Ion Torrent data. The comprehensive miRNA analysis pipeline, developed by the Rahman-O'Rielly bioinformatician, was more tailored for Ion Torrent data analysis and therefore produced different values for the sequencing

summary (**Table 3.18** vs. **Table 3.22**). The raw data from the Ion Torrent System used for the comprehensive miRNA analyses generated different results because of the differential pipeline parameters such as datasets and cut-offs used. Read-depth filtering was set at 5x coverage for known miRNAs as this coverage level is standard in the field. (Conesa et al., 2016) These analyses were performed using a relatively small dataset, (n=9) therefore attaining suggestive significance, and to a greater extent statistical significance, for the identified associations was difficult. As the cohort size increases or other datasets contribute to the analyses, a greater number of significant findings are more probable (see Future Directions – **Section 4.8**).

4.4.1 miRNA Variant and Novel miRNAs Analyses

miRNA variant analyses are used to determine associations between variants within the precursor or mature miRNAs and clinical phenotypes. Variants in precursor miRNAs can affect the binding affinity of the RISC complex thereby influencing the mRNA-inhibition capacity of that miRNA. Variants in the mature miRNA can affect miRNA-mRNA binding which could influence the expression level of that mRNA transcript. To investigate these findings further predictive binding analyses would have to be performed by incorporating the miRNA variant into the algorithm. miRNA variant analyses were performed as part of the comprehensive analysis; however, they were not investigated fully given they were not the main focus of this project.

Novel miRNA analyses are discovery-based and are used to identify unannotated miRNAs that could be responsible for a clinical phenotype. Identification of novel miRNAs is one of the strengths of using NGS technologies when investigating miRNAs. Other

miRNA investigation techniques, such as qPCR or microarrays, are targeted approaches and therefore only examine the targeted transcripts. To investigate these findings further, predictive binding analyses of the novel transcript would have to be performed. Novel miRNA analyses were performed as part of the comprehensive analysis; however, they were not investigated fully given they were not the main focus of this project.

4.4.2 Differential miRNA Expression Analyses

Normalization is a technique used to remove potential biases that are produced by technical differences that occur during sample processing (Gonzalez, 2014). These technical differences can occur at various stages during sample processing: differential concentrations of prepared libraries, differential proportion of libraries that are miRNA reads, differential molarities and/or number of libraries loaded into the OneTouch, differential percentages of template positive ISPs loaded onto the P1 chip, and differential number of reads in samples loaded onto the P1 chip – all of which can impact the total number of aligned reads. The pharmacogenomics dataset was normalized using edgeR software. Because read counts are considered proportional to miRNA expression, inter-sample normalization is required. In order to normalize the data, an appropriate baseline must be established and the read counts for each sample must be measured relative to this baseline (Gonzalez, 2014). Normalization of read counts was done using edgeR software for more accurate differential expression analyses.

There are some limitations associated with normalization. These limitations pertain to miRNAs that are unique to a sample or to miRNAs that are highly expressed in a sample contributing to a decrease in available space for remaining miRNAs (Gonzalez, 2014). If

the data does not undergo normalization, then sampling limitations such as this can compromise the integrity of miRNA differential expression analyses (Gonzalez, 2014).

Once normalized, read depths across the same sample (which is sequenced under different multiplexing conditions) should result in the same level of coverage of a miRNA. If normalization is executed correctly, the within-replicate correlation will be very high. Standards for depth of coverage differ depending on the chip loading conditions. For the purpose of this project, the read-depth cut off was set at 5x coverage. Coverage for miRNA-Seq investigations can range from 5-20 distinct mapping per genome. Because this project was exploratory in nature, a low depth of coverage was applied during filtering to increase the size of available datasets (Conesa et al., 2016).

4.4.2.1 Differential miRNA Expression Analyses of ACR50 Response Groupings

Identifying differential miRNA expression and its associations with treatment response in a PSA cohort was used to explore the capabilities of the comprehensive miRNA analyses pipeline. Differential expression is often measure by an intra-individual comparison between two time points; however, for the purpose of this study the expression level of a particular miRNA in a responder was compared to the mean expression level of that miRNA in the non-responder group.

Seven differentially expressed miRNA were associated with response groupings; however, this association was lost after correcting for multiple testing. The limited associations found were in keeping with the poor clustering results observed on the MDS plot. The published literature on the differentially expressed miRNAs identified between

ACR50 responders and non-responders pertaining to drug response or related disease pathogenesis are provided in **Table 4.2** and **Table 4.3**, respectively. Of the seven differentially expressed miRNA, only miR-150-5p has been reported to be involved in response to biologics in patients with PS (TNF α -inhibitors). miR-96-5p has been investigated for possible involvement in differential response to other monoclonal antibodies. Increased expression of miR-150-5p was found to be associated with the pathogenesis of myasthenia gravis, autoimmune pancreatitis, and other autoimmune diseases.

Because no significance was found after correcting for multiple testing, the top 100 differentially expressed miRNAs were prioritized for investigations into collectively targeted genes. No functional annotation was performed on the 24 collectively targeted genes; this was because the top 100 differentially expressed miRNAs (and corresponding targeted genes) were analyzed using pathway enrichment and network analyses to better define biological function.

Table 4.2 – The published literature related to drug response in identified differentially expressed miRNAs between ACR50 response groupings and in clinical datasets.

Mature miRNA ID	Clinical Dataset(s)	Publications Related Differential miRNA Expression leading to Differential Drug Response			
		Differential Expression	Related Disease or Model Used	Treatment Response	Reference
miR-106a-3p	Responders vs. Non-responders	N/A	N/A	N/A	N/A
miR-96-5p	Responders vs. Non-responders	Decrease	CRC cell lines	response to cetuximab and panitumumab	(Ress et al., 2015)
miR-296-5p	Responders vs. Non-responders	Increase	early stage laryngeal carcinoma	resistance to radiotherapy	(Maia et al., 2015)
		Decrease	general carcinogenesis	resistance to ionizing radiation (IR), alkylating agents, anthracyclines, and platinum-containing compounds	(van Jaarsveld et al., 2014)
miR-3194-5p	Responders vs. Non-responders	N/A	N/A	N/A	N/A
miR-150-5p	Responders vs. Non-responders, CDAI 1 month, HAQ-DI 3 months	Increase	PS	Response to TNF α inhibitors	(Torri et al., 2017)
		Decrease	non-small cell lung cancer	respond well to radiation	(Menon et al., 2016)
		Decrease	murine model	adverse reaction to radiation	(Dinh et al., 2016)
miR-183-5p	Responders vs. Non-responders	Increase	triple-negative breast cancer	sensitivity to anthracyclines or taxanes-based adjuvant chemotherapy	(Ouyang et al., 2014)
miR-193a-5p	Responders vs. Non-responders	Increase	Human and murine squamous cell carcinoma cell lines	Treatment with cisplatin	(Ory et al., 2011)
		Decrease	Wilms' tumor blastema	resistance to neoadjuvant chemotherapy followed by nephrectomy	(Watson et al., 2013)

Mature miRNA ID	Clinical Dataset(s)	Publications Related Differential miRNA Expression leading to Differential Drug Response			
		Differential Expression	Related Disease or Model Used	Treatment Response	Reference
miR-193a-5p		Increase	osteosarcoma	response to ifosfamide	(Gougelet et al., 2011)
		Decrease	ovarian cancer	response to decitabine followed by carboplatin	(Benson, Skaar, Liu, Nephew, & Matei, 2015)
		Decrease	bladder cancer cells lines	cisplatin sensitivity	(J. Zhou et al., 2016)
miR-124-3p	CDAI 1 month, HAQ-DI 1 month, HAQ-DI 3 months, ESR 3 months	Decrease	Crohn's Disease	response to exclusive enteral nutrition therapy	(Guo et al., 2016)
		Decrease	Type 2 Diabetes	post-gastric bypass surgery	(Zhu, Yin, Li, & Mao, 2017)
miR-1275	CDAI 1 month, HAQ-DI 3 months	Increase	endothelial cells lines	post-curcumin treatment	(Bai, Wang, Sun, Zhang, & Dong, 2016)
miR-582-5p	CDAI 1 month, CDAI 3 months, HAQ-DI 1 month, HAQ-DI 3 months	Decrease	Chronic morphine or heroin users	opioid-induced immunosuppression	(Long et al., 2016)
miR-31-5p	CDAI 1 month, HAQ-DI 3 months	Increase	colorectal cancer	shorter progression-free survival after treatment with anti-EGFR therapeutics	(Igarashi et al., 2015)
		Increase	colorectal cancer	progression-free survival after treatment with cetuximab	(Kiss et al., 2016)
		Increase	metastatic CRC	response to cetuximab	(Mlcochova et al., 2015)
		Decrease	human colonic epithelial cells	Protected against radiation induced apoptosis	(Kim, Zhang, Barron, & Shay, 2014)
		Decrease	human keratinocytes	response to protein kinase C inhibitors	(Liu et al., 2017)
miR-27a-5p	HAQ-DI 3 months	N/A	N/A	N/A	N/A
miR-4433b-3p	HAQ-DI 3 months	N/A	N/A	N/A	N/A
miR-146a-3p	ESR 3 months	N/A	N/A	N/A	N/A

Table 4.3 - The published literature pertaining to related disease pathogenesis in identified differentially expressed miRNAs identified between ACR50 response groupings and in clinical datasets.

Mature miRNA ID	Clinical Dataset(s)	Publications Related to Differential miRNA Expression leading to Related Disease Pathogenesis		
		Differential Expression	Related Disease	Reference
miR-106a-3p	Responders vs. Non-responders	N/A	N/A	N/A
miR-96-5p	Responders vs. Non-responders	N/A	N/A	N/A
miR-296-5p	Responders vs. Non-responders	Decrease	Asthma	(Davis et al., 2017)
miR-3194-5p	Responders vs. Non-responders	N/A	N/A	N/A
miR-150-5p	Responders vs. Non-responders, CDAI 1 month, HAQ-DI 3 months	Increased	Myasthenia Gravis	(Punga, Andersson, Alimohammadi, & Punga, 2015)
		Increased	Myasthenia Gravis	(Punga et al., 2014)
		Increase	Autoimmune Pancreatitis	(Hamada, Masamune, Kanno, & Shimosegawa, 2015)
		Decrease	primary Sjögren's syndrome	(Chen et al., 2017)
		Decrease	type 1 diabetes mellitus	(Assmann, Recamonde-Mendoza, De Souza, & Crispim, 2017)
miR-183-5p	Responders vs. Non-responders	Decrease	Anterior Uveitis in Rat Model	(Hsu, Chang, Lin, & Yang, 2015)
		Increase	Reduces Osteogenic Differentiation in Bone Marrow Stromal (Stem) Cells	(Davis et al., 2017)
miR-193a-5p	Responders vs. Non-responders	N/A	N/A	N/A

Mature miRNA ID	Clinical Dataset(s)	Publications Related to Differential miRNA Expression leading to Related Disease Pathogenesis		
		Differential Expression	Related Disease	Reference
miR-124-3p	CDAI 1 month, HAQ-DI month, HAQ-DI 3 months, ESR 3 months	N/A	N/A	N/A
miR-1275	CDAI 1 month, HAQ-DI 3 months	Decrease	type 1 diabetes mellitus	(Assmann et al., 2017)
		Increase	immune thrombocytopenic purpura	(Zuo et al., 2017)
miR-582-5p	CDAI 1 month, CDAI 3 months, HAQ-DI 1 month, HAQ-DI 3 months	N/A	N/A	N/A
miR-31-5p	CDAI 1 month, HAQ-DI 3 months	Increase	hypertrophic scar formation	(Wang et al., 2017)
		Decrease	cemento-ossifying fibroma (in silico prediction)	(Pereira et al., 2017)
		Decrease	Celiac Disease	(Magni et al., 2014)
		Increase	Crohn's Disease	(Peck et al., 2015)
		Decrease	Celiac Disease	(Vaira et al., 2014)
		Decrease	Celiac Disease	(Buoli Comani et al., 2015)
		Increase	In Keloid Fibroblasts	(Li et al., 2013)
Decrease	In osteoarthritic cartilage-derived mesenchymal stem cell	(Xia et al., 2016)		
miR-27a-5p	HAQ-DI 3 months	N/A	N/A	N/A
miR-4433b-3p	HAQ-DI 3 months	N/A	N/A	N/A
miR-146a-3p	ESR 3 months	N/A	N/A	N/A

4.4.2.2 Differential miRNA Expression Analyses Incorporating Clinical Data

When the associations between differential expression of miRNAs and ACR50 response groupings were deemed insignificant, they did not qualify for further analysis. Instead the clinical datasets were investigated for clinical contributions that could be affecting differential expression. For example, the ESR is known to lower as PsA symptoms subside; a lower ESR may be associated with differential expression of a miRNA that may be implicated in inflammation.

This method of data analysis was slightly more informative than the differential response grouping analysis, with some miRNAs approaching significance. The published literature on the differentially expressed miRNAs identified in clinical datasets that pertain to drug response or related disease pathogenesis are provided in **Table 4.2** and **Table 4.3**. miR-31-5p was found to be correlated with involvement in differential response to other monoclonal antibodies; this is in keeping with improved CDAI at one month and HAQ-DI at three months. miR-31-5p has also been investigated in other autoimmune diseases such as celiac and Crohn's disease. Increased expression of miR-150-5p was found to be associated with the pathogenesis of myasthenia gravis, a chronic autoimmune disease involving dysregulation of T-cell differentiation. Upregulation of miR-31-5p was seen in fibrocytes during hypertrophic scar formation, showing a possible association to dermatological issues.

The published literature on the differentially expressed miRNAs associated with HAQ-DI values at one-month and three-months post treatment is displayed in **Table 4.2**

and **Table 4.3**. Similar results of differential miRNA expression were seen between CDAI and HAQ-DI over time. Associations to miR-150-5p, and miR-31-5p were found; these miRNAs are known to be implicated in the development of autoimmune diseases or response to treatment with monoclonal antibodies, as mentioned above.

No differentially expressed miRNAs reached suggestive significance for the ESR values at one-month post treatment. The published literature on the differentially expressed miRNAs associated with ESR values at three-months post treatment is displayed in **Table 4.2** and **Table 4.3**. As in CDAI and HAQ-DI, differential expression of miR-124-3p was found in the development and treatment of Crohn's disease, with a decrease in expression as symptoms subsided.

4.4.2.3 Pathway Analysis Using Top 100 Differentially Expressed miRNAs

The pathway analysis was performed on the top 100 differentially expressed miRNAs to identify pathways that might be implicated in treatment response. Proteoglycans in Cancer was the pathway with the strongest association to the differentially expressed miRNAs identified between ACR50 response groupings and the differentially expressed miRNAs that was identified relative to CDAI values at one- and three-months post treatment. These proteoglycans are known to contribute to cancer development by affecting proliferation, adhesion, angiogenesis, and metastasis. Morphine Addiction was the pathway with the strongest association with differentially expressed miRNA relative to the HAQ-DI values at one-month post treatment. This pathway influences neuronal function, inter-neuronal communication, and the brain-reward circuit. TGF-beta Signalling

Pathways was the pathway with the strongest association to the differentially expressed miRNAs relative to HAQ-DI values at three-month post treatment and ESR values at one-month post treatment. The TGF-beta protein family includes activins and bone morphogenetic protein (BMPs), which are both highly conserved cytokines. Axon Guidance is the pathway with the strongest association to the differentially expressed miRNAs relative to ESR values at three-months post treatment. The Axon Guidance pathway is critical for the development of the neuronal network.

The identified pathways associated with ACR50 response groupings and with clinical datasets did not suggest a biological consequence of the differentially expressed miRNAs. This lack of potential causative factors is likely to do with the increased amount of data generated from research in other fields, such as cancer, when compared to research into autoimmune disorders. These results are minimally informative due to the lack of significance in the data used for the analyses and due to the bias of accessible information in the disease category that is being investigated.

4.4.2.4 miRNA-mRNA Network Analyses and an *in silico* Functional Analysis of Top 100 Differentially Expressed miRNAs

The network analysis generated as a visualization of the miRNA-mRNA interactions contains ten collectively targeted mRNAs by 26 of the top 100 differentially expressed miRNAs between ACR50 responders and non-responders. Of the ten collectively targeted genes, *CNOT6L*, *EZH2*, *NME7*, *ERGIC2*, and *PTHLH* are amongst the most frequently targeted. All miRNA-mRNA interactions in this network, as depicted by all lines being of equal thickness, have an equal likelihood of occurrence. miRNAs not

included in the visualization did not have a predictive binding score of >0.3 for any of the ten collectively targeted genes.

The network analysis of the differentially expressed miRNAs relative to the CDAI values at one-month post treatment showed ten collectively targeted genes and 25 miRNAs. Of the ten collectively targeted genes, *CNOT6L*, *BTG3*, *PTHLH*, *SPRY1*, *ERGIC2*, and *RBI* are amongst the most frequently targeted. Not only are these the genes most likely to be targeted, the target prediction of these genes has a higher likelihood of occurrence indicated by the thicker lines on the network. The network analysis of the differentially expressed miRNAs relative to the CDAI values at three-months post treatment showed ten collectively targeted genes and 23 miRNAs. Of the ten collectively targeted genes, *EPC2*, *TRAPPC8*, *ERGIC2*, *IRX5*, and *SPRY1* are amongst the most frequently targeted. The target prediction of these genes has a higher likelihood of occurrence indicated by the thicker lines in the network.

The network analysis of the differentially expressed miRNAs relative to the HAQ-DI values at one-month post treatment showed ten collectively targeted genes and 20 miRNAs. Of the ten collectively targeted genes, *BTG3*, *ERGIC2*, *PTHLH*, *HSP90B1*, and *ANKHDI* are amongst the most frequently targeted. All miRNA-mRNA interactions in this network, as depicted by all lines being of equal thickness, have an equal likelihood of occurrence. The network analysis of the differentially expressed miRNAs relative to the HAQ-DI values at three-months post treatment showed ten collectively targeted genes and 15 miRNAs. Of the ten collectively targeted genes, *RBI*, *SPRY1*, *ERGIC2*, *TAF4B*, and

CNOT6L are amongst the most frequently targeted. The target prediction of these genes has a higher likelihood of occurrence indicated by the thicker lines in the network.

The network analysis of the differentially expressed miRNAs relative to the ESR values at one-month post treatment showed ten collectively targeted genes and 20 miRNAs. Of the ten collectively targeted genes, *PTHLH*, *BTG3*, *CNOT6L*, and *RBI* are amongst the most frequently targeted. The target prediction of these genes has a higher likelihood of occurrence indicated by the thicker lines in the network. The network analysis of the differentially expressed miRNAs relative to the ESR values at three-months post treatment showed ten collectively targeted genes and 22 miRNAs. Of the ten collectively targeted genes *BTG3*, *ERGIC2*, *CNOT6L*, and *PTHLH* are amongst the most frequently targeted. The target prediction of these genes has a higher likelihood of occurrence indicated by the thicker lines in the network.

These networks were generated as a preliminary analysis and were exploratory in nature. Genes common to multiple network analyses such as *CNOT6L*, *ERGIC2*, *BTG3*, and *PTHLH* would be investigated further if increased significance was found. As the cohort size of the PsA patients treated with IL-12/23 and IL-17 inhibitors increases, and the TNF α cohort (see Future Directions – **Section 4.8**) is included in these analyses, the networks will provide more accurate and informative predictive binding results.

An *in silico* functional enrichment analysis was done on the top 100 differentially expressed miRNAs between ACR50 responders and non-responders and the collectively targeted genes to examine biological function associated with the miRNA-mRNA interaction. At present, there appears to be no clear link between the three main functional

modules (skeletal muscle satellite cell maintenance involved in skeletal muscle regeneration, purine nucleoside biosynthetic process, and cytoplasmic mRNA processing body assembly) from miRNA studies and known pathogenesis of PsA or secukinumab/ustekinumab treatment. Increases in sample size and independent validation is required before the significance of these findings can be determined.

In the case of this exploratory project, some figures generated by software (such as Cytoscape) are difficult to read because of the larger number of data points and the lack of significant findings. As shown in **Figure 3.26**, the software depicted all possible interactions. In the broader project, which will have a larger dataset and the possibility of significant findings, these diagrams will become more refined and legible.

4.5 Clinical Relevance

Precision medicine is important in terms of the patient; at the moment, precision medicine is largely conducted on a trial-and-error basis, which is neither the safest nor the most cost-effective approach. Precision medicine initiatives are currently underway for diagnostic markers, prognostic markers, and predictive markers for response to treatment. With regards to response to treatment, the field of pharmacogenomics is currently oriented towards predicting response or non-response but also predicting the development of adverse events. Predicting response is of the greatest value for patients who do not respond to treatment as their disease progression would otherwise continue while the cost of treatment would constitute a large financial burden (\$20,000 to \$30,000 per year).

Pharmacogenomics of PsA is focused primarily on treatment with TNF α inhibitors, which are a more traditionally used biologic, and on IL-17 pathway inhibitors, which are a newer type of biologic. Currently, clinicians have limited evidence as to which type of biologic to prescribe. This project, as well as the associated broader project, will help to indicate which patients should be prescribed which biologic. To determine which biologic is most appropriate, different pharmacogenomics approaches could be used including DNA profiles, epigenetics profiles, and RNA profiles. RNA profiles allow for the investigation of mRNAs, intracellular miRNAs, and circulating miRNAs. The most clinically relevant profile, without resorting to a tissue biopsy, would be circulating miRNAs as it lends insight to the inter-cellular communication occurring in the disease tissue.

Circulating miRNA pharmacogenomic profiling (as with all RNA pharmacogenomics profiling) is of particular clinical utility when a predictive marker is available at baseline, which may suggest an efficacious course of treatment for a patient. Intra-individual comparison of miRNA profiles can also be of clinical utility as they indicate up- and down-regulation of miRNAs, which could lend insight into the mechanism of action of the drug or the pathogenesis of disease.

The results generated from this project at this time are not clinically actionable. Given the sample size this is exploratory data for hypothesis generation and must still be validated. This project's aim was to develop and optimize a framework of assays and analyses that can be used to identify associations that may be clinically relevant once the cohort size is large enough to reach significance. The goal of the broader project is to

increase the patient cohort being prescribed IL-17 pathway inhibitors to 20 and to match that cohort with 20 patients being prescribed TNF α inhibitors. With an increased sample intake and dataset size, a multi time point comparison of response profiling between patients prescribed IL-17 pathway inhibitors and patients prescribed TNF α inhibitors will be performed. Findings from this investigation will then be validated by an independent cohort and prospectively tested in clinic to determine the relevance. Clinically predicting response to biologics in PsA patients would improve the current response rate (50% to 60% reaching ACR20 score). If a clinically relevant predictive marker or profile is found, response rates would ideally increase in a subset of patients, as 40% of non-responders will be removed.

4.6 Limitations

Although circulating miRNA profiles show great promise as a non-invasive biomarker for diagnosis, prognosis, and prediction of drug response, there are still some limitations to this type of investigation. Examining circulating miRNA profiles from plasma may not accurately represent what is occurring at the level of the involved tissue. This limitation can be addressed by increasing the cohort size or by the addition of other “-omics” datasets thereby increasing the likelihood of identifying accurate markers. Furthermore, future studies assessing the correlation between intracellular miRNA from serial synovial biopsies and circulating miRNA may also add further weight to the validity of assessing circulating miRNA as potential biomarkers.

During the optimization portion of this project, limiting factors such as R&D Systems' 'Optimized' adaptors and the flawed TF protocol were the cause of serious delays. The R&D Systems' 'Optimized' adaptors were of unknown volume and concentration and therefore should not have been used in such a lengthy and costly protocol. The updated protocol which has since been published on the TF website for use with the Ion RNA-Seq, is reflective of the Cheng et al. protocol.

Numerous points during the library preparation procedure could have resulted in downstream inhibition if they were incorrectly performed. These potential points of contamination include: if phenol chloroform was transferred with the aqueous phase during RNA extraction, if DNase inactivation reagent was transferred with the sample-containing supernatant after DNase treatment, and if beads were incorrectly transferred at any point during the magnetic bead clean up modules (particularly in final transfer of each module). Another potential limitation in the library preparation procedure was the percentage of alcohol used. The TH and CH protocol both state that 100% ethanol must be used to ensure accurate size selection. Due to shipping restrictions, the highest percentage of alcohol that can be shipped to NF is 95%. To address each of these potential laboratory limitations, extra care was taken to ensure no contamination occurred and that fresh alcohol was used daily to maintain as high a percentage of alcohol as possible.

Ideally all the PGx samples would be loaded onto the same chip to ensure no inter-run variability. This was not possible due to the barcoding system used to accommodate the broader project. The read bias that potentially occurred when the samples were run on different chips was addressed during normalization. As mentioned above there are many

points during sample processing, such as chip loading, which could bias the sequencing results. Normalization of the data using edgeR software should remedy these issues; however, these biases could still be possible.

The moderately low prevalence of PsA and the frequency of patients prescribed biologics made patient recruitment a limiting factor given the timeframe of this project. Due to the small sample size of this project, it was difficult to control for aspects such as co-medications, comorbidities, and sample ascertainment. The only co-medication controlled for in this project was concurrent treatment with other biologics; however, other medications such as steroids, NSAIDs, and methotrexate were not controlled for and could have therefore limited the quality of the results. Comorbidities such as other autoimmune diseases, which occur more frequently in patients already diagnosed with an autoimmune disease, can cause differential miRNA expression and confound the results generated. Co-medications and comorbidities are only possible confounding factors in this project where the differential expression of miRNAs is compared between patients. However, in the broader project where differential expression of miRNAs is compared within an individual, it is less likely that these factors will confound the data. Data quality could have also been limited by the method of sample ascertainment and whether fresh samples are delivered to the lab in order to attain realistic inter-cellular communication. This can be difficult to do in practice and is dependent on a laboratory's capacity.

Another limitation to the quality of results generated from this project is the response status of a patient. Response status is measured on a continuum. When a patient does not reach ACR50 and was therefore not deemed to be a responder, it does not

necessarily indicate that there was no response whatsoever (ie., they could have only reached ACR20 by the primary endpoint). Because half of the ACR50 criteria is reported by the patients, which is not always truly reflective of response status, miscategorization of responders is possible. This possibility of partial response (ACR20) or inappropriate self-categorization will confound the data associated with response and limit the quality of results of the project. However, this type of bias will minimize any potential findings as the non-responder pool is being contaminated with partial responders, so the error will be towards the null. The ACR50 was selected as the response criteria as it represents a more meaningful clinical response. The ideal control group would be non-responders, as determined by patients not reaching ACR20. Given the magnitude of effect from the present biologics in standard clinical practice, our sample size was insufficient to retrieve a large group of non-responders that failed to reach ACR20.

Phase III registration studies for TNF α inhibitors and IL-17A monoclonal antibodies have reported slight differences in the incidence of opportunistic and serious infections. Although there is no head-to-head studies between these two classes of medications, numerically there appears to be a lower rate of infections among IL-17A blockade. Also, IL-17A monoclonal antibodies are unlikely to aggravate diseases such as systemic lupus and multiple sclerosis. As patients for this study were selected from a real-world setting, there would be a tendency to select patients with a slightly lower risk of infection. This may affect the generalizability of our results.

Due to the small sample size, which limits the power of the study, an overall lack of significant findings was consistent across datasets, therefore the validation process and

subsequent functional studies were not possible. The furthest possible point of investigation for this project was network and the *in silico* functional analyses. These analyses are important because of how unlikely is it to find a single gene or miRNA dysregulation causing drug response or pathogenesis in a complex disease. It is more likely that a combination of dysregulated genes and miRNAs are responsible, which would necessitate a multi-omic approach to such research. As of yet, there are no FDA-approved clinical tests that are based on a pattern of dysregulation or are generated from multi-omic approaches; in the future, however, such steps will likely be necessary when treating complex diseases.

4.7 Summary and Conclusions

The development and optimization of a framework capable of preparing and sequencing circulating miRNA libraries was explored with a pharmacogenomic analyses of a PsA patient cohort. miRNA library preparation was optimized through attempting two protocols and multiple modifications. After an optimal library preparation protocol was established, the loading capacity of the PI chip was tested to create a reference for an increase in multiplexing without a decrease in sequencing quality. This library preparation and sequencing framework was used to investigate the miRNA profiles of PsA patients being treated with biologics, a very expensive class of pharmaceutical with a ~50% response rate. Nine PsA patients treated with IL-17 pathway inhibitors consented to the study and their blood samples were drawn pre-treatment, one-month post treatment, and three-month post treatment. Patients who reached the primary endpoint (ACR50) were deemed responders and the other were deemed non-responders. The baseline patient

samples were sequenced by the Ion Torrent System, and the data underwent numerous analyses using a comprehensive miRNA pipeline. Differential miRNA expression analyses were performed both between ACR50 response groupings and on clinical datasets in attempt to identify a miRNA or a miRNA profile that could predict treatment outcome. Statistical significance was difficult to attain due to the small cohort size; however, the results of these analyses show the potential for identifying a predictive marker or profile. A comprehensive literature review was conducted to identify differentially expressed miRNAs for potential implications in treatment response of PsA pathogenesis, as would have been done if findings had been significant. The data was then analyzed using pathway analyses, network analyses, and functional enrichment analysis for associated signalling cascades, collectively targeted genes, and relevance to biological functions. These results demonstrated the complexity of miRNA and their mRNA regulatory capacity. Although this study found minimal statistically significant findings. However, statistically significant associations between differentially expressed miRNAs and clinical outcomes can be thoroughly investigated with these analyses to determine potential causative mechanisms for differential drug response or disease development.

In conclusion, the circulating miRNA sequencing framework developed for this project has proven capable of effectively extracting miRNA from plasma, preparing high-quality libraries, sequence libraries in a high-throughput manner, and analyzing the sequencing data for potential associations. This project is part of a larger research agenda that could identify significant differential expression of cellular or circulating miRNAs that may have association with response to biologics in future PsA patient cohorts.

4.8 Future Directions

An RNA sequencing framework was developed to investigate variants and differential expression of mRNA, intracellular miRNA, and circulating miRNA. This RNA sequencing framework (**Figure 4.1**) was designed and implemented by the author through a review of pertinent literature and by consulting the FAS from TF.

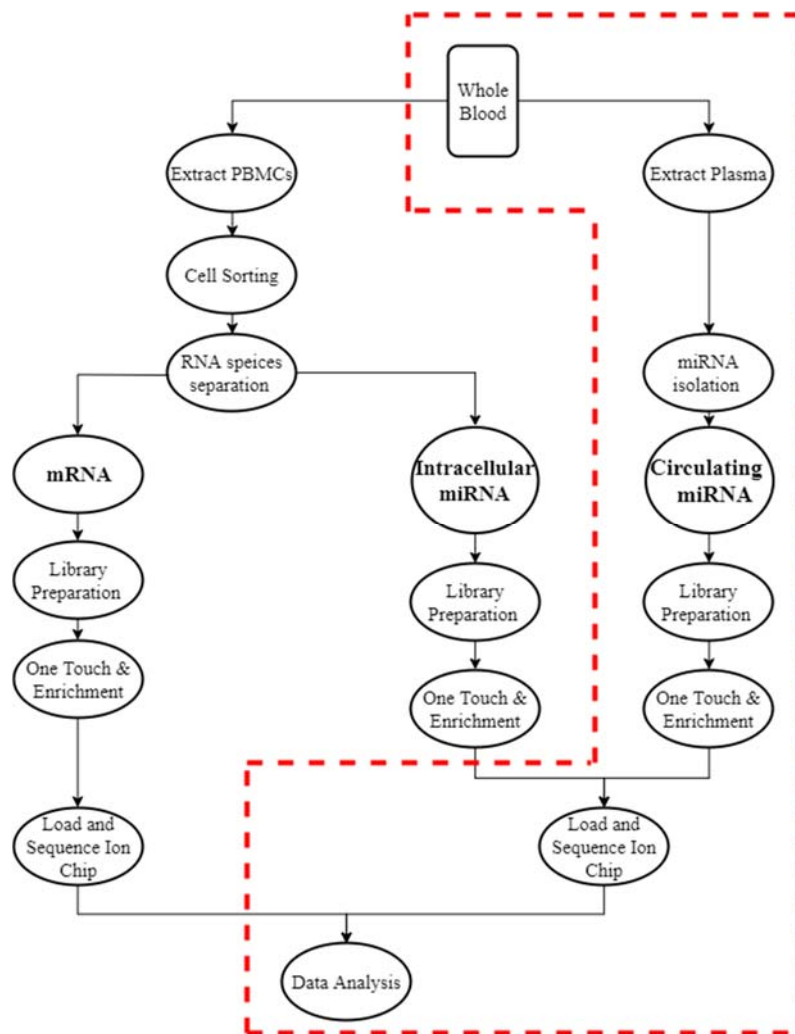


Figure 4.1 – Summary of RNA sequencing framework for the broader project that enables mRNA and intercellular miRNA sequencing and collective data analysis. Highlighted is the focus of this project.

The mRNA sequencing branch of this framework now enables researchers in the Rahman/O’Rielly lab group to gain insight into gene expression, gene expression levels, alternative splicing, and variants in the transcripts of expressed genes. The intracellular miRNA sequencing branch of the framework enables the examination of intracellular regulation of gene expression. Understanding the source of intracellular miRNAs can also provide insight into cell types that are responsible for disease development. The peripheral blood mononucleocytes of the PsA patients will be sorted by cell types in order to perform more informative intracellular miRNA analyses. The circulating miRNA sequencing branch of the framework enables investigations on the intercellular regulation of gene expression. While this framework has the capacity to sequence mRNA, intracellular miRNA, and circulating miRNA, this project solely investigated circulating miRNAs.

Patients recruited for this study were prescribed either TNF α inhibitors, IL-17 inhibitors, or IL-12/23 inhibitors. As the TNF α inhibitor cohort size increases, a collective comparative analysis of these biologics will be done in an attempt to identify therapeutic markers.

Examining circulating miRNA profiles can indicate intracellular communication occurring at the level of the tissue, making these miRNAs particularly important in PsA as an alternative to biopsing deteriorating psoriatic joints. Research into circulating miRNAs as a non-invasive source of biomarkers is expanding. The majority of these studies are done using microarray and qPCR but are limited by their targeted approach. Sequencing miRNA using NGS is preferable due to the sensitivity of detection, dynamic range of detection, and accuracy of measuring differential expression levels. Given the high prevalence of psoriatic

disease in NF, interpatient variability and the high cost associated with biological therapy, the lack of access to tissue of primary pathology, and the advent of NGS to sequence circulating miRNA, a marker for response to treatment with biologics would have great clinical utility. This project has assembled a framework to enable the identification of circulating miRNAs or circulating miRNA profiles that may have clinical utility. The results generated from the broader project will represent the most comprehensive investigation of treatment response in PSA patients.

References

- Al-Heresh, A. M., Proctor, J., Jones, S. M., Dixey, J., Cox, B., Welsh, K., & McHugh, N. (2002). Tumour necrosis factor-alpha polymorphism and the HLA-Cw*0602 allele in psoriatic arthritis. *Rheumatology (Oxford, England)*, *41*(5), 525-530.
- American Academy of Dermatology Work Group, Menter, A., Korman, N. J., Elmets, C. A., Feldman, S. R., Gelfand, J. M., . . . Bhushan, R. (2011). Guidelines of care for the management of psoriasis and psoriatic arthritis: Section 6. guidelines of care for the treatment of psoriasis and psoriatic arthritis: Case-based presentations and evidence-based conclusions. *Journal of the American Academy of Dermatology*, *65*(1), 137-174. doi:10.1016/j.jaad.2010.11.055 [doi]
- Assmann, T. S., Recamonde-Mendoza, M., De Souza, B. M., & Crispim, D. (2017). MicroRNA expression profiles and type 1 diabetes mellitus: Systematic review and bioinformatic analysis. *Endocrine Connections*, *6*(8), 773-790. doi:10.1530/EC-17-0248 [doi]
- Baerveldt, E. M., Onderdijk, A. J., Kurek, D., Kant, M., Florencia, E. F., Ijpma, A. S., . . . Prens, E. P. (2013). Ustekinumab improves psoriasis-related gene expression in noninvolved psoriatic skin without inhibition of the antimicrobial response. *The British Journal of Dermatology*, *168*(5), 990-998. doi:10.1111/bjd.12175 [doi]
- Bai, Y., Wang, W., Sun, G., Zhang, M., & Dong, J. (2016). Curcumin inhibits angiogenesis by up-regulation of microRNA-1275 and microRNA-1246: A promising therapy for treatment of corneal neovascularization. *Cell Proliferation*, *49*(6), 751-762. doi:10.1111/cpr.12289 [doi]
- Balato, A., Schiattarella, M., Di Caprio, R., Lembo, S., Mattii, M., Balato, N., & Ayala, F. (2014). Effects of adalimumab therapy in adult subjects with moderate-to-severe psoriasis on Th17 pathway. *Journal of the European Academy of Dermatology and Venereology : JEADV*, *28*(8), 1016-1024. doi:10.1111/jdv.12240 [doi]
- Balding, J., Kane, D., Livingstone, W., Mynett-Johnson, L., Bresnihan, B., Smith, O., & FitzGerald, O. (2003). Cytokine gene polymorphisms: Association with psoriatic arthritis susceptibility and severity. *Arthritis and Rheumatism*, *48*(5), 1408-1413. doi:10.1002/art.10935 [doi]
- Barnas, J. L., & Ritchlin, C. T. (2015). Etiology and pathogenesis of psoriatic arthritis. *Rheumatic Diseases Clinics of North America*, *41*(4), 643-663. doi:10.1016/j.rdc.2015.07.006 [doi]
- Bartel, D. P. (2004). MicroRNAs: Genomics, biogenesis, mechanism, and function. *Cell*, *116*(2), 281-297. doi:S0092867404000455 [pii]
- Benson, E. A., Skaar, T. C., Liu, Y., Nephew, K. P., & Matei, D. (2015). Carboplatin with decitabine therapy, in recurrent platinum resistant ovarian cancer, alters circulating miRNAs concentrations: A pilot study. *PloS One*, *10*(10), e0141279. doi:10.1371/journal.pone.0141279 [doi]

- Betel, D., Koppal, A., Agius, P., Sander, C., & Leslie, C. (2010). Comprehensive modeling of microRNA targets predicts functional non-conserved and non-canonical sites. *Genome Biology*, *11*(8), R90-2010-11-8-r90. Epub 2010 Aug 27. doi:10.1186/gb-2010-11-8-r90 [doi]
- Bowes, J., Loehr, S., Budu-Aggrey, A., Uebe, S., Bruce, I. N., Feletar, M., . . . Barton, A. (2015). PTPN22 is associated with susceptibility to psoriatic arthritis but not psoriasis: Evidence for a further PsA-specific risk locus. *Annals of the Rheumatic Diseases*, *74*(10), 1882-1885. doi:10.1136/annrheumdis-2014-207187 [doi]
- Boyd, T., & Kavanaugh, A. (2015). Novel approaches to biological therapy for psoriatic arthritis. *Expert Opinion on Biological Therapy*, , 1-14. doi:10.1517/14712598.2016.1118045 [doi]
- Budu-Aggrey, A., Bowes, J., Stuart, P. E., Zawistowski, M., Tsoi, L. C., Nair, R., . . . Raychaudhuri, S. (2017). A rare coding allele in IFIH1 is protective for psoriatic arthritis. *Annals of the Rheumatic Diseases*, *76*(7), 1321-1324. doi:10.1136/annrheumdis-2016-210592 [doi]
- Buoli Comani, G., Panceri, R., Dinelli, M., Biondi, A., Mancuso, C., Meneveri, R., & Barisani, D. (2015). miRNA-regulated gene expression differs in celiac disease patients according to the age of presentation. *Genes & Nutrition*, *10*(5), 482-015-0482-2. Epub 2015 Aug 2. doi:10.1007/s12263-015-0482-2 [doi]
- Butt, C. (2009). *The genetics of psoriatic arthritis.. Memorial University of Newfoundland*, (Thesis (Doctoral (PhD)))
- Campalani, E., Arenas, M., Marinaki, A. M., Lewis, C. M., Barker, J. N., & Smith, C. H. (2007). Polymorphisms in folate, pyrimidine, and purine metabolism are associated with efficacy and toxicity of methotrexate in psoriasis. *The Journal of Investigative Dermatology*, *127*(8), 1860-1867. doi:5700808 [pii]
- Campbell, J. D., Liu, G., Luo, L., Xiao, J., Gerrein, J., Juan-Guardela, B., . . . Lenburg, M. E. (2015). Assessment of microRNA differential expression and detection in multiplexed small RNA sequencing data. *RNA (New York, N.Y.)*, *21*(2), 164-171. doi:10.1261/rna.046060.114 [doi]
- Canadian Psoriasis Guidelines Addendum Committee. (2016). 2016 addendum to the canadian guidelines for the management of plaque psoriasis 2009. *Journal of Cutaneous Medicine and Surgery*, *20*(5), 375-431. doi:10.1177/1203475416655705 [doi]
- Carmona, R., MD. (2012). Clinical disease activity index (CDAI). Retrieved from <http://www.rheumtutor.com/clinical-disease-activity-index-cdai/>
- Carron, P., Varkas, G., Cypers, H., Van Praet, L., Elewaut, D., Van den Bosch, F., & CRESPA investigator group. (2017). Anti-TNF-induced remission in very early peripheral spondyloarthritis: The CRESPA study. *Annals of the Rheumatic Diseases*, *76*(8), 1389-1395. doi:10.1136/annrheumdis-2016-210775 [doi]
- Chandran, V. (2013). The genetics of psoriasis and psoriatic arthritis. *Clinical Reviews in Allergy & Immunology*, *44*(2), 149-156. doi:10.1007/s12016-012-8303-5 [doi]

- Chandran, V., Bull, S. B., Pellett, F. J., Ayearst, R., Rahman, P., & Gladman, D. D. (2013). Human leukocyte antigen alleles and susceptibility to psoriatic arthritis. *Human Immunology*, *74*(10), 1333-1338. doi:10.1016/j.humimm.2013.07.014 [doi]
- Chandran, V., Schentag, C. T., Brockbank, J. E., Pellett, F. J., Shanmugarajah, S., Toloza, S. M., . . . Gladman, D. D. (2009). Familial aggregation of psoriatic arthritis. *Annals of the Rheumatic Diseases*, *68*(5), 664-667. doi:10.1136/ard.2008.089367 [doi]
- Chandran, V., Siannis, F., Rahman, P., Pellett, F. J., Farewell, V. T., & Gladman, D. D. (2010). Folate pathway enzyme gene polymorphisms and the efficacy and toxicity of methotrexate in psoriatic arthritis. *The Journal of Rheumatology*, *37*(7), 1508-1512. doi:10.3899/jrheum.091311 [doi]
- Chen, J. Q., Papp, G., Poliska, S., Szabo, K., Tarr, T., Balint, B. L., . . . Zeher, M. (2017). MicroRNA expression profiles identify disease-specific alterations in systemic lupus erythematosus and primary sjogren's syndrome. *PloS One*, *12*(3), e0174585. doi:10.1371/journal.pone.0174585 [doi]
- Cheng, L., Sharples, R. A., Scicluna, B. J., & Hill, A. F. (2014). Exosomes provide a protective and enriched source of miRNA for biomarker profiling compared to intracellular and cell-free blood. *Journal of Extracellular Vesicles*, *3*, 10.3402/jev.v3.23743. eCollection 2014. doi:10.3402/jev.v3.23743 [doi]
- Chien, A. L., Elder, J. T., & Ellis, C. N. (2009). Ustekinumab: A new option in psoriasis therapy. *Drugs*, *69*(9), 1141-1152. doi:10.2165/00003495-200969090-00001 [doi]
- Chiu, H. Y., Wang, T. S., Chan, C. C., Cheng, Y. P., Lin, S. J., & Tsai, T. F. (2014). Human leukocyte antigen-Cw6 as a predictor for clinical response to ustekinumab, an interleukin-12/23 blocker, in chinese patients with psoriasis: A retrospective analysis. *The British Journal of Dermatology*, *171*(5), 1181-1188. doi:10.1111/bjd.13056 [doi]
- Coates, L. C., Fransen, J., & Helliwell, P. S. (2010). Defining minimal disease activity in psoriatic arthritis: A proposed objective target for treatment. *Annals of the Rheumatic Diseases*, *69*(1), 48-53. doi:10.1136/ard.2008.102053 [doi]
- Cock, P. J., Fields, C. J., Goto, N., Heuer, M. L., & Rice, P. M. (2010). The sanger FASTQ file format for sequences with quality scores, and the solexa/illumina FASTQ variants. *Nucleic Acids Research*, *38*(6), 1767-1771. doi:10.1093/nar/gkp1137 [doi]
- Cole, C. N. (2001). Choreographing mRNA biogenesis. *Nature Genetics*, *29*(1), 6-7. doi:10.1038/ng0901-6 [doi]
- Conesa, A., Madrigal, P., Tarazona, S., Gomez-Cabrero, D., Cervera, A., McPherson, A., . . . Mortazavi, A. (2016). A survey of best practices for RNA-seq data analysis. *Genome Biology*, *17*, 13-016-0881-8. doi:10.1186/s13059-016-0881-8 [doi]

- Creemers, E. E., Tijssen, A. J., & Pinto, Y. M. (2012). Circulating microRNAs: Novel biomarkers and extracellular communicators in cardiovascular disease? *Circulation Research*, *110*(3), 483-495. doi:10.1161/CIRCRESAHA.111.247452 [doi]
- Cubino, N., Montilla, C., Usategui-Martin, R., Cieza-Borrel, C., Carranco, T., Calero-Paniagua, I., . . . Gonzalez-Sarmiento, R. (2016). Association of IL1Beta (-511 A/C) and IL6 (-174 G > C) polymorphisms with higher disease activity and clinical pattern of psoriatic arthritis. *Clinical Rheumatology*, *35*(7), 1789-1794. doi:10.1007/s10067-016-3301-2 [doi]
- Cuchacovich, R., Perez-Alamino, R., Zea, A. H., & Espinoza, L. R. (2014). Distinct genetic profile in peripheral blood mononuclear cells of psoriatic arthritis patients treated with methotrexate and TNF-inhibitors. *Clinical Rheumatology*, *33*(12), 1815-1821. doi:10.1007/s10067-014-2807-8 [doi]
- Das, K. M., & Dubin, R. (1976). Clinical pharmacokinetics of sulphasalazine. *Clinical Pharmacokinetics*, *1*(6), 406-425.
- Davila, L., & Ranganathan, P. (2015). Corrigendum: Pharmacogenetics: Implications for therapy in rheumatic diseases. *Nature Reviews.Rheumatology*, *11*(5), 258. doi:10.1038/nrrheum.2015.32 [doi]
- Davis, C., Dukes, A., Drewry, M., Helwa, I., Johnson, M. H., Isales, C. M., . . . Hamrick, M. W. (2017). MicroRNA-183-5p increases with age in bone-derived extracellular vesicles, suppresses bone marrow stromal (stem) cell proliferation, and induces stem cell senescence. *Tissue Engineering.Part A*, *23*(21-22), 1231-1240. doi:10.1089/ten.TEA.2016.0525 [doi]
- Davis, J. S., Sun, M., Kho, A. T., Moore, K. G., Sylvia, J. M., Weiss, S. T., . . . Tantisira, K. G. (2017). Circulating microRNAs and association with methacholine PC20 in the childhood asthma management program (CAMP) cohort. *PloS One*, *12*(7), e0180329. doi:10.1371/journal.pone.0180329 [doi]
- Dayangac-Erden, D., Karaduman, A., & Erdem-Yurter, H. (2007). Polymorphisms of vitamin D receptor gene in turkish familial psoriasis patients. *Archives of Dermatological Research*, *299*(10), 487-491. doi:10.1007/s00403-007-0782-5 [doi]
- Deeks, E. D. (2015). Apremilast: A review in psoriasis and psoriatic arthritis. *Drugs*, *75*(12), 1393-1403. doi:10.1007/s40265-015-0439-1 [doi]
- Diani, M., Altomare, G., & Reali, E. (2015). T cell responses in psoriasis and psoriatic arthritis. *Autoimmunity Reviews*, *14*(4), 286-292. doi:10.1016/j.autrev.2014.11.012 [doi]
- Dinh, T. K., Fendler, W., Chalubinska-Fendler, J., Acharya, S. S., O'Leary, C., Deraska, P. V., . . . Kozono, D. (2016). Circulating miR-29a and miR-150 correlate with delivered dose during thoracic radiation therapy for non-small cell lung cancer. *Radiation Oncology (London, England)*, *11*, 61-016-0636-4. doi:10.1186/s13014-016-0636-4 [doi]

- Dougados, M., & Baeten, D. (2011). Spondyloarthritis. *Lancet (London, England)*, 377(9783), 2127-2137. doi:10.1016/S0140-6736(11)60071-8 [doi]
- Eder, L., Haddad, A., Rosen, C. F., Lee, K. A., Chandran, V., Cook, R., & Gladman, D. D. (2016). The incidence and risk factors for psoriatic arthritis in patients with psoriasis: A prospective cohort study. *Arthritis & Rheumatology (Hoboken, N.J.)*, 68(4), 915-923. doi:10.1002/art.39494 [doi]
- Edson-Heredia, E., Banerjee, S., Zhu, B., Maeda-Chubachi, T., Cameron, G. S., Shen, W., . . . Leonardi, C. L. (2016). A high level of clinical response is associated with improved patient-reported outcomes in psoriasis: Analyses from a phase 2 study in patients treated with ixekizumab. *Journal of the European Academy of Dermatology and Venereology : JEADV*, 30(5), 864-865. doi:10.1111/jdv.13032 [doi]
- Ellinghaus, D., Ellinghaus, E., Nair, R. P., Stuart, P. E., Esko, T., Metspalu, A., . . . Franke, A. (2012). Combined analysis of genome-wide association studies for crohn disease and psoriasis identifies seven shared susceptibility loci. *American Journal of Human Genetics*, 90(4), 636-647. doi:10.1016/j.ajhg.2012.02.020 [doi]
- Feuk, L., Carson, A. R., & Scherer, S. W. (2006). Structural variation in the human genome. *Nature Reviews.Genetics*, 7(2), 85-97. doi:nrg1767 [pii]
- Filer, C., Ho, P., Smith, R. L., Griffiths, C., Young, H. S., Worthington, J., . . . Barton, A. (2008). Investigation of association of the IL12B and IL23R genes with psoriatic arthritis. *Arthritis and Rheumatism*, 58(12), 3705-3709. doi:10.1002/art.24128 [doi]
- Franconi, F., & Campesi, I. (2014). Pharmacogenomics, pharmacokinetics and pharmacodynamics: Interaction with biological differences between men and women. *British Journal of Pharmacology*, 171(3), 580-594. doi:10.1111/bph.12362 [doi]
- Friedlander, M. R., Mackowiak, S. D., Li, N., Chen, W., & Rajewsky, N. (2012). miRDeep2 accurately identifies known and hundreds of novel microRNA genes in seven animal clades. *Nucleic Acids Research*, 40(1), 37-52. doi:10.1093/nar/gkr688 [doi]
- Gaffen, S. L., Jain, R., Garg, A. V., & Cua, D. J. (2014). The IL-23-IL-17 immune axis: From mechanisms to therapeutic testing. *Nature Reviews.Immunology*, 14(9), 585-600. doi:10.1038/nri3707 [doi]
- Gallo, E., Cabaleiro, T., Roman, M., Solano-Lopez, G., Abad-Santos, F., Garcia-Diez, A., & Dauden, E. (2013). The relationship between tumour necrosis factor (TNF)-alpha promoter and IL12B/IL-23R genes polymorphisms and the efficacy of anti-TNF-alpha therapy in psoriasis: A case-control study. *The British Journal of Dermatology*, 169(4), 819-829. doi:10.1111/bjd.12425 [doi]
- Galluzzo, M., Boca, A. N., Botti, E., Potenza, C., Malara, G., Malagoli, P., . . . Costanzo, A. (2015). IL12B (p40) gene polymorphisms contribute to ustekinumab response prediction in psoriasis. *Dermatology (Basel, Switzerland)*, doi:000441719 [pii]

- Gao, X., Single, R. M., Karacki, P., Marti, D., O'Brien, S. J., & Carrington, M. (2006). Diversity of MICA and linkage disequilibrium with HLA-B in two north american populations. *Human Immunology*, *67*(3), 152-158. doi:S0198-8859(06)00030-9 [pii]
- Gedebjerg, A., Johansen, C., Kragballe, K., & Iversen, L. (2013). IL-20, IL-21 and p40: Potential biomarkers of treatment response for ustekinumab. *Acta Dermato-Venereologica*, *93*(2), 150-155. doi:10.2340/00015555-1440 [doi]
- Gilbert, L., He, X., Farmer, P., Boden, S., Kozlowski, M., Rubin, J., & Nanes, M. S. (2000). Inhibition of osteoblast differentiation by tumor necrosis factor-alpha. *Endocrinology*, *141*(11), 3956-3964. doi:10.1210/endo.141.11.7739 [doi]
- Gladman, D. D. (2015). Clinical features and diagnostic considerations in psoriatic arthritis. *Rheumatic Diseases Clinics of North America*, *41*(4), 569-579. doi:10.1016/j.rdc.2015.07.003 [doi]
- Gladman, D. D., Anhorn, K. A., Schachter, R. K., & Mervart, H. (1986). HLA antigens in psoriatic arthritis. *The Journal of Rheumatology*, *13*(3), 586-592.
- Gladman, D. D., Helliwell, P., Mease, P. J., Nash, P., Ritchlin, C., & Taylor, W. (2004). Assessment of patients with psoriatic arthritis: A review of currently available measures. *Arthritis and Rheumatism*, *50*(1), 24-35. doi:10.1002/art.11417 [doi]
- Gladman, D. D., Ritchlin, C. (Sep 28, 2016). Treatment of psoriatic arthritis. Retrieved from <https://www.uptodate.com/contents/treatment-of-psoriatic-arthritis>
- Gladman, D. D., Ziouzina, O., Thavaneswaran, A., & Chandran, V. (2013). Dactylitis in psoriatic arthritis: Prevalence and response to therapy in the biologic era. *The Journal of Rheumatology*, *40*(8), 1357-1359. doi:10.3899/jrheum.130163 [doi]
- Goldminz, A. M., Suarez-Farinas, M., Wang, A. C., Dumont, N., Krueger, J. G., & Gottlieb, A. B. (2015). CCL20 and IL22 messenger RNA expression after adalimumab vs methotrexate treatment of psoriasis: A randomized clinical trial. *JAMA Dermatology*, *151*(8), 837-846. doi:10.1001/jamadermatol.2015.0452 [doi]
- Gonzalez, I. (2014). Statistical analysis of RNA-seq data. *Tutorial* (pp. 1-75). Plateforme Biostatistique – IMT Universite Toulouse III: Plateforme Bioinformatique – INRA Toulouse.
- Gonzalez, S., Martinez-Borra, J., Lopez-Vazquez, A., Garcia-Fernandez, S., Torre-Alonso, J. C., & Lopez-Larrea, C. (2002). MICA rather than MICB, TNFA, or HLA-DRB1 is associated with susceptibility to psoriatic arthritis. *The Journal of Rheumatology*, *29*(5), 973-978.
- Gottlieb, A. B., Chamian, F., Masud, S., Cardinale, I., Abello, M. V., Lowes, M. A., . . . Krueger, J. G. (2005). TNF inhibition rapidly down-regulates multiple proinflammatory pathways in psoriasis plaques. *Journal of Immunology (Baltimore, Md.: 1950)*, *175*(4), 2721-2729. doi:175/4/2721 [pii]

- Gougelet, A., Pissaloux, D., Besse, A., Perez, J., Duc, A., Dutour, A., . . . Alberti, L. (2011). MicroRNA profiles in osteosarcoma as a predictive tool for ifosfamide response. *International Journal of Cancer*, *129*(3), 680-690. doi:10.1002/ijc.25715 [doi]
- Grimson, A., Farh, K. K., Johnston, W. K., Garrett-Engele, P., Lim, L. P., & Bartel, D. P. (2007). MicroRNA targeting specificity in mammals: Determinants beyond seed pairing. *Molecular Cell*, *27*(1), 91-105. doi:S1097-2765(07)00407-8 [pii]
- Gudjonsson, J. E., & Krueger, G. (2012). A role for epigenetics in psoriasis: Methylated cytosine-guanine sites differentiate lesional from nonlesional skin and from normal skin. *The Journal of Investigative Dermatology*, *132*(3 Pt 1), 506-508. doi:10.1038/jid.2011.364 [doi]
- Gulliver, W. P., Macdonald, D., Gladney, N., Alaghehbandan, R., Rahman, P., & Adam Baker, K. (2011). Long-term prognosis and comorbidities associated with psoriasis in the newfoundland and labrador founder population. *Journal of Cutaneous Medicine and Surgery*, *15*(1), 37-47. doi:10.2310/7750.2010.10013 [doi]
- Gunda, P., Syeda, S. S., & Jugl, S. M. (2015). Understanding the relationship between health assessment questionnaire-disability index (haq-di), psoriasis area severity index (pasi), and quality of life (qol) and its influence on cost-effectiveness in psoriatic arthritis (psa). *Value in Health : The Journal of the International Society for Pharmacoeconomics and Outcomes Research*, *18*(7), A653. doi:10.1016/j.jval.2015.09.2354 [doi]
- Guo, Z., Gong, J., Li, Y., Gu, L., Cao, L., Wang, Z., . . . Li, J. (2016). Mucosal MicroRNAs expression profiles before and after exclusive enteral nutrition therapy in adult patients with crohn's disease. *Nutrients*, *8*(8), 10.3390/nu8080519. doi:10.3390/nu8080519 [doi]
- Haddad, A., & Zisman, D. (2017). Comorbidities in patients with psoriatic arthritis. *Rambam Maimonides Medical Journal*, *8*(1), 10.5041/RMMJ.10279. doi:10.5041/RMMJ.10279 [doi]
- Halsall, J. A., Osborne, J. E., Pringle, J. H., & Hutchinson, P. E. (2005). Vitamin D receptor gene polymorphisms, particularly the novel A-1012G promoter polymorphism, are associated with vitamin D3 responsiveness and non-familial susceptibility in psoriasis. *Pharmacogenetics and Genomics*, *15*(5), 349-355. doi:01213011-200505000-00011 [pii]
- Hamada, S., Masamune, A., Kanno, A., & Shimosegawa, T. (2015). Comprehensive analysis of serum microRNAs in autoimmune pancreatitis. *Digestion*, *91*(4), 263-271. doi:10.1159/000381283 [doi]
- Head, S. R., Komori, H. K., LaMere, S. A., Whisenant, T., Van Nieuwerburgh, F., Salomon, D. R., & Ordoukhanian, P. (2014). Library construction for next-generation sequencing: Overviews and challenges. *BioTechniques*, *56*(2), 61-4, 66, 68, passim. doi:10.2144/000114133 [doi]
- Hein, D. W., & Doll, M. A. (2012). Accuracy of various human NAT2 SNP genotyping panels to infer rapid, intermediate and slow acetylator phenotypes. *Pharmacogenomics*, *13*(1), 31-41. doi:10.2217/pgs.11.122 [doi]

- Helliwell, P. S., & Taylor, W. J. (2005). Classification and diagnostic criteria for psoriatic arthritis. *Annals of the Rheumatic Diseases*, *64* Suppl 2, ii3-8. doi:64/suppl_2/ii3 [pii]
- Hohler, T., Grossmann, S., Stradmann-Bellinghausen, B., Kaluza, W., Reuss, E., de Vlam, K., . . . Marker-Hermann, E. (2002). Differential association of polymorphisms in the TNFalpha region with psoriatic arthritis but not psoriasis. *Annals of the Rheumatic Diseases*, *61*(3), 213-218.
- Hsu, K. C., Chida, S., Geraghty, D. E., & Dupont, B. (2002). The killer cell immunoglobulin-like receptor (KIR) genomic region: Gene-order, haplotypes and allelic polymorphism. *Immunological Reviews*, *190*, 40-52. doi:imr19004 [pii]
- Hsu, Y. R., Chang, S. W., Lin, Y. C., & Yang, C. H. (2015). Expression of MicroRNAs in the eyes of lewis rats with experimental autoimmune anterior uveitis. *Mediators of Inflammation*, *2015*, 457835. doi:10.1155/2015/457835 [doi]
- Hueber, W., Patel, D. D., Dryja, T., Wright, A. M., Koroleva, I., Bruin, G., . . . Di Padova, F. (2010). Effects of AIN457, a fully human antibody to interleukin-17A, on psoriasis, rheumatoid arthritis, and uveitis. *Science Translational Medicine*, *2*(52), 52ra72. doi:10.1126/scitranslmed.3001107 [doi]
- Huffmeier, U., Uebe, S., Ekici, A. B., Bowes, J., Giardina, E., Korendowych, E., . . . Reis, A. (2010). Common variants at TRAF3IP2 are associated with susceptibility to psoriatic arthritis and psoriasis. *Nature Genetics*, *42*(11), 996-999. doi:10.1038/ng.688 [doi]
- Husted, J. A., Gladman, D. D., Long, J. A., & Farewell, V. T. (1995). A modified version of the health assessment questionnaire (HAQ) for psoriatic arthritis. *Clinical and Experimental Rheumatology*, *13*(4), 439-443.
- Igarashi, H., Kurihara, H., Mitsuhashi, K., Ito, M., Okuda, H., Kanno, S., . . . Shinomura, Y. (2015). Association of MicroRNA-31-5p with clinical efficacy of anti-EGFR therapy in patients with metastatic colorectal cancer. *Annals of Surgical Oncology*, *22*(8), 2640-2648. doi:10.1245/s10434-014-4264-7 [doi]
- Invitrogen by Life Technologies. (28 June 2012a). *Ion total RNA-seq v2* (Revision E, Publication Number 4476286 ed.) Thermo Fisher Scientific Inc.
- Invitrogen by Life Technologies. (28 June 2012b). *Total exosome RNA and protein isolation kit for isolation of RNA and protein from exosomes* (Revision A, Publication Number MAN0006962 ed.) Thermo Fisher Scientific Inc.
- Jani, M., Barton, A., & Ho, P. (2015). Pharmacogenetics of treatment response in psoriatic arthritis. *Current Rheumatology Reports*, *17*(7), 44-015-0518-z. doi:10.1007/s11926-015-0518-z [doi]
- Johnsson, H. J., & McInnes, I. B. (2015). Interleukin-12 and interleukin-23 inhibition in psoriatic arthritis. *Clinical and Experimental Rheumatology*, *33*(5 Suppl 93), S115-8. doi:9895 [pii]

- Julia, A., Ferrandiz, C., Dauden, E., Fonseca, E., Fernandez-Lopez, E., Sanchez-Carazo, J. L., . . . Marsal, S. (2015). Association of the PDE3A-SLCO1C1 locus with the response to anti-TNF agents in psoriasis. *The Pharmacogenomics Journal*, *15*(4), 322-325. doi:10.1038/tpj.2014.71 [doi]
- Julia, M., Guilabert, A., Lozano, F., Suarez-Casasus, B., Moreno, N., Carrascosa, J. M., . . . Mascaro, J. M., Jr. (2013). The role of fegamma receptor polymorphisms in the response to anti-tumor necrosis factor therapy in psoriasis A pharmacogenetic study. *JAMA Dermatology*, *149*(9), 1033-1039. doi:10.1001/jamadermatol.2013.4632 [doi]
- Kaltwasser, J. P. (2007). Leflunomide in psoriatic arthritis. *Autoimmunity Reviews*, *6*(8), 511-514. doi:S1568-9972(06)00215-1 [pii]
- Kamath, A. V. (2016). Translational pharmacokinetics and pharmacodynamics of monoclonal antibodies. *Drug Discovery Today. Technologies*, *21-22*, 75-83. doi:S1740-6749(16)30025-7 [pii]
- Karason, A., Gudjonsson, J. E., Upmanyu, R., Antonsdottir, A. A., Hauksson, V. B., Runasdottir, E. H., . . . Gulcher, J. R. (2003). A susceptibility gene for psoriatic arthritis maps to chromosome 16q: Evidence for imprinting. *American Journal of Human Genetics*, *72*(1), 125-131. doi:S0002-9297(07)60510-2 [pii]
- Katagiri, F., & Glazebrook, J. (2009). Overview of mRNA expression profiling using DNA microarrays. *Current Protocols in Molecular Biology*, *Chapter 22*, Unit 22.4. doi:10.1002/0471142727.mb2204s85 [doi]
- Kim, S. B., Zhang, L., Barron, S., & Shay, J. W. (2014). Inhibition of microRNA-31-5p protects human colonic epithelial cells against ionizing radiation. *Life Sciences in Space Research*, *1*, 67-73. doi:10.1016/j.lssr.2014.02.001 [doi]
- Kiss, I., Mlcochova, J., Bortlicek, Z., Poprach, A., Drabek, J., Vychytilova-Faltejskova, P., . . . Slaby, O. (2016). Efficacy and toxicity of panitumumab after progression on cetuximab and predictive value of MiR-31-5p in metastatic wild-type KRAS colorectal cancer patients. *Anticancer Research*, *36*(9), 4955-4959. doi:36/9/4955 [pii]
- Koch, A. E. (2005). Chemokines and their receptors in rheumatoid arthritis: Future targets? *Arthritis and Rheumatism*, *52*(3), 710-721. doi:10.1002/art.20932 [doi]
- Kosaka, N., Iguchi, H., Yoshioka, Y., Takeshita, F., Matsuki, Y., & Ochiya, T. (2010). Secretory mechanisms and intercellular transfer of microRNAs in living cells. *The Journal of Biological Chemistry*, *285*(23), 17442-17452. doi:10.1074/jbc.M110.107821 [doi]
- Krueger, G. G., Langley, R. G., Leonardi, C., Yeilding, N., Guzzo, C., Wang, Y., . . . CNTO 1275 Psoriasis Study Group. (2007). A human interleukin-12/23 monoclonal antibody for the treatment of psoriasis. *The New England Journal of Medicine*, *356*(6), 580-592. doi:356/6/580 [pii]

- Krueger, J. G., Fretzin, S., Suarez-Farinas, M., Haslett, P. A., Phipps, K. M., Cameron, G. S., . . . Hoffman, R. W. (2012). IL-17A is essential for cell activation and inflammatory gene circuits in subjects with psoriasis. *The Journal of Allergy and Clinical Immunology*, *130*(1), 145-54.e9. doi:10.1016/j.jaci.2012.04.024 [doi]
- Lane, C., & Crawford, G. (1937). Psoriasis: A statistical study of two hundred and thirty-one cases. *Archives of Dermatology and Syphilology* Pages = {1051-1061}, *35*(6) doi:10.1001/archderm.1937.01470240043003 [doi]
- Lembo, S., Balato, N., Caiazzo, G., Megna, M., Ayala, F., & Balato, A. (2016). The effects of etanercept on replication, proliferation, survival, and apoptosis markers in moderate to severe psoriasis. *Journal of the European Academy of Dermatology and Venereology : JEADV*, doi:10.1111/jdv.13583 [doi]
- Leonardi, C., Matheson, R., Zachariae, C., Cameron, G., Li, L., Edson-Heredia, E., . . . Banerjee, S. (2012). Anti-interleukin-17 monoclonal antibody ixekizumab in chronic plaque psoriasis. *The New England Journal of Medicine*, *366*(13), 1190-1199. doi:10.1056/NEJMoa1109997 [doi]
- Li, C., Bai, Y., Liu, H., Zuo, X., Yao, H., Xu, Y., & Cao, M. (2013). Comparative study of microRNA profiling in keloid fibroblast and annotation of differential expressed microRNAs. *Acta Biochimica Et Biophysica Sinica*, *45*(8), 692-699. doi:10.1093/abbs/gmt057 [doi]
- Li, H., Handsaker, B., Wysoker, A., Fennell, T., Ruan, J., Homer, N., . . . 1000 Genome Project Data Processing Subgroup. (2009). The sequence alignment/map format and SAMtools. *Bioinformatics (Oxford, England)*, *25*(16), 2078-2079. doi:10.1093/bioinformatics/btp352 [doi]
- Liu, Y., Helms, C., Liao, W., Zaba, L. C., Duan, S., Gardner, J., . . . Bowcock, A. M. (2008). A genome-wide association study of psoriasis and psoriatic arthritis identifies new disease loci. *PLoS Genetics*, *4*(3), e1000041. doi:10.1371/journal.pgen.1000041 [doi]
- Liu, Y., Zhong, L., Liu, D., Ye, H., Mao, Y., & Hu, Y. (2017). Differential miRNA expression profiles in human keratinocytes in response to protein kinase C inhibitor. *Molecular Medicine Reports*, *16*(5), 6608-6619. doi:10.3892/mmr.2017.7447 [doi]
- Long, X., Li, Y., Qiu, S., Liu, J., He, L., & Peng, Y. (2016). MiR-582-5p/miR-590-5p targeted CREB1/CREB5-NF-kappaB signaling and caused opioid-induced immunosuppression in human monocytes. *Translational Psychiatry*, *6*, e757. doi:10.1038/tp.2016.4 [doi]
- Lopez-Ferrer, A., Laiz, A., & Puig, L. (2017). The safety of ustekinumab for the treatment of psoriatic arthritis. *Expert Opinion on Drug Safety*, *16*(6), 733-742. doi:10.1080/14740338.2017.1323864 [doi]
- Lovendorf, M. B., Zibert, J. R., Gyldenlove, M., Ropke, M. A., & Skov, L. (2014). MicroRNA-223 and miR-143 are important systemic biomarkers for disease activity in psoriasis. *Journal of Dermatological Science*, *75*(2), 133-139. doi:10.1016/j.jdermsci.2014.05.005 [doi]

- Lucas, D., Campillo, J. A., Lopez-Hernandez, R., Martinez-Garcia, P., Lopez-Sanchez, M., Botella, C., . . . Muro, M. (2008). Allelic diversity of MICA gene and MICA/HLA-B haplotypic variation in a population of the murcia region in southeastern Spain. *Human Immunology*, *69*(10), 655-660. doi:10.1016/j.humimm.2008.07.011 [doi]
- Lunavat, T. R., Cheng, L., Kim, D. K., Bhadury, J., Jang, S. C., Lasser, C., . . . Lotvall, J. (2015). Small RNA deep sequencing discriminates subsets of extracellular vesicles released by melanoma cells--evidence of unique microRNA cargos. *RNA Biology*, *12*(8), 810-823. doi:10.1080/15476286.2015.1056975 [doi]
- Magni, S., Buoli Comani, G., Elli, L., Vanessi, S., Ballarini, E., Nicolini, G., . . . Barisani, D. (2014). miRNAs affect the expression of innate and adaptive immunity proteins in celiac disease. *The American Journal of Gastroenterology*, *109*(10), 1662-1674. doi:10.1038/ajg.2014.203 [doi]
- Maia, D., de Carvalho, A. C., Horst, M. A., Carvalho, A. L., Scapulatempo-Neto, C., & Vettore, A. L. (2015). Expression of miR-296-5p as predictive marker for radiotherapy resistance in early-stage laryngeal carcinoma. *Journal of Translational Medicine*, *13*, 262-015-0621-y. doi:10.1186/s12967-015-0621-y [doi]
- Mangoni, A. A., & Jackson, S. H. (2004). Age-related changes in pharmacokinetics and pharmacodynamics: Basic principles and practical applications. *British Journal of Clinical Pharmacology*, *57*(1), 6-14. doi:2007 [pii]
- Martin, M. (2011). Cutadapt removes adapter sequences from high-throughput sequencing reads. *EMBnet journal*, *17*, 10-12. doi:<https://doi.org/10.14806/ej.17.1.200>
- Martinez, C., Blanco, G., Ladero, J. M., Garcia-Martin, E., Taxonera, C., Gamito, F. G., . . . Agundez, J. A. (2004). Genetic predisposition to acute gastrointestinal bleeding after NSAIDs use. *British Journal of Pharmacology*, *141*(2), 205-208. doi:10.1038/sj.bjp.0705623 [doi]
- Martinez-Borra, J., Gonzalez, S., Santos-Juanes, J., Sanchez del Rio, J., Torre-Alonso, J. C., Lopez-Vazquez, A., . . . Lopez-Larrea, C. (2003). Psoriasis vulgaris and psoriatic arthritis share a 100 kb susceptibility region telomeric to HLA-C. *Rheumatology (Oxford, England)*, *42*(9), 1089-1092. doi:10.1093/rheumatology/keg304 [doi]
- McAlexander, M. A., Phillips, M. J., & Witwer, K. W. (2013). Comparison of methods for miRNA extraction from plasma and quantitative recovery of RNA from cerebrospinal fluid. *Frontiers in Genetics*, *4*, 83. doi:10.3389/fgene.2013.00083 [doi]
- McInnes, I. B., Mease, P. J., Kirkham, B., Kavanaugh, A., Ritchlin, C. T., Rahman, P., . . . FUTURE 2 Study Group. (2015). Secukinumab, a human anti-interleukin-17A monoclonal antibody, in patients with psoriatic arthritis (FUTURE 2): A randomised, double-blind, placebo-controlled, phase 3 trial. *Lancet (London, England)*, *386*(9999), 1137-1146. doi:10.1016/S0140-6736(15)61134-5 [doi]
- McInnes, I. B., Mease, P. J., Ritchlin, C. T., Rahman, P., Gottlieb, A. B., Kirkham, B., . . . Mpfu, S. (2017). Secukinumab sustains improvement in signs and symptoms of psoriatic arthritis: 2

- year results from the phase 3 FUTURE 2 study. *Rheumatology (Oxford, England)*, doi:10.1093/rheumatology/kex301 [doi]
- Mease, P., & McInnes, I. B. (2016). Secukinumab: A new treatment option for psoriatic arthritis. *Rheumatology and Therapy*, 3(1), 5-29. doi:10.1007/s40744-016-0031-5 [doi]
- Mease, P. J. (2002). Tumour necrosis factor (TNF) in psoriatic arthritis: Pathophysiology and treatment with TNF inhibitors. *Annals of the Rheumatic Diseases*, 61(4), 298-304.
- Mease, P. J., McInnes, I. B., Kirkham, B., Kavanaugh, A., Rahman, P., van der Heijde, D., . . . FUTURE 1 Study Group. (2015). Secukinumab inhibition of interleukin-17A in patients with psoriatic arthritis. *The New England Journal of Medicine*, 373(14), 1329-1339. doi:10.1056/NEJMoa1412679 [doi]
- Menon, N., Rogers, C. J., Lukaszewicz, A. I., Axtelle, J., Yadav, M., Song, F., . . . Jacob, N. K. (2016). Detection of acute radiation sickness: A feasibility study in non-human primates circulating miRNAs for triage in radiological events. *PloS One*, 11(12), e0167333. doi:10.1371/journal.pone.0167333 [doi]
- Menter, A., Gottlieb, A., Feldman, S. R., Van Voorhees, A. S., Leonardi, C. L., Gordon, K. B., . . . Bhushan, R. (2008). Guidelines of care for the management of psoriasis and psoriatic arthritis: Section 1. overview of psoriasis and guidelines of care for the treatment of psoriasis with biologics. *Journal of the American Academy of Dermatology*, 58(5), 826-850. doi:10.1016/j.jaad.2008.02.039 [doi]
- Mi, S., Zhang, J., Zhang, W., & Huang, R. S. (2013). Circulating microRNAs as biomarkers for inflammatory diseases. *MicroRNA (Sharjah, United Arab Emirates)*, 2(1), 63-71. doi:10.2174/2211536611302010007 [doi]
- Miossec, P. (2017). Update on interleukin-17: A role in the pathogenesis of inflammatory arthritis and implication for clinical practice. *RMD Open*, 3(1), e000284-2016-000284. eCollection 2017. doi:10.1136/rmdopen-2016-000284 [doi]
- Mizutani, H., Ohmoto, Y., Mizutani, T., Murata, M., & Shimizu, M. (1997). Role of increased production of monocytes TNF-alpha, IL-1beta and IL-6 in psoriasis: Relation to focal infection, disease activity and responses to treatments. *Journal of Dermatological Science*, 14(2), 145-153. doi:S0923-1811(96)00562-2 [pii]
- Mlcochova, J., Faltejskova-Vychytilova, P., Ferracin, M., Zagatti, B., Radova, L., Svoboda, M., . . . Slaby, O. (2015). MicroRNA expression profiling identifies miR-31-5p/3p as associated with time to progression in wild-type RAS metastatic colorectal cancer treated with cetuximab. *Oncotarget*, 6(36), 38695-38704. doi:10.18632/oncotarget.5735 [doi]
- Moll, J. M., & Wright, V. (1973). Psoriatic arthritis. *Seminars in Arthritis and Rheumatism*, 3(1), 55-78. doi:0049-0172(73)90035-8 [pii]

- Morales-Lara, M. J., Canete, J. D., Torres-Moreno, D., Hernandez, M. V., Pedrero, F., Celis, R., . . . Conesa-Zamora, P. (2012). Effects of polymorphisms in TRAILR1 and TNFR1A on the response to anti-TNF therapies in patients with rheumatoid and psoriatic arthritis. *Joint, Bone, Spine : Revue Du Rhumatisme*, 79(6), 591-596. doi:10.1016/j.jbspin.2012.02.003 [doi]
- Moret, I., Sanchez-Izquierdo, D., Iborra, M., Tortosa, L., Navarro-Puche, A., Nos, P., . . . Beltran, B. (2013). Assessing an improved protocol for plasma microRNA extraction. *PLoS One*, 8(12), e82753. doi:10.1371/journal.pone.0082753 [doi]
- Motta, V., Angelici, L., Nordio, F., Bollati, V., Fossati, S., Frascati, F., . . . Baccarelli, A. A. (2013). Integrative analysis of miRNA and inflammatory gene expression after acute particulate matter exposure. *Toxicological Sciences : An Official Journal of the Society of Toxicology*, 132(2), 307-316. doi:10.1093/toxsci/kft013 [doi]
- Murdaca, G., Gulli, R., Spano, F., Lantieri, F., Burlando, M., Parodi, A., . . . Puppo, F. (2014). TNF-alpha gene polymorphisms: Association with disease susceptibility and response to anti-TNF-alpha treatment in psoriatic arthritis. *The Journal of Investigative Dermatology*, 134(10), 2503-2509. doi:10.1038/jid.2014.123 [doi]
- Naesens, M., Kuypers, D. R., & Sarwal, M. (2009). Calcineurin inhibitor nephrotoxicity. *Clinical Journal of the American Society of Nephrology : CJASN*, 4(2), 481-508. doi:10.2215/CJN.04800908 [doi]
- Nair, R. P., Ruether, A., Stuart, P. E., Jenisch, S., Tejasvi, T., Hiremagalore, R., . . . Weichenthal, M. (2008). Polymorphisms of the IL12B and IL23R genes are associated with psoriasis. *The Journal of Investigative Dermatology*, 128(7), 1653-1661. doi:10.1038/sj.jid.5701255 [doi]
- Nair, R. P., Stuart, P. E., Nistor, I., Hiremagalore, R., Chia, N. V., Jenisch, S., . . . Elder, J. T. (2006). Sequence and haplotype analysis supports HLA-C as the psoriasis susceptibility 1 gene. *American Journal of Human Genetics*, 78(5), 827-851. doi:S0002-9297(07)63817-8 [pii]
- Nash, P., Kirkham, B., Okada, M., Rahman, P., Combe, B., Burmester, G. R., . . . SPIRIT-P2 Study Group. (2017). Ixekizumab for the treatment of patients with active psoriatic arthritis and an inadequate response to tumour necrosis factor inhibitors: Results from the 24-week randomised, double-blind, placebo-controlled period of the SPIRIT-P2 phase 3 trial. *Lancet (London, England)*, 389(10086), 2317-2327. doi:S0140-6736(17)31429-0 [pii]
- National Clinical Guideline Centre (UK). (2012 Oct). Psoriasis: Assessment and management of psoriasis. London: Royal College of Physicians (UK); NICE Clinical Guidelines, (No. 153.) doi:NBK247829 [bookaccession]
- Nelson, G. W., Martin, M. P., Gladman, D., Wade, J., Trowsdale, J., & Carrington, M. (2004). Cutting edge: Heterozygote advantage in autoimmune disease: Hierarchy of protection/susceptibility conferred by HLA and killer ig-like receptor combinations in psoriatic arthritis. *Journal of Immunology (Baltimore, Md.: 1950)*, 173(7), 4273-4276. doi:173/7/4273 [pii]

- Olshaker, J. S., & Jerrard, D. A. (1997). The erythrocyte sedimentation rate. *The Journal of Emergency Medicine*, *15*(6), 869-874. doi:S0736467997001972 [pii]
- Orbai, A. M., & Ogdie, A. (2016). Patient-reported outcomes in psoriatic arthritis. *Rheumatic Diseases Clinics of North America*, *42*(2), 265-283. doi:10.1016/j.rdc.2016.01.002 [doi]
- O'Rielly, D. D., & Rahman, P. (2011). Pharmacogenetics of psoriasis. *Pharmacogenomics*, *12*(1), 87-101. doi:10.2217/pgs.10.166 [doi]
- O'Rielly, D. D., & Rahman, P. (2014). Genetics of psoriatic arthritis. *Best Practice & Research. Clinical Rheumatology*, *28*(5), 673-685. doi:10.1016/j.berh.2014.10.010 [doi]
- Ory, B., Ramsey, M. R., Wilson, C., Vadysirisack, D. D., Forster, N., Rocco, J. W., . . . Ellisen, L. W. (2011). A microRNA-dependent program controls p53-independent survival and chemosensitivity in human and murine squamous cell carcinoma. *The Journal of Clinical Investigation*, *121*(2), 809-820. doi:10.1172/JCI43897 [doi]
- Ouyang, M., Li, Y., Ye, S., Ma, J., Lu, L., Lv, W., . . . Wang, W. (2014). MicroRNA profiling implies new markers of chemoresistance of triple-negative breast cancer. *PloS One*, *9*(5), e96228. doi:10.1371/journal.pone.0096228 [doi]
- Paraskevi, A., Theodoropoulos, G., Papaconstantinou, I., Mantzaris, G., Nikiteas, N., & Gazouli, M. (2012). Circulating MicroRNA in inflammatory bowel disease. *Journal of Crohn's & Colitis*, *6*(9), 900-904. doi:10.1016/j.crohns.2012.02.006 [doi]
- Pasch, M. C. (2016). Nail psoriasis: A review of treatment options. *Drugs*, *76*(6), 675-705. doi:10.1007/s40265-016-0564-5 [doi]
- Peck, B. C., Weiser, M., Lee, S. E., Gipson, G. R., Iyer, V. B., Sartor, R. B., . . . Sheikh, S. Z. (2015). MicroRNAs classify different disease behavior phenotypes of crohn's disease and may have prognostic utility. *Inflammatory Bowel Diseases*, *21*(9), 2178-2187. doi:10.1097/MIB.0000000000000478 [doi]
- Peddle, L., Butt, C., Snelgrove, T., & Rahman, P. (2005). Interleukin (IL) 1alpha, IL1beta, IL receptor antagonist, and IL10 polymorphisms in psoriatic arthritis. *Annals of the Rheumatic Diseases*, *64*(7), 1093-1094. doi:64/7/1093 [pii]
- Pedersen, O. B., Svendsen, A. J., Ejstrup, L., Skytthe, A., & Junker, P. (2008). On the heritability of psoriatic arthritis. disease concordance among monozygotic and dizygotic twins. *Annals of the Rheumatic Diseases*, *67*(10), 1417-1421. doi:10.1136/ard.2007.078428 [doi]
- Pereira, T. D. S. F., Brito, J. A. R., Guimaraes, A. L. S., Gomes, C. C., de Lacerda, J. C. T., de Castro, W. H., . . . Gomez, R. S. (2017). MicroRNA profiling reveals dysregulated microRNAs and their target gene regulatory networks in cemento-ossifying fibroma. *Journal of Oral Pathology & Medicine : Official Publication of the International Association of Oral Pathologists and the American Academy of Oral Pathology*, doi:10.1111/jop.12650 [doi]

- PhUSE Wiki contributors. (2012). ACR response criteria. Retrieved from http://www.phusewiki.org/wiki/index.php?title=ACR_Response_Criteria&oldid=2838
- Pivarcsi, A., Meisgen, F., Xu, N., Stahle, M., & Sonkoly, E. (2013). Changes in the level of serum microRNAs in patients with psoriasis after antitumour necrosis factor-alpha therapy. *The British Journal of Dermatology*, *169*(3), 563-570. doi:10.1111/bjd.12381 [doi]
- Popa, O. M., Cherciu, M., Cherciu, L. I., Dutescu, M. I., Bojinca, M., Bojinca, V., . . . Popa, L. O. (2016). ERAP1 and ERAP2 gene variations influence the risk of psoriatic arthritis in romanian population. *Archivum Immunologiae Et Therapiae Experimentalis*, *64*(Suppl 1), 123-129. doi:10.1007/s00005-016-0444-4 [doi]
- Prieto-Perez, R., Solano-Lopez, G., Cabaleiro, T., Roman, M., Ochoa, D., Talegon, M., . . . Abad-Santos, F. (2015). The polymorphism rs763780 in the IL-17F gene is associated with response to biological drugs in patients with psoriasis. *Pharmacogenomics*, *16*(15), 1723-1731. doi:10.2217/pgs.15.107 [doi]
- Puig, L. (2014). Methotrexate: New therapeutic approaches. *Actas Dermo-Sifiliograficas*, *105*(6), 583-589. doi:10.1016/j.ad.2012.11.017 [doi]
- Punga, A. R., Andersson, M., Alimohammadi, M., & Punga, T. (2015). Disease specific signature of circulating miR-150-5p and miR-21-5p in myasthenia gravis patients. *Journal of the Neurological Sciences*, *356*(1-2), 90-96. doi:10.1016/j.jns.2015.06.019 [doi]
- Punga, T., Le Panse, R., Andersson, M., Truffault, F., Berrih-Aknin, S., & Punga, A. R. (2014). Circulating miRNAs in myasthenia gravis: miR-150-5p as a new potential biomarker. *Annals of Clinical and Translational Neurology*, *1*(1), 49-58. doi:10.1002/acn3.24 [doi]
- Rader, R. A. (2008). (Re)defining biopharmaceutical. *Nature Biotechnology*, *26*(7), 743-751. doi:10.1038/nbt0708-743 [doi]
- Rahman, P., Bartlett, S., Siannis, F., Pellett, F. J., Farewell, V. T., Peddle, L., . . . Gladman, D. D. (2003). CARD15: A pleiotropic autoimmune gene that confers susceptibility to psoriatic arthritis. *American Journal of Human Genetics*, *73*(3), 677-681. doi:10.1086/378076 [doi]
- Rahman, P., & Elder, J. T. (2005). Genetic epidemiology of psoriasis and psoriatic arthritis. *Annals of the Rheumatic Diseases*, *64* Suppl 2, ii37-9; discussion ii40-1. doi:64/suppl_2/ii37 [pii]
- Rahman, P., Inman, R. D., Maksymowych, W. P., Reeve, J. P., Peddle, L., & Gladman, D. D. (2009). Association of interleukin 23 receptor variants with psoriatic arthritis. *The Journal of Rheumatology*, *36*(1), 137-140. doi:10.3899/jrheum.080458 [doi]
- Rahman, P., Puig, L., Gottlieb, A. B., Kavanaugh, A., McInnes, I. B., Ritchlin, C., . . . PSUMMIT 1 and 2 Study Groups. (2016). Ustekinumab treatment and improvement of physical function and health-related quality of life in patients with psoriatic arthritis. *Arthritis Care & Research*, *68*(12), 1812-1822. doi:10.1002/acr.23000 [doi]

- Ramirez, J., Fernandez-Sueiro, J. L., Lopez-Mejias, R., Montilla, C., Arias, M., Moll, C., . . . Canete, J. D. (2012). FCGR2A/CD32A and FCGR3A/CD16A variants and EULAR response to tumor necrosis factor-alpha blockers in psoriatic arthritis: A longitudinal study with 6 months of followup. *The Journal of Rheumatology*, *39*(5), 1035-1041. doi:10.3899/jrheum.110980 [doi]
- Ranganathan, P., & McLeod, H. L. (2006). Methotrexate pharmacogenetics: The first step toward individualized therapy in rheumatoid arthritis. *Arthritis and Rheumatism*, *54*(5), 1366-1377. doi:10.1002/art.21762 [doi]
- Ratain, M. MD, and Plunkett Jr, W. PhD. (2003). In Kufe DW, Pollock RE, Weichselbaum RR, et al., editors. (Ed.), *Holland-frei cancer medicine. chapter 46, pharmacology* (6th edition ed.). Hamilton (ON): BC Decker. Retrieved from <https://www.ncbi.nlm.nih.gov/books/NBK12354/>
- Raychaudhuri, S. K., Saxena, A., & Raychaudhuri, S. P. (2015). Role of IL-17 in the pathogenesis of psoriatic arthritis and axial spondyloarthritis. *Clinical Rheumatology*, *34*(6), 1019-1023. doi:10.1007/s10067-015-2961-7 [doi]
- Reich, K., Huffmeier, U., Konig, I. R., Lascorz, J., Lohmann, J., Wendler, J., . . . Burkhardt, H. (2007). TNF polymorphisms in psoriasis: Association of psoriatic arthritis with the promoter polymorphism TNF*-857 independent of the PSORS1 risk allele. *Arthritis and Rheumatism*, *56*(6), 2056-2064. doi:10.1002/art.22590 [doi]
- Ress, A. L., Stiegelbauer, V., Winter, E., Schwarzenbacher, D., Kiesslich, T., Lax, S., . . . Pichler, M. (2015). MiR-96-5p influences cellular growth and is associated with poor survival in colorectal cancer patients. *Molecular Carcinogenesis*, *54*(11), 1442-1450. doi:10.1002/mc.22218 [doi]
- Reyes-Herrera, P. H., Ficarra, E., Acquaviva, A., & Macii, E. (2011). miREE: miRNA recognition elements ensemble. *BMC Bioinformatics*, *12*, 454-2105-12-454. doi:10.1186/1471-2105-12-454 [doi]
- Ribas, F., Oliveira, L. A., Petzl-Erler, M. L., & Bicalho, M. G. (2008). Major histocompatibility complex class I chain-related gene A polymorphism and linkage disequilibrium with HLA-B alleles in euro-brazilians. *Tissue Antigens*, *72*(6), 532-538. doi:10.1111/j.1399-0039.2008.01142.x [doi]
- Ritchlin, C. T., Kavanaugh, A., Gladman, D. D., Mease, P. J., Helliwell, P., Boehncke, W. H., . . . Group for Research and Assessment of Psoriasis and Psoriatic Arthritis (GRAPPA). (2009). Treatment recommendations for psoriatic arthritis. *Annals of the Rheumatic Diseases*, *68*(9), 1387-1394. doi:10.1136/ard.2008.094946 [doi]
- Roberts, J., O'Rielly, D.D., Rahman, P.,. (2017). *A review of ustekinumab in the treatment of psoriatic arthritis*. Unpublished manuscript.

- Ryan, C., Leonardi, C. L., Krueger, J. G., Kimball, A. B., Strober, B. E., Gordon, K. B., . . . Menter, A. (2011). Association between biologic therapies for chronic plaque psoriasis and cardiovascular events: A meta-analysis of randomized controlled trials. *Jama*, *306*(8), 864-871. doi:10.1001/jama.2011.1211 [doi]
- Ryan, C., Renfro, L., Collins, P., Kirby, B., & Rogers, S. (2010). Clinical and genetic predictors of response to narrowband ultraviolet B for the treatment of chronic plaque psoriasis. *The British Journal of Dermatology*, *163*(5), 1056-1063. doi:10.1111/j.1365-2133.2010.09985.x [doi]
- Sankowski, A. J., Lebkowska, U. M., Cwikla, J., Walecka, I., & Walecki, J. (2013). Psoriatic arthritis. *Polish Journal of Radiology*, *78*(1), 7-17. doi:10.12659/PJR.883763 [doi]
- Schageman, J., Zeringer, E., Li, M., Barta, T., Lea, K., Gu, J., . . . Vlassov, A. V. (2013). The complete exosome workflow solution: From isolation to characterization of RNA cargo. *BioMed Research International*, *2013*, 253957. doi:10.1155/2013/253957 [doi]
- Shingara, J., Keiger, K., Shelton, J., Laosinchai-Wolf, W., Powers, P., Conrad, R., . . . Labourier, E. (2005). An optimized isolation and labeling platform for accurate microRNA expression profiling. *RNA (New York, N.Y.)*, *11*(9), 1461-1470. doi:rna.2610405 [pii]
- Skarmoutsou, E., Trovato, C., Granata, M., Rossi, G. A., Mosca, A., Longo, V., . . . Mazzarino, M. C. (2015). Biological therapy induces expression changes in notch pathway in psoriasis. *Archives of Dermatological Research*, *307*(10), 863-873. doi:10.1007/s00403-015-1594-7 [doi]
- Smith, G., Weidlich, S., Dawe, R. S., & Ibbotson, S. H. (2011). Glutathione S-transferase M1 (GSTM1) genotype but not GSTT1 or MC1R genotype influences erythral sensitivity to narrow band (TL-01) UVB phototherapy. *Pharmacogenetics and Genomics*, *21*(4), 217-224. doi:10.1097/FPC.0b013e32833efb36 [doi]
- Stuart, P. E., Nair, R. P., Ellinghaus, E., Ding, J., Tejasvi, T., Gudjonsson, J. E., . . . Elder, J. T. (2010). Genome-wide association analysis identifies three psoriasis susceptibility loci. *Nature Genetics*, *42*(11), 1000-1004. doi:10.1038/ng.693 [doi]
- Sutherland, A., Power, R. J., Rahman, P., & O'Rielly, D. D. (2016). Pharmacogenetics and pharmacogenomics in psoriasis treatment: Current challenges and future prospects. *Expert Opinion on Drug Metabolism & Toxicology*, , 1-13. doi:10.1080/17425255.2016.1194394 [doi]
- Suzuki, E., Mellins, E. D., Gershwin, M. E., Nestle, F. O., & Adamopoulos, I. E. (2014). The IL-23/IL-17 axis in psoriatic arthritis. *Autoimmunity Reviews*, *13*(4-5), 496-502. doi:10.1016/j.autrev.2014.01.050 [doi]
- Suzuki, Y., Hamamoto, Y., Ogasawara, Y., Ishikawa, K., Yoshikawa, Y., Sasazuki, T., & Muto, M. (2004). Genetic polymorphisms of killer cell immunoglobulin-like receptors are associated with susceptibility to psoriasis vulgaris. *The Journal of Investigative Dermatology*, *122*(5), 1133-1136. doi:10.1111/j.0022-202X.2004.22517.x [doi]

- Talamonti, M., Botti, E., Galluzzo, M., Teoli, M., Spallone, G., Bavetta, M., . . . Costanzo, A. (2013). Pharmacogenetics of psoriasis: HLA-Cw6 but not LCE3B/3C deletion nor TNFAIP3 polymorphism predisposes to clinical response to interleukin 12/23 blocker ustekinumab. *The British Journal of Dermatology*, *169*(2), 458-463. doi:10.1111/bjd.12331 [doi]
- Tam, S., de Borja, R., Tsao, M. S., & McPherson, J. D. (2014). Robust global microRNA expression profiling using next-generation sequencing technologies. *Laboratory Investigation; a Journal of Technical Methods and Pathology*, *94*(3), 350-358. doi:10.1038/labinvest.2013.157 [doi]
- Taylor, W., Gladman, D., Helliwell, P., Marchesoni, A., Mease, P., Mielants, H., & CASPAR Study Group. (2006). Classification criteria for psoriatic arthritis: Development of new criteria from a large international study. *Arthritis and Rheumatism*, *54*(8), 2665-2673. doi:10.1002/art.21972 [doi]
- Tejasvi, T., Stuart, P. E., Chandran, V., Voorhees, J. J., Gladman, D. D., Rahman, P., . . . Nair, R. P. (2012). TNFAIP3 gene polymorphisms are associated with response to TNF blockade in psoriasis. *The Journal of Investigative Dermatology*, *132*(3 Pt 1), 593-600. doi:10.1038/jid.2011.376 [doi]
- Teng, M. W., Bowman, E. P., McElwee, J. J., Smyth, M. J., Casanova, J. L., Cooper, A. M., & Cua, D. J. (2015). IL-12 and IL-23 cytokines: From discovery to targeted therapies for immune-mediated inflammatory diseases. *Nature Medicine*, *21*(7), 719-729. doi:10.1038/nm.3895 [doi]
- Tong, Q., Zhao, L., Qian, X. D., Zhang, L. L., Xu, X., Dai, S. M., . . . Zhao, D. B. (2013). Association of TNF-alpha polymorphism with prediction of response to TNF blockers in spondyloarthritis and inflammatory bowel disease: A meta-analysis. *Pharmacogenomics*, *14*(14), 1691-1700. doi:10.2217/pgs.13.146 [doi]
- Torre Alonso, J. C. (2010). Use and application in clinical practice of the CASPAR criteria. [Utilidad y aplicacion en la practica clinica de los criterios CASPAR] *Reumatologia Clinica*, *6 Suppl 1*, 18-21. doi:10.1016/j.reuma.2009.12.002 [doi]
- Torri, A., Carpi, D., Bulgheroni, E., Crosti, M. C., Moro, M., Gruarin, P., . . . de Candia, P. (2017). Extracellular MicroRNA signature of human helper T cell subsets in health and autoimmunity. *The Journal of Biological Chemistry*, *292*(7), 2903-2915. doi:10.1074/jbc.M116.769893 [doi]
- Ustekinumab (Stelara) Injection. (2016 Nov). Cost comparison table for biologics used for the treatment of psoriatic arthritis. *Canadian Agency for Drugs and Technologies in Health, Appendix 1* doi:Bookshelf ID: NBK409642
- Vageli, D. P., Exarchou, A., Zafiriou, E., Doukas, P. G., Doukas, S., & Roussaki-Schulze, A. (2015). Effect of TNF-alpha inhibitors on transcriptional levels of pro-inflammatory interleukin-33 and toll-like receptors-2 and -9 in psoriatic plaques. *Experimental and Therapeutic Medicine*, *10*(4), 1573-1577. doi:10.3892/etm.2015.2688 [doi]

- Vaira, V., Roncoroni, L., Barisani, D., Gaudio, G., Bosari, S., Bulfamante, G., . . . Elli, L. (2014). microRNA profiles in coeliac patients distinguish different clinical phenotypes and are modulated by gliadin peptides in primary duodenal fibroblasts. *Clinical Science (London, England : 1979)*, *126*(6), 417-423. doi:10.1042/CS20130248 [doi]
- van Jaarsveld, M. T., Wouters, M. D., Boersma, A. W., Smid, M., van Ijcken, W. F., Mathijssen, R. H., . . . Pothof, J. (2014). DNA damage responsive microRNAs misexpressed in human cancer modulate therapy sensitivity. *Molecular Oncology*, *8*(3), 458-468. doi:10.1016/j.molonc.2013.12.011 [doi]
- Vasilopoulos, Y., Manolika, M., Zafiriou, E., Sarafidou, T., Bagiatis, V., Kruger-Krasagaki, S., . . . Roussaki-Schulze, A. (2012). Pharmacogenetic analysis of TNF, TNFRSF1A, and TNFRSF1B gene polymorphisms and prediction of response to anti-TNF therapy in psoriasis patients in the greek population. *Molecular Diagnosis & Therapy*, *16*(1), 29-34. doi:10.2165/11594660-000000000-00000 [doi]
- Vasilopoulos, Y., Sarri, C., Zafiriou, E., Patsatsi, A., Stamatis, C., Ntoumou, E., . . . Sarafidou, T. (2014). A pharmacogenetic study of ABCB1 polymorphisms and cyclosporine treatment response in patients with psoriasis in the greek population. *The Pharmacogenomics Journal*, *14*(6), 523-525. doi:10.1038/tpj.2014.23 [doi]
- Wang, C. Q., Suarez-Farinas, M., Nograles, K. E., Mimoso, C. A., Shrom, D., Dow, E. R., . . . Krueger, J. G. (2014). IL-17 induces inflammation-associated gene products in blood monocytes, and treatment with ixekizumab reduces their expression in psoriasis patient blood. *The Journal of Investigative Dermatology*, *134*(12), 2990-2993. doi:10.1038/jid.2014.268 [doi]
- Wang, X., Zhang, Y., Jiang, B. H., Zhang, Q., Zhou, R. P., Zhang, L., & Wang, C. (2017). Study on the role of hsa-miR-31-5p in hypertrophic scar formation and the mechanism. *Experimental Cell Research*, doi:S0014-4827(17)30491-3 [pii]
- Warren, R. B., Smith, R. L., Campalani, E., Eyre, S., Smith, C. H., Barker, J. N., . . . Griffiths, C. E. (2008). Genetic variation in efflux transporters influences outcome to methotrexate therapy in patients with psoriasis. *The Journal of Investigative Dermatology*, *128*(8), 1925-1929. doi:10.1038/jid.2008.16 [doi]
- Watson, J. A., Bryan, K., Williams, R., Popov, S., Vujanic, G., Coulomb, A., . . . O'Sullivan, M. (2013). miRNA profiles as a predictor of chemoresponsiveness in wilms' tumor blastema. *PloS One*, *8*(1), e53417. doi:10.1371/journal.pone.0053417 [doi]
- Weger, W. (2010). Current status and new developments in the treatment of psoriasis and psoriatic arthritis with biological agents. *British Journal of Pharmacology*, *160*(4), 810-820. doi:10.1111/j.1476-5381.2010.00702.x [doi]
- Weilner, S., Skalicky, S., Salzer, B., Keider, V., Wagner, M., Hildner, F., . . . Hackl, M. (2015). Differentially circulating miRNAs after recent osteoporotic fractures can influence osteogenic differentiation. *Bone*, *79*, 43-51. doi:10.1016/j.bone.2015.05.027 [doi]

- Wiese, M. D., Alotaibi, N., O'Doherty, C., Sorich, M. J., Suppiah, V., Cleland, L. G., & Proudman, S. M. (2014). Pharmacogenomics of NAT2 and ABCG2 influence the toxicity and efficacy of sulphasalazine containing DMARD regimens in early rheumatoid arthritis. *The Pharmacogenomics Journal*, *14*(4), 350-355. doi:10.1038/tpj.2013.45 [doi]
- Williams, F., Meenagh, A., Sleator, C., Cook, D., Fernandez-Vina, M., Bowcock, A. M., & Middleton, D. (2005). Activating killer cell immunoglobulin-like receptor gene KIR2DS1 is associated with psoriatic arthritis. *Human Immunology*, *66*(7), 836-841. doi:S0198-8859(05)00084-4 [pii]
- Wright, V. (1956). Psoriasis and arthritis. *Annals of the Rheumatic Diseases*, *15*(4), 348-356.
- Wright, V. (1978). Seronegative polyarthritis: A unified concept. *Arthritis and Rheumatism*, *21*(6), 619-633.
- Wu, F., Zhang, S., Dassopoulos, T., Harris, M. L., Bayless, T. M., Meltzer, S. J., . . . Kwon, J. H. (2010). Identification of microRNAs associated with ileal and colonic crohn's disease. *Inflammatory Bowel Diseases*, *16*(10), 1729-1738. doi:10.1002/ibd.21267 [doi]
- Xia, Z., Ma, P., Wu, N., Su, X., Chen, J., Jiang, C., . . . Wu, Z. (2016). Altered function in cartilage derived mesenchymal stem cell leads to OA-related cartilage erosion. *American Journal of Translational Research*, *8*(2), 433-446.
- Zhai, G., Zhou, J., Woods, M. O., Green, J. S., Parfrey, P., Rahman, P., & Green, R. C. (2016). Genetic structure of the newfoundland and labrador population: Founder effects modulate variability. *European Journal of Human Genetics : EJHG*, *24*(7), 1063-1070. doi:10.1038/ejhg.2015.256 [doi]
- Zhou, B., Wang, S., Mayr, C., Bartel, D. P., & Lodish, H. F. (2007). miR-150, a microRNA expressed in mature B and T cells, blocks early B cell development when expressed prematurely. *Proceedings of the National Academy of Sciences of the United States of America*, *104*(17), 7080-7085. doi:0702409104 [pii]
- Zhou, J., Duan, H., Xie, Y., Ning, Y., Zhang, X., Hui, N., . . . Zhou, J. (2016). MiR-193a-5p targets the coding region of AP-2alpha mRNA and induces cisplatin resistance in bladder cancers. *Journal of Cancer*, *7*(12), 1740-1746. doi:10.7150/jca.15620 [doi]
- Zhu, Z., Yin, J., Li, D. C., & Mao, Z. Q. (2017). Role of microRNAs in the treatment of type 2 diabetes mellitus with roux-en-Y gastric bypass. *Brazilian Journal of Medical and Biological Research = Revista Brasileira De Pesquisas Medicas E Biologicas*, *50*(3), e5817-431X20175817. doi:S0100-879X2017000300705 [pii]
- Zuo, B., Zhai, J., You, L., Zhao, Y., Yang, J., Weng, Z., . . . He, Y. (2017). Plasma microRNAs characterising patients with immune thrombocytopenic purpura. *Thrombosis and Haemostasis*, *117*(7), 1420-1431. doi:10.1160/TH-16-06-0481 [doi]

APPENDICES

Appendix A – Procedures preformed that did not contribute to the optimization of miRNA library preparation

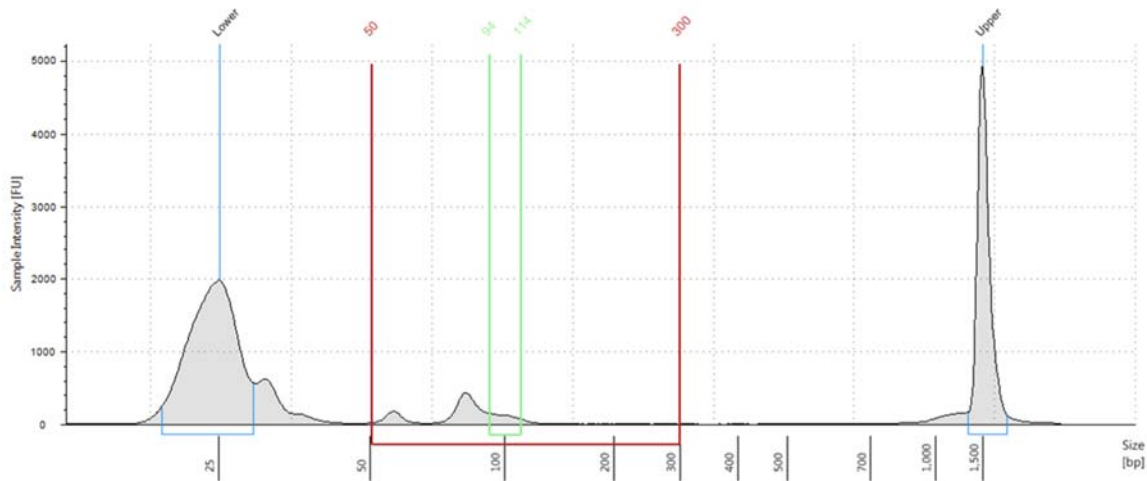


Figure A1 – Result when incorrect concentration of ethanol was added in error during the last stages of library preparation causing the majority of the miRNAs to lose the adaptors resulting in an oversized lower marker.

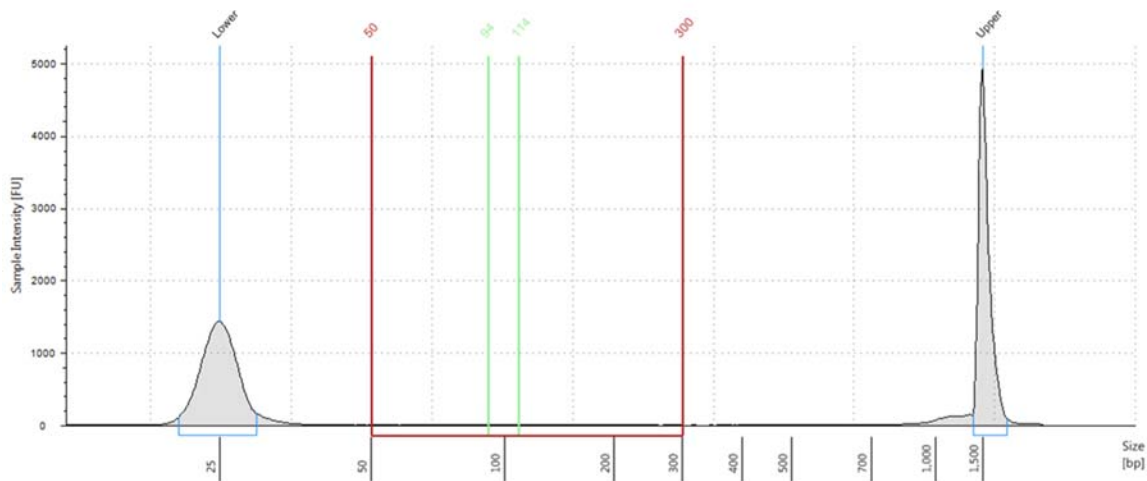


Figure A2 – Result when unknown error occurred at an unknown point during library preparation resulting in a sample concentration of zero

Appendix B – Pharmacogenomics PsA Cohort Library Preparations

Patient 2

The miRNA library of this patient was quantified as having a total molarity of 142 nmol/l and a regional molarity of 83.5 nmol/l, resulting in a regional molarity percentage of 58.8%. The electropherogram showed a slight adaptor dimer in the shoulder of the sample peak located at 106 bps and minimal large RNA species (**Figure B1**). The library sequenced 4,671,889 miRNA reads and detected a total of 741 different miRNAs

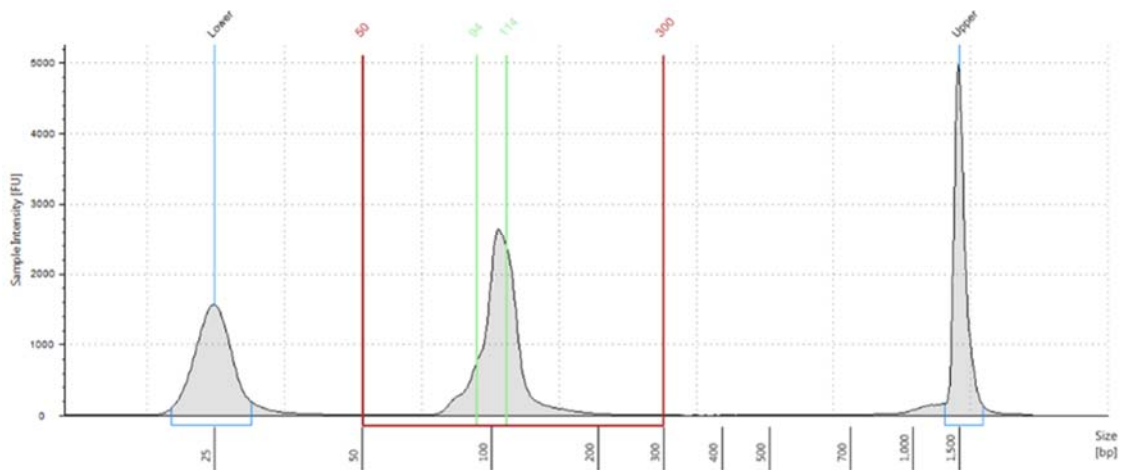


Figure B1 - Electropherogram depicting the size distribution and concentration of small RNA in the library of Patient 2.

Patient 6

The miRNA library of this patient was quantified as having a total molarity of 111 nmol/l and a regional molarity of 49.4 nmol/l, resulting in a regional molarity percentage of 44.5%. The electropherogram showed a very small adaptor dimer peak at 86 bps, a sample peak at 117 bps (falling slightly outside of the desired size range), and some large RNA species (**Figure B2**). The library sequenced 4,355,535 miRNA reads and detected a total of 686 different miRNAs.

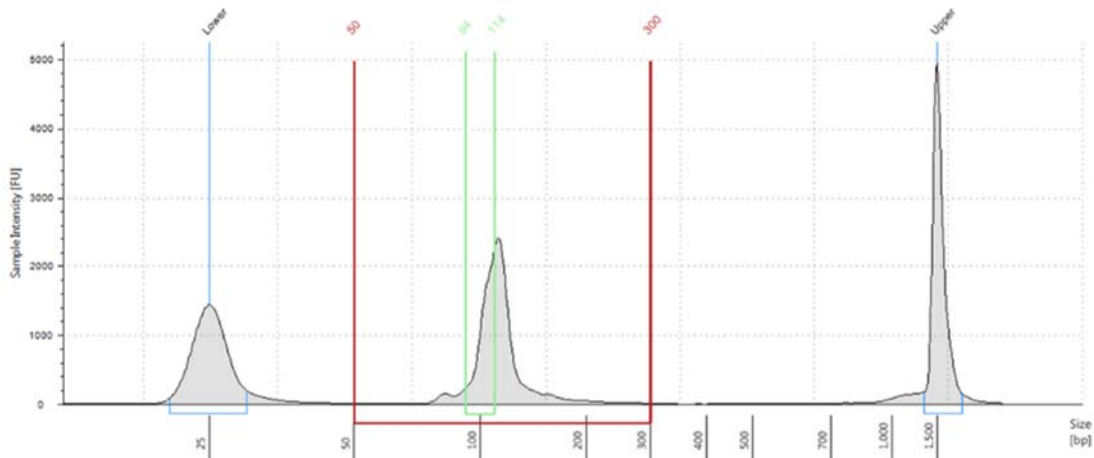


Figure B2 - Electropherogram depicting the size distribution and concentration of small RNA in the library of Patient 6.

Patient 7

The miRNA library of this patient was quantified as having a total molarity of 130 nmol/l and a regional molarity of 69.2 nmol/l, resulting in a regional molarity percentage of 53.2%. The electropherogram showed a small adaptor dimer peak at 86 bps, a sample peak at 109 bps, and minimal large RNA species (**Figure B3**). The library sequenced 4,715,021 miRNA reads and detected a total of 731 different miRNAs.

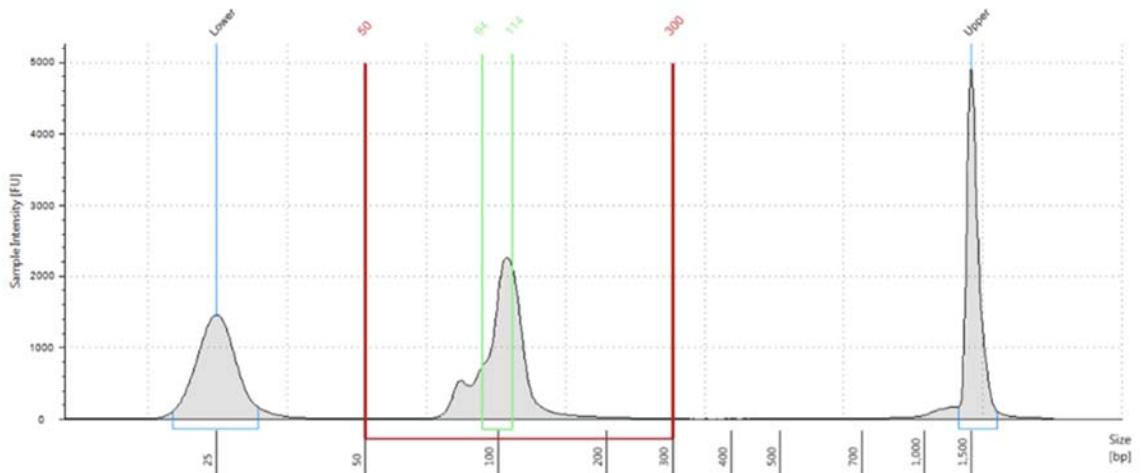


Figure B3 - Electropherogram depicting the size distribution and concentration of small RNA in the library of Patient 7.

Patient 8

The miRNA library of this patient was quantified as having a total molarity of 190 nmol/l and a regional molarity of 115 nmol/l, resulting in a regional molarity percentage of 60.5%. The electropherogram showed a small adaptor dimer peak at 85 bps, a sample peak at 111 bps, and minimal large RNA species (**Figure B4**). The library sequenced 4,165,755 miRNA reads and detected a total of 683 different miRNAs.

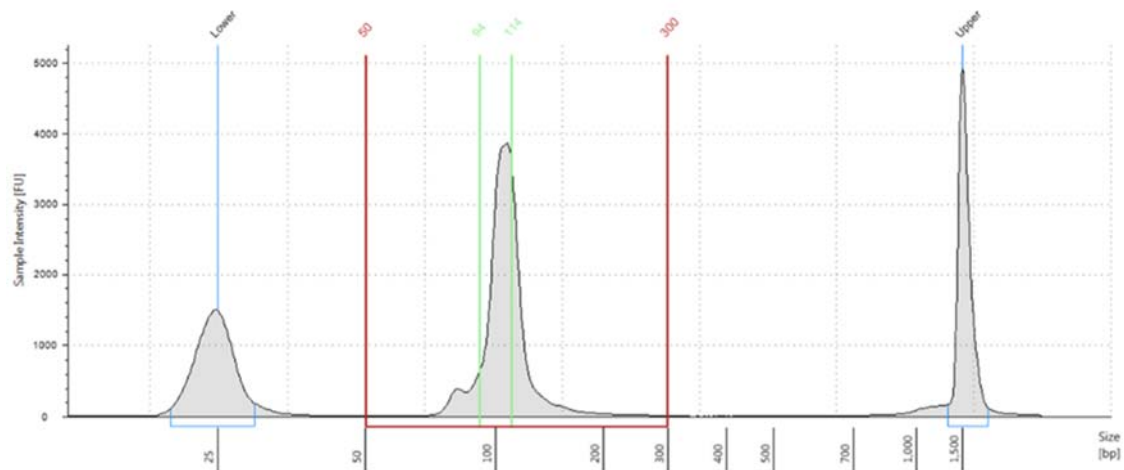


Figure B4 - Electropherogram depicting the size distribution and concentration of small RNA in the library of Patient 8.

Patient 10

The miRNA library of this patient was quantified as having a total molarity of 162 nmol/l and a regional molarity of 98.7 nmol/l, resulting in a regional molarity percentage of 60.9%. The electropherogram showed a slight adaptor dimer in the shoulder of the sample peak located at 109 bps and minimal large RNA species (**Figure B5**). The library sequenced 5,538,278 miRNA reads and detected a total of 725 different miRNAs.

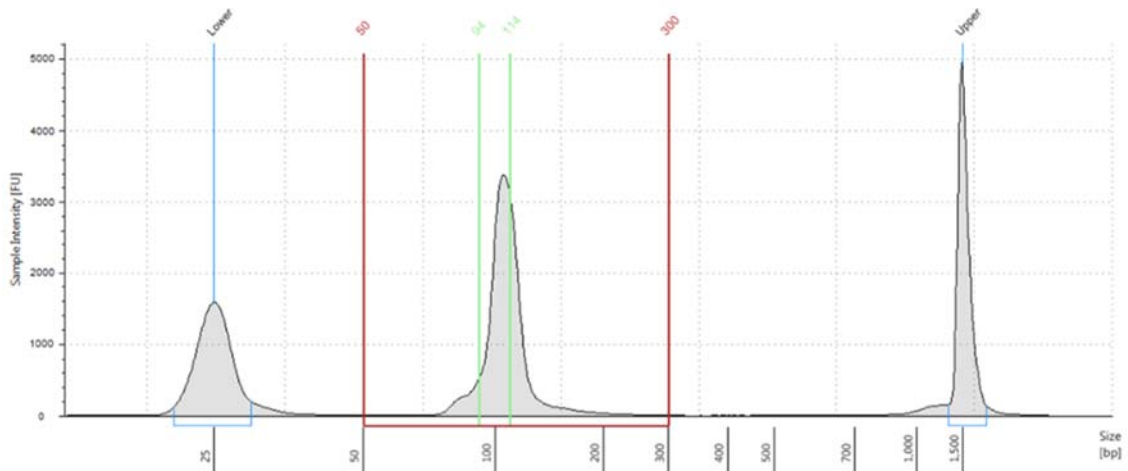


Figure B5 - Electropherogram depicting the size distribution and concentration of small RNA in the library of Patient 10.

Patient 11

The miRNA library of this patient was quantified as having a total molarity of 362 nmol/l and a regional molarity of 157 nmol/l, resulting in a regional molarity percentage of 43.4%. The electropherogram showed a large adaptor dimer peak at 86, a sample peak at 107 bps, and some large RNA species peaks at 164 bps, 226 bps, and 277 bps (**Figure B6**). The library sequenced 5,968,026 miRNA reads and detected a total of 711 different miRNAs.

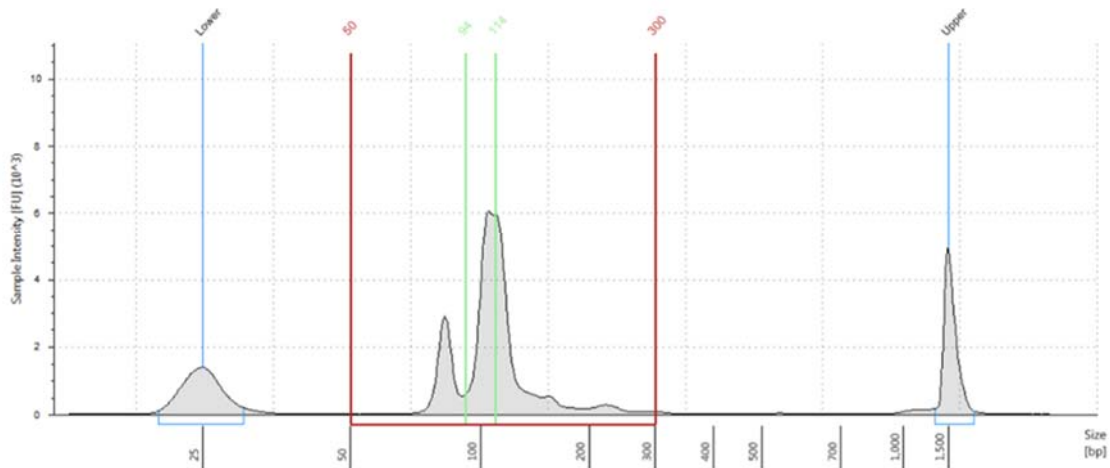


Figure B6 - Electropherogram depicting the size distribution and concentration of small RNA in the library of Patient 11.

Patient 12

The miRNA library of this patient was quantified as having a total molarity of 234 nmol/l and a regional molarity of 135 nmol/l, resulting in a regional molarity percentage of 57.7%. The electropherogram showed a sample peak at 111 bps, and a large RNA species peak at 162 bps (**Figure B7**). The library sequenced 6,619,036 miRNA reads and detected a total of 776 different miRNAs.

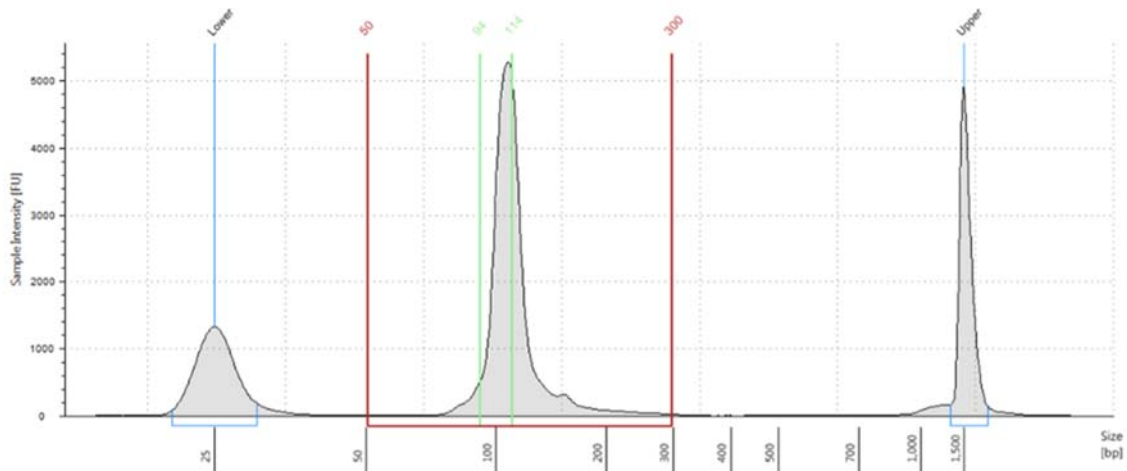


Figure B7 - Electropherogram depicting the size distribution and concentration of small RNA in the library of Patient 12.

Patient 13

The miRNA library of this patient was quantified as having a total molarity of 180 nmol/l and a regional molarity of 119 nmol/l, resulting in a regional molarity percentage of 66.1%. The electropherogram showed a small adaptor dimer in the shoulder of the sample peak located at 104 bps, and minimal large RNA species (**Figure B8**). The library sequenced 6,695,083 miRNA reads and detected a total of 794 different miRNAs.

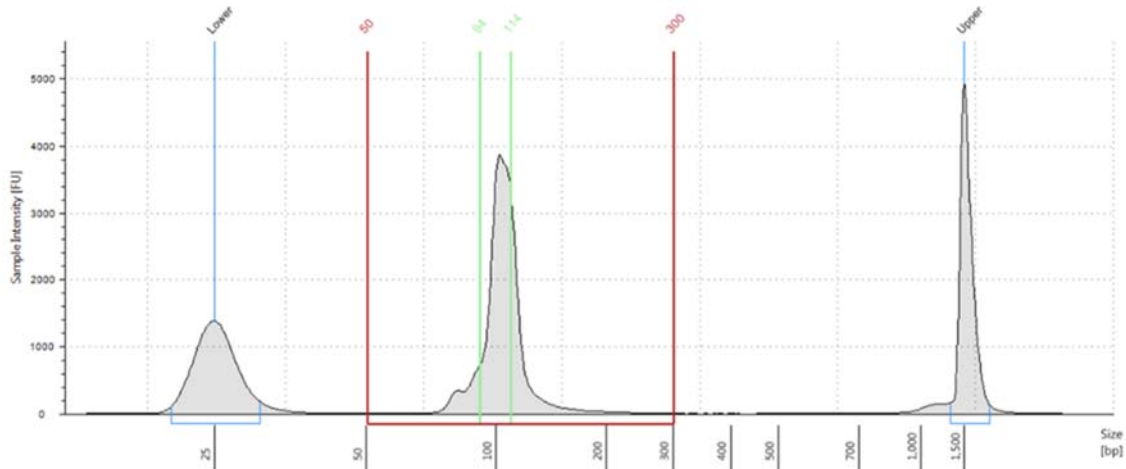


Figure B8 - Electropherogram depicting the size distribution and concentration of small RNA in the library of Patient 13.

Patient 14

The miRNA library of this patient was quantified as having a total molarity of 275 nmol/l and a regional molarity of 165 nmol/l, resulting in a regional molarity percentage of 60.0%. The electropherogram showed a sample peak located at 107 bps and minimal large RNA species (**Figure B9**). The library sequenced 9,061,954 miRNA reads and detected a total of 810 different miRNAs.

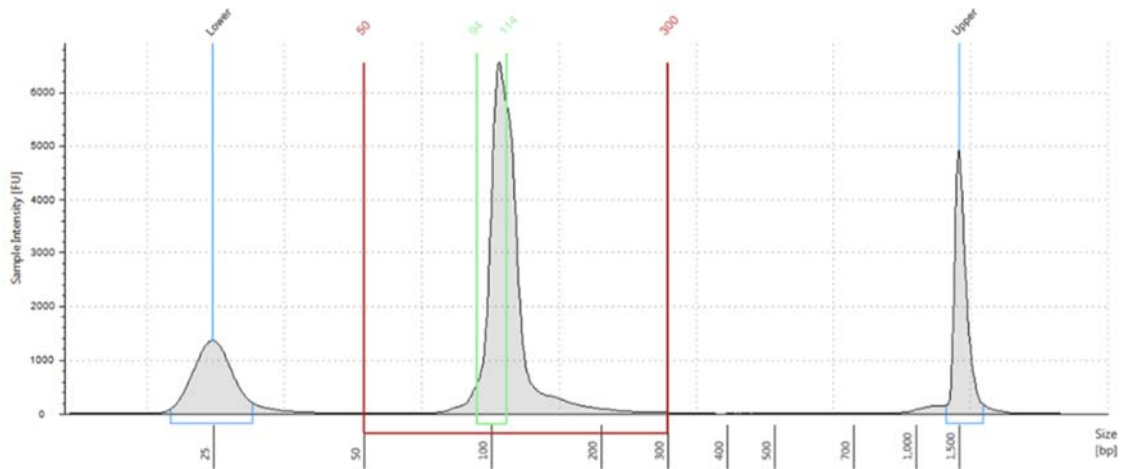


Figure B9 – Electropherogram depicting the size distribution and concentration of small RNA in the library of Patient 14.

Appendix C – Consent form for patients taking part in the pharmacogenomics project

HREB Version: October 2015

Faculty of Medicine, Schools of Nursing and Pharmacy of Memorial
University of Newfoundland; Eastern Health, St. John's; Newfoundland Cancer Treatment
and Research Foundation

CONSENT TO TAKE PART IN GENETIC RESEARCH

TITLE: Drug Response for Psoriatic Arthritis Treatment Study

INVESTIGATOR(S): Ms. Alison Sutherland, Dr. P. Rahman, & Dr. D. O'Rielly

SPONSOR: Atlantic Canada Opportunities Agency (ACOA)

You have been asked to take part in a research study. It is up to you to decide whether to be in the study or not. Before you decide, you need to understand what the study is for, what risks you might take and what benefits you might receive. This consent form explains the study.

The researchers will:

- discuss the study with you
- answer your questions
- keep confidential any information which could identify you or family members personally
- be available during the study to deal with problems and answer questions

If you decide not to take part or to leave the study this will not affect your usual health care.

1. Introduction/Background:

Genes are made of DNA and are tiny packets of information that contain the instructions for how our bodies develop. Some illnesses or conditions occur in families due to changes in genes. There can be variation in the way your DNA is expressed (RNA). If variation is found in your gene expression profile, we may do further testing to determine the cause of this change. A recent scientific method, called *Next Generation Sequencing* (NGS) is now available that can rapidly identify many genes that cause rare genetic disorders. This method allows a person's genes to be examined. It increases the number of genes we can look at in a single test.

Psoriatic Arthritis is a disease which is treated by various drugs. The effect of these drugs on a patient may be different depending on their genetics. Some patients can respond negatively and some patients will not respond at all. Finding genetic markers for how different patients will respond to the drugs is important for the treatment of future patients. Having a method of predicting negative responders or non-responders can help avoid avoidable harm and unnecessary cost.

One way to identify the genes responsible for the difference in response is to study patients who are currently being treated with these drugs. You have been identified as having Psoriatic Arthritis and have not yet been treated with this category of drug. Taking part in this study is completely voluntary. You do not have to be in the study if you do not want to. Your course of treatment will not be affected by this choice. This consent gives you important information about the study.

Version date:

1

Participant's Initials: _____

2. Purpose of study:

- The purpose of this study is to identify markers of drug response in the treatment of Psoriatic Arthritis. This study may eventually lead to a better understanding of the treatment of this disease.
- The researchers will use a technique called *Next Generation Sequencing* in an attempt to identify gene(s) expressed in Psoriatic Arthritis.

3. Description of the study procedures and tests:

- Review your medical records.
- Have genetic blood tests using a biological sample; prior to starting treatment and after one month of treatment (up to 3 tablespoons (30mls) per sampling).
- You will be asked to return every 3 months for a clinical assessment, as is standard procedure with the treatment.

4. Possible risks and discomforts:

- There is a risk of slight pain or bruising when your blood is drawn.
- The laboratory scientists will analyze your DNA, and the part that is expressed (RNA), looking for changes in genes that are related to Psoriatic Arthritis. The tests that will be run in the laboratory are designed to find new Psoriatic Arthritis genes, however this method of DNA analysis occasionally leads to finding other disease-causing genes that may be important to your family's health. These are called "secondary findings" and will be shared with you if the condition has medical implications, for example if screening tests or medical therapies are available which will lessen the impact of the disease or prevent it from developing. These findings will be discussed with you by a member of our research team at a convenient for you. If an actionable result is found and a referral to the Provincial Medical Genetics Program occurs, there is a possibility of a negative impact on future insurance coverage.
- Depending on which gene is affected in the secondary finding, it may be medically actionable. Secondary findings that can be treated are called actionable genes. There is a list of 63 actionable genes. If additional testing reveals a change in an actionable gene, the clinician will report this finding to you in a follow up appointment. If you do not wish to receive these secondary findings, you will not be enrolled in the study.
- In order to interpret the results of genetic research, we need to have correct information about parents. Sometimes the research shows new information about birth parents. This could happen in the case of an adoption or a mistake in the identity of a mother or father. This information will not be given to anyone, including yourself or family members, unless it is medically important to do so.

5. Benefits:

It is not known whether this study will benefit you. It is possible that the genetic cause for Psoriatic Arthritis may be found. While we cannot know this for sure, we do know that your participation will allow researchers to gain insight into the causes and treatments of Psoriatic Arthritis and perhaps other related conditions.

6. Liability statement:

Signing this form gives us your consent to be in this study. It tells us that you understand the information about the research study. When you sign this form, you do not give up your legal rights. Researchers or agencies involved in this research study still have their legal and professional responsibilities.

Version date:

2

Participant's Initials: _____

7. Confidentiality:

Protecting your privacy is an important part of this study. Every effort to protect your privacy will be made. However it cannot be guaranteed. For example we may be required by law to allow access to research records.

When you sign this consent form you give us permission to:

- Collect information from you;
- Collect information from your health records;
- Share information with the people conducting the study; and
- Share information with the people responsible for protecting your safety.

Use of records

The research team will collect and use only the information they need for this research study. This information will include:

- Date of birth;
- Sex;
- Medical conditions;
- Medications; and
- Results of tests and procedures you had before and during the study.

Names and contact information will be kept secure by the research team. It will not be shared with others without your permission.

8. Storage and Future Use:

The biologic samples and data collected for this study will be kept for an indefinite period of time.

In order to preserve a valuable resource, your DNA/RNA samples may be stored at the end of this research project. It is possible that these samples may be useful in a future research project which may or may not be related to the current research project. Any future research would have to be approved by a Health Research Ethics Board (HREB).

Please tick **one** of the following three options:

1. I agree that my DNA/RNA samples can be used for any HREB-approved research project (about inflammatory diseases), including those in which my name is given to the researchers, without obtaining further consent from me.
2. Specific consent must be obtained from me before using my DNA/RNA samples in any future research project in which my name is associated with the sample.
3. Under no circumstances may my DNA/RNA samples be used for any future research project. The samples must be destroyed at the end of the present project.

If you decide to withdraw from the study, the information collected up to that time will continue to be used by the research team. It may not be removed. This information will only be used for the purposes of this study.

Biologic samples and data collected and used by the research team will be stored in the Rahman/O'Rielly Laboratory, Memorial University of Newfoundland. Dr. Proton Rahman &

Version date:

3

Participant's Initials: _____

Dr. Darren O'Rielly are the people responsible for keeping it secure.

If at any time you wish to withdraw from the study or wish to have your biologic sample destroyed or returned, you can do so by contacting Dr. Proton Rahman at 709-777-5733.

9. Data Sharing Policy:

Much of the recent progress in understanding genetic disorders has come from research teams sharing the "de-identified" clinical and genetic information that they have collected with other researchers in the same field. The word "de-identified" means that the information is sent without names or any other information that could link it back to you. It is standard procedure to share de-identified data with other researchers. The databases where your de-identified information will be sent have strict access policies.

10. Questions or problems:

If you have any questions about taking part in this study, you can meet with the investigator who is in charge of the study at this institution. That person is:

Dr. Proton Rahman 709-777-5733

Or you can talk to someone who is not involved with the study at all, but can advise you on your rights as a participant in a research study. This person can be reached through:

**Office of the Health Research Ethics Board at 709-777-6974
Email at info@hrea.ca**

This study has been reviewed and given ethics approval by the Newfoundland and Labrador Health Research Ethics Board.

After signing this consent you will be given a copy.

Version date:

4

Participant's Initials: _____

Signature Page

To be filled out and signed by the participant:

Please check as appropriate:

- I have read the consent Yes { } No { }
- I have had the opportunity to ask questions/to discuss this study. Yes { } No { }
- I have received satisfactory answers to all of my questions. Yes { } No { }
- I have received enough information about the study. Yes { } No { }
- I have spoken to a qualified member of the study team. Yes { } No { }
- I understand that I am free to withdraw from the study Yes { } No { }
 - at any time
 - without having to give a reason
 - without affecting my future care
- I understand that it is my choice to be in the study and that I may not benefit. Yes { } No { }
- I understand how my privacy is protected and my records kept confidential. Yes { } No { }
- I agree that the study team may examine the biologic sample from me. Yes { } No { }
- I agree that the study doctor or investigator may read the parts of my hospital records which are relevant to the study. Yes { } No { }
- I agree to take part in this study. Yes { } No { }

Signature of Participant **Name Printed** **Date**

Signature of Witness **Name Printed** **Date**

To be signed by the investigator:

I have explained this study to the best of my ability. I invited questions and gave answers. I believe that the participant fully understands what is involved in being in the study, any potential risks of the study and that he or she has freely chosen to be in the study.

Signature of Investigator **Name Printed** **Date**

Telephone number: _____

Version date:

5

Participant's Initials: _____

Appendix D – Copyright approval to use a figure from Suzuki *et al.*, 2014

ELSEVIER LICENSE TERMS AND CONDITIONS	
	Nov 29, 2017
<hr/>	
<p>This Agreement between Alison Sutherland ("You") and Elsevier ("Elsevier") consists of your license details and the terms and conditions provided by Elsevier and Copyright Clearance Center.</p>	
License Number	4237650532774
License date	Nov 28, 2017
Licensed Content Publisher	Elsevier
Licensed Content Publication	Autoimmunity Reviews
Licensed Content Title	The IL-23/IL-17 axis in psoriatic arthritis
Licensed Content Author	Erika Suzuki,Elizabeth D. Mellins,M. Eric Gershwin,Frank O. Nestle,Iannis E. Adamopoulos
Licensed Content Date	April–May 2014
Licensed Content Volume	13
Licensed Content Issue	4-5
Licensed Content Pages	7
Start Page	496
End Page	502
Type of Use	reuse in a thesis/dissertation
Intended publisher of new work	other
Portion	figures/tables/illustrations
Number of figures/tables/illustrations	1
Format	both print and electronic
Are you the author of this Elsevier article?	No
Will you be translating?	No
Original figure numbers	Fig. 1. IL-23, IL-17 and RANK receptor signaling. - Will modify to remove RANKL trigger pathway
Title of your thesis/dissertation	Pharmacogenomics of Psoriatic Arthritis
Expected completion date	Dec 2017
Estimated size (number of pages)	140
Requestor Location	Alison Sutherland 87A Bond St. St. John's, NL A1C1T3 Canada Attn: Alison Sutherland
Total	0.00 USD
Terms and Conditions	

INTRODUCTION

1. The publisher for this copyrighted material is Elsevier. By clicking "accept" in connection with completing this licensing transaction, you agree that the following terms and conditions apply to this transaction (along with the Billing and Payment terms and conditions established by Copyright Clearance Center, Inc. ("CCC"), at the time that you opened your Rightslink account and that are available at any time at <http://myaccount.copyright.com>).

GENERAL TERMS

2. Elsevier hereby grants you permission to reproduce the aforementioned material subject to the terms and conditions indicated.

3. Acknowledgement: If any part of the material to be used (for example, figures) has appeared in our publication with credit or acknowledgement to another source, permission must also be sought from that source. If such permission is not obtained then that material may not be included in your publication/copies. Suitable acknowledgement to the source must be made, either as a footnote or in a reference list at the end of your publication, as follows:

"Reprinted from Publication title, Vol /edition number, Author(s), Title of article / title of chapter, Pages No., Copyright (Year), with permission from Elsevier [OR APPLICABLE SOCIETY COPYRIGHT OWNER]." Also Lancet special credit - "Reprinted from The Lancet, Vol. number, Author(s), Title of article, Pages No., Copyright (Year), with permission from Elsevier."

4. Reproduction of this material is confined to the purpose and/or media for which permission is hereby given.

5. Altering/Modifying Material: Not Permitted. However figures and illustrations may be altered/adapted minimally to serve your work. Any other abbreviations, additions, deletions and/or any other alterations shall be made only with prior written authorization of Elsevier Ltd. (Please contact Elsevier at permissions@elsevier.com). No modifications can be made to any Lancet figures/tables and they must be reproduced in full.

6. If the permission fee for the requested use of our material is waived in this instance, please be advised that your future requests for Elsevier materials may attract a fee.

7. Reservation of Rights: Publisher reserves all rights not specifically granted in the combination of (i) the license details provided by you and accepted in the course of this licensing transaction, (ii) these terms and conditions and (iii) CCC's Billing and Payment terms and conditions.

8. License Contingent Upon Payment: While you may exercise the rights licensed immediately upon issuance of the license at the end of the licensing process for the transaction, provided that you have disclosed complete and accurate details of your proposed use, no license is finally effective unless and until full payment is received from you (either by publisher or by CCC) as provided in CCC's Billing and Payment terms and conditions. If full payment is not received on a timely basis, then any license preliminarily granted shall be deemed automatically revoked and shall be void as if never granted. Further, in the event that you breach any of these terms and conditions or any of CCC's Billing and Payment terms and conditions, the license is automatically revoked and shall be void as if never granted. Use of materials as described in a revoked license, as well as any use of the materials beyond the scope of an unrevoked license, may constitute copyright infringement and publisher reserves the right to take any and all action to protect its copyright in the materials.

9. Warranties: Publisher makes no representations or warranties with respect to the licensed material.

10. Indemnity: You hereby indemnify and agree to hold harmless publisher and CCC, and their respective officers, directors, employees and agents, from and against any and all claims arising out of your use of the licensed material other than as specifically authorized pursuant to this license.

11. **No Transfer of License:** This license is personal to you and may not be sublicensed, assigned, or transferred by you to any other person without publisher's written permission.
12. **No Amendment Except in Writing:** This license may not be amended except in a writing signed by both parties (or, in the case of publisher, by CCC on publisher's behalf).
13. **Objection to Contrary Terms:** Publisher hereby objects to any terms contained in any purchase order, acknowledgment, check endorsement or other writing prepared by you, which terms are inconsistent with these terms and conditions or CCC's Billing and Payment terms and conditions. These terms and conditions, together with CCC's Billing and Payment terms and conditions (which are incorporated herein), comprise the entire agreement between you and publisher (and CCC) concerning this licensing transaction. In the event of any conflict between your obligations established by these terms and conditions and those established by CCC's Billing and Payment terms and conditions, these terms and conditions shall control.
14. **Revocation:** Elsevier or Copyright Clearance Center may deny the permissions described in this License at their sole discretion, for any reason or no reason, with a full refund payable to you. Notice of such denial will be made using the contact information provided by you. Failure to receive such notice will not alter or invalidate the denial. In no event will Elsevier or Copyright Clearance Center be responsible or liable for any costs, expenses or damage incurred by you as a result of a denial of your permission request, other than a refund of the amount(s) paid by you to Elsevier and/or Copyright Clearance Center for denied permissions.

LIMITED LICENSE

The following terms and conditions apply only to specific license types:

15. **Translation:** This permission is granted for non-exclusive world **English** rights only unless your license was granted for translation rights. If you licensed translation rights you may only translate this content into the languages you requested. A professional translator must perform all translations and reproduce the content word for word preserving the integrity of the article.
16. **Posting licensed content on any Website:** The following terms and conditions apply as follows: Licensing material from an Elsevier journal: All content posted to the web site must maintain the copyright information line on the bottom of each image; A hyper-text must be included to the Homepage of the journal from which you are licensing at <http://www.sciencedirect.com/science/journal/xxxxx> or the Elsevier homepage for books at <http://www.elsevier.com>; Central Storage: This license does not include permission for a scanned version of the material to be stored in a central repository such as that provided by Heron/XanEdu. Licensing material from an Elsevier book: A hyper-text link must be included to the Elsevier homepage at <http://www.elsevier.com>. All content posted to the web site must maintain the copyright information line on the bottom of each image.

Posting licensed content on Electronic reserve: In addition to the above the following clauses are applicable: The web site must be password-protected and made available only to bona fide students registered on a relevant course. This permission is granted for 1 year only. You may obtain a new license for future website posting.

17. **For journal authors:** the following clauses are applicable in addition to the above:

Preprints:

A preprint is an author's own write-up of research results and analysis, it has not been peer-reviewed, nor has it had any other value added to it by a publisher (such as formatting, copyright, technical enhancement etc.).

Authors can share their preprints anywhere at any time. Preprints should not be added to or enhanced in any way in order to appear more like, or to substitute for, the final versions of articles however authors can update their preprints on arXiv or RePEc with their Accepted Author Manuscript (see below).

If accepted for publication, we encourage authors to link from the preprint to their formal publication via its DOI. Millions of researchers have access to the formal publications on ScienceDirect, and so links will help users to find, access, cite and use the best available version. Please note that Cell Press, The Lancet and some society-owned have different preprint policies. Information on these policies is available on the journal homepage.

Accepted Author Manuscripts: An accepted author manuscript is the manuscript of an article that has been accepted for publication and which typically includes author-incorporated changes suggested during submission, peer review and editor-author communications.

Authors can share their accepted author manuscript:

- immediately
 - via their non-commercial person homepage or blog
 - by updating a preprint in arXiv or RePEc with the accepted manuscript
 - via their research institute or institutional repository for internal institutional uses or as part of an invitation-only research collaboration work-group
 - directly by providing copies to their students or to research collaborators for their personal use
 - for private scholarly sharing as part of an invitation-only work group on commercial sites with which Elsevier has an agreement
- After the embargo period
 - via non-commercial hosting platforms such as their institutional repository
 - via commercial sites with which Elsevier has an agreement

In all cases accepted manuscripts should:

- link to the formal publication via its DOI
- bear a CC-BY-NC-ND license - this is easy to do
- if aggregated with other manuscripts, for example in a repository or other site, be shared in alignment with our hosting policy not be added to or enhanced in any way to appear more like, or to substitute for, the published journal article.

Published journal article (JPA): A published journal article (PJA) is the definitive final record of published research that appears or will appear in the journal and embodies all value-adding publishing activities including peer review co-ordination, copy-editing, formatting, (if relevant) pagination and online enrichment.

Policies for sharing publishing journal articles differ for subscription and gold open access articles:

Subscription Articles: If you are an author, please share a link to your article rather than the full-text. Millions of researchers have access to the formal publications on ScienceDirect, and so links will help your users to find, access, cite, and use the best available version. Theses and dissertations which contain embedded PJAs as part of the formal submission can be posted publicly by the awarding institution with DOI links back to the formal publications on ScienceDirect.

If you are affiliated with a library that subscribes to ScienceDirect you have additional private sharing rights for others' research accessed under that agreement. This includes use for classroom teaching and internal training at the institution (including use in course packs and courseware programs), and inclusion of the article for grant funding purposes.

Gold Open Access Articles: May be shared according to the author-selected end-user license and should contain a [CrossMark logo](#), the end user license, and a DOI link to the formal publication on ScienceDirect.

Please refer to Elsevier's [posting policy](#) for further information.

18. **For book authors** the following clauses are applicable in addition to the above:

Authors are permitted to place a brief summary of their work online only. You are not

allowed to download and post the published electronic version of your chapter, nor may you scan the printed edition to create an electronic version. **Posting to a repository:** Authors are permitted to post a summary of their chapter only in their institution's repository.

19. **Thesis/Dissertation:** If your license is for use in a thesis/dissertation your thesis may be submitted to your institution in either print or electronic form. Should your thesis be published commercially, please reapply for permission. These requirements include permission for the Library and Archives of Canada to supply single copies, on demand, of the complete thesis and include permission for Proquest/UMI to supply single copies, on demand, of the complete thesis. Should your thesis be published commercially, please reapply for permission. Theses and dissertations which contain embedded PJAs as part of the formal submission can be posted publicly by the awarding institution with DOI links back to the formal publications on ScienceDirect.

Elsevier Open Access Terms and Conditions

You can publish open access with Elsevier in hundreds of open access journals or in nearly 2000 established subscription journals that support open access publishing. Permitted third party re-use of these open access articles is defined by the author's choice of Creative Commons user license. See our [open access license policy](#) for more information.

Terms & Conditions applicable to all Open Access articles published with Elsevier:

Any reuse of the article must not represent the author as endorsing the adaptation of the article nor should the article be modified in such a way as to damage the author's honour or reputation. If any changes have been made, such changes must be clearly indicated. The author(s) must be appropriately credited and we ask that you include the end user license and a DOI link to the formal publication on ScienceDirect.

If any part of the material to be used (for example, figures) has appeared in our publication with credit or acknowledgement to another source it is the responsibility of the user to ensure their reuse complies with the terms and conditions determined by the rights holder.

Additional Terms & Conditions applicable to each Creative Commons user license:

CC BY: The CC-BY license allows users to copy, to create extracts, abstracts and new works from the Article, to alter and revise the Article and to make commercial use of the Article (including reuse and/or resale of the Article by commercial entities), provided the user gives appropriate credit (with a link to the formal publication through the relevant DOI), provides a link to the license, indicates if changes were made and the licensor is not represented as endorsing the use made of the work. The full details of the license are available at <http://creativecommons.org/licenses/by/4.0>.

CC BY NC SA: The CC BY-NC-SA license allows users to copy, to create extracts, abstracts and new works from the Article, to alter and revise the Article, provided this is not done for commercial purposes, and that the user gives appropriate credit (with a link to the formal publication through the relevant DOI), provides a link to the license, indicates if changes were made and the licensor is not represented as endorsing the use made of the work. Further, any new works must be made available on the same conditions. The full details of the license are available at <http://creativecommons.org/licenses/by-nc-sa/4.0>.

CC BY NC ND: The CC BY-NC-ND license allows users to copy and distribute the Article, provided this is not done for commercial purposes and further does not permit distribution of the Article if it is changed or edited in any way, and provided the user gives appropriate credit (with a link to the formal publication through the relevant DOI), provides a link to the license, and that the licensor is not represented as endorsing the use made of the work. The full details of the license are available at <http://creativecommons.org/licenses/by-nc-nd/4.0>. Any commercial reuse of Open Access articles published with a CC BY NC SA or CC BY NC ND license requires permission from Elsevier and will be subject to a fee.

Commercial reuse includes:

- Associating advertising with the full text of the Article
- Charging fees for document delivery or access
- Article aggregation
- Systematic distribution via e-mail lists or share buttons

Posting or linking by commercial companies for use by customers of those companies.

20. Other Conditions:

v1.9

Questions? customercare@copyright.com or +1-855-239-3415 (toll free in the US) or +1-978-646-2777.

Appendix E - Copyright approval to use a figure from Creemers *et al.*, 2012

WOLTERS KLUWER HEALTH, INC. LICENSE TERMS AND CONDITIONS	
	Nov 16, 2017
<hr/>	
<p>This Agreement between Alison Sutherland ("You") and Wolters Kluwer Health, Inc. ("Wolters Kluwer Health, Inc.") consists of your license details and the terms and conditions provided by Wolters Kluwer Health, Inc. and Copyright Clearance Center.</p>	
License Number	4230901284884
License date	Nov 16, 2017
Licensed Content Publisher	Wolters Kluwer Health, Inc.
Licensed Content Publication	Circulation Research
Licensed Content Title	Circulating MicroRNAs
Licensed Content Author	Esther E. Creemers, Anke J. Tijssen, Yigal M. Pinto
Licensed Content Date	Feb 3, 2012
Licensed Content Volume	110
Licensed Content Issue	3
Type of Use	Dissertation/Thesis
Requestor type	Individual
Portion	Figures/table/illustration
Number of figures/tables/illustrations	1
Figures/tables/illustrations used	Cellular release mechanisms and extracellular transportation systems of miRNAs
Author of this Wolters Kluwer article	No
Title of your thesis / dissertation	Pharmacogenomics of Psoriatic Arthritis
Expected completion date	Dec 2017
Estimated size(pages)	140
Requestor Location	Alison Sutherland 87A Bond St. St. John's, NL A1C1T3 Canada Attn: Alison Sutherland
Billing Type	Invoice
Billing Address	Alison Sutherland 87A Bond St. St. John's, NL A1C1T3 Canada Attn: Alison Sutherland
Total	0.00 USD

Wolters Kluwer Terms and Conditions

1. **Transfer of License:** Wolters Kluwer hereby grants you a non-exclusive license to reproduce this material for this purpose, and for no other use, subject to the conditions herein.
2. **Credit Line:** will be prominently placed and include: For books – the author(s), title of book, editor, copyright holder, year of publication; For journals – the author(s), title of article, title of journal, volume number, issue number, inclusive pages and website URL to the journal page.
3. **Warranties:** The requestor warrants that the material shall not be used in any manner which may be considered derogatory to the title, content, or authors of the material, or to Wolters Kluwer.
4. **Indemnity:** You hereby indemnify and hold harmless Wolters Kluwer and their respective officers, directors, employees and agents, from and against any and all claims, costs, proceeding or demands arising out of your unauthorized use of the Licensed Material.
5. **Geographical Scope:** Permission granted is non-exclusive, and is valid throughout the world in the English language and the languages specified in your original request.
6. Wolters Kluwer cannot supply the requestor with the original artwork, electronic files or a "clean copy."
7. Permission is valid if the borrowed material is original to a Wolters Kluwer imprint (Lippincott-Raven Publishers, Williams & Wilkins, Lea & Febiger, Harwal, Rapid Science, Little Brown & Company, Harper & Row Medical, American Journal of Nursing Co, and Urban & Schwarzenberg - English Language, Raven Press, Paul Hoeber, Springhouse, Ovid).
8. **Termination of contract:** If you opt not to use the material requested above please notify RightsLink or Wolters Kluwer within 90 days of the original invoice date.
9. This permission does not apply to images that are credited to publications other than Wolters Kluwer books/journals or its Societies. For images credited to non-Wolters Kluwer books or journals, you will need to obtain permission from the source referenced in the figure or table legend or credit line before making any use of the image(s) or table(s).
10. **Modifications:** With the exception of text size or color, no Wolters Kluwer material is permitted to be modified or adapted without publisher approval.
11. **Third party material:** Adaptations are protected by copyright, so if you would like to reuse material that we have adapted from another source, you will need not only our permission, but the permission of the rights holder of the original material. Similarly, if you want to reuse an adaptation of original LWW content that appears in another publishers work, you will need our permission and that of the next publisher. The adaptation should be credited as follows: Adapted with permission from Wolters Kluwer: Book author, title, year of publication or Journal name, article author, title, reference citation, year of publication. Modifications are permitted on an occasional basis only and permission must be sought by Wolters Kluwer.
12. **Duration of the license:** Permission is granted for a one-time use only within 12 months from the date of this invoice. Rights herein do not apply to future reproductions, editors, revisions, or other derivative works. Once the 12 - month term has expired, permission to renew must be submitted in writing.
 - i. For content reused in another journal or book, in print or electronic format, the license is one-time use and lasts for the 1st edition of a book or for the life of the edition in case of journals.
 - ii. If your Permission Request is for use on a website (which is not a journal or a book), internet, intranet, or any publicly accessible site, you agree to remove the material from such site after 12 months or else renew your permission request.
13. **Contingent on payment:** While you may exercise the rights licensed immediately upon issuance of the license at the end of the licensing process for the transaction, provided that you have disclosed complete and accurate details of your proposed use, no license is finally effective unless and until full payment is received from you (either by publisher or by CCC) as provided in CCC's Billing and Payment terms and conditions. If full payment is not received on a timely basis, then any license preliminarily granted shall be deemed automatically revoked and shall be void as if never granted. Further, in the event that you breach any of these terms and conditions or any of CCC's Billing and Payment terms and conditions, the license is automatically revoked and shall be void as if never granted. Use

of materials as described in a revoked license, as well as any use of the materials beyond the scope of an unrevoked license, may constitute copyright infringement and publisher reserves the right to take any and all action to protect its copyright in the materials.

14. **Waived permission fee:** If the permission fee for the requested use of our material has been waived in this instance, please be advised that your future requests for Wolters Kluwer materials may incur a fee.
15. **Service Description for Content Services:** Subject to these terms of use, any terms set forth on the particular order, and payment of the applicable fee, you may make the following uses of the ordered materials:
 - i. **Content Rental:** You may access and view a single electronic copy of the materials ordered for the time period designated at the time the order is placed. Access to the materials will be provided through a dedicated content viewer or other portal, and access will be discontinued upon expiration of the designated time period. An order for Content Rental does not include any rights to print, download, save, create additional copies, to distribute or to reuse in any way the full text or parts of the materials.
 - ii. **Content Purchase:** You may access and download a single electronic copy of the materials ordered. Copies will be provided by email or by such other means as publisher may make available from time to time. An order for Content Purchase does not include any rights to create additional copies or to distribute copies of the materials.

For Journals Only:

1. Please note that articles in the **ahead-of-print stage** of publication can be cited and the content may be re-used by including the date of access and the unique DOI number. Any final changes in manuscripts will be made at the time of print publication and will be reflected in the final electronic version of the issue. Disclaimer: Articles appearing in the Published Ahead-of-Print section have been peer-reviewed and accepted for publication in the relevant journal and posted online before print publication. Articles appearing as publish ahead-of-print may contain statements, opinions, and information that have errors in facts, figures, or interpretation. Accordingly, Wolters Kluwer, the editors and authors and their respective employees are not responsible or liable for the use of any such inaccurate or misleading data, opinion or information contained in the articles in this section.
2. Where a journal is being published by a learned society, the details of that society must be included in the credit line.
 - i. **For Open Access journals:** The following statement needs to be added when reprinting the material in Open Access journals only: "promotional and commercial use of the material in print, digital or mobile device format is prohibited without the permission from the publisher Wolters Kluwer. Please contact healthpermissions@wolterskluwer.com for further information."
 - ii. **Exceptions:** In case of reuse from **Diseases of the Colon & Rectum, Plastic Reconstructive Surgery, The Green Journal, Critical Care Medicine, Pediatric Critical Care Medicine, the American Heart Association Publications and the American Academy of Neurology** the following guideline applies: no drug/ trade name or logo can be included in the same page as the material re-used.
3. **Translations:** If granted permissions to republish a full text article in another language, Wolters Kluwer should be sent a copy of the translated PDF. Please include disclaimer below on all translated copies:
 - i. ***Wolters Kluwer and its Societies take no responsibility for the accuracy of the translation from the published English original and are not liable for any errors which may occur.***
4. **Full Text Articles:** Reuse of full text articles in English is prohibited.

STM Signatories Only:

1. Any permission granted for a particular edition will apply also to subsequent editions and for editions in other languages, provided such editions are for the work as a whole in situ and does not involve the separate exploitation of the permitted illustrations or excerpts. Please click [here](#) to view the STM guidelines.

Other Terms and Conditions:

v1.17

Questions? customercare@copyright.com or +1-855-239-3415 (toll free in the US) or +1-978-646-2777.

Appendix E – The usage terms for draw.io, all flow charts created for this project were made using draw.io software.

The screenshot shows a Stack Overflow question page. At the top, there is a search bar with the text "What do you want to know?" and an "Ask question" button. Below the search bar, there are navigation links for "Questions", "Topics", and "Experts". The main content area features a question titled "What are the usage terms for diagrams produced by draw.io?". The question is asked by David Benson on June 04, 2015, and has 0 votes. The question text is: "Can they be used for any purpose under commercial usage conditions, for example? Does that extend to using the built-in icons that are copyrighted to JGraph?". There are tags for "draw.io", "usage", "license", "terms", "commercial", "icons", and "faq". A "Comment" button is visible below the question. The answer section shows "1 answer" and a response from David Benson on June 04, 2015, with 0 votes. The answer text is: "There are no restrictions on the usage of any output generated. The generated diagram belongs to you and we grant you a license to use any of our copyrighted icons for both persistence and making raster and vector outputs of your diagrams, using draw.io, for any purpose." A "Comment" button is also present below the answer. A link to a solution article by Mate Egri from October 18, 2016, is provided: "https://desk.draw.io/solution/articles/16000042494-what-are-the-usage-terms-for-diagrams-produced-by-draw-io-". At the bottom of the answer section, there is a text input field with the placeholder "Add your comment..." and a "Log in to answer" button. On the right side of the page, there is a "Watch" section and a "RELATED QUESTIONS" section with several links to other questions.